12-2009

“Saccharomyces cerevisiae G protein Coupled Receptor, Ste2p Interactions with its Ligand, α-factor and Cognate Gα protein, Gpa1p

George Kwabena Essien Umanah
University of Tennessee - Knoxville

To the Graduate Council:

I am submitting herewith a dissertation written by George Kwabena Essien Umanah entitled ""Saccharomyces cerevisiae G protein Coupled Receptor, Ste2p Interactions with its Ligand, α-factor and Cognate Gα protein, Gpa1p." I have examined the final electronic copy of this dissertation for form and content and recommend that it be accepted in partial fulfillment of the requirements for the degree of Doctor of Philosophy, with a major in Microbiology.

Jeffrey M. Becker, Major Professor

We have read this dissertation and recommend its acceptance:

Cynthia B. Peterson, Todd B. Reynolds, Timothy E. Sparer, Elias J. Fernandez

Accepted for the Council:

Carolyn R. Hodges

Vice Provost and Dean of the Graduate School

(Original signatures are on file with official student records.)

To the Graduate Council:

I am submitting herewith a dissertation written by George Kwabena Essien Umanah entitled "*Saccharomyces cerevisiae* G protein Coupled Receptor, Ste2p Interactions with its Ligand, α-factor and Cognate Gα protein, Gpa1p." I have examined the final electronic copy of this thesis for form and content and recommend that it be accepted in partial fulfillment of the requirements for the degree of Doctor of Philosophy with a major in Microbiology.

Jeffrey M. Becker
Major Professor

We have read this dissertation
and recommend its acceptance:

Cynthia B. Peterson

Todd B. Reynolds

Timothy E. Sparer

Elias J. Fernandez

Accepted for the Council:

Carolyn R. Hodges
Vice Provost and Dean of the Graduate School

(Original signatures are on file with official student records.)

Saccharomyces cerevisiae G protein Coupled Receptor, Ste2p Interactions with its Ligand, α-factor and Cognate Gα protein, Gpa1p.

A Dissertation Presented for the

Doctor of Philosophy Degree

The University of Tennessee, Knoxville

George Kwabena Essien Umanah

December 2009

DEDICATION

This dissertation is dedicated to my parents, Charles and Comfort Umanah, Beatrice Eshun and my Auntie, Mavis Odame for their love and care that have seen me through all these years of studying away from home. I would not be able to achieve any of this without the sacrifices they made in order for me to receive the best education possible. I would also like to dedicate this work to my wife, Trisha L. Horton-Umanah, for all the support she provided. I appreciate your help during these difficulty times and God bless you.

ACKNOWLEDGEMENTS

I would like to thank everybody who helped me throughout my studies. My first and warmest gratitude goes to my mentor and "fearless Boss" Dr. Jeffrey M. Becker, it was really a great pleasure to work for such an enthusiastic scientist. Dr. Becker has provided me with knowledge, confidence, support and directions that will be with me for the rest of my career. I am thankful that he was so patient and supportive during the times I was struggling with my projects. His critical suggestions and guidance helped me overcome lots of setbacks that I would not even try without him. I am honored to work for you. I also would like to thank Dr. Fred Naider for his support and valuable ideas on critical decisions throughout these studies. My appreciation goes to my committee members: Cynthia B. Peterson, Todd B. Reynolds, Timothy E. Sparer and Elias J. Fernandez for their suggestions, critical reviews, and guidance during my studies.

I appreciate the hard working members of Dr. Naider's laboratory for synthesizing the peptides that were used in this study. I am thankful for working with Dr. Steve Wright who introduced me to the G protein studies. Without your advice and suggestions this would not have been possible. I would like to thank Dr. Yaa Difie Osei (University of Ghana) for recommending me to Dr. Becker's lab.

A heartfelt appreciation and hugs to all members in Dr. Becker's laboratory, who kept me alive during my studies. I want to thank Dr. Melinda Hauser (Mother of the Lab, you are awesome and will be missed), Dr. Byung-Kwon Lee and Dr. Tom Masi for their help, wise criticism and insightful thoughts. My deepest appreciate goes to Li-Yin Huang (aka Proline) for being my best lab-mate and partner. It was great working with you Li-Yin; you are such a hard working and wonderful person. It was great to work in the same lab with Sarah Kauffman, Dr.

Steve Minkin, Dr. Hee-Jung Kim, Kyung Sik, and Seraj Uddin. I appreciate the help from Julie Maccarone; you were my best student ever. Thanks to Jonathan Lockhart, Andrew Johns, Amanda Deyo, Jenna Burton, Benjamin Goldman and Adam Schwartz for all the fun in Dr. Becker's Lab.

Thanks to Dr. Larry Thompson and Nancy Horn of Dr. Peterson's lab for helping with the analyses of the mass spectrometric data. I also want to acknowledge Dr. Nathan Verberkmoes and Dr. Andrew Link (Vanderbilt University) for helping with the MS/MS data. Thanks to Joseph A. May for running all the DNA sequences. Finally I want to thank my family in Ghana, England, my wife and her family in Tennessee, all members of Second Presbyterian Church (Knoxville), and members of my soccer club in Knoxville (The Ligers) for all the support that they gave me during all these years.

ABSTRACT

The *Saccharomyces cerevisiae* alpha-factor receptor, Ste2p, belongs to the G protein-coupled receptors (GPCRs), a class of integral membrane proteins that are characterized by seven-transmembrane (TM) domains. Ste2p-alpha-factor pair has been used extensively as a paradigm for investigating GPCRs structure and function. Upon binding of alpha-factor to Ste2p, a signal is transduced via an associated guanine-nucleotide binding protein, Gpa1p, initiating a cascade of events similar to those for mammalian GPCRs signal transduction. GPCRs are essential in many physiological processes associated with human diseases. Many aspects of structure and function are highly conserved across GPCRs, irrespective of primary amino acid sequence. This dissertation investigated the interactions of Ste2p with alpha-factor and Gpa1p. An overview of GPCRs in general with specific emphasis on Ste2p interactions with alpha-factor and Gpa1p are discussed in part I. Cross-linking studies of alpha-factor analogs containing 3,4-dihydroxylphenylalanine (DOPA) at positions 1 and 13 indicated that Trp^{1} and Tyr^{13} of α-factor are in close proximity to Lys269 and Cys59 of Ste2p, respectively when alpha-factor is bound to Ste2p. An alpha-factor synergist lacking the last two amino acids required for binding could only inhibit the cross-linking of DOPA at position 1 suggesting that the alpha-factor synergist interacts with the N-terminus of alpha-factor (described in part II). Part III describes the first report of an unnatural amino acid, *p*-benzoyl-*L*-phenylalanine (Bpa), replacement in a GPCR expressed in its native environment, and the use these receptors to photocapture a peptide ligand. Many of the Bpa-substituted Ste2p receptors exhibited biological activity and two of them, Phe55-Bpa and Tyr193-Bpa, were able to selectively capture alpha-factor in the ligand binding site after photoactivation; indicating that these residues may be in direct contact or in close proximity to alpha-factor when bound to Ste2p. Part IV reports for the

first time the involvement of the third intracellular loop (IL3) in Ste2p homo-dimer formation, and also conformational changes at the cytoplasmic ends of TM5-TM6 of Ste2p induced by alpha-factor binding. Conformational changes in the C-terminus of Gpa1p occurring during Ste2p and Gpa1p activation are also discussed for the first time in part V. Variants of Ste2p-Gpa1p fusion proteins that displayed activities similar to Ste2p and Gpa1p are described in part VI. The final part of this dissertation discusses the overall conclusions and contains suggestions for future studies. The results obtained during this study should provide very important information about the mechanisms underlying the activation of GPCRs and G proteins.

TABLE OF CONTENTS

CHAPTER **PAGE**

LIST OF TABLES

TABLE **PAGE**

LIST OF FIGURES

FIGURE **PAGE**

PART I: General Introduction

PART II: Cross-linking of DOPA-containing α-factor Pheromone analogs of *Saccharomyces cerevisiae* into its G Protein-Coupled Receptor, Ste2p

PART III: Unnatural Amino Acid Replacement in a Yeast G Protein-Coupled Receptor in its Native Environment

PART VI: Activities of *Saccharomyces cerevisiae* α-factor Pheromone Receptor (Ste2p) and its G alpha protein (Gpa1p) fusion protein

PART VII: General Conclusions and Future Studies

PART I

General Introduction

CHAPTER 1

G Protein-coupled Receptors: An overview

G-protein-coupled receptors (GPCRs) are the largest but the most diverse group of cell surface proteins present in fungi, plants, and the animal kingdom. They are characterized by the presence of seven membrane spanning α-helical segments separated by alternating intracellular and extracellular loop regions (*1*). They are essential for communication between the internal and external environments of cells. Although they share a common structure they can be activated by very diverse extracellular signals such as light, peptides, proteins, lipids, organic odorants, taste molecules, nucleotides or nucleosides (*1-7*). Despite the diverse ligands for GPCRs they all perform a similar function: coupling the binding of ligands to the activation of specific heterotrimeric guanine nucleotide-binding proteins (G proteins) leading to the modulation of downstream effector proteins. Thus, they are called G protein-coupled receptors (GPCRs). However, individual group of GPCRs have unique combinations of signal-transduction activities involving multiple G-protein subtypes, as well as G-protein-independent signaling pathways and regulatory processes (*8-10*). These signal-transductions are involved in a large number of physiological functions (see Figure 1).

Ligand binding to a GPCR initiates a cascade of intracellular events, including changes in levels of second messengers, ionic conductance, and other signaling activity. The activated GPCR induces a conformational change in the associated heteromeric G proteins. This change initiates activation of the alpha (α) subunit of G protein leading to release of GDP followed by binding of GTP and the dissociation of the beta(β) and gamma (γ) dimer subunits.

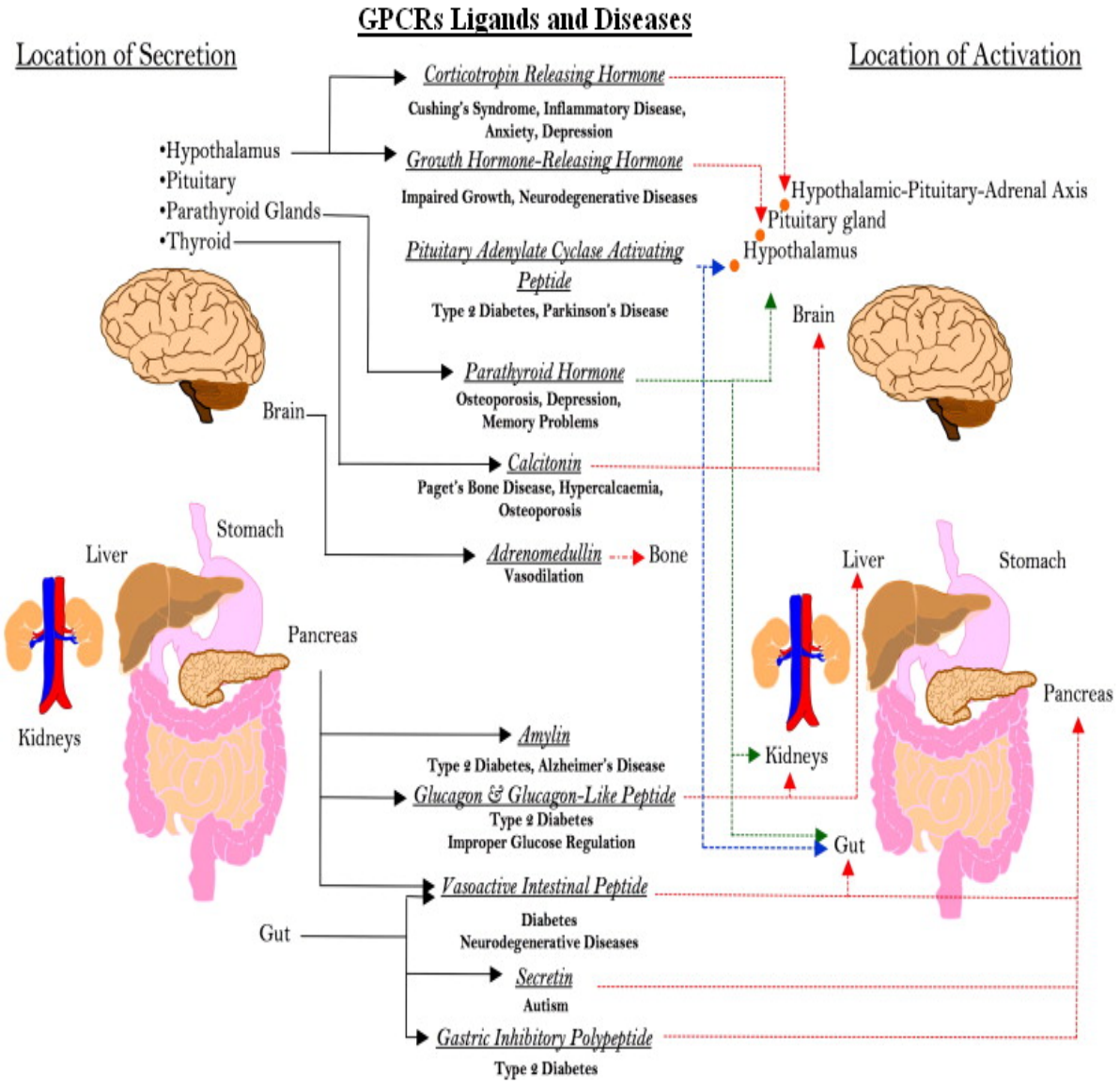

Figure 1: The role of GPCRs in pathophysiology. A large variety of large peptide hormones are secreted that mediate multiple physiological functions at various target sites via the activations of their GPCRs. Mutations and/or defects in expression of both ligands and GPCRs can result in multiple acute and chronic diseases. Figure taken from Chapter et al., (*7*).

Both the GTP bound Gα-subunit and the released Gβγ-dimer can mediate the stimulation or inhibition of a diverse collection of effectors (*6, 11, 12*). For example, the binding of adrenaline or noradrenaline to β_2AR, the human GPCR for adrenergic agents, during sympathetic neurotransmission leads to the activation of Gα proteins, the stimulation of adenylyl cyclase, the accumulation of cyclic AMP (cAMP), and the phosphorylation of proteins involved in muscle-cell contraction (*11, 12*). Due to their involvement in physiological functions GPCRs are potential drug targets for many human diseases and are targets for approximately 50-60% of the human drugs currently marketed with annual sales revenue of about 44 billion US dollars(*4, 5, 7*). The human genome encodes about 1000 different GPCRs, however the marketed drugs currently target only about 50 GPCRs (*4*). There is no doubt that the field of GPCR research, drug discovery and development will continue to be very critical in the years ahead.

GPCRs Classification:

GPCRs are classified by several systems based on characteristics, such as how their ligand binds, and other criteria like physiological and structural features. The most commonly used classification systems divide GPCRs into clans A, B, C, D, E, and F, and subclans (families) that cover all GPCRs in both vertebrates and invertebrates (*13, 14*). A GPCR 'Clan' consists of receptors whose protein sequences share greater than 20% sequence identity in their transmembrane regions, and are thought to have evolved from a common ancestor, whereas families within a clan share obvious common biochemical properties (see Table 1). Examples of invertebrate GPCRs are bacterial opsin receptors in clan A, and archaebacterial opsins in clan F. Clans D and E (fungal pheromone receptors) contain the STE2 and the STE3 receptors respectively (*14-16*). These clans will be discussed in detail in the next chapter.

Table 1: Sequence-based groupings within the G protein-coupled receptors.

Clan A: Rhodopsin-like receptors	
Family I	Olfactory receptors, adenosine receptors, melanocortin receptors, and others
Family II	Biogenic amine receptors
Family III	Vertebrate opsins and neuropeptide receptors
Family IV	Invertebrate opsins
Family V	Chemokine, chemotactic, somatostatin, opioids and others
Family VI	Melatonin receptors and others
Clan B: Calcitonin and related receptors	
Family I	Calcitonin, calcitonin-like, and CRF receptors
Family II	PTH/PTHrP receptors
Family III	Glucagon, secretin receptors and others
Family IV	Latrotoxin receptors and others
Clan C: Metabotropic glutamate and related receptors	
Family I	Metabotropic glutamate receptors
Family II	Calcium receptors
Family II	GABA-B receptors
Family IV	Putative pheromone receptors
Clan D: STE2 pheromone receptors	
Clan E: STE3 pheromone receptors	
Clan F: cAMP and archaebacterial opsin receptors	

Table adapted from Flower D. R.(*14*)

GPCRs in vertebrates are classified into clans and families on the basis of their sequence and structural similarity. These are the rhodopsin (clan A), secretin (clan B), glutamate (clan C), and adhesion Frizzled/Taste2 receptor families (*16*). The most diverse is found among the rhodopsin family members that are characterized by conserved sequence motifs. Most of these members have the NSxxNPxxY motif in transmembrane (TM) 7 and the DRY motif or D(E)-R-Y(F) at the border between TM3 and intracellular loop (IL) 2 that are essential for receptor activities (*17-19*). The ligands for most of the rhodopsin receptors bind within a pocket between the TM regions (*20*). The rhodopsin family is further divided into two categories, α- and β-groups. This α-group consists of the prostaglandin, amine, opsin, and melatonin receptors. The β-group group is composed of about 36 classes of peptide binding receptors, such as the growth hormone secretagogues, chemokine, thyrotropin releasing hormone, hypocretin, neuropeptide, cholecystokinin, neurotensin, and gonadotropin-releasing hormone receptors. The rhodopsin family has been studied and characterized more than any of the other GPCRs families (*16*).

The secretin family, also termed "secretin-like receptor" has an N terminus between 60 and 80 amino acids long, and it contains conserved cyteines bridges that are important for binding of the ligand to these receptors. These receptors bind rather large peptides that share high amino acid identity compared to the rhodopsin family (*14, 16*). The family of glutamate receptors consists of the ion-sensing, and some taste receptors. Several of these receptors found in human are also ion channels. The ligand recognition region is found in the N terminus and is 280 to 580 amino acids long. Some of them are believed to have N termini that form two distinct lobes separated by a cavity in which the ligand binds (*16*). The adhesion family consists of

receptors with GPCR-like transmembrane-spanning regions fused together with domains of adhesion-like motifs in the N terminus.

The N termini are about 200 to 280 amino acids long, rich in glycosylation sites and proline residues that are important for cell adhesion (*21-24*). The Frizzled/Taste2 receptor family is divided into two groups, the frizzled and TAS2 (taste2) receptors. They have consensus sequence of IFL SFLL in in TM2, TM5, and SxKTL in TM7. The TAS2 receptors have short N termini and are expressed in the tongue and palate epithelium (*16*). The frizzled receptors have about 200-amino acid in the N terminus with conserved cysteines that are required for ligand binding. This family regulates cell fate, proliferation, and polarity during metazoan development by mediating signals from secreted molecules (*16, 25, 26*). Though GPCRs may have different amino acids sequences they all have overall similar structure-function relationships.

The structure and organization of GPCRs:

A recent focus in structural biology has been the determination of the structure of GPCRs. Information about their structures is crucial for the understanding of their functions and importance for diseases and drug development. Though intensive academic and industrial studies have been carried out on GPCRs, little is known about the structural basis of GPCR function (*1, 5, 12*). Some of the methods used to gather information about protein structure include X-ray crystallography, electron microscopy or diffraction, NMR spectroscopy and molecular modeling. However, these methods require high concentrations of dissolved purified protein and they are mostly insoluble in media that provide a good environment for crystallization or NMR study. The fact that need to be in a lipid-like environment to maintain their native structure makes their crystallization and NMR study much more difficult to achieve.

These characteristics of GPCRs make it difficult to determine the crystal structure. Recently, different tricks have been used to achieve the stability and conformational homogeneity required for GPCR crystallization including the use of antibody complexes, fusion proteins, binding ligands, stabilizing mutants, and special crystallization environments (*27-35*). The crystal structures of four (bovine rhodopsin, human β_2 adrenergic receptor (β_2AR), the avian β_1AR and the human A_{2A} adenosine receptor) GPCRs obtained recently have been very crucial for the understanding of how GPCR structure dictates the unique functional properties of the complex signal transductions (*1*).

The first crystal structure of GPCRs came from the protein bovine rhodopsin. The structure revealed a highly organized seven helical transmembrane (TM) bundle connected by alternating intracellular (IL) and extracellular loop (EL) regions (*17, 36, 37*). The comparison of the 3D structures of rhodopsin and recently solved GPCR structures showed differences in the length of the loop and helix segments and of the arrangement, tilts, and kinks of the individual helices among the GPCRs. Though rhodopsin is unique in that it has no soluble ligand, superimposing of all four known crystal structures on to each other indicated that they have a similar overall architecture (*1*). The structure of rhodopsin has EL2 connected to TM3 via a disulfide bridge and fits tightly into the helix bundle of seven TMs. On the extracellular surface, the EL2 forms a short β-sheet that creates a pocket for ligand binding. The glycosylated amino terminus is important for ligand interactions (*28-30, 38-40*). On the other hand, the EL2 regions of β_1AR and β_2AR receptors consist of a short α-helix that is stabilized by intra- and inter-loop disulfide bonds, and the cytoplasmic N-terminal regions are disordered, that is, they are not part of the solved crystal structure, possibly due to their flexible nature (*32, 35, 41*).

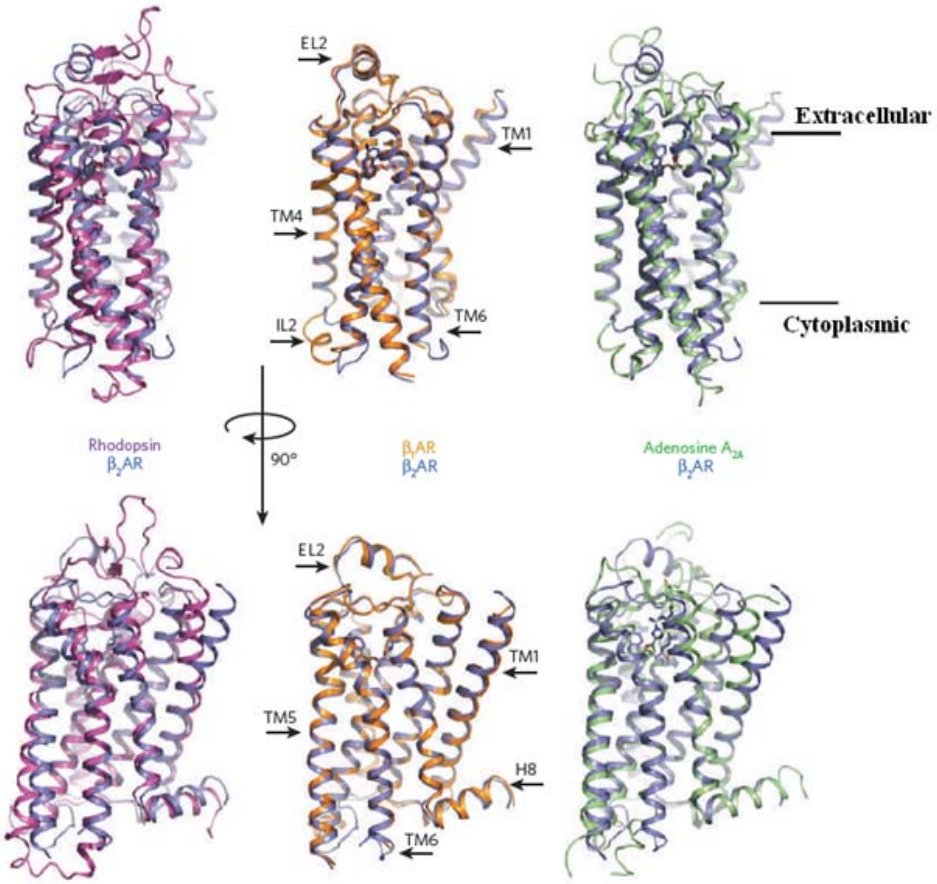

Figure 2 : Comparison of GPCR structures. Bovine rhodopsin (purple), avian β_1AR (orange) and human A_{2A} adenosine receptor (green) are each superimposed on the human β_2AR structure (blue). The extracellular loop 2 (EL2), intracellular loop 2 (IL2), cytoplasmic helix 8 (H8) and transmembrane (TM) segments are labeled on one of the structures. Figure adapted from Rosenbaum et al.(*1*).

However, unlike rhodopsin the EL2 regions of β_1AR and β_2AR receptors have multiple disulfide bonds that form a cavity essential for ligand binding. The ligand-binding pockets observed in all four structures have also been observed in other GPCRs such as dopamine, serotonin (*32, 35, 41*).

Rhodopsin has in the cytoplasmic surface an 'ionic lock' that is formed between the highly conserved E/DRY motif on TM3 and a glutamate residue on TM6. In rhodopsin the ionic lock stabilize the receptor in its inactive state. Mutations of the ionic lock in the β_1AR and β_2AR receptors increase constitutive activity (*42-46*). Network interactions between adjacent acidic and basic residues on TM3 of the E/DRY motif are present in all four GPCR structures. These interactions are important for conformational changes leading to the active state of the receptors. The IL2 of β_1AR and A_{2A} structures have a short α-helix that forms a hydrogen-bonding interaction with the E/DRY motif. This interaction is not observed in β_2AR and rhodopsin structures (*35, 37*). All four structures have the highly conserved NPXXY motif at the cytoplasmic end of TM7 that plays an essential role in conformational changes during the activation of the receptors. The proline in this motif is responsible for the distortion in TM7 observed in all structures. Interestingly, all crystal structures also revealed a short 8th cytoplasmic helix (H8), which runs parallel to the cytoplasmic membrane and a fourth intracellular loop (IL4). The H8 and IL4 are thought to play a role in the coupling of the receptor with G proteins (*1, 19, 37*). Thus, although GPCRs solved to date may have differences in helical packing interactions they all have a similar overall structure.

The crystal structures of these GPCRs have been used as a template to model other GPCRs. The low sequence similarity among GPCRs makes the homology modeling difficult for GPCRs in non-rhodopsin families. However, this problem has been overcome in some cases by the development of secondary structure predictions and *ab initio* 3D modeling techniques with experimental constraints. The modeling of GPCRs based on biophysical studies has also been very crucial for determining the structure and helical arrangements in GPCRs (*14, 47-51*). This dissertation uses modeling programs to build models based on data collected.

GPCRs in the membrane exist as monomers, dimers, or oligomers, with the dimer often regarded as the minimal oligomeric arrangement required for functional coupling to the G-protein. Experimental studies using animal models support a specific role for GPCR oligomerization in vivo and in human pathologies (*52-54*). Detail analyses of oligomerization in rhodopsin have suggested that the dimer, or even a larger oligomer form of the receptor, is involved in the functional coupling of rhodopsin to the G protein transducin. The monomer of rhodopsin is capable of activating transducin however, the dimeric form couples the G protein more efficiently (*55-57*). It is not clear whether GPCR oligomerization plays a role in the chaperoning and cell transport of receptors, or in the control of signaling specificity and efficacy. Nevertheless, evidence of essential roles for dimerization in all GPCR families makes it an important phenomenon that needs investigation (*52-54*).

Biophysical studies and computational analyses have been used to identify and predict the interface of GPCR oligomers. One of the earliest studies to show evidence of GPCR dimerization demonstrated that overexpressed differentially tagged β_2-adrenergic receptors (β_2AR) form dimers and also showed that a peptide corresponding to the TM6 region of the β_2AR could be used to disrupt the dimer and decrease receptor function implying that TM6 is important for dimer formation in β_2AR (*58*). Another study also showed that a dimer between the two different GABA receptors, $GABA_BR1$ and $GABA_BR2$, was required to form fully functional GABA receptors. This study also suggested both GPCR subunits in a dimer seem to have distinct roles in the complex and that the $GABA_BR1$ seems to be responsible for ligand binding while the $GABA_BR2$ is required for G-protein coupling. Thus, whereas some GPCRs such as the metabotropic glutamate (mGlu) receptors are strict dimers other GPCRs like the GABA receptors form oligomers (Figure 2A) that may couple with only one G protein (*53*).

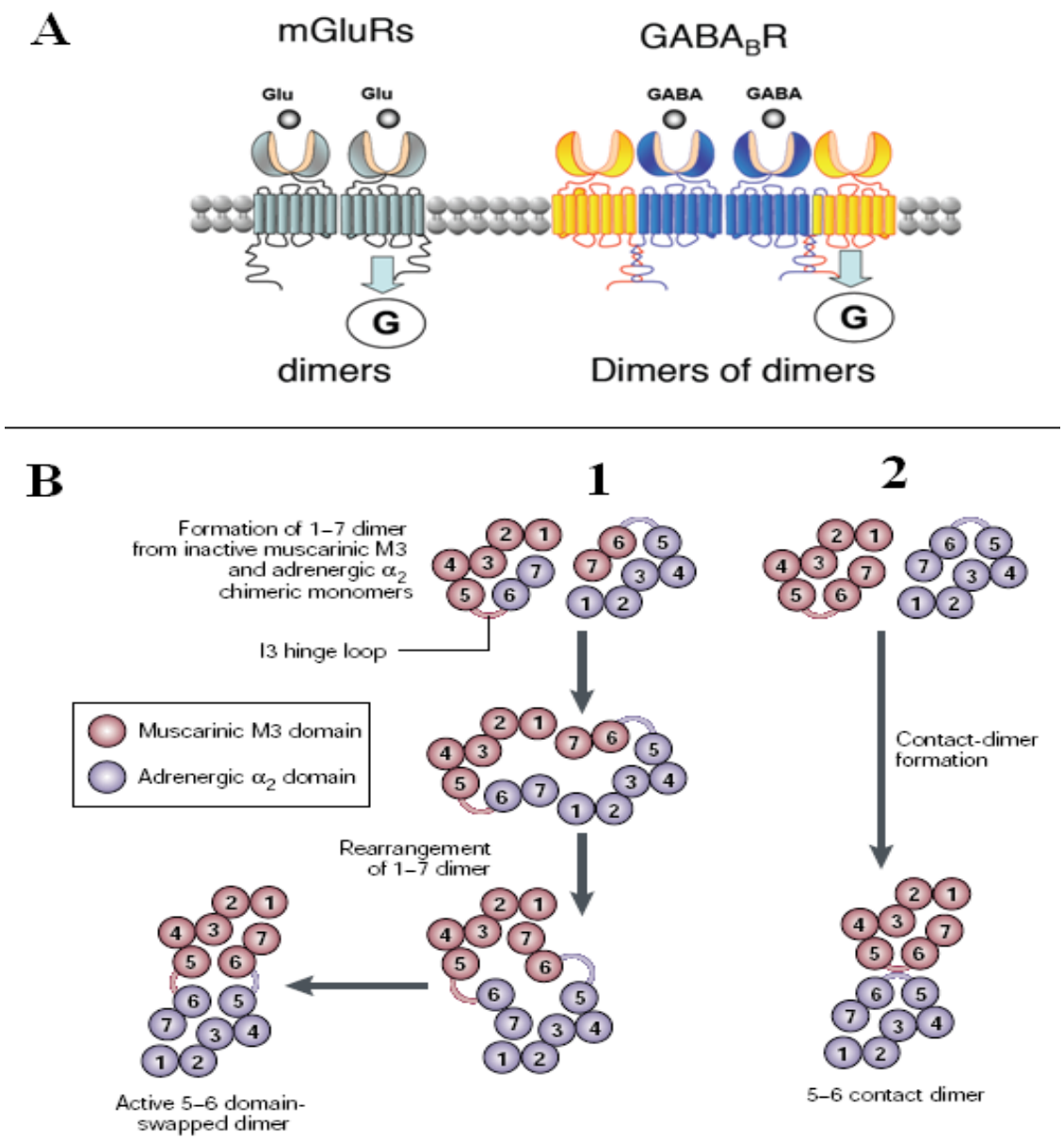

Figure 2: Oligomerization in GPCRs. **A**; schematic oligomeric assembly of mGlu and GABAB receptors. Whereas the mGlu receptors are strict dimers, the GABA receptor assemble into dimers of dimers with possibly a single receptor entity activating G protein at a time. The figure was taken from Pin et al (*53*). **B**; proposed models for GPCRs organization. **1**; the domain-swapping model. **2**; the contact model in which each receptor unit touches the other through interactions involving TM5 and TM6. Figure taken from Bouvier (*59*).

Data from atomic force microscopy and the crystallographic structure of rhodopsin suggested that TM1, TM2, TM4, TM5, second intracellular loop (IL2), and the third intracellular loop (IL3) are involved in the formation of rhodopsin oligomers (*55-57*). Some GPCRs have been shown to use different oligomerization interfaces to achieve functional activities (*53*). The use of truncated receptors and other studies suggest that GPCR dimer formation may involve domain swapping or direct contacts of the receptor subunits (see Figure 2B). Mutation and computational analyses all provide evidence of the involvement of TM5 and TM6 in the dimerization interface in both the swapping and direct-contact models in some GPCRs tested (*59*). Although intensive studies have been done on GPCR oligomerization, the functional bases of these interactions are not well defined. Knowledge about the interaction in GPCR oligomerization will enhance understanding of the molecular mechanisms underlying GPCR cellular function, with the promise of new and improved therapeutics targeting the complex structures and their mechanisms. Part IV of this dissertation will discuss a dimer interface contact observed in vivo in a yeast GPCR.

Ligand Binding in GPCRs:

Despite variations in ligand specificity of the GPCRs, there are some similarities in the ligand interactions among the GPCR families. GPCRs ligands are classified as full agonist, partial agonists, inverse agonists, antagonist, and allosteric regulators. These ligands induce different conformational changes in GPCRs and as well as produce different intracellular signals (*4, 6, 11, 60, 61*). A full agonist produces a wild-type effect. The partial agonists bind to GPCRs resulting in a lesser effect than full agonists. Inverse agonists induce opposite effects on

the same GPCR as full agonists. For example, whereas norepinephrine stimulates the β-adrenergic receptor to increase adenylyl cyclase activity, inverse agonists would bind to constitutively active receptor to decrease adenylyl cyclase activity. The antagonists on the other hand bind to GPCRs but have no intrinsic activity or effect other than blocking the binding of agonists. Inverse and partial agonists are able to block the binding of full agonists to GPCRs by binding at similar binding pockets, which affect the activation of the GPCRs (*11, 62*). Allosteric regulators interact with GPCRs at sites different from the ligand binding domains. Most allosteric regulators such as G proteins interact with the cytoplasmic domains of GPCRs (*4, 63-65*).

Another group of ligands known as synergists have also been identified. Unlike the antagonist, inverse or partial agonists, the synergist does not show significant binding to the receptor but serves to increase the activities of the receptor in the presence of full agonist. Thus, synergists do not block the binding of the full agonist but rather enhances its activities. Synergists have been found in the yeast α-factor pheromone receptor, Ste2p, but not much is known in other GPCR families (*66, 67*). The developments of drugs targeting GPCRs are mostly based on the mechanisms of full, partial, and inverse agonists, as well as antagonist, synergists and allosteric modulators. Thus, understanding the activities of these ligands will facilitate the design of drugs that target GPCRs (*5, 11, 12*).

The binding mechanisms of ligands in GPCRs vary within different ligand groups. Large ligands, such as proteins, bind to the extracellular loops of GPCRs, whereas the small molecules like ions bind within the transmembrane region of receptor. Within the peptide-binding GPCRs a combination of ligand binding to the extracellular loops followed by ligand penetrating the transmembrane region and interacting with receptor residues buried in the membrane has been

observed (*11, 68-70*). Ligand binding to GPCRs is predicted to trigger conformational changes within the receptor core (TM bundle), which are then propagated to the cytoplasmic surface of the receptor, which is involved in G protein recognition and activation. Thus, ligand binding leads to the disruption of existing interhelical interactions, thereby promoting a set of interactions that leads to a new, energetically favorable conformational state of the receptor. Ligands which bind to extracellular loops induce different conformational changes compared to small molecules that interact only with residues deep within the receptor core (*69, 71-73*). The multiplicity of recognition sites in peptide receptors are thought to provide the basis for understanding ligand interactions with GPCRs. Understanding the peptide ligand interactions with its cognate GPCR is critical for elucidating other GPCRs-ligand interactions (*7, 11*). However, less information exists concerning the binding sites of peptide-responsive GPCRs in comparision with the knowledge of binding of GPCRs activated by small ligands.

Structure-activity relationships involving ligand analogues and mutagenesis of receptors have been employed to discern receptor-peptide ligands interactions and how binding is transduced to activate intracellular signaling. One of the most commonly used strategies is to label the peptide with a cross-linker that will attach to the receptor upon activation of the cross-linker. In most cases the cross-linking studies are followed by enzymatic and/or chemical cleavage and mass spectrometry analysis of the fragmented product to identify the receptor region that cross-linked to the ligand (*74-81*). For example, photocross-linking using photoactivatable peptide analogs carrying 4-benzoyl-*L*-phenylalanine (Bpa) have been used to provide biochemical evidence for contacts between the ligand and its receptor (*82-85*). Other techniques and methods such as double-mutant cycle analyses have also been used to provide thermodynamic evidence for the interaction between groups within one protein or in ligand-

protein complexes (*86, 87*). Nevertheless, there are limitations to using these approaches including low yield of product and multiple cross-linked products making it difficult to define the exact residue-residue interactions involved in GPCR binding.

The recent advent of the use of 3,4-dihydroxyphenyl-alanine (DOPA) to label protein or peptide ligand for cross-liking has been very effective. DOPA-containing compounds were oxidized to form an *o*-quinone intermediate that could be attacked by a nearby nucleophile resulting in a stable, covalent cross-link (*88-90*). The cross-linked product is resistant to chemical and enzymatic peptide cleavage. Unlike most cross-linking methods, DOPA crosslinking produces a high yield with little or no nonspecific products observed, even in complex protein mixtures (*89, 90*). The second part of this dissertation will focus on the use of peptide analogs carrying DOPA for cross-linking the peptide to its GPCR, and analysis of the results by mass spectrometry and site-directed mutagenesis. The discussions of these methodologies are expanded in part II of this dissertation.

Agonist-induced conformational changes in GPCRs:

How agonist binding and the resulting changes upon interactions at the ligand-binding pocket lead to conformational changes that are transferred from the extracellular region to the cytoplasmic surface to activate G proteins for signaling still remains a fundamental puzzle in GPCR biology. There are two models for GPCR activation. The first model also known as the "two-state model" is an extended ternary complex model which predicts that the receptor exists in an equilibrium between an inactive conformation (R) and an active conformation (R*). In the absence of agonist, the inactive R state is predominant; however, the energy required to convert R to R* is low enough to allow a certain fraction of the receptors spontaneously to assume the

R* state. Thus, the receptors isomerize between inactive (R) and active (R*) conformations; inverse agonists and agonists function by stabilizing R and R*, respectively (*91-94*).

The second model is known as the "multi-state model" and suggests that the receptor alternates spontaneously between multiple active and inactive conformations. Most experiments have provided strong support that GPCRs may exist in multiple conformational states making the second model more likely than the first (*95*). This model also suggests that the ligand might play an active role to induce conformational changes in the receptor during activation that give rise to multiple states of the receptor. Recently, the crystal structures and biophysical studies of rhodopsin, opsin and β_1AR and β_2AR receptors have shown that the activation of these GPCRs by their ligands is accompanied by similar changes in transmembrane helix packing and G protein signaling mechanism. Thus, helical rearrangements of GPCRs induced by agonist are critical for activation and coupling with G proteins (*1, 3, 96-100*).

Initial conformational changes in GPCRs during activation occur at the extracellular surface. For example, in β_2AR and β_1AR agonists binding induce conformational changes at the ligand binding site accompanied by the movement of the upper region of TM5 to TM3. The interaction of the ligand with TM5 via hydrogen-bonding and TM3/TM7–amine polar contacts initiate changes in the packing of nearby aromatic amino acids. These movements at the extracellular surface results in a conformational change involving tightly packed rearrangements that shifts the helical bundles of the receptor towards the cytoplasmic surface. It has been observed that adrenergic receptors have a disruption of the packing interactions allowing free transmembrane helix motions in the absence of an agonist (*42, 44-46, 101*). Cysteine disulfide cross-linking studies of M3 muscarinic acetylcholine and metal-ion-mediated showed that receptor activation involves movements of the extracellular segments of TM7 and TM6 inward

towards TM3 (*1*). It was proposed that the inward movement of the extracellular ends of TM6 and TM7 may be a common structural feature of GPCRs (*3*). These studies also suggested that a rotation and straightening of conserved proline bends found in TM5–TM7 may mediate these conformational changes. It is not clear how these series of events, which occur at the extracellular region and within the receptor core, propagate changes at the intracellular receptor surface where G protein coupling occurs. Overall structural changes observed at the extracellular surface of these receptors may be common in all GPCRs during activation (*1, 3*).

GPCRs undergo more structural changes at the cytoplasmic surface than the extracellular surface. Comparing the crystal structure of opsin and rhodopsin shows that the cytoplasmic end of TM6 is shifted more than 6 Å outwards from the centre of the bundle relative to its position in the inactive state closer to TM5 in the active state. It was observed that the cytoplasmic end of TM6 is stabilized by changes in interactions with TM5 (*19, 102-105*). The ionic lock observed in the inactive state is broken and new interactions are formed between TM3 and TM5 as well as between TM6 and TM5. TM7 undergoes conformational changes and occupies the original position of TM6 (*46*). Other studies have also shown that light-induced rhodopsin activation triggers an outward movement of the cytoplasmic ends of TM6 accompanied by a clockwise rotation of ~30^{o} (*103*). These movements have also been observed in other receptor such as M3 and adrenergic receptors (Figure 3). In M3 agonist binding increased the proximity between the cytoplasmic ends of TM5 and TM6. Possible TM6 rotational movements were also observed in M3 receptor (*3*). It remains unclear whether these conformational changes occur in a concerted manner or whether a primary structural change triggers secondary changes in the structure and orientation of other TM helices.

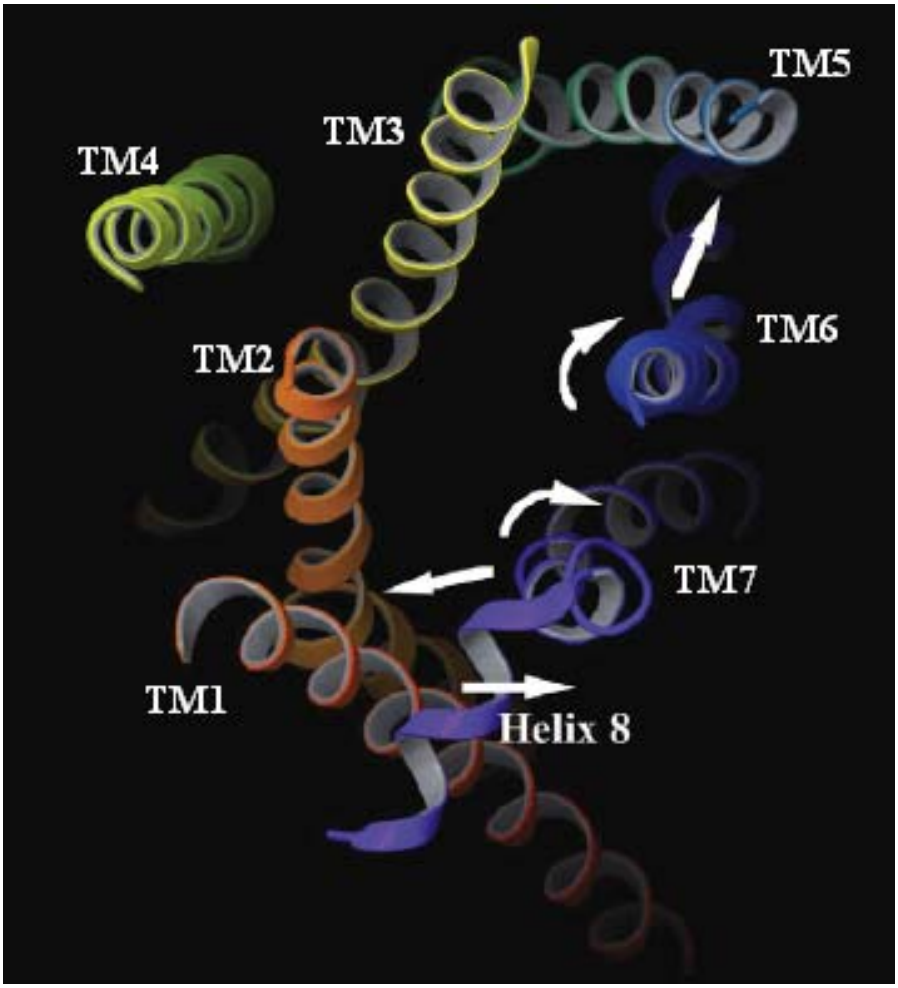

Figure 3: Conformational changes at the cytoplasmic surface GPCRs. Conformational changes at the cytoplasmic surface GPCRs. This model of the M3 receptor was built based on disulfide cross-linking and other studies. Agonist binding to the M3 receptor causes TM6 to undergo a rotational movement and to move closer to the TM5. Whereas the C-terminal portion of TM7 move closer to TM1, accompanied by a rotational movement and the N-terminal portion of helix 8 is move away from the cytoplasmic end of TM1. The agonist-induced structural changes are thought to expose previously inaccessible receptor residues or surfaces such as the cytoplasmic ends of TM3, TM6 and TM7. Figure taken from Wess *et al*.(*3*)

The result of these changes is the creation of a hydrophobic environment between TM3, TM5 and TM6 in which the Gα protein interacts with the receptor as observed in opsin. These phenomena are believed to be common features of all GPCRs (*34*). Agonist induced conformational changes at cytoplasmic ends of TM5 and TM6 in a yeast GPCR is discussed in part IV of this dissertation.

GPCRs interactions with G proteins:

The cytoplasmic surfaces of GPCRs contain multiple contact regions responsible for receptor coupling to signal transduction complexes. The most prominent domains in GPCRs for coupling are the second and third intracellular loops as well as the C-terminal tail and TM boundaries (*10, 11, 106-108*). G proteins, which link GPCRs to second messenger systems, are among the intracellular modulators contacted by GPCRs. The G protein consists of heterotrimeric complexes of α, β and γ subunits. There are 18 Gα, 5 Gβ, and 11 Gγ subunits, involved in distinct heterotrimeric complexes in humans that are critical for signal transductions through the activation of different GPCRs (*6, 11*). Following agonist induced conformational changes in GPCRs, a cascade of events known as the G protein cycle is initiated. The G protein cycle (Figure 4) involves receptor interaction with the Gα subunit in an inactive state with GDP bound, which then switches to a state where the guanine nucleotide binding site is empty, and finally an active state where GTP is bound to the empty guanine nucleotide binding site, causing dissociation of the α subunit from the agonist-occupied receptor and the βγ subunits. The α subunit in the active state now interacts with specific effector proteins which results in changes in intracellular signaling.

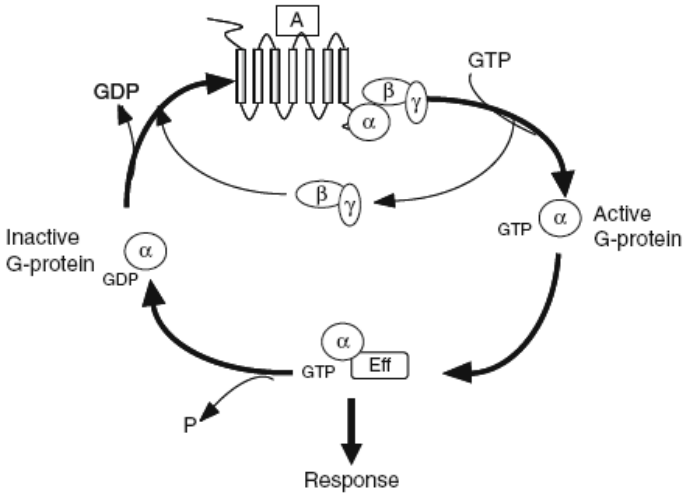

Figure 4: The GPCR-G protein cycle. Following agonist [A] binding to a GPCR, changes in the conformation of the receptor leads to the activation of heterotrimeric G protein (α, β, γ). The α subunit, in the active state, interacts with specific effector [Eff] proteins which results in changes in the concentration of intracellular signaling molecules. Figure taken from Williams and Hill (*6*).

The GTPase activity of the α subunit hydrolyzes GTP to GDP, resulting in conformational changes such that it dissociates from the effector(s). The inactive α subunit now reassociates with the βγ subunits and the cycle is repeated if an appropriate agonist-occupied receptor is available (*9, 61, 63, 64, 109, 110*). The GPCR–G protein association has recently found to have interesting implications with regards to drug discovery. If drugs can be identified to change the pattern of GPCR–G protein associations or cause a GPCR to preferentially associate with one G protein and not others, then it would be possible to regulate the activities and functions of a specific receptor (*4, 5, 11, 12*).

The Gα subunit of the heterotrimeric G protein is made up of GTPase domain (binding and hydrolysis of GTP) and a helical domain that buries the GTP within the core of the protein. The helical domain is also known to play a role in directing specificity of receptor- and effector-G protein coupling. The structure-function relationship of the helical domain is well documented, however, little is known about the structure of the extreme N- and C- terminal domains (*9*). Comparison of inactive and active state crystal structures revealed that Gα has three flexible regions, known as switches I, II, and III, which become more rigid and well ordered in the GTP-bound active conformation. The N-terminal region of Gα has been found to interact with the Gβ as well as receptor through an N-terminal coiled coil. Some studies on the C-terminus showed that C-terminal synthetic peptide and/or antibodies against the C-terminal domain inhibited receptor-G protein signaling (*111, 112*). The α4-helix, α2-helix, α2-β4 loop regions, and α4-β6 loop domain are all shown to be critical mediators of receptor-G protein coupling (*113, 114*).

The recent crystal structure of opsin bound to a carboxy-terminal peptide of transducin (Gα of rhodopsin) reveals a cleft on the receptor that provides the interaction surface for the Gα protein. The hydrophobic residues on one face of the transducin-derived peptide helix bind to a hydrophobic surface at the cytoplasmic ends of TM5 and TM6. Here the rearranged ionic-lock residues are thought to be critical for the formation of the receptor–transducin peptide complex. The orientation of the peptide binding is stabilized by a hydrogen-bonding network between the transducin residues and TM3, TM5, TM6 and helix 8 of opsin. The peptide was also found to induce long-range stabilization effects into the ligand binding pocket (*34*). Though the crystal structure of opsin bound to transducin peptide has provided information about the crucial binding epitope of the G protein on GPCRs cytoplasmic surfaces, the question of how the conformational

changes in GPCRs activate G protein and whether G proteins undergo any specific changes during this activation remains unsolved. The fifth part of this dissertation will focus on the interactions of residues in the cytoplasmic ends of TM5-TM6 and intracellular loop 3 (IL3) of a GPCR with the C-terminus of a Gα.

CHAPTER 2

α-factor Pheromone and its G Protein-coupled Receptor (Ste2p) of *Saccharomyces cerevisiae*

The complexity of eukaryotic systems is one of the major roadblocks in GPCR research. The cross-talk between different types of receptors and a variety of G proteins regulating many different pathways that involve different modulators but similar signaling complicates biochemical and physiological studies in this complex biological system. It is therefore convenient to use a simple biological system that will provide information on a given GPCR interacting with a specific modulator (G protein) that will reflect the specific activities of the given GPCR. *Saccharomyces cerevisiae* is an attractive system because it has the genetics of a typical eucaryote while possessing only a few GPCRs and G proteins (*2, 115*). There is a high homology between the yeast pheromone signaling pathway that involves a mitogen-activated protein kinase (MAPK) system and that of mammalian GPCRs (figure 4). Different GPCRs from mammalian and other systems have been successfully expressed in *S. cerevisiae* and have been shown to couple functionally to either the endogenous yeast Gα (Gpa1p), or co-expressed mammalian Gα subunits and respond to their native agonists or antagonists (*115*). *S. cerevisiae* has only three GPCRs, two pheromone receptors (either Ste2p or Ste3p) and Gpr1p, which is a carbohydrate sensor. While the pheromone and carbohydrate-sensing pathways share some down-stream components, there is no crosstalk between the two systems as the pheromone receptors and the Gpr1p couple to two different G proteins. The binding of the pheromones, α- and a-factor to their GPCRs, Ste2p and Ste3p respectively, in *S. cerevisiae* and activation of

these GPCRs have been observed to be similar to other peptide-responsive GPCRs. These characteristics make *S. cerevisiae* an attractive biological system for studying GPCRs (*2, 115, 116*).

GPCRs signal transductions in *S. cerevisiae*:

S. cerevisiae exist as haploid or diploid cell. The haploid cells exist as one of two mating types, *MAT**a*** and *MAT*α. The *MAT**a*** cells express the GPCR Ste2p and secrete the pheromone, **a**-factor, a hydrophobic farnesylated, carboxymethylated, dodecapeptide with the sequence YIIKGVFWDPAC(Farnesyl)-OCH3. The *MAT*α cells express the GPCR Ste3p and secrete the pheromone, α-factor, a tridecapeptide with the sequence WHWLQLKPGQPMY. The binding of the pheromones, α-factor and **a-**factor, to Ste2p and Ste3p respectively, initiate mating and eventual fusion of two haploid cells resulting in a diploid cell. The mating pathway in each haploid cell is mediated by the intracellular heterotrimeric G protein interactions. The yeast G proteins, which consist of Gpa1p, Ste4p and Ste18p subunits, are structurally and functionally similar to the mammalian Gα-, β- and γ-subunits, respectively. Activation of Ste2p and Ste3p by the pheromones leads to G1 cell cycle arrest, and polarized cell growth before cellular fusion (*2, 115, 116*).

Like all GPCRs, Ste2p and Ste3p activation is followed by GDP exchanged for GTP in Gpa1p and dissociates from the Ste4/Ste18 complex which in turn signals to Ste20p, a p21-activated protein kinase-like kinase. Ste20 activates the Ste5p-scaffolded MAP kinase modules composed of Ste11p, Ste7p and Fus3p. Activation of MAP kinase cascade by phosphorylation of the transcription factor Ste12p results in the expression of mating genes (Figure 5).

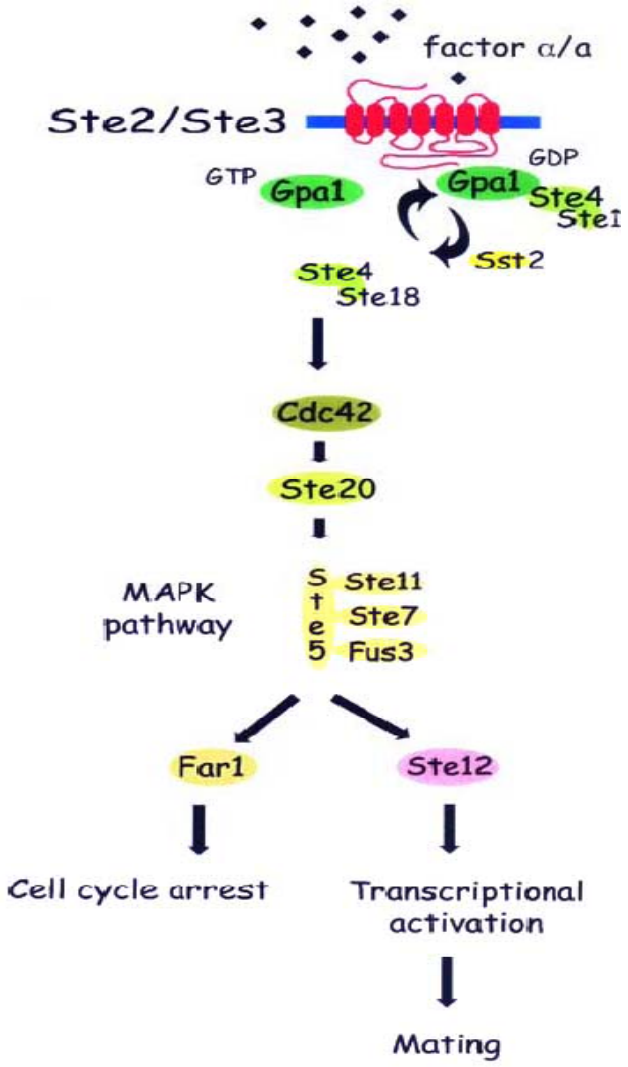

Figure 5: S. cerevisiae GPCRs and pheromone signaling pathway. Pheromone (α/a factor) binding and activation of receptors (Ste2p/Ste3p) activates the MAP kinase cascade via Gpa1p activation and results in activation of nuclear proteins that control transcription, cell polarity and progression through the cell cycle. The figure was taken from Minic et al., (*115*).

Some of the effects of downstream MAPK cascades involve stabilization of the cyclin-dependent kinase inhibitor Far1p by Fus3p and Cdc28 protein kinase resulting in arrest of cell division in the G1 phase of the cell cycle. Other downstream effects include inducing cell and nuclear fusion and also regulating genes that are involve in the mating process (*117, 118*). The tips of the projections fuse to form a conjugation bridge followed by the nuclear migration across the bridge, and subsequent fusion to produce a diploid nucleus in the zygote. The negative regulator of the pathway is the Gpa1-specific GTPase-activating protein, Sst2, a member of the RGS (regulator of G protein signaling). Thus, pheromone stimulation of yeast results in phosphorylation of proteins in the MAP kinase cascade and activation of nuclear proteins that control transcription, which is similar to mammalian MAP kinase cascade. *S. cerevisiae,* with its GPCR signaling pathway, is indeed a powerful tool for GPCR-ligand screening studies, and it has been successful used in pharmacological screenings (*115*).

Structural analysis of Ste2p:

The *S. cerevisiae* GPCR for α-factor pheromone, Ste2p, is a member of clan D GPCRs and shares common structure-function relationships with other GPCRs. Though the underlying mechanisms of GPCR function may be well conserved, Ste2p shares only a few recognizable sequence similarities to mammalian GPCRs or the cognate yeast pheromone **a**-factor receptor,Ste3p. Ste2p lacks the highly conserved E/DRY motif in the intracellular end of TM3 present in most mammalian GPCRs. However, comparison of Ste2p with some mammalian GPCRs (clan A) shows that they share an overall common structure (*116*). Like most mammalian GPCRs, the core region of the seven TMs of Ste2p functions in ligand binding and the third intracellular loop plays a key role in G-protein activation (*84-86, 116*). Ste2p has

conserved amino acids at specific positions similar to clan A receptors where mutations affect receptor activities. Strong polar amino acids that mediate helix interactions and weakly polar amino acids that facilitate tight helix packing in clan A receptors are also identified in Ste2p at similar positions (*116*). Proline residues in TM6 and TM7 that are essential for conformational changes during activation of clan A receptors as well as amino acids and sites of constitutively active mutations on TM3, TM6 and TM7 are identical in clan A and D (Ste2p) receptors (*119*). Thus, there are similarities in the mechanism of receptor structure-function relationships among clan A and D receptors.

A detailed structural analysis of Ste2p using x-ray crystallography has been difficult to obtain due to the difficulties in obtaining sufficient amounts of pure protein, as in other GPCRs. Analysis of mutant receptors for structure-function studies has been an alternative to crystallographic information on GPCRs. Scanning cysteine accessibility mutagenesis (SCAM) on each residues of the first extracellular loop (EL1) of Ste2p was used to create a structural model for the EL1. This study predicted that the EL1 is comprised of a helix corresponding to EL1 residues 106 to 114 followed by two short β-strands comprising residues 126 to 135 (*120*). Hauser, *et al*, (*121*), using SCAM, also proposed that EL1 of Ste2p is structured such that parts of the loop are buried in the membrane making it inaccessible for interaction with the extracellular part of the TM bundle. Other SCAM studies on the TMs of Ste2p showed that the TMs vary in length and that some of the TMs are buried and tilted relative to the plane of the membrane similar to the rhodopsin GPCR. Ste2p shows overall similarity to many mammalian GPCRs in that the core region containing the TMs is involved in signal transduction and the C terminal tail is a target for posttranslational modifications (*122*).

Ste2p has been identified as oligomeric in intact cells and membranes. Coexpression of Ste2p tagged with the cyan or yellow fluorescent proteins (CFP or YFP) resulted in efficient fluorescence resonance energy transfer (FRET). The study also showed that dominant-interfering receptor mutants inhibited signaling by interacting with wild-type receptors rather than by sequestering G proteins (*123, 124*). Analysis of Ste2p truncated mutants showed that the N-terminal extracellular domain, TM1, and TM2, are involved in stabilizing receptor oligomers (*125*). Recently, disulfide cross-linking studies have shown TM1 and TM4 as dimer contacts in Ste2p similar to that of the rhodopsin family of GPCRs. The study suggests that similar dimer interface sites in Ste2p and rhodopsin-like receptors provide further evidence that many aspects of structure and function are highly conserved across GPCRs (*126*). Subunits of Ste2p in a dimer complex have been found to be activated independently rather than cooperatively by agonist, but function together to promote G protein activation, possibly by contacting different subunits or regions of the G protein (*127*). Despite the intensive studies on the structure-function relationship of Ste2p the mechanism underlying its activation is not well defined. The fourth part of this dissertation will examine some of the possible helical movements that occur during the activation of Ste2p and also discuss dimer contacts involving the third intracellular loop.

***Function analysis of* α*-factor pheromone*:**

The tridecapeptide α-factor pheromone (WHWLQLKPGQPMY) induces signal transduction upon binding to Ste2p. Studies of α-factor indicated that Trp1-Leu4 residues are associated with receptor activation and signal transduction; Lys^{7}-Gln^{10} residues are involved in the biologically active conformation and Gln^{10}-Tyr^{13} residues are essential for receptor binding (*66, 67, 128-131*). Alanine scanning studies showed that *D*-Ala series analogs, near the N-

terminus, specifically [*D*-Ala2]α-factor, [*D*-Ala3]α-factor and [*D*-Ala4]α-factor had no detectable activity. However, these peptides bound to Ste2p and antagonized the biological activity of the native α-factor. Other studies from our laboratory showed that most of the antagonists discovered involved changes in residues near the N-terminus. Thus, residues at the N-terminus are critical for Ste2p activation and/or in stabilizing the activated state of this receptor (*66, 67*).

Alanine scanning studies of the carboxyl terminus of α-factor revealed that this region strongly influenced binding to Ste2p. Substitution of these residues with alanine caused decreases in binding affinity of up to about 3000-fold. Deletion of the carboxyl terminal residues result in pheromones with drastically reduced receptor affinity and, in some cases, also with complete loss of affinity. Interestingly, some of these C-terminal deleted analogs have synergist activities (*67*). For example, an analog with the last two amino acids deleted (WHWLQLKPGQP) does not show any significant binding and does not block the binding of the agonist but rather enhances its activity as evidenced by the increased in signaling when the two peptides (synergist and agonist) were mixed together for Ste2p activity. Whereas deletion of the C-terminus results in synergist activity, the deletion of the N-terminus results in antagonist activities implying that α-factor contains domains that are critical for specific functions (*67, 132*).

The central residues of α-factor comprising of sequence Lys^{7} to Gln^{10} assume a β-turn structure that is essential for the proper orientation of the signaling and the binding domains. This region is critical for maintaining the biologically active conformation of α-factor during the activation of Ste2p (*128, 130, 131*). Alanine scanning studies of this portion of the peptide showed that whereas D-Ala^{9} analog had high activity and affinity, D-Ala^{7}, D-Ala^{8} and D-Ala^{10}

analogs had reduced receptor affinities and activities. Other studies with biologically-active, covalently constrained analogs formed by synthetic cross-links between residues 7 and 10 indicated that this region of the pheromone was involved in forming a conformationally active peptide (*67, 130*). These data suggest that the middle portion of α-factor serves to create the proper overall biologically active conformation (*67*). It can therefore be concluded that α-factor is comprised of three domains (Figure 6), the N-terminus (activation domain), the C-terminus (binding domain) central residues (loop domain). Other peptides with specific functional domains that bind GPCRs have been reported (*133-136*).

Ste2p interaction with α-factor:

The interaction between α-factor pheromone and its receptor Ste2p is one of the most extensively studied models for the peptide ligand-GPCR relationship. Despite many techniques used to study the structure-function relationship for this receptor and its ligand, the question of exactly how and where the ligand binds to activate the receptor still remains not fully elucidated. This dissertation will discuss some of the possible residue-to-residue contacts (interaction) between Ste2p and α-factor. Most of the information obtained from Ste2p and α-factor activities comes from the characterization of mutant receptors and α-factor analogs (*2, 116*). Another promising approach which has been adapted to the study of the dynamics of GPCR structure is the use of orthogonal pairs of tRNA/ aminoacyl-tRNA synthetases evolved and expressed in the target cell to incorporate unnatural amino acids (*137-139*). In *S. cerevisiae* this approach has been used to incorporate a variety of unnatural amino acids, including the photoactivatable amino acid analog *p*-benzoyl-*L*-phenylalanine (Bpa) into soluble protein (*140, 141*). Details and success of this system for Ste2p studies is described in part three of this dissertation.

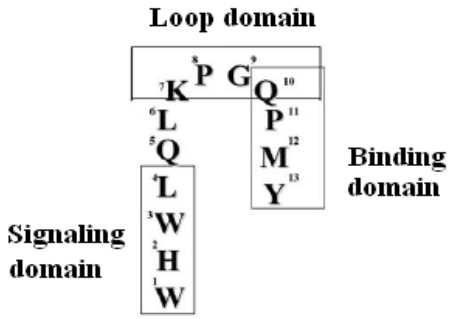

Figure 6: Functional domains of α-factor pheromone. The cartoon indicates that the pheromone may be divided into three domains based biophysical studies. The N-terminus (signaling domain) is critical for receptor activation and signaling; the central residues (loop domain) are required for conformational stability of the ligand; and the C-terminus (binding domains) is essential for receptor recognition and binding (*2*).

Ste2p crosslinking studies using biotinylated α-factor analogs containing Bpa at different positions indicated that Trp1, Trp3, Gln5 and Tyr13 residues in α-factor interacts with residues of the extracellular domains of Ste2p. The N-terminus of α-factor interacts with the receptor signaling domain, consisting of residues from extracellular ends of TMD5-TMD7 and parts of second (EL2) and third (EL3) extracellular loops, most likely Ser251-Met294 (*85*). It was also shown that Tyr13 of α-factor may interact with Phe55 – Arg58 residues in Ste2p (*84, 85, 142*). Mutagenesis studies of residues 262 – 270 in Ste2p showed that the Tyr266 residue in the TMD6 plays an essential role in ligand specificity and receptor activation (*143*). Double-mutant cysteine cycle scanning of the interaction of α- factor with Ste2p also showed that the amino terminus of α- factor interact with Asn205 and Tyr266 (*86, 87*). The interactions of synthetic α-factor (position 10) analogs with mutations in Ste2p showed that Gln^{10} in α- factor interacts with Ser47

and Thr48 residues in Ste2p (*144*). Replacing aspartic acid at position 275 in EL3 with asparagine affected both pheromone binding and signaling, suggesting that this position interacts directly with α-factor. Mutagenesis studies of Ala281 and Thr282 in TM7 suggested that these residues are involved in receptor activation. These residues are in approximately the same position as Lys296 in rhodopsin, which is covalently linked to retinal (*119*).

Studies using a fluorescent α-factor analogue in conjunction with flow cytometry and fluorescence microscopy showed that α-factor binding to Ste2p involves multiple steps. The initial interactions involve the binding of α-factor in a hydrophobic environment in Ste2p, followed by a conversion to a state in which the ligand moves to a more polar environment (*145*). Based on biophysical studies from our lab a model showing possible contacts between α-factor and Ste2p has been proposed (Figure 7). In this model α-factor is shown to bend around the Gly9-Pro11 residues with the Lys13 side chain interacting with a receptor binding pocket. The Gln10 side chain is proximal to residues 47 and 48 of Ste2p, whereas the Trp1 side chain is near a pocket formed by TM6-EL3-TM7. It is likely that Trp1 and Trp3 interact with an aromatic group near the interface of the transmembrane domains and the outside surface of the membrane (*2, 144*). Detailed analyses of Trp1 and Tyr13 interactions with Ste2p are discussed in part II of this dissertation.

Ste2p interactions with Gpa1p:

S. cerevisiae has two different Gα subunits, Gpa1p that interacts with Ste2p or Ste3p and Gpa2p that interacts with Gpr1p which is a carbohydrate sensor.

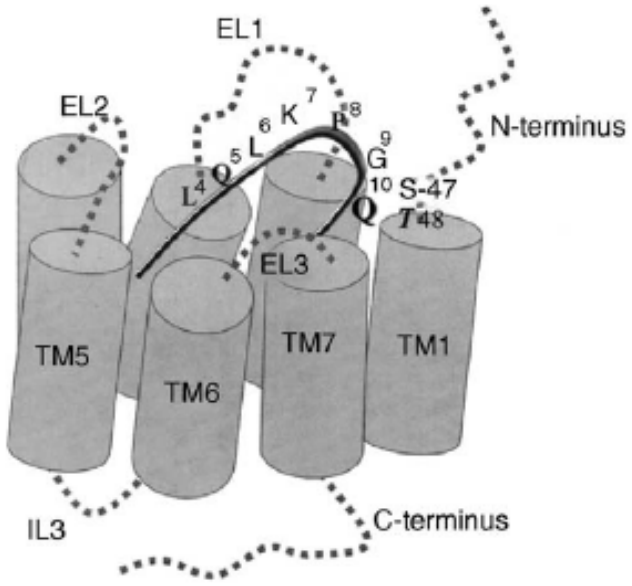

Figure 7: Model of α-factor binding to its receptor, Ste2p. Only residues 4–10 (Leu-Gln) of α-factor are labeled. The N-terminus and C-terminus are in close proximity to TM1 and TM6 respectively. Gln10 is shown to interact with Ser47 and Thr48 of the receptor (*144*).

Like all Gα subunits, Gpa1p is made up of a GTPase domain (binding and hydrolysis of GTP) and a helical domain that buries the GTP within the core of the protein. The helical domain is also known to play a role in directing specificity of receptor- and effector-G protein coupling (*9*).

Gpa1p shows about 45% identity with mammalian Gα proteins and is most closely related to the Gαi subfamily. The binding pockets of mammalian Gα subunits on their GPCRs are shown to contain a high number of hydrophobic residues that create an environment favoring Gα coupling. Similar binding pockets have been predicted for Gpa1p suggesting that the underlying mechanism for interactions between the mammalian GPCRs and their Gα subunits is similar to that of Ste2p and Gpa1p interactions (*118, 146*).

Although Ste2p lacking a full C-terminal tail is still capable of signaling upon binding of α-factor, the asparagine-to-serine substitution (N388S) in the C-terminal tail of Ste2p resulted in defects in growth arrest, and impaired mating competence. This study suggests that the C-terminal tail of Ste2p may interact with G proteins in *S. cerevisiae* (*147*). Cysteine scanning studies of the intracellular loops of Ste2p indicated that the central regions were all highly accessible (to solvent?) whereas residues near the ends of the loops (TMs boundaries) were less accessible. However, these boundary regions are enriched in hydrophobic residues, suggesting that they may form a hydrophobic pocket for interaction with the G proteins (*122*). Other studies of specific intracellular domains have also shown that the intracellular loop 3 (IL3) of Ste2p might be involved in Ste2p-Gpa1p coupling (*148, 149*). However, alanine scanning and random mutagenesis of IL3 residues show that relatively conservative mutations did not result in strong defects, making it difficult to pinpoint specific residues that directly interact with Gpa1p (*150-152*).

The region of Gpa1p that has been predicted to most likely interact directly with Ste2p is the C-terminus. Gpa1p C-terminus mutants in *S. cerevisiae* showed that truncation of the last amino acids and lysine-to-proline substitution (K467P) lead to mating defects. This suggests that the C-terminal residues of Gpa1p, especially the last five amino acids, may be involved in Ste2p-Gpa1p interactions (*153*). Another group also proposed that the C-terminal domain of Gpa1p is essential for Ste2p-coupling, and that the C-terminus of Gpa1p forms a β-turn that correlates with the C-terminal region of mammalian Gα (*154*). Screening for mutations in the N-terminal region of yeast Gpa1p also indicated some interactions with Ste2p (*155*). Other mutagenesis studies suggest that residues in different interface regions of Gpa1p contribute to activation of Ste2p and signaling (*114*). To date no study has pinpointed specific residue-to-residue

interactions between Ste2p and Gpa1p. In this dissertation specific residue-residue interactions between Ste2p and Gpa1p have been identified. This is discussed in part four. The findings of this study reveal strong evidence for similarities between Ste2p-Gpa1p mechanism of interaction and that of the mammalian GPCR transduction pathway. Thus, knowledge about Ste2p structure-function relationship will be very helpful in understanding the mechanism of activation and signaling in other GPCR systems.

This dissertation describes the use of α-factor analogs as probes to study receptor binding and activation and also examines the interactions between Ste2p and its cognate Gα subunit, Gpa1p. Part two details the characterization and use of α-factor that contain DOPA (3,4-dihydroxyphenyl-alanine) in determining ligand-receptor contact sites. A proposed ligand binding mechanism is also discussed. The capturing of α-factor by Ste2p containing the unnatural amino acid *p*-benzoyl-*L*-phenylalanine (Bpa) via photoactivation cross-linking to determine which Ste2p residues interact with α-factor is discussed in Part three. Part four investigates specific contacts between Ste2p and Gpa1p. Conformational changes in both proteins upon ligand binding are examined. The use of a Ste2p-Gpa1p fused protein as a tool to study the interactions between Ste2p and Gpa1p is presented in Part five. Finally part 6 is an overall evaluation of these studies, contributions to the working model of α-factor-Ste2p and Ste2p-Gpa1p interactions, and future studies that could be performed to refine these models. This dissertation will provide better understanding of how peptide ligands interacts with their GPCRs, and also how these interactions promote activation of the associated G proteins which ultimately result in signal transduction.

List of References for Part I

1. Rosenbaum, D. M., Rasmussen, S. G., and Kobilka, B. K. (2009) The structure and function of G-protein-coupled receptors, *Nature 459*, 356-363.
2. Naider, F., and Becker, J. M. (2004) The alpha-factor mating pheromone of Saccharomyces cerevisiae: a model for studying the interaction of peptide hormones and G protein-coupled receptors, *Peptides 25*, 1441-1463.
3. Wess, J., Han, S. J., Kim, S. K., Jacobson, K. A., and Li, J. H. (2008) Conformational changes involved in G-protein-coupled-receptor activation, *Trends Pharmacol Sci 29*, 616-625.
4. De Amici, M., Dallanoce, C., Holzgrabe, U., Trankle, C., and Mohr, K. (2009) Allosteric ligands for G protein-coupled receptors: A novel strategy with attractive therapeutic opportunities, *Med Res Rev*.
5. Lundstrom, K. (2009) An overview on GPCRs and drug discovery: structure-based drug design and structural biology on GPCRs, *Methods Mol Biol 552*, 51-66.
6. Williams, C., and Hill, S. J. (2009) GPCR signaling: understanding the pathway to successful drug discovery, *Methods Mol Biol 552*, 39-50.
7. Chapter, M. C., White, C. M., De Ridder, A., Chadwick, W., Martin, B., and Maudsley, S. (2009) Chemical modification of Class II G-protein-coupled receptor ligands: Frontiers in the development of peptide analogs as neuroendocrine pharmacological therapies, *Pharmacol Ther*.
8. Pierce, K. L., Premont, R. T., and Lefkowitz, R. J. (2002) Seven-transmembrane receptors, *Nat Rev Mol Cell Biol 3*, 639-650.

9. Cabrera-Vera, T. M., Vanhauwe, J., Thomas, T. O., Medkova, M., Preininger, A., Mazzoni, M. R., and Hamm, H. E. (2003) Insights into G protein structure, function, and regulation, *Endocr Rev 24*, 765-781.

10. Sato, M., and Ishikawa, Y. (2009) Accessory proteins for heterotrimeric G-protein: Implication in the cardiovascular system, *Pathophysiology*.

11. Eglen, R. M., and Reisine, T. (2009) New insights into GPCR function: implications for HTS, *Methods Mol Biol 552*, 1-13.

12. Ratnala, V. R., and Kobilka, B. (2009) Understanding the ligand-receptor-G protein ternary complex for GPCR drug discovery, *Methods Mol Biol 552*, 67-77.

13. Attwood, T. K., and Findlay, J. B. (1994) Fingerprinting G-protein-coupled receptors, *Protein Eng 7*, 195-203.

14. Flower, D. R. (1999) Modelling G-protein-coupled receptors for drug design, *Biochim Biophys Acta 1422*, 207-234.

15. Kolakowski, L. F., Jr. (1994) GCRDb: a G-protein-coupled receptor database, *Receptors Channels 2*, 1-7.

16. Fredriksson, R., Lagerstrom, M. C., Lundin, L. G., and Schioth, H. B. (2003) The G-protein-coupled receptors in the human genome form five main families. Phylogenetic analysis, paralogon groups, and fingerprints, *Mol Pharmacol 63*, 1256-1272.

17. Palczewski, K., Kumasaka, T., Hori, T., Behnke, C. A., Motoshima, H., Fox, B. A., Le Trong, I., Teller, D. C., Okada, T., Stenkamp, R. E., Yamamoto, M., and Miyano, M. (2000) Crystal structure of rhodopsin: A G protein-coupled receptor, *Science 289*, 739-745.

18. Lodowski, D. T., and Palczewski, K. (2009) Chemokine receptors and other G protein-coupled receptors, *Curr Opin HIV AIDS 4*, 88-95.

19. Ludeke, S., Mahalingam, M., and Vogel, R. (2009) Rhodopsin activation switches in a native membrane environment, *Photochem Photobiol 85*, 437-441.

20. Baldwin, J. M. (1994) Structure and function of receptors coupled to G proteins, *Curr Opin Cell Biol 6*, 180-190.

21. Harmar, A. J. (2001) Family-B G-protein-coupled receptors, *Genome Biol 2*, REVIEWS3013.

22. Hayflick, J. S. (2000) A family of heptahelical receptors with adhesion-like domains: a marriage between two super families, *J Recept Signal Transduct Res 20*, 119-131.

23. McKnight, A. J., and Gordon, S. (1998) The EGF-TM7 family: unusual structures at the leukocyte surface, *J Leukoc Biol 63*, 271-280.

24. Stacey, M., Lin, H. H., Gordon, S., and McKnight, A. J. (2000) LNB-TM7, a group of seven-transmembrane proteins related to family-B G-protein-coupled receptors, *Trends Biochem Sci 25*, 284-289.

25. Barnes, M. R., Duckworth, D. M., and Beeley, L. J. (1998) Frizzled proteins constitute a novel family of G protein-coupled receptors, most closely related to the secretin family, *Trends Pharmacol Sci 19*, 399-400.

26. Slusarski, D. C., Corces, V. G., and Moon, R. T. (1997) Interaction of Wnt and a Frizzled homologue triggers G-protein-linked phosphatidylinositol signalling, *Nature 390*, 410-413.

27. Cherezov, V., and Caffrey, M. (2007) Membrane protein crystallization in lipidic mesophases. A mechanism study using X-ray microdiffraction, *Faraday Discuss 136*, 195-212; discussion 213-129.

28. Cherezov, V., Rosenbaum, D. M., Hanson, M. A., Rasmussen, S. G., Thian, F. S., Kobilka, T. S., Choi, H. J., Kuhn, P., Weis, W. I., Kobilka, B. K., and Stevens, R. C. (2007) High-resolution crystal structure of an engineered human beta2-adrenergic G protein-coupled receptor, *Science 318*, 1258-1265.

29. Day, P. W., Rasmussen, S. G., Parnot, C., Fung, J. J., Masood, A., Kobilka, T. S., Yao, X. J., Choi, H. J., Weis, W. I., Rohrer, D. K., and Kobilka, B. K. (2007) A monoclonal antibody for G protein-coupled receptor crystallography, *Nat Methods 4*, 927-929.

30. Rasmussen, S. G., Choi, H. J., Rosenbaum, D. M., Kobilka, T. S., Thian, F. S., Edwards, P. C., Burghammer, M., Ratnala, V. R., Sanishvili, R., Fischetti, R. F., Schertler, G. F., Weis, W. I., and Kobilka, B. K. (2007) Crystal structure of the human beta2 adrenergic G-protein-coupled receptor, *Nature 450*, 383-387.

31. Rosenbaum, D. M., Cherezov, V., Hanson, M. A., Rasmussen, S. G., Thian, F. S., Kobilka, T. S., Choi, H. J., Yao, X. J., Weis, W. I., Stevens, R. C., and Kobilka, B. K. (2007) GPCR engineering yields high-resolution structural insights into beta2-adrenergic receptor function, *Science 318*, 1266-1273.

32. Jaakola, V. P., Griffith, M. T., Hanson, M. A., Cherezov, V., Chien, E. Y., Lane, J. R., Ijzerman, A. P., and Stevens, R. C. (2008) The 2.6 angstrom crystal structure of a human A2A adenosine receptor bound to an antagonist, *Science 322*, 1211-1217.

33. Park, J. H., Scheerer, P., Hofmann, K. P., Choe, H. W., and Ernst, O. P. (2008) Crystal structure of the ligand-free G-protein-coupled receptor opsin, *Nature 454*, 183-187.

34. Scheerer, P., Park, J. H., Hildebrand, P. W., Kim, Y. J., Krauss, N., Choe, H. W., Hofmann, K. P., and Ernst, O. P. (2008) Crystal structure of opsin in its G-protein-interacting conformation, *Nature 455*, 497-502.

35. Warne, T., Serrano-Vega, M. J., Baker, J. G., Moukhametzianov, R., Edwards, P. C., Henderson, R., Leslie, A. G., Tate, C. G., and Schertler, G. F. (2008) Structure of a beta1-adrenergic G-protein-coupled receptor, *Nature 454*, 486-491.

36. Krebs, A., Villa, C., Edwards, P. C., and Schertler, G. F. (1998) Characterisation of an improved two-dimensional p22121 crystal from bovine rhodopsin, *J Mol Biol 282*, 991-1003.

37. Lodowski, D. T., Angel, T. E., and Palczewski, K. (2009) Comparative analysis of GPCR crystal structures, *Photochem Photobiol 85*, 425-430.

38. Edwards, P. C., Li, J., Burghammer, M., McDowell, J. H., Villa, C., Hargrave, P. A., and Schertler, G. F. (2004) Crystals of native and modified bovine rhodopsins and their heavy atom derivatives, *J Mol Biol 343*, 1439-1450.

39. Li, J., Edwards, P. C., Burghammer, M., Villa, C., and Schertler, G. F. (2004) Structure of bovine rhodopsin in a trigonal crystal form, *J Mol Biol 343*, 1409-1438.

40. Ruprecht, J. J., Mielke, T., Vogel, R., Villa, C., and Schertler, G. F. (2004) Electron crystallography reveals the structure of metarhodopsin I, *EMBO J 23*, 3609-3620.

41. Hanson, M. A., Cherezov, V., Griffith, M. T., Roth, C. B., Jaakola, V. P., Chien, E. Y., Velasquez, J., Kuhn, P., and Stevens, R. C. (2008) A specific cholesterol binding site is established by the 2.8 A structure of the human beta2-adrenergic receptor, *Structure 16*, 897-905.

42. Ballesteros, J. A., Jensen, A. D., Liapakis, G., Rasmussen, S. G., Shi, L., Gether, U., and Javitch, J. A. (2001) Activation of the beta 2-adrenergic receptor involves disruption of an ionic lock between the cytoplasmic ends of transmembrane segments 3 and 6, *J Biol Chem 276*, 29171-29177.

43. Okada, T., Fujiyoshi, Y., Silow, M., Navarro, J., Landau, E. M., and Shichida, Y. (2002) Functional role of internal water molecules in rhodopsin revealed by X-ray crystallography, *Proc Natl Acad Sci U S A 99*, 5982-5987.

44. Bond, R. A., and Ijzerman, A. P. (2006) Recent developments in constitutive receptor activity and inverse agonism, and their potential for GPCR drug discovery, *Trends Pharmacol Sci 27*, 92-96.

45. Yao, X., Parnot, C., Deupi, X., Ratnala, V. R., Swaminath, G., Farrens, D., and Kobilka, B. (2006) Coupling ligand structure to specific conformational switches in the beta2-adrenoceptor, *Nat Chem Biol 2*, 417-422.

46. Vogel, R., Mahalingam, M., Ludeke, S., Huber, T., Siebert, F., and Sakmar, T. P. (2008) Functional role of the "ionic lock"--an interhelical hydrogen-bond network in family A heptahelical receptors, *J Mol Biol 380*, 648-655.

47. Galaktionov, S., Nikiforovich, G. V., and Marshall, G. R. (2001) Ab initio modeling of small, medium, and large loops in proteins, *Biopolymers 60*, 153-168.

48. Nikiforovich, G. V., Galaktionov, S., Balodis, J., and Marshall, G. R. (2001) Novel approach to computer modeling of seven-helical transmembrane proteins: current progress in the test case of bacteriorhodopsin, *Acta Biochim Pol 48*, 53-64.

49. Nikiforovich, G. V., and Marshall, G. R. (2001) 3D model for TM region of the AT-1 receptor in complex with angiotensin II independently validated by site-directed mutagenesis data, *Biochem Biophys Res Commun 286*, 1204-1211.

50. Vaidehi, N., Floriano, W. B., Trabanino, R., Hall, S. E., Freddolino, P., Choi, E. J., Zamanakos, G., and Goddard, W. A., 3rd. (2002) Prediction of structure and function of G protein-coupled receptors, *Proc Natl Acad Sci U S A 99*, 12622-12627.

51. Blois, T. M., and Bowie, J. U. (2009) G-protein-coupled receptor structures were not built in a day, *Protein Sci 18*, 1335-1342.

52. Milligan, G., Canals, M., Pediani, J. D., Ellis, J., and Lopez-Gimenez, J. F. (2006) The role of GPCR dimerisation/oligomerisation in receptor signalling, *Ernst Schering Found Symp Proc*, 145-161.

53. Pin, J. P., Comps-Agrar, L., Maurel, D., Rives, M. L., Trinquet, E., Kniazeff, J., Rondard, P., and Prezeau, L. (2009) GPCR oligomers: two or more for what? Lessons from mGlu and GABAB receptors, *J Physiol*.

54. Panetta, R., and Greenwood, M. T. (2008) Physiological relevance of GPCR oligomerization and its impact on drug discovery, *Drug Discov Today 13*, 1059-1066.

55. Filizola, M., Wang, S. X., and Weinstein, H. (2006) Dynamic models of G-protein coupled receptor dimers: indications of asymmetry in the rhodopsin dimer from molecular dynamics simulations in a POPC bilayer, *J Comput Aided Mol Des 20*, 405-416.

56. Fotiadis, D., Liang, Y., Filipek, S., Saperstein, D. A., Engel, A., and Palczewski, K. (2003) Atomic-force microscopy: Rhodopsin dimers in native disc membranes, *Nature 421*, 127-128.

57. Park, P. S., Filipek, S., Wells, J. W., and Palczewski, K. (2004) Oligomerization of G protein-coupled receptors: past, present, and future, *Biochemistry 43*, 15643-15656.

58. Hebert, T. E., Moffett, S., Morello, J. P., Loisel, T. P., Bichet, D. G., Barret, C., and Bouvier, M. (1996) A peptide derived from a beta2-adrenergic receptor transmembrane domain inhibits both receptor dimerization and activation, *J Biol Chem 271*, 16384-16392.

59. Bouvier, M. (2001) Oligomerization of G-protein-coupled transmitter receptors, *Nat Rev Neurosci 2*, 274-286.

60. Gregory, K. J., Sexton, P. M., and Christopoulos, A. (2007) Allosteric modulation of muscarinic acetylcholine receptors, *Curr Neuropharmacol 5*, 157-167.

61. Leach, K., Sexton, P. M., and Christopoulos, A. (2007) Allosteric GPCR modulators: taking advantage of permissive receptor pharmacology, *Trends Pharmacol Sci 28*, 382-389.

62. Dinger, M. C., Bader, J. E., Kobor, A. D., Kretzschmar, A. K., and Beck-Sickinger, A. G. (2003) Homodimerization of neuropeptide y receptors investigated by fluorescence resonance energy transfer in living cells, *J Biol Chem 278*, 10562-10571.

63. Christopoulos, A. (2002) Allosteric binding sites on cell-surface receptors: novel targets for drug discovery, *Nat Rev Drug Discov 1*, 198-210.

64. Christopoulos, A., and Kenakin, T. (2002) G protein-coupled receptor allosterism and complexing, *Pharmacol Rev 54*, 323-374.

65. May, L. T., Avlani, V. A., Sexton, P. M., and Christopoulos, A. (2004) Allosteric modulation of G protein-coupled receptors, *Curr Pharm Des 10*, 2003-2013.

66. Eriotou-Bargiota, E., Xue, C. B., Naider, F., and Becker, J. M. (1992) Antagonistic and synergistic peptide analogues of the tridecapeptide mating pheromone of Saccharomyces cerevisiae, *Biochemistry 31*, 551-557.

67. Abel, M. G., Zhang, Y. L., Lu, H. F., Naider, F., and Becker, J. M. (1998) Structure-function analysis of the Saccharomyces cerevisiae tridecapeptide pheromone using alanine-scanned analogs, *J Pept Res 52*, 95-106.

68. Blake, A. D., Bot, G., and Reisine, T. (1996) Structure-function analysis of the cloned opiate receptors: peptide and small molecule interactions, *Chem Biol 3*, 967-972.

69. Gurrath, M. (2001) Peptide-binding G protein-coupled receptors: new opportunities for drug design, *Curr Med Chem 8*, 1605-1648.

70. Kolb, P., Rosenbaum, D. M., Irwin, J. J., Fung, J. J., Kobilka, B. K., and Shoichet, B. K. (2009) Structure-based discovery of beta2-adrenergic receptor ligands, *Proc Natl Acad Sci U S A 106*, 6843-6848.

71. Ghanouni, P., Steenhuis, J. J., Farrens, D. L., and Kobilka, B. K. (2001) Agonist-induced conformational changes in the G-protein-coupling domain of the beta 2 adrenergic receptor, *Proc Natl Acad Sci U S A 98*, 5997-6002.

72. Kobilka, B. K. (2007) G protein coupled receptor structure and activation, *Biochim Biophys Acta 1768*, 794-807.

73. Kobilka, B. K., and Deupi, X. (2007) Conformational complexity of G-protein-coupled receptors, *Trends Pharmacol Sci 28*, 397-406.

74. Labbe-Jullie, C., Barroso, S., Nicolas-Eteve, D., Reversat, J. L., Botto, J. M., Mazella, J., Bernassau, J. M., and Kitabgi, P. (1998) Mutagenesis and modeling of the neurotensin

receptor NTR1. Identification of residues that are critical for binding SR 48692, a nonpeptide neurotensin antagonist, *J Biol Chem 273*, 16351-16357.

75. Barroso, S., Richard, F., Nicolas-Etheve, D., Reversat, J. L., Bernassau, J. M., Kitabgi, P., and Labbe-Jullie, C. (2000) Identification of residues involved in neurotensin binding and modeling of the agonist binding site in neurotensin receptor 1, *J Biol Chem 275*, 328-336.

76. Flanagan, C. A., Rodic, V., Konvicka, K., Yuen, T., Chi, L., Rivier, J. E., Millar, R. P., Weinstein, H., and Sealfon, S. C. (2000) Multiple interactions of the Asp(2.61(98)) side chain of the gonadotropin-releasing hormone receptor contribute differentially to ligand interaction, *Biochemistry 39*, 8133-8141.

77. Chorev, M. (2002) Parathyroid hormone 1 receptor: insights into structure and function, *Receptors Channels 8*, 219-242.

78. Rihakova, L., Deraet, M., Auger-Messier, M., Perodin, J., Boucard, A. A., Guillemette, G., Leduc, R., Lavigne, P., and Escher, E. (2002) Methionine proximity assay, a novel method for exploring peptide ligand-receptor interaction, *J Recept Signal Transduct Res 22*, 297-313.

79. Hunyady, L., Vauquelin, G., and Vanderheyden, P. (2003) Agonist induction and conformational selection during activation of a G-protein-coupled receptor, *Trends Pharmacol Sci 24*, 81-86.

80. Kauer, J. C., Erickson-Viitanen, S., Wolfe, H. R., Jr., and DeGrado, W. F. (1986) p-Benzoyl-L-phenylalanine, a new photoreactive amino acid. Photolabeling of calmodulin with a synthetic calmodulin-binding peptide, *J Biol Chem 261*, 10695-10700.

81. Dorman, G., and Prestwich, G. D. (1994) Benzophenone photophores in biochemistry, *Biochemistry 33*, 5661-5673.

82. Shoelson, S. E., Lee, J., Lynch, C. S., Backer, J. M., and Pilch, P. F. (1993) BpaB25 insulins. Photoactivatable analogues that quantitatively cross-link, radiolabel, and activate the insulin receptor, *J Biol Chem 268*, 4085-4091.

83. Boucard, A. A., Wilkes, B. C., Laporte, S. A., Escher, E., Guillemette, G., and Leduc, R. (2000) Photolabeling identifies position 172 of the human AT(1) receptor as a ligand contact point: receptor-bound angiotensin II adopts an extended structure, *Biochemistry 39*, 9662-9670.

84. Henry, L. K., Khare, S., Son, C., Babu, V. V., Naider, F., and Becker, J. M. (2002) Identification of a contact region between the tridecapeptide alpha-factor mating pheromone of Saccharomyces cerevisiae and its G protein-coupled receptor by photoaffinity labeling, *Biochemistry 41*, 6128-6139.

85. Son, C. D., Sargsyan, H., Naider, F., and Becker, J. M. (2004) Identification of ligand binding regions of the Saccharomyces cerevisiae alpha-factor pheromone receptor by photoaffinity cross-linking, *Biochemistry 43*, 13193-13203.

86. Lee, Y. H., Naider, F., and Becker, J. M. (2006) Interacting residues in an activated state of a G protein-coupled receptor, *J Biol Chem 281*, 2263-2272.

87. Naider, F., Becker, J. M., Lee, Y. H., and Horovitz, A. (2007) Double-mutant cycle scanning of the interaction of a peptide ligand and its G protein-coupled receptor, *Biochemistry 46*, 3476-3481.

88. Burdine, L., Gillette, T. G., Lin, H. J., and Kodadek, T. (2004) Periodate-triggered cross-linking of DOPA-containing peptide-protein complexes, *J Am Chem Soc 126*, 11442-11443.

89. Liu, B., Burdine, L., and Kodadek, T. (2006) Chemistry of periodate-mediated cross-linking of 3,4-dihydroxylphenylalanine-containing molecules to proteins, *J Am Chem Soc 128*, 15228-15235.

90. Lim, H. S., Cai, D., Archer, C. T., and Kodadek, T. (2007) Periodate-triggered cross-linking reveals Sug2/Rpt4 as the molecular target of a peptoid inhibitor of the 19S proteasome regulatory particle, *J Am Chem Soc 129*, 12936-12937.

91. Hall, D. A. (2000) Modeling the functional effects of allosteric modulators at pharmacological receptors: an extension of the two-state model of receptor activation, *Mol Pharmacol 58*, 1412-1423.

92. Rubenstein, L. A., Zauhar, R. J., and Lanzara, R. G. (2006) Molecular dynamics of a biophysical model for beta2-adrenergic and G protein-coupled receptor activation, *J Mol Graph Model 25*, 396-409.

93. Ehlert, F. J., and Griffin, M. T. (2008) Two-state models and the analysis of the allosteric effect of gallamine at the M2 muscarinic receptor, *J Pharmacol Exp Ther 325*, 1039-1060.

94. Youn, H., Koh, J., and Roberts, G. P. (2008) Two-state allosteric modeling suggests protein equilibrium as an integral component for cyclic AMP (cAMP) specificity in the cAMP receptor protein of Escherichia coli, *J Bacteriol 190*, 4532-4540.

95. Kobilka, B. (2004) Agonist binding: a multistep process, *Mol Pharmacol 65*, 1060-1062.

96. Bhattacharya, S., Hall, S. E., and Vaidehi, N. (2008) Agonist-induced conformational changes in bovine rhodopsin: insight into activation of G-protein-coupled receptors, *J Mol Biol 382*, 539-555.

97. Weis, W. I., and Kobilka, B. K. (2008) Structural insights into G-protein-coupled receptor activation, *Curr Opin Struct Biol 18*, 734-740.

98. Granier, S., Kim, S., Fung, J. J., Bokoch, M. P., and Parnot, C. (2009) FRET-based measurement of GPCR conformational changes, *Methods Mol Biol 552*, 253-268.

99. Reynolds, K. A., Katritch, V., and Abagyan, R. (2009) Identifying conformational changes of the beta(2) adrenoceptor that enable accurate prediction of ligand/receptor interactions and screening for GPCR modulators, *J Comput Aided Mol Des 23*, 273-288.

100. Yao, X. J., Velez Ruiz, G., Whorton, M. R., Rasmussen, S. G., DeVree, B. T., Deupi, X., Sunahara, R. K., and Kobilka, B. (2009) The effect of ligand efficacy on the formation and stability of a GPCR-G protein complex, *Proc Natl Acad Sci U S A 106*, 9501-9506.

101. Rasmussen, S. G., Jensen, A. D., Liapakis, G., Ghanouni, P., Javitch, J. A., and Gether, U. (1999) Mutation of a highly conserved aspartic acid in the beta2 adrenergic receptor: constitutive activation, structural instability, and conformational rearrangement of transmembrane segment 6, *Mol Pharmacol 56*, 175-184.

102. Altenbach, C., Yang, K., Farrens, D. L., Farahbakhsh, Z. T., Khorana, H. G., and Hubbell, W. L. (1996) Structural features and light-dependent changes in the cytoplasmic interhelical E-F loop region of rhodopsin: a site-directed spin-labeling study, *Biochemistry 35*, 12470-12478.

103. Farrens, D. L., Altenbach, C., Yang, K., Hubbell, W. L., and Khorana, H. G. (1996) Requirement of rigid-body motion of transmembrane helices for light activation of rhodopsin, *Science 274*, 768-770.

104. Yang, K., Farrens, D. L., Hubbell, W. L., and Khorana, H. G. (1996) Structure and function in rhodopsin. Single cysteine substitution mutants in the cytoplasmic interhelical E-F loop region show position-specific effects in transducin activation, *Biochemistry 35*, 12464-12469.

105. Altenbach, C., Kusnetzow, A. K., Ernst, O. P., Hofmann, K. P., and Hubbell, W. L. (2008) High-resolution distance mapping in rhodopsin reveals the pattern of helix movement due to activation, *Proc Natl Acad Sci U S A 105*, 7439-7444.

106. Saidak, Z., Blake-Palmer, K., Hay, D. L., Northup, J. K., and Glass, M. (2006) Differential activation of G-proteins by mu-opioid receptor agonists, *Br J Pharmacol 147*, 671-680.

107. Nguyen-Ngoc, T., Afshar, K., and Gonczy, P. (2007) Coupling of cortical dynein and G alpha proteins mediates spindle positioning in Caenorhabditis elegans, *Nat Cell Biol 9*, 1294-1302.

108. Ahuja, S., and Smith, S. O. (2009) Multiple switches in G protein-coupled receptor activation, *Trends Pharmacol Sci 30*, 494-502.

109. Simon, M. I., Strathmann, M. P., and Gautam, N. (1991) Diversity of G proteins in signal transduction, *Science 252*, 802-808.

110. Spiegel, A. M., and Weinstein, L. S. (2004) Inherited diseases involving g proteins and g protein-coupled receptors, *Annu Rev Med 55*, 27-39.

111. McFadzean, I., Mullaney, I., Brown, D. A., and Milligan, G. (1989) Antibodies to the GTP binding protein, Go, antagonize noradrenaline-induced calcium current inhibition in NG108-15 hybrid cells, *Neuron 3*, 177-182.

112. Gilchrist, A., Mazzoni, M. R., Dineen, B., Dice, A., Linden, J., Proctor, W. R., Lupica, C. R., Dunwiddie, T. V., and Hamm, H. E. (1998) Antagonists of the receptor-G protein interface block Gi-coupled signal transduction, *J Biol Chem 273*, 14912-14919.

113. Blahos, J., 2nd, Mary, S., Perroy, J., de Colle, C., Brabet, I., Bockaert, J., and Pin, J. P. (1998) Extreme C terminus of G protein alpha-subunits contains a site that discriminates between Gi-coupled metabotropic glutamate receptors, *J Biol Chem 273*, 25765-25769.

114. Gladue, D. P., and Konopka, J. B. (2008) Scanning mutagenesis of regions in the Galpha protein Gpa1 that are predicted to interact with yeast mating pheromone receptors, *FEMS Yeast Res 8*, 71-80.

115. Minic, J., Sautel, M., Salesse, R., and Pajot-Augy, E. (2005) Yeast system as a screening tool for pharmacological assessment of g protein coupled receptors, *Curr Med Chem 12*, 961-969.

116. Eilers, M., Hornak, V., Smith, S. O., and Konopka, J. B. (2005) Comparison of class A and D G protein-coupled receptors: common features in structure and activation, *Biochemistry 44*, 8959-8975.

117. Burchett, S. A., Scott, A., Errede, B., and Dohlman, H. G. (2001) Identification of novel pheromone-response regulators through systematic overexpression of 120 protein kinases in yeast, *J Biol Chem 276*, 26472-26478.

118. Dohlman, H. G., and Thorner, J. W. (2001) Regulation of G protein-initiated signal transduction in yeast: paradigms and principles, *Annu Rev Biochem 70*, 703-754.

119. Lin, J. C., Duell, K., and Konopka, J. B. (2004) A microdomain formed by the extracellular ends of the transmembrane domains promotes activation of the G protein-coupled alpha-factor receptor, *Mol Cell Biol 24*, 2041-2051.

120. Akal-Strader, A., Khare, S., Xu, D., Naider, F., and Becker, J. M. (2002) Residues in the first extracellular loop of a G protein-coupled receptor play a role in signal transduction, *J Biol Chem 277*, 30581-30590.

121. Hauser, M., Kauffman, S., Lee, B. K., Naider, F., and Becker, J. M. (2007) The first extracellular loop of the Saccharomyces cerevisiae G protein-coupled receptor Ste2p undergoes a conformational change upon ligand binding, *J Biol Chem 282*, 10387-10397.

122. Choi, Y., and Konopka, J. B. (2006) Accessibility of cysteine residues substituted into the cytoplasmic regions of the alpha-factor receptor identifies the intracellular residues that are available for G protein interaction, *Biochemistry 45*, 15310-15317.

123. Gehret, A. U., Bajaj, A., Naider, F., and Dumont, M. E. (2006) Oligomerization of the yeast alpha-factor receptor: implications for dominant negative effects of mutant receptors, *J Biol Chem 281*, 20698-20714.

124. Overton, M. C., and Blumer, K. J. (2000) G-protein-coupled receptors function as oligomers in vivo, *Curr Biol 10*, 341-344.

125. Overton, M. C., and Blumer, K. J. (2002) The extracellular N-terminal domain and transmembrane domains 1 and 2 mediate oligomerization of a yeast G protein-coupled receptor, *J Biol Chem 277*, 41463-41472.

126. Wang, H. X., and Konopka, J. B. (2009) Identification of amino acids at two dimer interface regions of the alpha-factor receptor (Ste2), *Biochemistry 48*, 7132-7139.

127. Chinault, S. L., Overton, M. C., and Blumer, K. J. (2004) Subunits of a yeast oligomeric G protein-coupled receptor are activated independently by agonist but function in concert to activate G protein heterotrimers, *J Biol Chem 279*, 16091-16100.

128. Xue, C. B., Eriotou-Bargiota, E., Miller, D., Becker, J. M., and Naider, F. (1989) A covalently constrained congener of the Saccharomyces cerevisiae tridecapeptide mating pheromone is an agonist, *J Biol Chem 264*, 19161-19168.

129. Xue, C. B., McKinney, A., Lu, H. F., Jiang, Y., Becker, J. M., and Naider, F. (1996) Probing the functional conformation of the tridecapeptide mating pheromone of Saccharomyces cerevisiae through study of disulfide-constrained analogs, *Int J Pept Protein Res 47*, 131-141.

130. Antohi, O., Marepalli, H. R., Yang, W., Becker, J. M., and Naider, F. (1998) Conformational analysis of cyclic analogues of the Saccharomyces cerevisiae alpha-factor pheromone, *Biopolymers 45*, 21-34.

131. Zhang, Y. L., Marepalli, H. R., Lu, H. F., Becker, J. M., and Naider, F. (1998) Synthesis, biological activity, and conformational analysis of peptidomimetic analogues of the Saccharomyces cerevisiae alpha-factor tridecapeptide, *Biochemistry 37*, 12465-12476.

132. Liu, S., Henry, L. K., Lee, B. K., Wang, S. H., Arshava, B., Becker, J. M., and Naider, F. (2000) Position 13 analogs of the tridecapeptide mating pheromone from Saccharomyces cerevisiae: design of an iodinatable ligand for receptor binding, *J Pept Res 56*, 24-34.

133. Carpenter, K. A., Wilkes, B. C., and Schiller, P. W. (1998) The octapeptide angiotensin II adopts a well-defined structure in a phospholipid environment, *Eur J Biochem 251*, 448-453.

134. Chauvin, S., Berault, A., Lerrant, Y., Hibert, M., and Counis, R. (2000) Functional importance of transmembrane helix 6 Trp(279) and exoloop 3 Val(299) of rat gonadotropin-releasing hormone receptor, *Mol Pharmacol 57*, 625-633.

135. de Gasparo, M., Catt, K. J., Inagami, T., Wright, J. W., and Unger, T. (2000) International union of pharmacology. XXIII. The angiotensin II receptors, *Pharmacol Rev 52*, 415-472.

136. Greenberg, Z., Bisello, A., Mierke, D. F., Rosenblatt, M., and Chorev, M. (2000) Mapping the bimolecular interface of the parathyroid hormone (PTH)-PTH1 receptor complex: spatial proximity between Lys(27) (of the hormone principal binding domain) and leu(261) (of the first extracellular loop) of the human PTH1 receptor, *Biochemistry 39*, 8142-8152.

137. Wang, L., Xie, J., and Schultz, P. G. (2006) Expanding the genetic code, *Annu Rev Biophys Biomol Struct 35*, 225-249.

138. Ryu, Y., and Schultz, P. G. (2006) Efficient incorporation of unnatural amino acids into proteins in Escherichia coli, *Nat Methods 3*, 263-265.

139. Liu, W., Brock, A., Chen, S., and Schultz, P. G. (2007) Genetic incorporation of unnatural amino acids into proteins in mammalian cells, *Nat Methods 4*, 239-244.

140. Chen, S., Schultz, P. G., and Brock, A. (2007) An improved system for the generation and analysis of mutant proteins containing unnatural amino acids in Saccharomyces cerevisiae, *J Mol Biol 371*, 112-122.

141. Chin, J. W., Cropp, T. A., Anderson, J. C., Mukherji, M., Zhang, Z., and Schultz, P. G. (2003) An expanded eukaryotic genetic code, *Science 301*, 964-967.

142. Son, C. D., Sargsyan, H., Hurst, G. B., Naider, F., and Becker, J. M. (2005) Analysis of ligand-receptor cross-linked fragments by mass spectrometry, *J Pept Res 65*, 418-426.

143. Lee, B. K., Lee, Y. H., Hauser, M., Son, C. D., Khare, S., Naider, F., and Becker, J. M. (2002) Tyr266 in the sixth transmembrane domain of the yeast alpha-factor receptor plays key roles in receptor activation and ligand specificity, *Biochemistry 41*, 13681-13689.

144. Lee, B. K., Khare, S., Naider, F., and Becker, J. M. (2001) Identification of residues of the Saccharomyces cerevisiae G protein-coupled receptor contributing to alpha-factor pheromone binding, *J Biol Chem 276*, 37950-37961.

145. Bajaj, A., Celic, A., Ding, F. X., Naider, F., Becker, J. M., and Dumont, M. E. (2004) A fluorescent alpha-factor analogue exhibits multiple steps on binding to its G protein coupled receptor in yeast, *Biochemistry 43*, 13564-13578.

146. Dohlman, H. G. (2002) G proteins and pheromone signaling, *Annu Rev Physiol 64*, 129-152.

147. Duran-Avelar, M. J., Ongay-Larios, L., Zentella-Dehesa, A., and Coria, R. (2001) The carboxy-terminal tail of the Ste2 receptor is involved in activation of the G protein in the Saccharomyces cerevisiae alpha-pheromone response pathway, *FEMS Microbiol Lett 197*, 65-71.

148. Slessareva, J. E., Ma, H., Depree, K. M., Flood, L. A., Bae, H., Cabrera-Vera, T. M., Hamm, H. E., and Graber, S. G. (2003) Closely related G-protein-coupled receptors use multiple and distinct domains on G-protein alpha-subunits for selective coupling, *J Biol Chem 278*, 50530-50536.

149. Kristiansen, K. (2004) Molecular mechanisms of ligand binding, signaling, and regulation within the superfamily of G-protein-coupled receptors: molecular modeling and mutagenesis approaches to receptor structure and function, *Pharmacol Ther 103*, 21-80.

150. Clark, C. D., Palzkill, T., and Botstein, D. (1994) Systematic mutagenesis of the yeast mating pheromone receptor third intracellular loop, *J Biol Chem 269*, 8831-8841.

151. Stefan, C. J., and Blumer, K. J. (1994) The third cytoplasmic loop of a yeast G-protein-coupled receptor controls pathway activation, ligand discrimination, and receptor internalization, *Mol Cell Biol 14*, 3339-3349.

152. Celic, A., Martin, N. P., Son, C. D., Becker, J. M., Naider, F., and Dumont, M. E. (2003) Sequences in the intracellular loops of the yeast pheromone receptor Ste2p required for G protein activation, *Biochemistry 42*, 3004-3017.

153. Hirsch, J. P., Dietzel, C., and Kurjan, J. (1991) The carboxyl terminus of Scg1, the G alpha subunit involved in yeast mating, is implicated in interactions with the pheromone receptors, *Genes Dev 5*, 467-474.

154. Kallal, L., and Kurjan, J. (1997) Analysis of the receptor binding domain of Gpa1p, the G(alpha) subunit involved in the yeast pheromone response pathway, *Mol Cell Biol 17*, 2897-2907.

155. Roginskaya, M., Connelly, S. M., Kim, K. S., Patel, D., and Dumont, M. E. (2004) Effects of mutations in the N terminal region of the yeast G protein alpha-subunit Gpa1p on signaling by pheromone receptors, *Mol Genet Genomics 271*, 237-248.

PART II

Cross-linking of DOPA-containing α-factor Pheromone analogs of *Saccharomyces cerevisiae* into its G Protein-Coupled Receptor, Ste2p.

Part II was published (excluding the data on DOPA[1] α-factor analogs) in its entirety as: Umanah, G. K., Son, C., Ding, F., Naider, F., Becker, J. M. (2009). *Biochemistry*, **48** (9), 2033-44. George K. Umanah was responsible for the characterization of the α-factor peptide analogs and carried out all cross-linking studies. Fa-Xiang Ding in Dr. Naider's laboratory was responsible for synthesis and purification of the peptides used in the study.

CHAPTER 1

Introduction

G protein-coupled receptors (GPCRs) are a large family of integral membrane proteins associated with signaling systems present in mammalians, plants, protozoans, fungi, and metazoans (1). Malfunctions of GPCRs contribute to diseases such as Alzheimer's, Parkinson's disease, diabetes, color blindness, asthma, depression, hypertension, stress, cardiovascular, and immune disorders (*2, 3*). All GPCRs share a common structure consisting of seven transmembrane domains (TMDs) connected by three extracellular and three intracellular loops (*1, 4, 5*). Upon binding of their ligands, GPCRs undergo conformational changes that transduce the signal into the cell by activating a cascade of protein-protein interactions initiated through a heterotrimeric G protein complex (6).

Ste2p, the *Saccharomyces cerevisiae* α-factor pheromone receptor, has been studied as a model for peptide-responsive GPCRs (*7, 8*). Though Ste2p does not share recognizable sequence similarity with mammalian GPCRs or even with Ste3p, the **a**-factor pheromone receptor of yeast, all GPCRs have strong structural and functional similarities (*9, 10*). For example, the packing and interactions between the fifth and sixth transmembrane domains are essential for proper signal transduction to the G protein in both rhodopsin and Ste2p (*11, 12*). Though there have been considerable studies on the GPCR binding sites of small ligands, less is known about the binding sites of peptide-responsive GPCRs.

Studies on the tridecapeptide α-factor pheromone (Trp-His-Trp-Leu-Gln-Leu-Lys-Pro-Gly-Gln-Pro-Met-Tyr) have contributed to the understanding of structure and function of peptide hormones. Alanine scanning studies of α-factor indicated that Trp1-Leu4 residues are associated

with receptor activation and signal transduction; Lys7-Gln10 residues are involved in formation of the biologically active conformation and Gln10-Tyr13 residues are essential for receptor binding (13). Photoreactive cross-linking studies, using 4-benzoyl-L-phenylalanine (Bpa)-containing α-factor analogs at different positions indicated that position one, three, and thirteen in α-factor interacted with residues on the extracellular face of Ste2p (14-16). The N-terminus of α-factor was shown to interact with Ste2p residues from extracellular ends of the fifth, sixth and seventh TMDs and parts of the second and third extracellular loops, whereas the C-terminus interacted with part of the first transmembrane domain (*14, 16, 17*). All of these studies revealed that generation of covalently linked ligand-receptor conjugates followed by detailed product analysis were an attractive approach to identify and map residues involved in Ste2p-ligand interactions. Nevertheless, limitations of using the cross-linking approaches performed to date are low yield of product and multiple cross-linked products making it difficult to define the exact residue-residue interactions involved in GPCR binding.

Recently, compounds containing 3,4-dihydroxylphenylalanine (DOPA) have been shown to cross-link efficiently to proteins (18). DOPA-containing compounds were oxidized by sodium periodate to form an ortho-quinone intermediate that could be attacked by a nearby nucleophile resulting in a stable, covalent cross-link. The ortho-quinone intermediate was shown to act as an electrophile that formed adducts with cysteine or histidine through the Michael addition reaction and also with lysine through the Schiff base formation (*18, 19*). Unlike most chemical cross-linking approaches, DOPA cross-linking occurs in high yield with little or no non-specific products observed even in complex protein mixtures (20). This method has been utilized to identify the yeast Rpt6/Sug1 and Rpt4/Sug2 proteins as the direct targets of Gal4 transcriptional

activation domains within the 26S proteasome (21). DOPA contained in RIP-1 (*R*egulatory Particle *I*nhibitor *P*eptoid-1) was also used to identify the yeast RIP-1 receptor (22).

Previously it was reported that an α-factor analog containing Bpa at positions 1 and 13 cross-linked into portions of Ste2p comprising residues Ser251-M294 and Phe55 – Arg58 respectively (*14-16*). However the exact residue of Ste2p that interacted with position 1 or 13 of α-factor was not defined. In this study we investigated the periodate-mediated chemical cross-linking of [DOPA^{1} Lys^{7}(BioACA),Nle^{12}]α-factor (Bio-DOPA^{1}) and [Lys^{7}(BioACA),Nle^{12}, DOPA^{13}]α-factor (Bio-DOPA^{13}) into Ste2p. These α-factor analogs were potent agonists; Bio-DOPA^{1} bound to Ste2p similar to the α-factor whereas Bio-DOPA^{13} bound with about 10-fold less affinity. Matrix-assisted laser-desorption ionization-time-of-flight (MALDI-TOF) analysis revealed that Bio-DOPA^{1} and Bio-DOPA^{13} α-factor analogs cross-linked to fragments of Ste2p comprising residues Leu264-Val280 (specifically Lys269) and Phe55 – Met69, respectively. Cross-linking of the Bio-DOPA^{13} α-factor analog into a Ste2p mutant (Cys59Ser) devoid of cysteine was greatly diminished suggesting that DOPA^{13} of the α-factor analog interacted directly with Cys^{59} of Ste2p. This represents the first time that DOPA oxidative cross-linking has been used to link a peptide hormone to a GPCR receptor and demonstrates the general utility of this method for studying contact points of biologically active peptides with their cognate receptors.

CHAPTER 2

Materials and Methods

***Media, Reagents, Strains and Plasmids*:**

Saccharomyces cerevisiae strain LM102 [*MAT**a**, bar1, leu2, ura3, FUS1-lacZ::URA3, ste2*Δ (23)] was used for growth arrest and binding assays and the protease deficient strain BJS21 [*MAT**a**, prc1-407 prb1-1122 pep4-3 leu2 trp1 ura3-52 ste2::Kan*^{R} (24)] was used for protein isolation and immunoblot analysis. The plasmid pBEC1 containing C-terminal FLAG and His tagged *STE2* (23) was transformed by the method of Geitz (25) into LM102 and BJS21 cells. Transformants were selected by growth on yeast media (26) lacking tryptophan (designated as MLT) to maintain selection for the plasmid. The Cells were cultured in MLT and grown to mid-log phase at 30 ^{o}C with shaking (200 rpm) for all assays.

Synthesis and characterization of Peptides:

The tridecapeptide pheromone α-factor analogs [DOPA^1 Lys^7(BioACA),Nle^{12}]α-factor (designated Bio-DOPA^1) and [Lys^7(BioACA),Nle^{12},DOPA^{13}]α-factor (designated Bio-DOPA^{13}) were synthesized using automated solid-phase peptide synthesis with Fmoc/OtBu protection schemes. The hydroxyl groups of DOPA were protected as the acetonide derivative. All protected amino reagents were purchased from Advanced Chem Tech (Louisville, KY) and all solvents and reagents were of the highest purity available. α-Factor and α-factor analogs used in this study all contain norleucine in place of the native Met^{12} residue. Norleucine is isosteric with methionine and [Nle^{12}] α-factor is isoactive and has the same receptor affinity as α-factor (27).

The syntheses of [Nle^{12}]α-factor, desTrp^{1},desHis^{2}[Nle^{12}]α-factor and [Biotin^{7}]α-factor were done as described previously (*14, 28*).

To pre-swollen wang resin (0.145g, 0.1 mmol, 0.69mmol/g) in DMF (10 mL) was added Fmoc-DOPA(acetonide)-OH (115mg, 0.25 mmol), N-hydroxybenzotriazole (34mg, 0.25 mmol), 4-dimethylaminopyridine (3.05 mg, 0.025 mmol) and diisopropylcarbodiimide (31.55 mg, 0.25 mmol) and the resulting mixture was stirred at room temperature for 1h. The mixture was filtered and the resin was treated again with the reagents above in DMF (10 mL) at room temperature for 1h. After filtration and washing with DMF (10 mLx2), the resin was further treated with acetic anhydride (102 mg, 1.0 mmol) and N,N diisopropylethyl- amine (128 mg, 1.0 mmol) in DMF (10 mL) for 30 min to cap unreacted hydroxyl groups, followed by washing with DMF (3x10 mL). The Fmoc-DOPA(acetonide)-O-Wang resin (0.1 mmol) was loaded on a Model 433A solid phase peptide synthesizer (Applied Biosystems, Foster City, CA) using 0.1 mmol single coupling chemistry and 2-(1H-benzotriazole-1-yl)-1,1,3,3-tetra-methyluronium hexafluorophosphate /N hydroxybenzotriazole as coupling reagents. After completing the chain assembly, the resin was dried under vacuum. To cleave the peptide the dry resin (550 mg) obtained above was added to a mixture of phenol (0.75g, ethanedithiol, 0.5mL, thioanisole (0.5mL), water (0.5mL) and 10 mL trifluoroacetic acid and the resulting mixture was stirred for 1.5h at room temperature. After filtration the volume of the filtrate was reduced by rotary evaporation *in vacuo*, the resulting residue was treated with 100 mL of ethyl ether and the precipitate was collected by filtration. The crude peptide (180 mg) was purified on preparative HPLC C18 column (19 mmX 300 mm) using gradient from 30% to 70% acetonitrile/H_2O (0.1%TFA) over 90 mins to give pure Fmoc-WHWLQLKPGQPNleDOPA-OH (70 mg).

To a vial covered with aluminum foil containing Fmoc-WHWLQLKPGQPNleDOPA-OH (12 mg) and DMF (1mL), was added piperidine (0.1 mL, 18% in DMF) at 4 °C under an Argon atmosphere, and the solution was stirred at 4 °C for 30 min. The solution was neutralized by 2% HCl, after filtration, the filtrate was loaded onto a preparative HPLC (C18 column, 19 mm X 300 mm) using a gradient of 20-50% acetonitrile (0.1% TFA) in water (0.1%TFA). 7.0 mg of pure WHWLQLKPGQPNleDOPA-OH ([DOPA^{13}]α-factor) was obtained. Yield: 64%, MW, calculated: 1681.97, found: 1680.9.

To the solution of Fmoc-WHWLQLKPGQPNleDopa-OH (22 mg, 5.16μmol) in DMF (1mL) and sodium borate (1mL, 50 mM), was added biotinamidohexanoic acid N-hydroxy succinimide ester (7.04 mg, 15.48μmol) at 4 °C. The solution was stirred for 1h. (when HPLC indicated that the starting material had been converted to product), neutralized by 2% HCl, filtered and the filtrate was loaded on preparative HPLC (C18 column, 19X300mm) using a gradient from 20-70% acetonitrile (0.1%TFA)/water (0.1%TFA). Highly purified Fmoc-WHWLQLK(BioACA)PGQPNleDOPA-OH (16mg; 72% yield) was recovered. This Fmoc-peptide (16 mg) was dissolved in DMF (1.2 mL) at 4 °C and piperidine (66 μL, 18% in DMF) was added. The solution was stirred for 1h and then was neutralized and filtered, and the filtrate was loaded on preparative HPLC using a gradient of 20-50% acetonitrile(0.1% TFA)/water(0.1%TFA). 5.4 mg of WHWLQLK(BioACA)PGQPNleDOPA-OH was obtained, yield: 34%. MW: calculated: 2021.43; observed: 2022.56 (Fig. 1B).

Mass spectrometric analysis of peptides:

For matrix-assisted laser-desorption ionization (MALDI) analysis the peptides were resuspended in 50:50 water-acetonitrile with 0.1% trifluoroacetic acid (TFA) at a final concentration of 0.1μg/μL. A 20mg/mL α-cyano-4-hydroxy-trans-cinnamic acid [(α-ACHA), Sigma/Aldrich Chemical Company, St. Louis, MO] matrix was prepared by dissolving recrystallized α-ACHA in 50:50 water-acetonitrile with 0.1% TFA. An equal volume (0.5 μL) of peptide solution was mixed with matrix before spotting on the MALDI plate. The MADLI-TOF spectra were acquired on a Bruker Daltonics (Boston, MA) Microflex using the reflector methods. The tandem mass spectrometry (MS/MS) data was acquired by MALDI post-source decay on a Bruker Daltonics Microflex. The interpretation of the MS/MS data was carried out using Bruker Daltonics BioTools software.

Growth Arrest Assays:

LM102 cells expressing C-terminal FLAG and His tagged Ste2p were grown at 30 ºC in MLT, harvested, washed three times with water and resuspended at a final concentration of 5 x 10^6 cells/ml (24). Cells (1 ml) were combined with 3.5 ml agar noble (1.1 %) and poured as a top agar lawn onto MLT medium agar plate. Filter disks (BD, Franklin Lakes, NJ) impregnated with α-factor or various α-factor analogs were placed on the top agar. The plates were incubated at 30 ºC for 18 hours and then observed for clear halos around the discs. The experiment was repeated at least three times and reported values represent the mean of these tests.

Binding Competition Assays:

This assay was performed using LM102 cells expressing C-terminal FLAG and His tagged Ste2p. Tritiated [^{3}H]-α-factor (10.2 Ci/mmol, 12 μM) prepared as previously described (*24, 27*) was used in competition binding assays on whole cells. The cells were grown at 30 ºC in MLT, harvested, washed three times with YM1 [0.5 M potassium phosphate (pH 6.24) containing 10 mM TAME, 10 mM sodium azide, 10 mM potassium fluoride,and 1% BSA] and adjusted to a final concentration of 2 x 10^7 cells per ml in YM1 plus protease inhibitors [YM1i (29)]. For the competition binding studies, cells (600 μl) were combined with 150 μl of ice cold 5X YM1i supplemented with 6nM [^{3}H]α-factor in the presence or absence α-factor or α-factor analogs and incubated at room temperature for 30 minutes. The final concentrations of α-factor and α-factor analogs ranged from 0.5 x 10^{-10} to 1 x 10^{-6} M. After incubation, triplicate samples of 200 μl aliquots were filtered and washed over glass fiber filter mats using the Standard Cell Harvester (Skatron Instruments, Sterling, VA) and placed in scintillation vials. The radioactivity [^{3}H] on the filter was counted by liquid scintillation spectroscopy. The binding data were analyzed by non-linear regression analysis for one-site competition binding using Prism software (GraphPad Software, San Diego, CA) to determine the binding affinity (K_d) and potency (EC_{50}) for each peptide. The *Ki* values were calculated by using the equation of Cheng and Prusoff, where $Ki = EC50 / (1 + [\text{ligand}] / Kd)$ (17).

DOPA chemical cross-linking:

BJS21 cells expressing C-terminal FLAG and His tagged *STE2* were grown and total cell membranes isolated as previously described (24). Protein concentration was determined by BioRad (BioRad, Hercules, CA) protein assay (23). The membranes were re-suspended in NE-Buffer [20mM HEPES, 20% glycerol, 100mM KCl, 12.5mM EDTA, 0.5mM DTT (18)] incubated with Bio-DOPA-α-factor analogs (1 μM) in the presence or absence of 100 μM α-factor (WHWLQLKPGQPNle^{12}Y), 100 μM α-factor antagonist [desW^{1}desH^{2}WLQLKPGQPNle^{12}Y] (28), 100 μM α-factor synergist [WHWLQLKPGQP] (28), or 2 μg of BSA (bovine serum albumin) for 120 minutes at4 ^{o}C. For periodate mediated cross-linking, a final concentration of 1.0mM $NaIO_4$ was added to the mixture and incubated for 2 minutes. A final concentration of 100mM DTT (1,4-Dithiothreitol) was used to quench the reaction (18). The cross-linked membranes were washed three times with CAPS buffer [N-cyclohexyl-3-aminopropanesulfonic acid (Sigma, St. Louis, MO.), 10 mM, pH 10] by centrifugation to remove non-bound Bio-DOPA. The washed, cross-linked samples were fractionated by SDS-PAGE and then immunoblotted. The blots were probed with an antibody directed against the N-terminal 60 amino acids of Ste2p [generously provided by J. Konopka (30)] and with Neutravidin-HRP conjugate (Pierce, Rockford, IL) to detect the biotin tag on Bio-DOPA pheromone covalently linked to the Ste2p. The signal generated were analyzed using Quantity One software (Version 4.5.1) on a Chemi-Doc XRS photodocumentation system (BioRad, Hercules, CA).

Purification of intact cross-linked Ste2p:

The cross-linked Ste2p was enriched using His-Select^{TM} HC-Nickel affinity gel (Sigma/Aldrich Chemical Co., St. Louis, MO) following the manufacturer's directions. Approximately 10 mg cell membrane containing cross-linked Ste2p were resuspended in ice-cold solubilization buffer (50 mM Tris HCl, pH 7.4, 150 mM NaCl, 1% Triton X-100) with protease inhibitors (PMSF, pepstatin A and leupeptin) and incubated overnight at 4ºC with end-over-end mixing, then centrifuged at 15,000 x g for 30 minutes to remove non-soluble material. The solubilized proteins were then mixed with His-HC-Nickel gel and incubated at 4ºC with end-over-end mixing for 1 hour. The gel was collected by centrifugation at low speed (500 x g, 1 minute) and resuspended and collected four times in wash buffer (50 mM sodium phosphate, pH 8.0, 0.3 M sodium chloride, and 5 mM imidazole). Ste2p was eluted by resuspending the resin in 1 mL ice cold elution buffer (50 mM sodium phosphate, pH 8.0, 0.3 M sodium chloride, and 250 mM imidazole) and incubated at 4ºC with end-over-end mixing for 10 minutes. The resin was pelleted by centrifugation (2000 x g, 1 minute) and the supernatant, containing the eluted Ste2p, transferred to a fresh tube. Purity and concentration of samples was estimated by Coomassie blue and silver staining of SDS-PAGE gels (data not shown). The samples were also analyzed by immunoblotting using an antibody directed against Ste2p (30) and with Neutravidin-HRP conjugate to detect the biotin tag on Bio-DOPA covalently linked to the Ste2p.

Digestion of Cross-linked Ste2p:

The enriched cross-linked Ste2p samples eluted from the His-Nickel column were digested with cyanogen bromide (CNBr). The eluted samples containing Ste2p (~20 μg) were dried by vacuum centrifugation (Thermo Scientific, Waltham, MA) then dissolved in 100%

trifluoroacetic acid (TFA) containing 10 mg/ml CNBr. Deionized distilled water (ddH_2O) was then added to adjust the final TFA concentration to 80%, and the samples incubated at 37°C in the dark for 18 hours (*24, 31*). The samples were dried by vacuum centrifugation and washed three times with ddH_2O, and then 1M Tris (pH 8.0) was added to neutralize the acidic mixture.

Purification of cross-linked Ste2p-fragments:

Fragments from the CNBr digestion of cross-linked Ste2p were resuspended in PBS buffer (0.1 M sodium phosphate, 0.15 M sodium chloride; pH 7), mixed with monomeric avidin resin (Pierce Thermo Scientific, Rockford, IL,USA) and incubated for 6 hours at 4ºC with end-over-end mixing (16). The resin was collected by centrifugation at low speed (1000 x g, 1 minute) and resuspended and collected four times in PBS buffer. The cross-linked Ste2p fragments were eluted by resuspending the resin in 200 µL ice cold elution buffer (0.1 M glycine, pH 2.5) and incubating at 4ºC with end-over-end mixing for 5 minutes. The resin was pelleted by centrifugation (2000 x g, 1 minute) and the supernatant, containing the eluted cross-linked Ste2p fragments, transferred to a fresh tube containing 20 µl of TBS (0.5 M Tris HCl, pH 7.4, 1.5 M NaCl).

MALDI-TOF analysis of cross-linked peptides:

The eluted samples from the avidin resin were further washed and concentrated using a pipette with C18 chromatographic media ($ZipTip_{C18}$ pipette tips; Millipore Corporation, Billerica, MA) following the manufacturer's directions and resuspended in 60% acetonitrile 40% water (0.1% TFA). For MALDI-TOF analysis α-CHCA [20 mg/ml (in 50:50 acetone-isopropanol)] was used as the matrix. The samples (0.5 µL), were either mixed with 0.5 µL of

matrix before spotting on the target or 1.0 μL of matrix was spotted and allowed to dry before applying 1.0 μL of samples (24). MADLI-TOF spectra were acquired on a Bruker Daltonics Microflex using the reflector method. Masses were calculated using PROWL peptide mass prediction tools (32) and also based on the chemistry of the DOPA cross-linking (19).

CHAPTER 3

Results

***Synthesis and Characterization of Bio-DOPA- α-factor**:*

The synthesis of analogs of α-factor containing 3,4-dihydroxyphenylalanine (DOPA) were carried out using automated solid phase synthesis on a WANG resin. The intermediate Fmoc protected peptide was obtained in high yield and purity and was used in the hydroxysuccinimiude mediated addition of biotinylamido caproate (14). The final peptides used in bioassays and cross-linking studies were virtually homogeneous as judged by gradient HPLC and had the expected molecular weights. The structures and MALDI-TOF analyses of α-factor and Bio-DOPA-α-factor analogs are shown in figures 1 and 2, respectively. The MS/MS spectra of the peptides are shown in figure 3. The observed mass of the peptides as determined by MALDI-TOF were similar to masses predicted by the PROWL peptide mass prediction tools (32). The α-factor was observed as 1666.086 Da (predicted, 1665.96 Da), Bio-DOPA^{1} was 1998.762 Da (predicted, 1998.221 Da) and Bio-DOPA^{13} was 2022.560 Da (predicted, 2021.43 Da). On both the α-factor and Bio-DOPA^{13} analogs spectra, 11 out of the 13 *b* ion fragments and 10 out of the 13 *y* ion fragments were observed whereas 9 out of the 13 *b* ion and 5 out of the 13 *y* ion fragments were observed on the Bio-DOPA^{1} spectrum (Figure 3). In the MS/MS analysis of the Bio-DOPA^{1} a mass shift of about 333 Da was observed in *b*7-*b*12 compared to α-factor due to the tagging of biotinylaminocaproate onto Lys7 and the replacement of Trp1 with DOPA. The tagging of biotinylaminocaproate onto Lys7 and the replacement of Tyr13 with DOPA in Bio-DOPA^{13} were observed as evidence of a mass shift of 356 Da from *y*7-*y*13 fragment ions compared to that of α-factor.

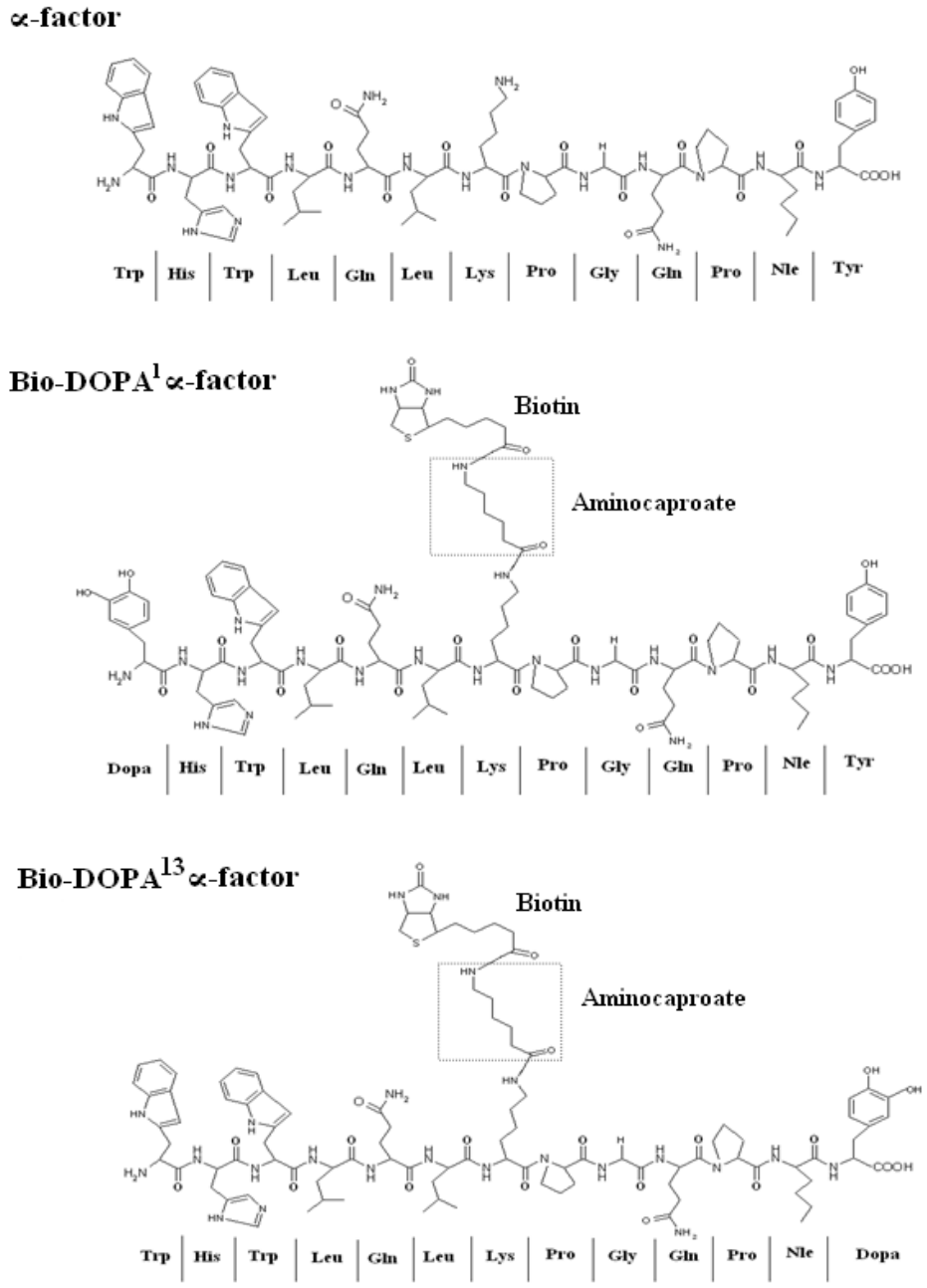

Figure 1: Structures of native and Bio-DOPA α-factor analogs. In Bio-DOAPA[1] and Bio-DOPA[13] Trp1 and Tyr13 residues of α-factor are replaced by DOPA, and biotin is conjugated through its carboxyl group to the ε–amine of Lys7 using aminocaproate as a linker.

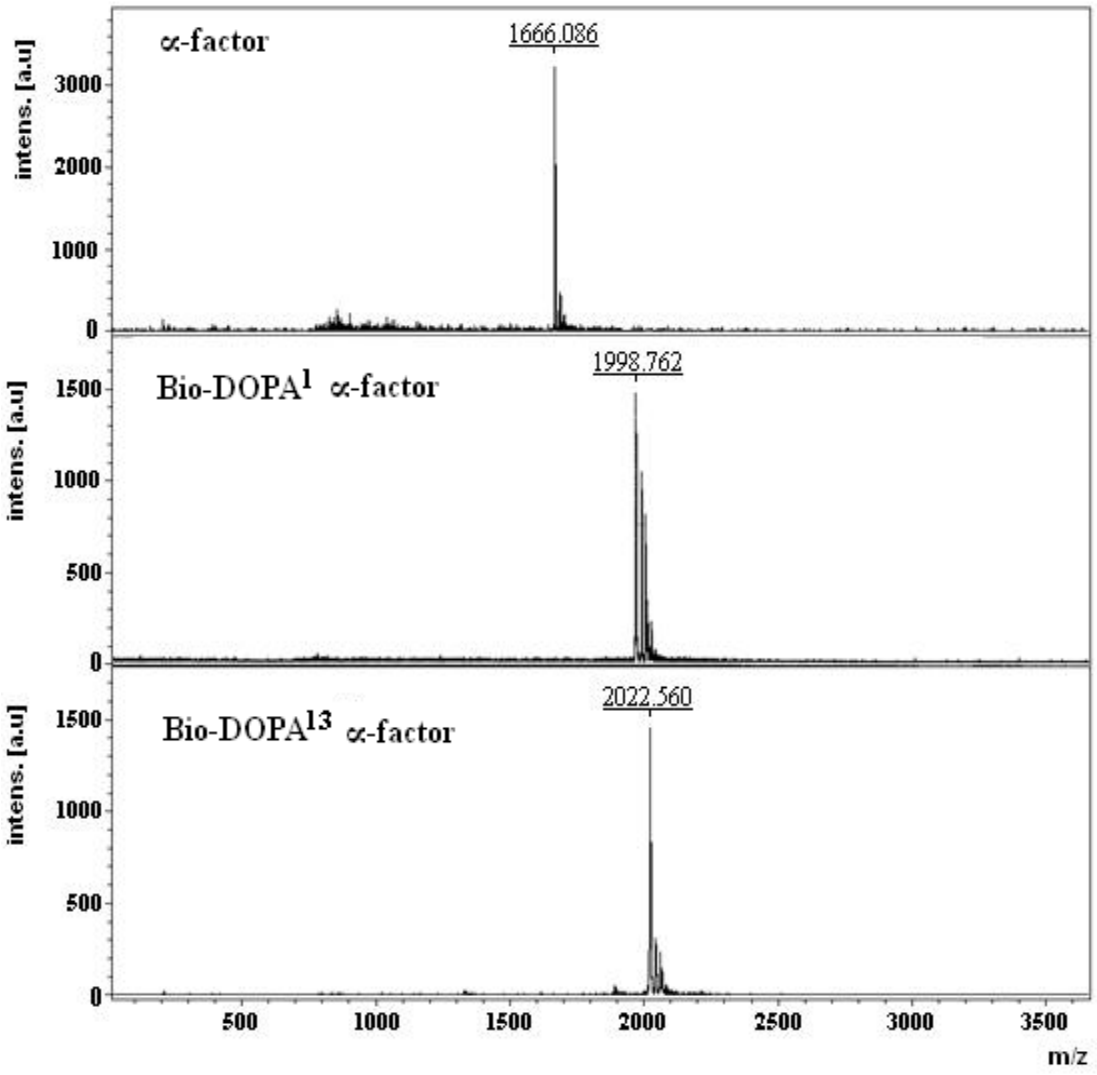

Figure 2: Mass spectrometric analysis of α-factor and Bio-DOPA analogs. The observed masses of the peptides as determined by MALDI-TOF were similar to masses predicted by the PROWL peptide mass prediction tools (32): α-Factor 1665.96 Da; Bio-DOPA^{1} 1998.221 Da and Bio-DOPA^{13} 2021.43 Da..

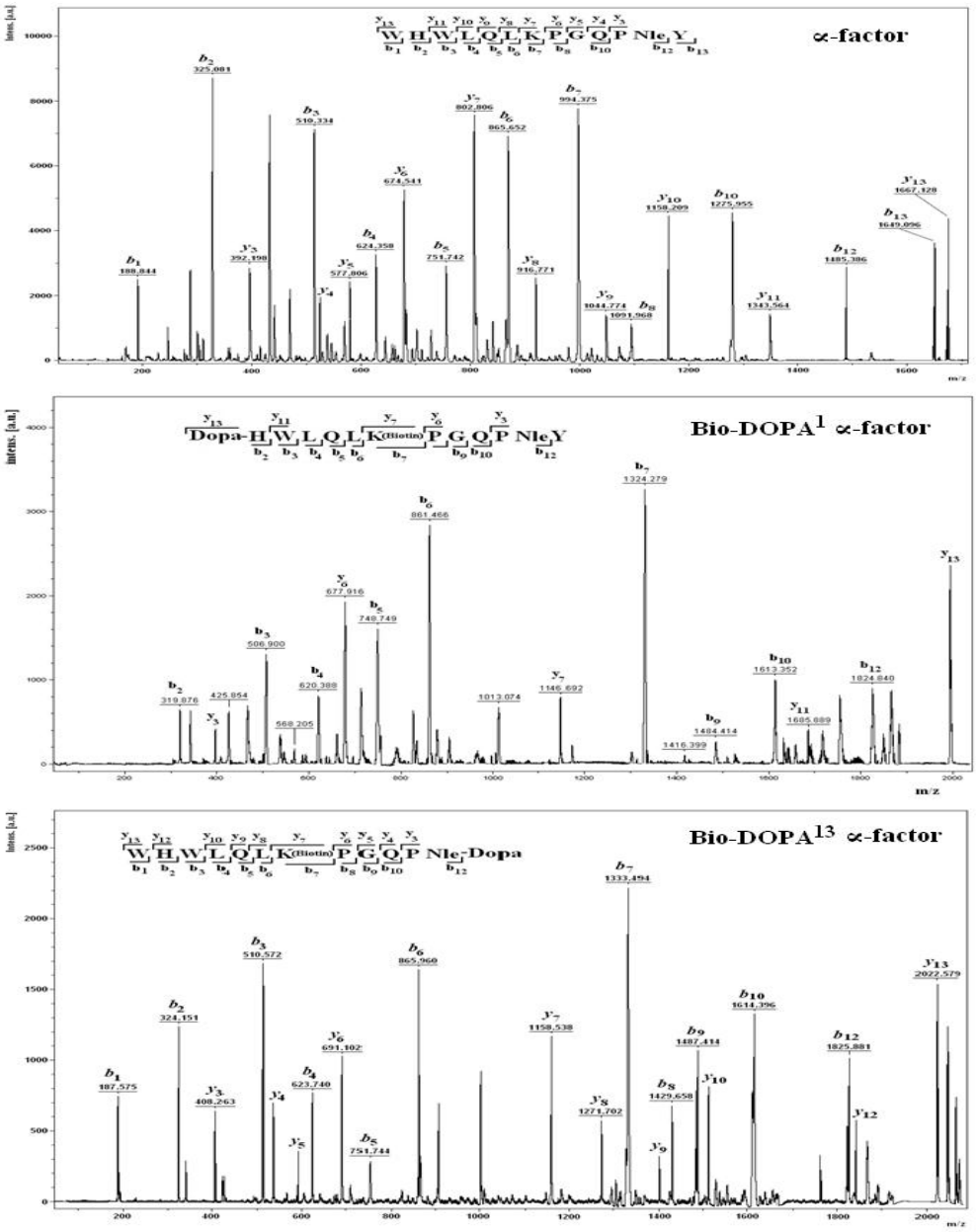

Figure 3: MALDI post-source decay spectra of α-factor and Bio-DOPA peptides. Inserts are one-letter amino acid residue abbreviations of the peptides labeled with the identified ion types. A mass shift of about 333 Da was observed in Bio-DOPA[1] *b*7 to *b*12 fragments whereas Bio-DOPA[13] fragments, *y*7 to *y*13 show a mass shift of 356 Da from fragment ions compared to that of α-factor.

Bioactivity and Binding of Bio-DOPA-α-factor.

Previously, it was reported that Bpa-α-factor analogs were useful for photoaffinity labeling of Ste2p (*14, 15*). The diphenylketone side chain in Bpa is considerably larger than the side chain of any natural amino acid. Because of the structural similarity of DOPA to Tyr and Trp (See Figure 1), we believed that DOPA would make an equal or better replacement than Bpa. Biotin was tagged onto Lys^7 for detection purposes (*16, 33*). α-factor analogs containing DOPA alone without biotin or biotin without DOPA were used as controls. The replacement of DOPA at position 13 [WHWLQLKPGQPNle-Dopa] or ($DOPA^{13}$) α-factor resulted in a biological activity of 83% and binding affinity (*Kd*, 19 nM) of 77 % compared to that of the native α-factor [WHWLQLKPGQPNleY] that had binding affinity (*Kd*) of 12nM (Figure 4B). Whereas Bio-α-factor [WHWLQLK(BiotinACA) PGQPNleY] exhibited a biological activity of 39% and binding affinity of 13%. For Bio-$DOPA^{13}$ [WHWLQLK(BiotinACA)PGQPNle-Dopa] about a 3-fold (35%) and 10-fold (10%) reduction were observed in the biological activity and binding affinity (*Kd*, ~100 nM), respectively (Figure 4B). We concluded that DOPA at position 13 did not significantly alter the interaction of the C-terminus of α-factor with Ste2p. The $DOPA^1$ [Dopa-HWLQLKPGQPNleY] and Bio-$DOPA^1$ [Dopa-HWLQLK(BiotinACA) PGQPNleY]α-factor analogs displayed 3- and 4-fold less activities than the wild-type α-factor, respectively (Figure 4A). For the binding activities, $DOPA^1$-α-factor displayed binding affinity of 20 nM and Bio-$DOPA^1$ was 66.4 nM (Figure 4B). Thus, the replacement of Trp at postion 1 with DOPA in α-factor affected the ability of the peptide to activate Ste2p but did not affect the binding affinity. Thus, the reduction in the activities of Bio-$DOPA^{13}$ and Bio-$DOPA^1$ were mainly due to tagging with biotin and not the DOPA replacement.

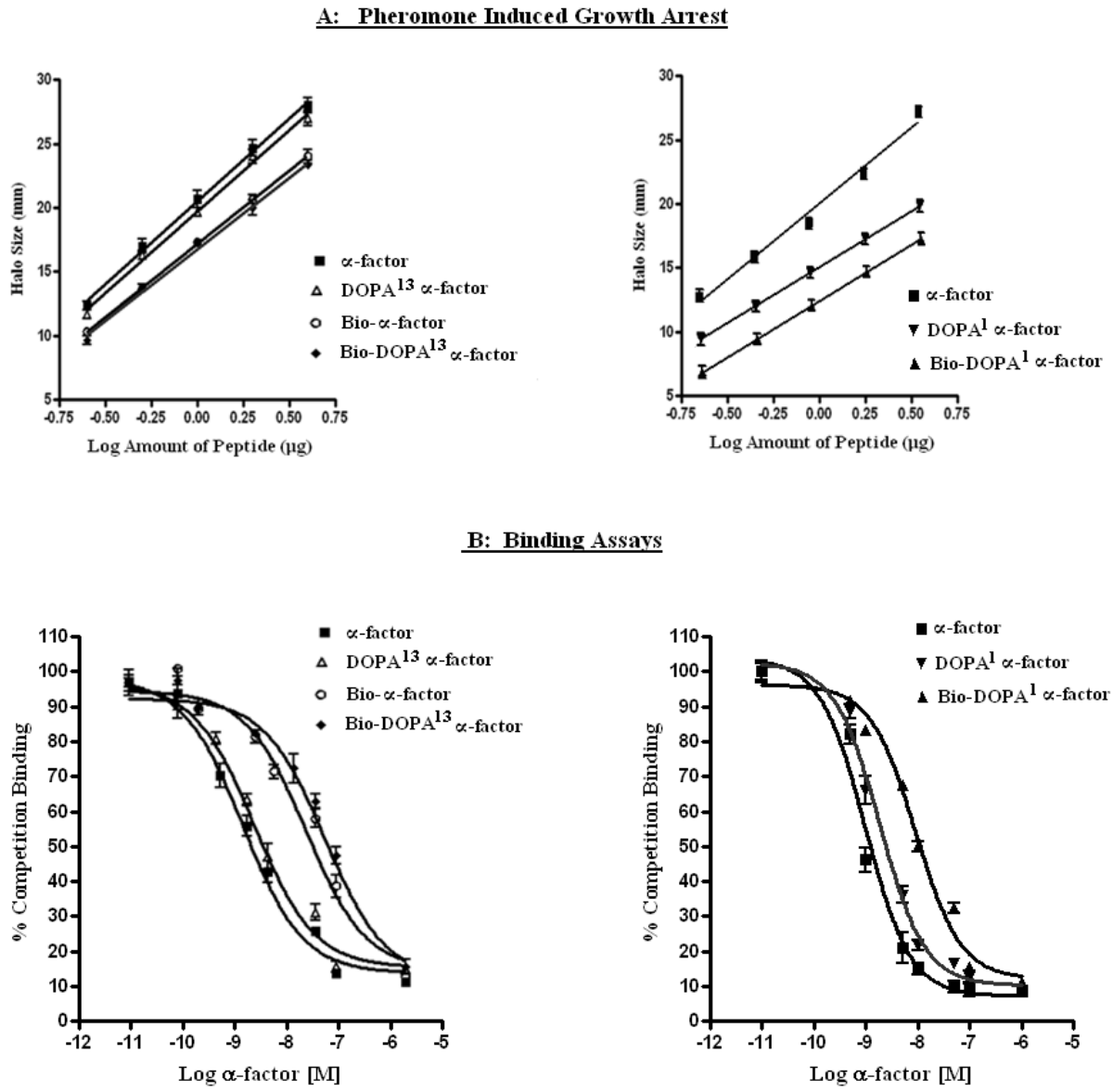

Figure 4: Biological and binding assays of DOPA-containing α-factor analogs. A: Growth arrest assay to determine the ability of the peptides to activate α-factor receptor, Ste2p. B: The binding of the peptides were determined by competition binding with [^{3}H]α-factor for Ste2p. The assays are described in detail in the Experimental Procedures

Bio-DOPA α-factor analogs Cross-link into Ste2p:

Membranes from cells expressing Ste2p (His and FLAG tagged) were incubated with Bio-DOPA-α-factor and cross-linked by periodate oxidation. Cross-linking was carried out in the absence or presence of α-factor, an α-factor antagonist, a synergist, or BSA as controls to evaluate the specificity of the cross-linking. The antagonist binds to Ste2p with high affinity and the synergist does not bind to Ste2p yet influences its biological activity (28). Following incubation with the peptide probes, the membranes were treated with sodium periodate to oxidize DOPA and initiate cross-linking. The reaction was quenched with DTT. Membrane proteins were resolved on SDS-PAGE, blotted, and then probed with anti-FLAG antibody to detect Ste2p (Ste2p tagged with FLAG epitope tag) or NeutrAvidin HRP (Na-RHP) to detect biotin attached to Bio-DOPA α-factor analogs (Figure 5). A band (~52-54 kDa) corresponding to the size of Ste2p was observed in all lanes on blots probed with the anti-FLAG and all these lanes shows similar signal intensity of the Ste2p band. When the immunoblots were probed with Na-HRP a distinct band at 54 kDa was detected in the lane where Bio-DOPA α-factor analogs were oxidized in the presence of Ste2p. This band was absent in samples that were not treated with Bio-DOPA α-factor analogs, indicating that the ~54 kDa is a Ste2p-[Bio-DOPA]α-factor (~52 kDa + ~2 kDa) cross-linked product. The cross-linking was nearly eliminated in the presence of excess (100-fold) α-factor and significantly reduced in the presence of a 100-fold excess of the α-factor antagonist in both the Bio-DOPA^{1} and Bio-DOPA^{13} reactions. In the presence of BSA no effect on the level of cross-linked product was observed. However, in the presence of α-factor synergist about 70% reduction of cross-linking signal was observed in Bio-DOPA^{1} but no significant reduction in the Bio-DOPA^{13} reaction.

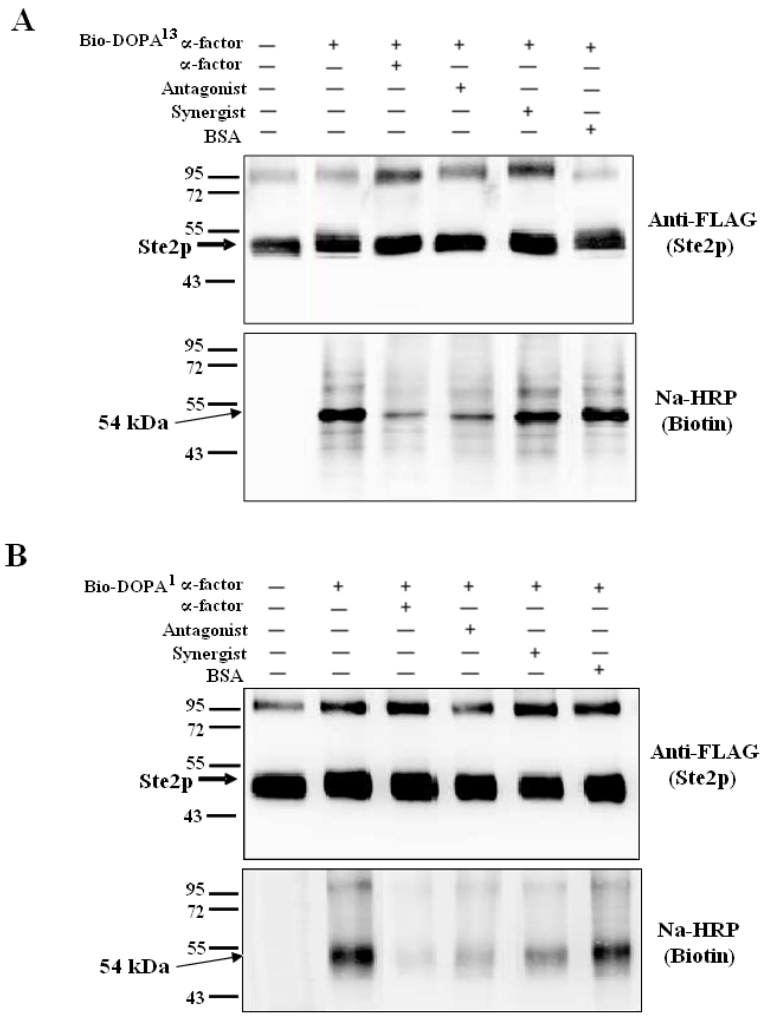

Figure 5: Bio-DOPA α-factor analogs chemical cross-linking into Ste2p. Cell membranes containing wild type Ste2p were incubated with Bio-DOPA analog alone or with Bio-DOPA analog in the presence of 100-fold wild-type α-factor, antagonist, synergist, or BSA. The membranes were treated with sodium periodate to oxidize DOPA and initiate cross-linking, and the reaction was quenched with DTT. The samples were resolved on SDS-PAGE and probed with anti-FLAG to detect Ste2p and with Neutravidin-HRP conjugate (Na-RHP) to detect the biotin tag on Bio-DOPA-α-factor. Blots images of Bio-DOPA^{13} (A) and Bio-DOPA^{1}.(B) cross-linking are shown.

As a control for the cross-linking of Bio-DOPA-α-factor into Ste2p, membranes prepared from cells devoid of Ste2p were mixed with Bio-DOPA α-factor analogs and treated with sodium periodate under the same conditions. No detectable signal was observed on the anti-Ste2p antibody blots in the Ste2p-devoid samples (Figure 6), however, a weak signal (~52 kD) similar in size to that of Ste2p was detected on blots of membranes probed with Na-HRP that was the result of non-specific association of the Bio-DOPA^{13} with a membrane protein(s) in a Ste2p-independent manner. To remove Bio-DOPA-α-factor that was noncovalently associated with Ste2p, Bio-DOPA-α-factor treated membranes from cells expressing Ste2p and lacking Ste2p were mixed with a His-HC Nickel resin after the cross-linking reaction. A distinct band (~54 kDa) corresponding to a cross-linked product of Ste2p and Bio-DOPA-α-factor was observed in enriched samples (Lanes labeled "P") from cross-linked membranes containing Ste2p both on the anti-Ste2p antibody and Na-HRP blots. However, this band was absent in the Ste2p deletion mutant (Lane "P"). Thus, Bio-DOPA^{13} remained linked to Ste2p even after the harsh treatment for purifying Ste2p, indicating that a stable cross-link existed between Ste2p and Bio-DOPA^{13}. Moreover, the Bio-DOPA^{13} that associated with non-Ste2p proteins could be completely removed by this treatment.

Phe^{55}-Met^{69} cross-linked to Bio-DOPA^{13}.

The cross-linked Ste2p samples were purified using His-HC Nickel resin and treated with CNBr to fragment Ste2p. The digest was mixed with avidin beads to capture the CNBr fragment of Ste2p cross-linked to Bio-DOPA-α-factor.

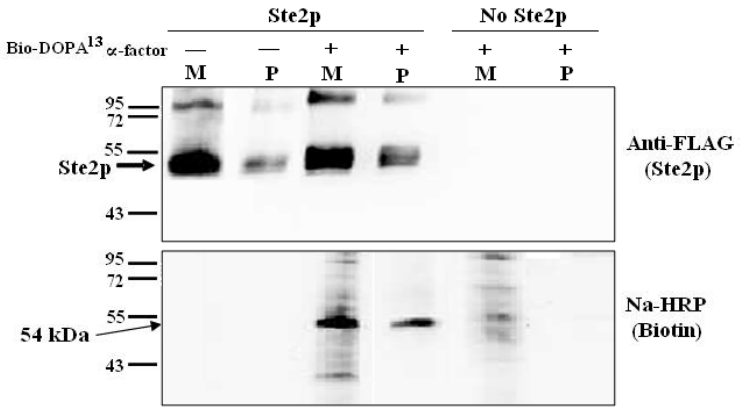

Figure 6: Immunoblot analysis of Bio-DOPA^{13} reaction with membranes lacking Ste2p. Cell membranes containing and lacking Ste2p were treated with Bio-DOPA^{13} for cross-linking. The samples were separated on SDS-PAGE and probed with an anti-FLAG antibody directed against Ste2p and with Na-HRP to detect Bio-DOPA^{13}. **M** indicates membrane extract; **P** indicates enriched (purified) samples from His-HC Nickel resin.

Samples were eluted from the avidin beads with 0.1M glycine, pH 2.5 and were concentrated using a Millipore ZipTip to remove detergent and compounds that might interfere with mass spectrometry analysis (34). MALDI-TOF analysis Bio-DOPA^{13} cross-linking (Figure 7A) showed that the eluted sample contained two peaks, 3497.01 and 3815.21 Da, corresponding to a CNBr-Ste2p fragment, F^{55}-M^{69} (1473.81 Da, assuming a homoserine lactone terminus) cross-linked to Bio-DOPA^{13} (2021.43 Da)[Total calculated mass = 3494.24; Observed mass = 3497.01], and a CNBr-Ste2p fragment F^{55}-M^{71} (1792.22 Da, assuming a homoserine lactone terminus) cross-linked to Bio-DOPA^{13} (2021.43 Da) [Total calculated mass = 3812.65, Observed mass = 3815.21], respectively. The calculated masses were based on M +1H (mass spectrometric ionization) and the loss of 2H from the cross-linking reaction.

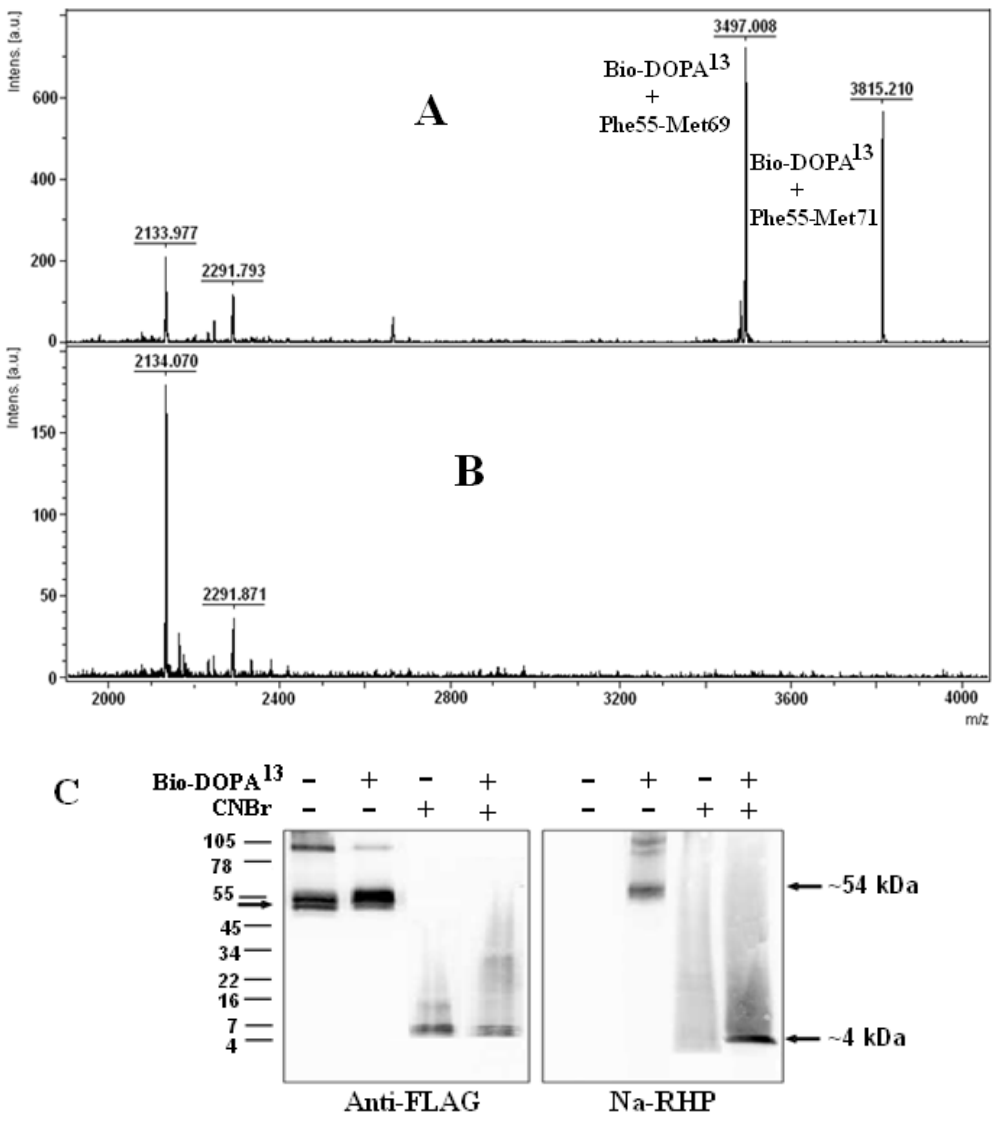

Figure 7: MALDI-TOF analysis of CNBr digested Ste2p-Bio-DOPA^{13} cross-linked peptides.

A: spectrum for samples eluted from avidin resin cross-linked Ste2p samples. The 3497 and 3815 Da peaks correspond to Ste2p fragments F^{55}-M^{69} and F^{55}-M^{71} cross-linked to Bio-DOPA^{13} respectively. **B**; spectrum for samples eluted from avidin resin from CNBr digested Ste2p without cross-linking. Two major peptides were detected which were also observed in cross-linked Ste2p samples. **C**: immunoblot analysis images of samples used for the MALDI-TOF.

Two additional peaks (2134 and 2291) were also found in the cross-linked sample and a sample eluted from avidin beads mixed with CNBr-treated Ste2p that had not been subjected to cross-linking (Figure 7B). Thus, these additional peaks were associated with peptides that were co-purified with Ste2p during the enrichment with the His-HC Nickel resin and were also retained by the avidin beads.The CNBr treated cross-linked Bio-DOPA^{13} purified samples used for the MALDI-TOF analysis were also resolved on SDS-PAGE. The results (Figure 7C) also suggested about a the Ste2p-Bio-DOPA^{13} cross-linked fragment is about 4 kDa as observed on the Na-RHP blot in lanes treated with Bio-DOPA^{13} but not in lanes without the Bio-DOPA^{13} treatment. A fragment of about 6 kDa corresponding to the C-terminus of the Ste2p containing the FLAG epitope tag was observed in all lanes treated with CNBr on the anti-FLAG blot. This implies that the Ste2p samples were digested by the CNBr.

Ser251-Met294 cross-linked to Bio-DOPA^{1}.

MALD-TOF analysis of the Bio-DOPA^{1} cross-linking samples (Figure 8A) show that the sample eluted from the avidin resins contained a 6571.883 Da fragment, but the Ste2p without crosslinking (8B) had no detectable fragment. The 6571.883 Da peak corresponds to Ste2p fragment Ser251-Met294 (4572.455 Da) cross-linked to Bio-DOPA^{1} α-factor (1998.221 Da). The observed mass (6571.883) on the MALDI-TOF spectrum is similar to the calculated mass (6568.676 Da). The same samples used for MALDI-TOF analysis revealed that the Ste2p-Bio-DOPA^{1} cross-linked fragment is about 7 kDa as observed on the Na-RHP immunoblot (Figure 8C, lanes treated with Bio-DOPA^{1}). The MS/MS analyses (Figure 9 and Table 1) confirmed that Bio-DOPA^{1} reacted with Ser251-Met294 and probably with Lys269.

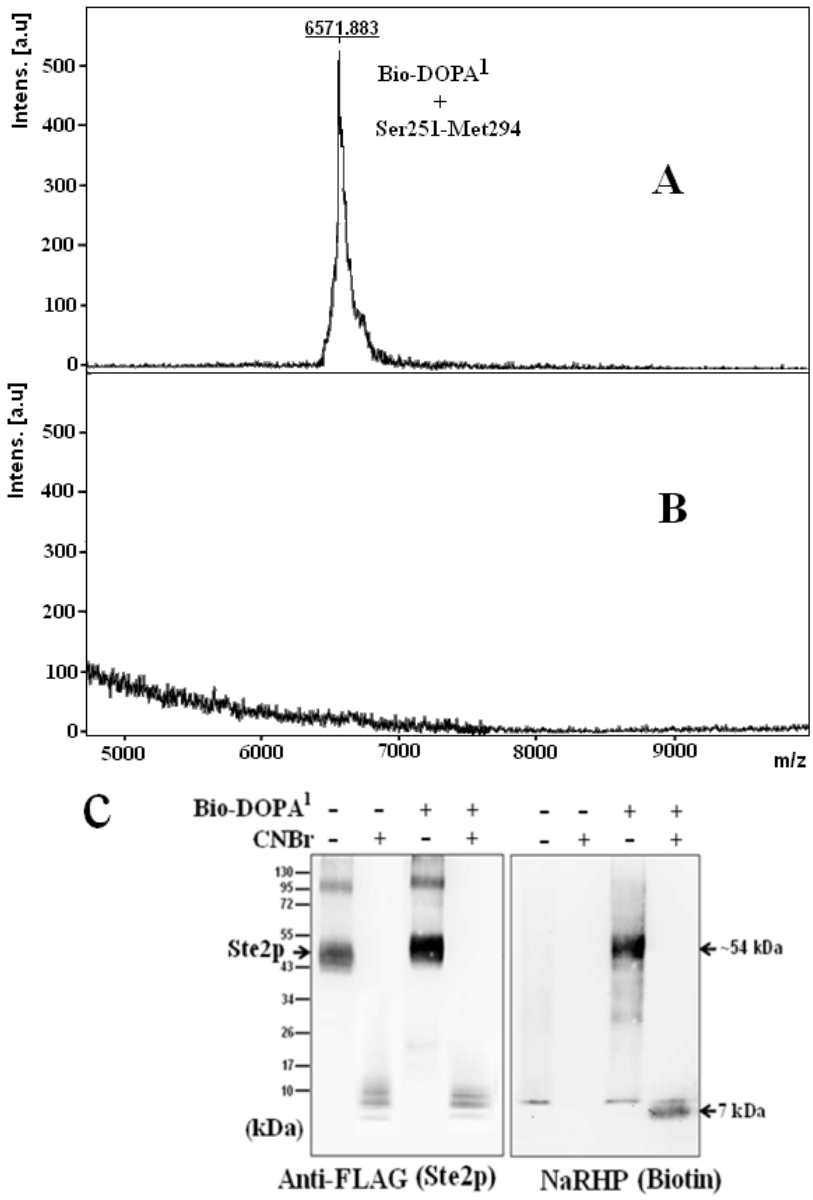

Figure 8: MALDI-TOF analysis of Ste2p-Bio-DOPA1 crosslinked fragment. **A**: Ste2p- Bio-DOPA[1] crosslinked spectrum of peptides eluted from avidin resin. A 6571.883 Da peak corresponds to Ste2p fragment, Ser251-Met294 (4572.455 Da) cross-linked to Bio-DOPA[1] α-factor (1998.221 Da) was observed. **B**: Spectrum sample eluted from avidin mixed with CNBr-treated Ste2p (without cross-linking). **C**: Image of immunoblot analysis of samples used for MALDI analysis. A band at about 7 kDa is observed in Bio-DOPA[1] treated lane.

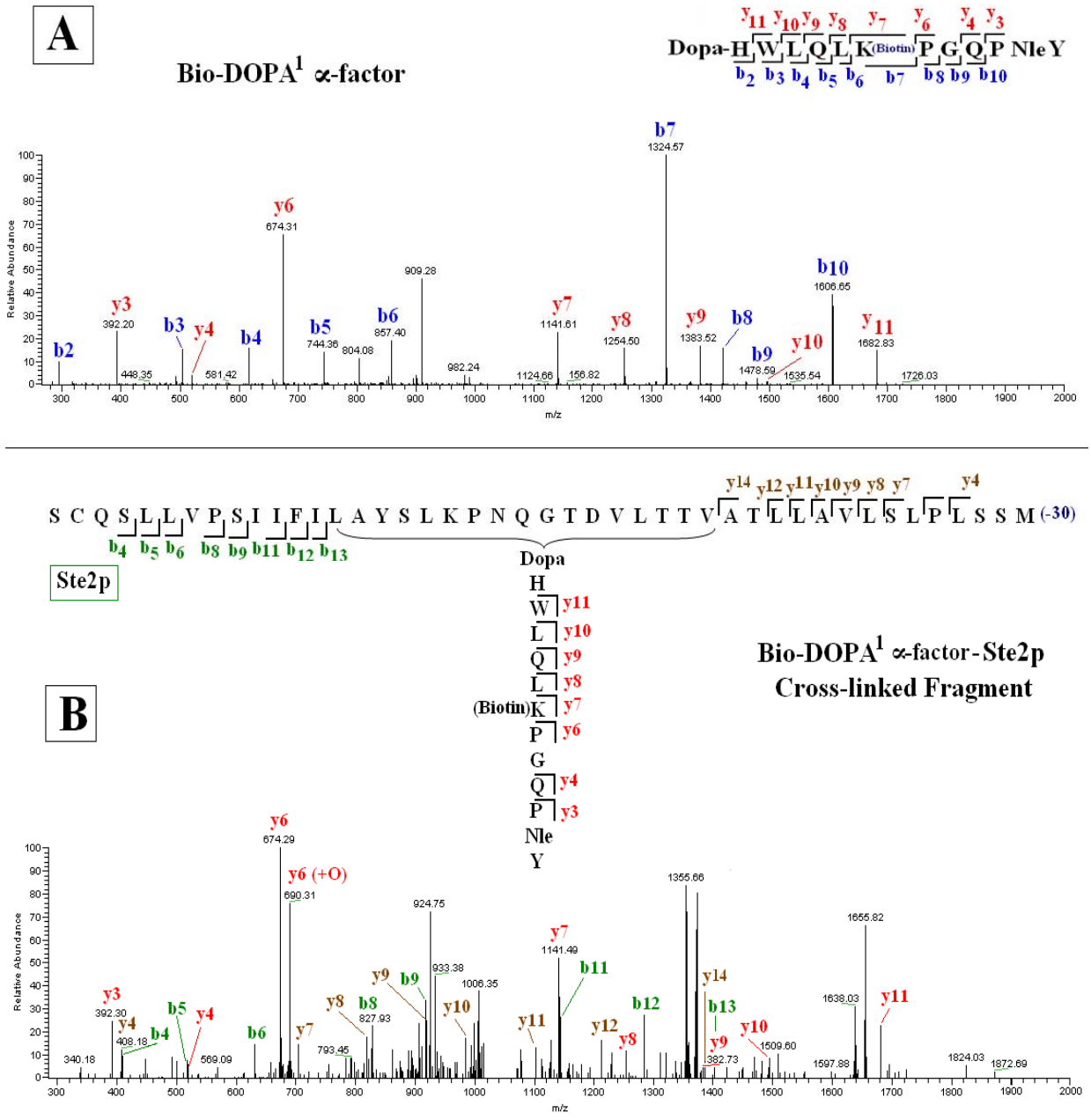
A
Bio-DOPA[1] ∝-factor
Dopa-H W L Q L K(Biotin) P G Q P NleY
b7
1324.57
y6
674.31
b10
1606.65
y3
392.20
b3
y4
b4
b5
744.36
b6
857.40
909.28
y7
1141.61
y8
1254.50
y9
1383.52
b8
y11
1682.83
b2
b9
1478.59
y10
1535.54
448.35
581.42
804.08
982.24
1124.66
156.82
1726.03
Relative Abundance
m/z
B
S C Q S L L V P S I I F I L A Y S L K P N Q G T D V L T T V A T L L A V L S L P L S S M (-30)
Ste2p
Dopa
H
W y11
L y10
Q y9
L y8
(Biotin)K y7
P y6
G
Q y4
P y3
Nle
Y
Bio-DOPA[1] ∝-factor-Ste2p
Cross-linked Fragment
y6
674.29
y6 (+O)
690.31
924.75
1355.66
1655.82
y7
1141.49
b11
933.38
1006.35
y14
y9
b9
y3
392.30
y8
b8
827.93
b13
y11
1638.03
b5
y4
y10
b12
y4
408.18
b4
y10
1509.60
b6
y7
y11
y12
y8
y9
793.45
382.73
340.18
569.09
1597.88
1824.03
1872.69
Relative Abundance
m/z

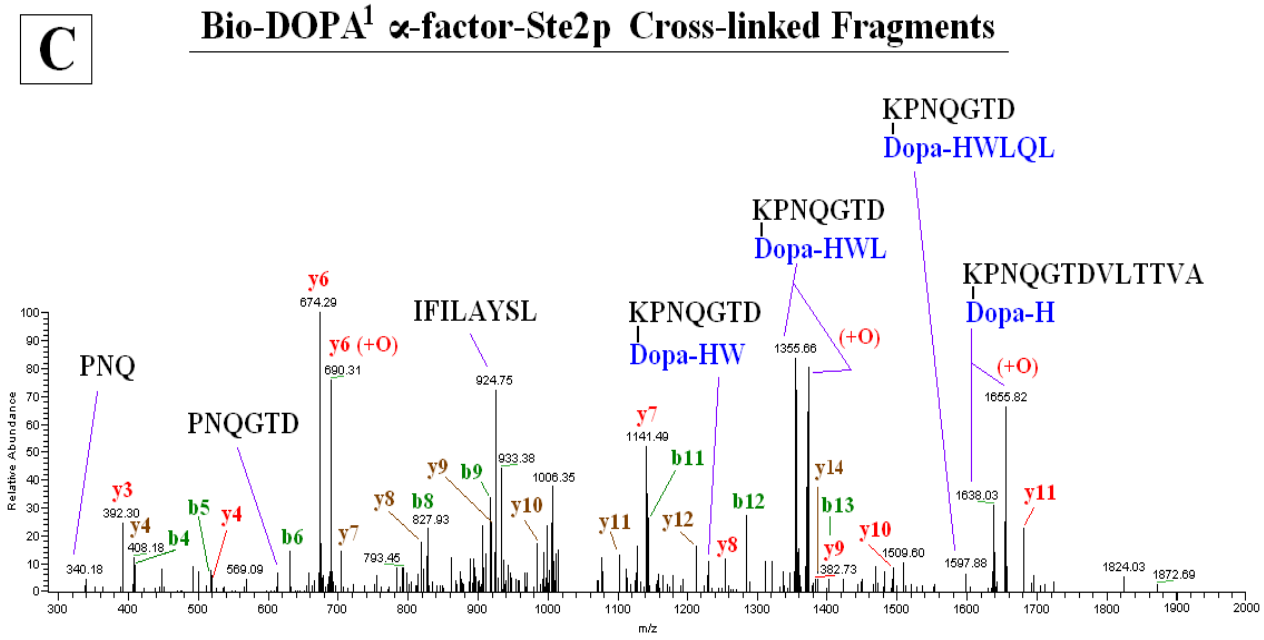

Figure 9: MS/MS analysis of Bio-DOPA[1]-Ste2p cross-linked fragments. Inserts are one-letter amino acid residue abbreviations of the fragment labeled with the identified ion types. **A:** MS/MS spectrum of fragment Bio-DOPA[1] α-factor. The spectrum shows that 9 and 8 out of 13 *b*- and *y*-ion fragments, respectively. **B:** MS/MS spectrum of the cross-linked fragment. Only the *y*-ions of Bio-DOPA[1] α-factor were identified. In the Ste2p fragment (Ser251-Met294) 8 b-ions representing the N-terminus and 8 y-ions representing the C-terminus were identified. C: fragment ions corresponding to internal fragments of the cross-linked peptide are labeled with their amino acid sequences. Lys269 in Step is observed to cross-link to Bio-DOPA[1] α-factor in some of the fragments. The oxidized form (+O) of some of the fragments were also observed. A list of observed masses (m/z) of the fragment ions in all the spectra compared to the theoretical masses are shown on Table 1 below.

Table 1. A list of observed masses of fragment ions in the Bio-DOPA[1] cross-linked spectra.

Bio-DOPA[1] Spectrum fragments				
ion number	b ions (m/z)		y ions (m/z)	
	Expected	Observed	Expected	Observed
2	317.33	317.15		
3	503.54	503.31	392.47	392.20
4	616.70	616.21	520.61	520.39
5	744.833	744.36		
6	857.99	857.40	674.77	674.31
7	1325.46	1324.57	1142.24	1141.61
8	1422.58	1421.70	1255.41	1254.50
9	1479.64	1478.59	1383.54	1383.52
10	1607.77	1606.65	1496.70	1496.92
11			1682.91	1682.83

Bio-DOPA[1]-Ste2p Cross-linked Spectrum fragments						
Fragment ion number	Ste2p fragments (S251-M294)				Bio-DOPA[1] fragments	
	b ions (m/z)		y ions (m/z)		y ions (m/z)	
	Expected	Observed	Expected	Observed	Expected	Observed
3	406.44	406.48	407.54	408.18	392.47	392.30
4	519.60	519.20			520.61	520.20
5	632.76	631.36				
6			704.89	704.47	674.77	674.29
7	829.01	827.93	818.05	819.21	1142.24	1141.49
8	916.09	916.68	917.18	918.01	1255.41	1254.66
9			988.26	988.82	1383.54	1382.73
10	1142.41	1142.65	1101.42	1102.53	1496.70	1497.92
11	1289.58	1289.02	1214.58	1213.59	1682.91	1681.60
12	1402.74	14021				
13						
14			1386.76	1386.48		

Bio-DOPA[1] -Ste2p Spectrum fragments		
	Fragment size (m/z)	
Residues	Expected	Observed
PNQ	339.37	340.18
PNQGTD	612.61	613.45
IFILAYSL	922.81	924.75
(Dopa-HW) $_+$ KPNQGTD	1243.32	1244.41
(Dopa-HWL) $_+$ KPNQGTD	1356.48	1355.66
(Dopa-HWL) $_+$ KPNQGTD (+O)	1374.56	1373.76
(Dopa-HWLQL) $_+$ KPNQGTD	1597.77	1597.88
(Dopa-H) $_+$ KPNQGTDVLTTVA	1639.82	1638.03
(Dopa-H) $_+$ KPNQGTDVLTTVA (+O)	1657.01	1655.82

Bio-DOPA^{13} cross-links to Cys59:

It has been shown previously that the sulfhydryl group of cysteine is able to covalently cross-link to DOPA upon sodium periodate-mediated oxidation (19). Since Cys is part of the Ste2p fragment detected in the Ste2p-Bio-DOPA^{13} fragment, we carried out a cross-linking experiment with a cysteine-less Ste2p (Cys59Ser, Cys252Ser). Membranes were prepared from cells expressing Ste2p wild-type, the cysteine-less mutant, or no Ste2p. The cross-linking and enrichment of Ste2p were carried out as described above. The immunoblot analysis (Figure 10A) showed that cross-linking of Bio-DOPA^{13} into the cysteine-less Ste2p was 83% less efficient in comparison to the wild-type receptor, although similar levels of Ste2p signal were detected in both the wild-type and Cys-less samples. Bio-DOPA^{13} cross-linked to a Cys59Ala in a wild-type background (maintaining Cys at 252) showed the same low level of cross-linking as that of the Cys59Ser mutant. Cross-linking of Bio-DOPA^{1} to the Cys-less receptor was not affected as (Figure 10C) indicating that the reaction of Bio-DOPA^{13} with Cys59 is specific.

Previous studies in our lab have suggested that the N-terminus of α-factor may interact with Tyr266 or Tyr203 in Ste2p (*35*). We therefore carried out the cross-linking of the Bio-DOPA^{1} with membranes of cells expressing Tyr266Cys (Y266C) and Tyr203Cys (Y203C) to test whether the presence of Cys at position 266 or 203 would affect cross-linking with Bio-DOPA^{1}. These Cys mutants have the endogenous two cysteine residues replaced with serine residues (C59S, C252S) similar to the Cys-less receptor and bind α-factor effectively (*35, 36*). The cross-linking results indicated that Bio-DOPA^{1} cross-linking with the Y266C or Y203C were similar to the wild type. However, Bio-DOPA^{13} cross-linking was reduced in the Y266C and Y203C similar to the Cys-less receptor.

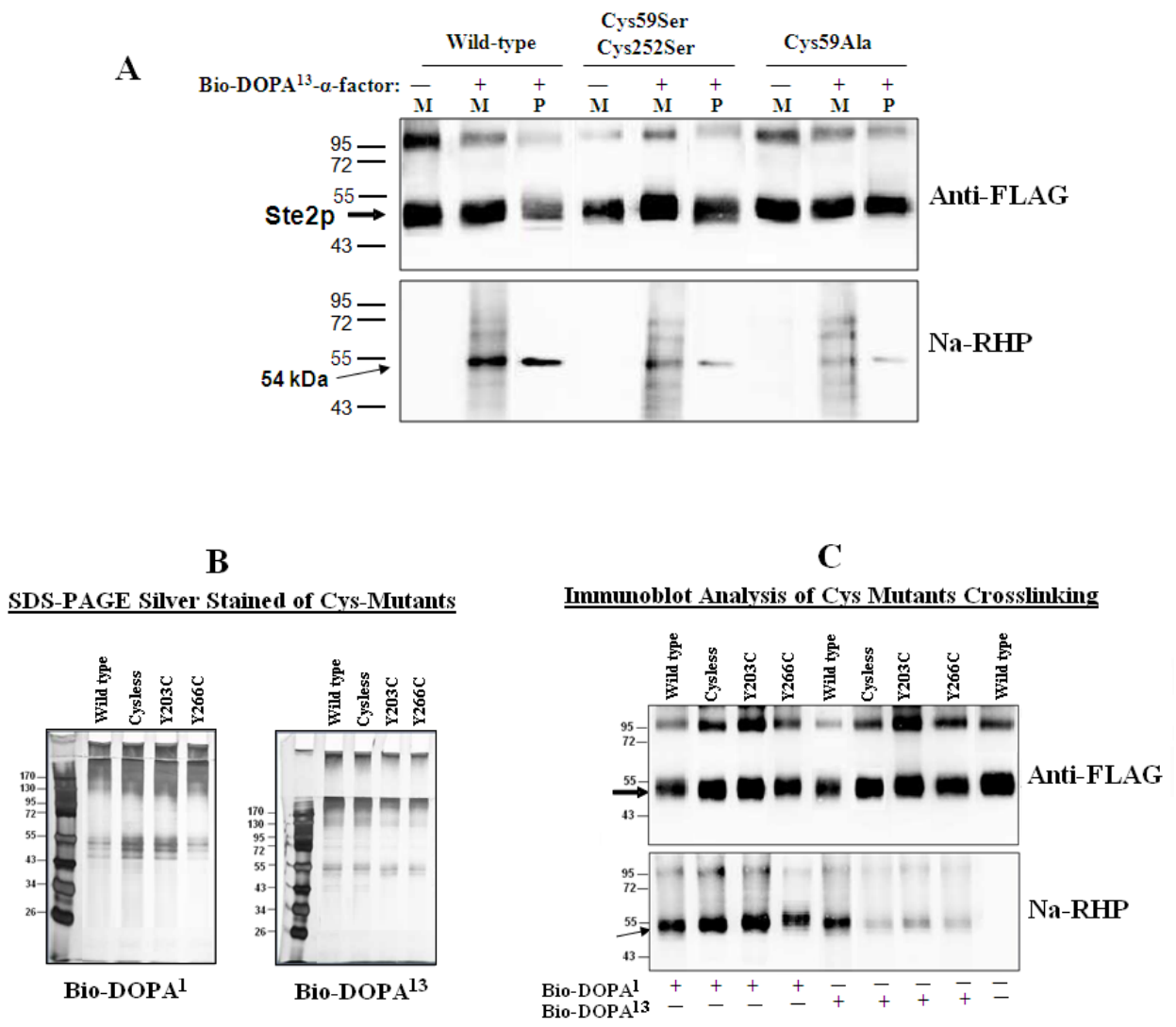

Figure 10: Cross-linking of Bio-DOPA α-factor analogs to Ste2p Cys mutants. A: immunoblot analysis of Cys-less and Cys59Ala mutant cross-linking with Bio-DOPA^{13}. M indicates membrane extract; P indicates enriched (purified) samples from His-HC Nickel resin. B: Silver stained SDS-PAGE of purified Cys-mutants cross-linked with Bio-DOPA analogs. C: immunoblot analysis of the cross-linked Cys mutants purified samples. All Cys mutants cross-linked efficiently with Bio-DOPA^{1} but showed reduced cross-linking with Bio-DOPA^{13}.

CHAPTER 4

Discussion

Cross-linking studies followed by mass spectrometry analysis of the product has become increasingly used to elucidate contacts between ligands and their cognate receptors (*37*). In addition, a few studies have pin-pointed a residue-to-residue interaction between a peptide and its GPCR using photoaffinity labeling (*38-42*). Ste2p, the α-factor pheromone receptor of *Saccharomyces cerevisiae*, has been used as a model for interactions between small peptides and GPCRs. Photochemical cross-linking, site-directed mutagenesis, and double mutant-cycle analysis approaches concluded that residues 1, 3, 10 and 13 of α-factor are involved in binding to Ste2p (*13, 43-46*). Several regions of Ste2p that contact α-factor were previously identified (*14-17, 24, 47*). However, in no case was the exact residue-residue interaction between α-factor and Ste2p determined.

Periodate-mediated cross-linking of DOPA has been shown to result in a stable covalent cross-link between interacting polypeptides (*19, 20*). DOPA-mediated cross-linking was previously shown to be efficient and specific as only one protein was labeled using a mixture of ten proteins (18). The methodology revealed contacts between Rpt6p/Sug1p and Rpt4p/Sug2p proteins and the Gal4 transcriptional activation domains (21) and was also used to investigate peptoid-inhibitor interactions with the 19S regulatory particle of the 26S proteasome (22). However, none of these studies defined the contact points between cross-linked molecules. The present study was conducted to explore the utility of 3,4-dihydroxylphenylalanine (DOPA) oxidative chemical cross-linking in analyzing hormone-receptor interactions. The interaction of GPCR, Ste2p, and its cognate peptide ligand, α-factor, was used as the test system.

The results presented in this paper show that replacement of Trp1 or Tyr13 by DOPA in α-factor results in a high affinity, potent agonist (Figure 4). Comparisons with control peptides allow the conclusion that the DOPA moiety in the Bio-DOPA α-factor peptides used in cross-linking studies likely binds similarly to the phenol side chain in the native peptide. Thus reaction of this moiety with groups on the receptor should lead to information relevant to the natural ligand.

DOPA chemical cross-linking studies carried out using membranes prepared from cells expressing Ste2p showed that Bio-DOPA^{1} and Bio-DOPA^{13} cross-linked into Ste2p. When the cross-linking was carried out using membranes lacking Ste2p under the same conditions only a small signal was observed and this was totally removed by treatment with an affinity column that recognized Ste2p (Figure 6). The cross-linking of Bio-DOPA-α-factor analogs to Ste2p was prevented by 100-fold molar excess native α-factor and highly reduced by a lower affinity α-factor antagonist (28) but it was not influenced by the presence of BSA. These results showed that Bio-DOPA-α-factor binds and cross-links to the ligand binding site in Ste2p and that it could be used to determine the contact between positions 1 and 13 of α-factor and this GPCR.

The strong interaction between avidin and biotin has been very useful in affinity purification of biotinylated peptides (34) and together with MS analysis is widely used for detection of cross-linked products with high sensitivity and accuracy (*48*). We reported previously on the purification and MS analysis of a biotinylated-α-factor cross-linked to a portion of Ste2p (16). We applied this approach to analyze the cross-linking between Bio-DOPA-α-factor and Ste2p. The cross-linked Ste2p samples were fragmented with cyanogen bromide (CNBr) and the biotinylated fragments were captured by affinity purification. MALDI-TOF analysis of the CNBr fragments from cross-linked Bio-DOPA^{13} with Ste2p showed two

major peaks, 3497 and 3815 Da (Figure 7A). In addition, two other peaks (2134 and 2291 Da) were detected which were also detected in samples from uncross-linked CNBr-treated Ste2p samples (Figure 7B). These two minor peaks (2134 and 2291 Da) were due to proteins that were co-purified with Ste2p during the enrichment with the His-HC Nickel resin as observed on silver and comassie stained SDS-PAGE gels (data not shown). Since the two major peaks (3497 and 3815 Da) were only observed in the cross-linked Ste2p samples, we concluded that these fragments are composed of parts of Ste2p cross-linked to Bio-DOPA-α-factor. Examination of the predicted sizes of CNBr fragments of Ste2p and the peaks detected revealed that the peak 3497.01 Da corresponded to a CNBr-digested Ste2p fragment, Phe^{55}-Met^{69} (1473.81 Da) cross-linked to Bio-DOPA (2021.43 Da), whereas the 3815.21 Da peak corresponded to a CNBr-digested Ste2p fragment Phe^{55}-Met^{71} (1792.22 Da) cross-linked to Bio-DOPA (2021.43 Da). The approximately 3 Da difference between both experimental peaks and the theoretical values was due to averaging the observed isotopic mass of the peptides (32). On the basis of this result and previous studies showing that [Bpa^{13}]α-factor analog cross-linked to residues Phe^{55}-Arg^{58} of Ste2p, we suggest that position 13 of α-factor interacts with a residue(s) within Phe^{55}-Met^{69}.

Previous investigations determined that the ε-amino of lysine, the imidazole of histidine, and the thiol of cysteine were capable of attacking the ortho-quinone obtained on periodate oxidation of DOPA (19). Based on these findings, the only nucleophilic side chain within the residues Phe^{55}-Met^{69} (^{55}FGVRCGAAALTLIVM^{69}) that could attack the ortho-quinone intermediate is Cys^{59}. To efficiently couple to DOPA, the thiol group of cysteine and DOPA must be in close proximity (19). Thus our results suggest that DOPA at position 13 of Bio-$DOPA^{13}$ cross-links to Cys^{59} of Ste2p and that residue 59 of Ste2p and residue 13 of the α-factor ligand must be close proximity in the ligand bound state of the receptor.

To investigate whether DOPA in Bio-DOPA^{13} cross-linked to Cys^{59} of Ste2p, experiments were repeated using membranes containing cysteine-less Ste2p mutant. This mutant receptor has similar activities as the wild-type receptor (23). Immunoblotting analysis (Figure 10) showed that cross-linking of Bio-DOPA^{13} into the cysteine-less Ste2p and Cys mutants (Y266C and Y203C) was over 80% less efficient compared to wild-type. This experiment was repeated at least three times and similar results were obtained. We also changed Cys to Ala at position 59 while maintaining Cys at position 252. This construct showed a similar reduction in cross-linking indicating that the majority of the cross-linked product involved Cys59 (Figure 10A). Thus, the substitution of cysteine with serine or alanine at position 59 of Ste2p reduced the cross-linking between linked Bio-DOPA^{13} and Ste2p, supporting the conclusion that the thiol functional group of Cys^{59} was cross-linked to Bio-DOPA^{13} and that Cys^{59} is in close proximity with position 13 of α-factor. The proposed mechanism for the cross-linking of Bio-DOPA^{13} to Cys^{59} of Ste2p follows a reaction scheme suggested by the Kodadek group (22) and is outlined Figure 11. The minor amount of cross-linking in the Cys-less still observed (about 20% of the wild-type level) may be due to other nucleophiles in proximity to position 59 of Ste2p. Potential candidates are Arg58, His94, and Lys100 according to the model of Ste2p based on the rhodopsin x-ray structure (*9, 10*). As stated above the significant reduction in cross-linking found with the Cys-less receptor is consistent with our conclusion that Cys59 is the contact point of Tyr^{13} and Ste2p.

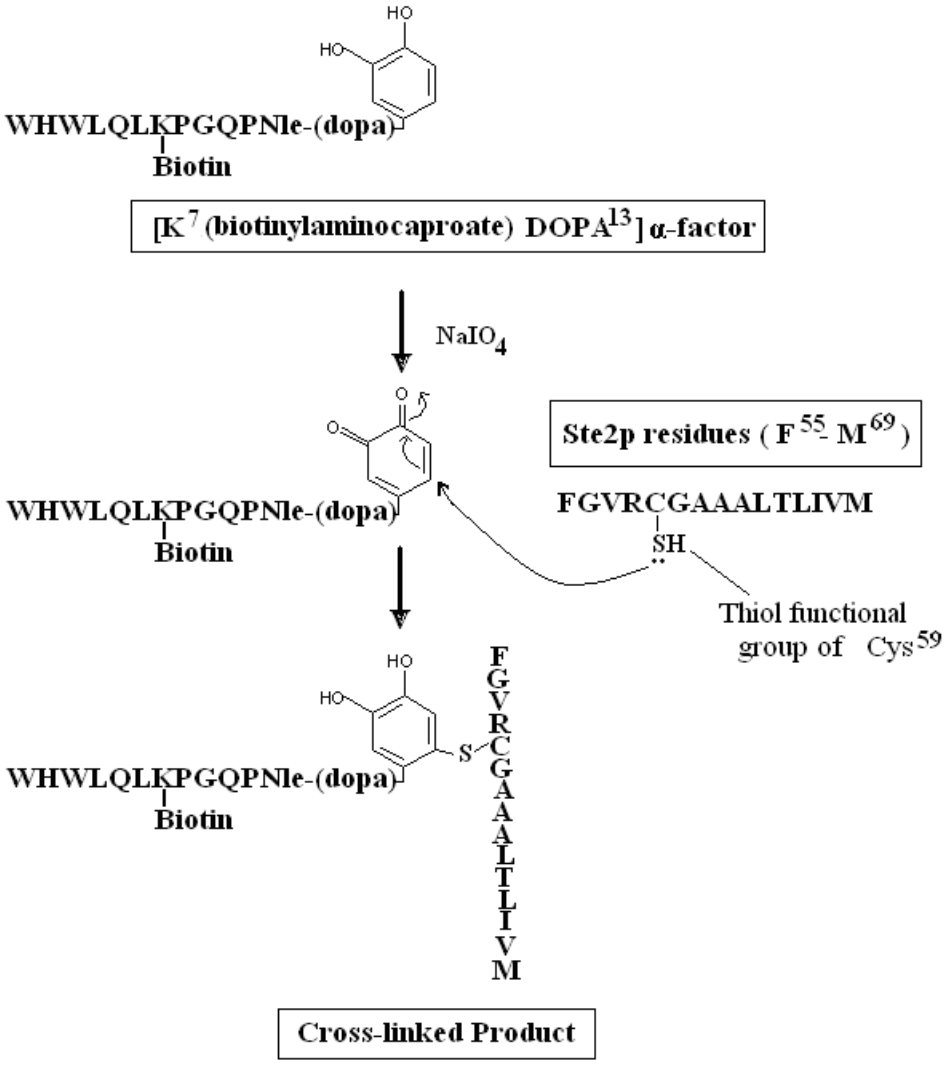

Figure 11: Proposed mechanism of cross-linking of DOPA at position 13 of α-factor and the Cys59 of Ste2p. DOPA is oxidized to an intermediate ortho-quinone which is then attacked by the thiol functional group of Cys^{59} to form a stable covalent cross-link according to (19).

Previous studies in our lab have suggested that the N-terminus of α-factor may interact with Tyr266 in Ste2p. It was suggested in that study that the highly aromatic and hydrophobic N-terminus ($W^1H^2W^3L^4$) of α-factor probably binds to hydrophobic residues comprising the receptor residues such as Tyr266 and some aromatic residues (Tyr203 and Phe204) at the second extracellular loop and transmembrane five boundary (*35*). To determine whether Trp^1 of α-factor is directly in contact or in close proximity with Tyr266 or Tyr203 in Step in its ligand-bound state, Bio-$DOPA^1$ cross-linking was carried out using membranes containing Cys-less, Tyr266Cys and Tyr203Cys Ste2p mutants. The cross-linking of Bio-$DOPA^1$ into all mutant receptors tested was similar to the wild type receptor (Figure 10C). Thus, Bio-$DOPA^1$ cross-linking was not affected in the presence or absence of Cys at Tyr203 or Tyr266 implying that Trp^1 in α-factor may not be in close proximity with Tyr203 or Tyr266 in the Ste2p-ligand bound state.

The cross-linking of Bio-$DOPA^1$ was reduced in the presence α-factor (~92%), α-factor antagonist (~85%) and α-factor synergist (~70%). The MALDI-TOF analysis of Bio-$DOPA^1$-α-factor cross-linking into Ste2p revealed that this peptide cross-linked to a region in Ste2p comprising of Ser251 to Met294 (TM6-EL3-TM7) consistent with previous studies using Bpa at the same position of the ligand (*15*). MS/MS analysis of Bio-$DOPA^1$ cross-linked product confirmed that the region Ser251 to Met 294 cross-linked with Bio-$DOPA^1$. Whereas both the *b*- and *y*-ion fragments of Bio-$DOPA^1$ were observed in the Bio-$DOPA^1$ spectrum (Figure 9), only the *y*-ions of the ligand were identified in the cross-linked spectrum suggesting that the N-terminus of the ligand containing DOPA is cross-linked to a fragment. The *b* ions of residues Ser251-Ile263 and *y* ions of residues Leu283-Met294 were identified in the Ste2p fragment, Ser251-Met294. The identification of the N- and C- termini of Ste2p fragment, Ser251-Met294

and C-terminus of Bio-DOPA^{1}-in one spectrum indicate that all these fragments are in one piece (cross-linked fragment). However, the instrument used for the MS/MS has a mass-charge ratio (m/z) limit of 2000 therefore it is not possible to obtain a fragment ion that is more than 2000 m/z on the spectrum examined. Since the Bio-DOPA^{1} is about 1999 Da (m/z) anything that cross-links with it will increase the mass to more than 2000 m/z hence will not be identified. Nevertheless the results implied that Bio-DOPA^{1} may cross-link with one of the residue in Leu264-Val280 (Figure 9B). Detailed examination of fragment ions observed in the cross-linked spectrum indicates that Bio-DOPA^{1} is cross-linked to Lys269 (Figure 9C) located at the TM6-EL3 boundary. The effect of this residue on Bio-DOPA^{1} cross-linking was not tested and remains a target for future studies.

The reduction of cross-linking in the presence of α-factor synergist observed in Bio-DOPA^{1} but not Bio-DOPA^{13} can be attributed to the fact that this synergist may interact within the ligand signaling pocket (interaction site of α-factor N-terminus) but not the binding site (interaction site of α-factor C-terminus). This α-factor synergist lacking the last two residues of wild type α-factor has been shown to have significantly reduced binding affinity for Ste2p however it enhances the activity of the wild-type α-factor (*28*). Thus, due to the absence of the last two amino acids (M^{12}W^{13}) critical for binding this synergist doe not bind to the inactive Ste2p conformation but it interacts with Ste2p-α-factor active complex and increases the activity of the receptor more than wild type levels (*28*). Exact interaction site of this synergist in Ste2p is unknown.

The different cross-linking reactions of Bio-DOPA^{1} and Bio-DOPA^{13} in presence of the synergist can be explained by the fact that the binding of α-factor to Ste2p may involve two

binding steps as proposed in a mechanism in figure 11. This mechanism is based on Trp^{1} and Tyr^{13} of α-factor cross-linking reactions with Ste2p residues Leu264-Thr282 and Phe55-Met69, respectively, reported in this study and other reports (*14-16*) as well as α-factor synergist inhibition of cross-liking at Leu264-Thr282. It is proposed that the binding of α-factor to Ste2p involves initial binding of the C-terminus to the binding pockets (may include region Phe55-Met69 and other regions) followed by The N-terminus penetrating the transmembrane regions of TM5-TM6 and interacting within the signal pocket (see Figure 12) required for receptor activation as observed in some peptide-responsive GPCRs (*49-52*). This binding mechanism explains why the synergist was able to inhibit the cross-linking of Bio-$DOPA^{1}$ but not Bio-$DOPA^{13}$. Thus, in the presence of synergist both Bio-$DOPA^{1}$ and Bio-$DOPA^{13}$ binds to Ste2p without any inhibition by the synergist (since it does not bind) but it may interact within the same site in Ste2p as the N-terminus of the Bio-DOPA analogs. These interactions of synergist do not affect binding of these peptides but interferes with the cross-linking of Bio-$DOPA^{1}$ that contains DOPA (replacing Trp1) at the N-terminus by blocking the reactions of DOPA. The same blocking effect of the N-terminus interaction is suggested to occur with Bio-$DOPA^{13}$ however because the DOPA is located at the C-terminus (replacing Tyr^{13}) in this peptide it does not affect the cross-linking in Bio-$DOPA^{13}$.

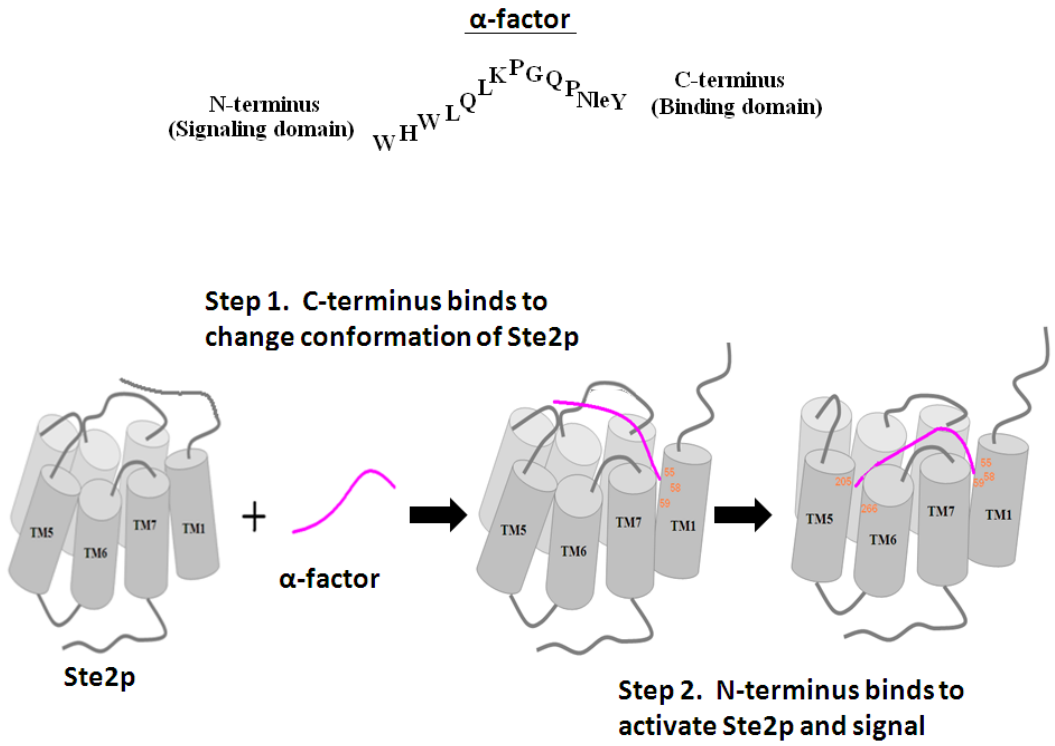

Figure 12: Proposed mechanism of α-factor binding to Step. The C-terminus of α-factor binds Ste2p close to the TM1 region (Phe55-Met69) this causes conformational changes in Ste2p allowing the N-terminus of α-factor to penetrate and bind within the signaling pocket that may involve TM5-TM6-TM7 residues. The extracellular loops are also involved in stabilizing the receptor-ligand complex.

In the presence of 100-fold excess α-factor antagonist both Bio-DOPA[1] or Bio-DOPA[13] cross-linking were inhibited because this antagonist binds efficiently and similar to α-factor (*28*); hence it is capable of blocking the binding (step 1 of mechanism shown above, of Bio-DOPA[1] and Bio-DOPA[13].

We therefore suggest that the synergist interacts within the same signaling pocket in Ste2p as the N-terminus of wild type α-factor in the receptor-ligand bound active complex

conformation. This interactions may be responsible for the increase in Ste2p activity observed in previous studies (*28*) when both the wild type α-factor and its synergist are present.

Previously we concluded that [Bpa^{13}]α-factor cross-linked to the F55-R58 fragment of Ste2p using photoactivation approaches (14). To probe this region further, site-directed single Ala mutations were constructed on residues 54-58 in Ste2p (data not shown). Ste2p mutants R58A, R58D, and R58E exhibited a large increase in the Kd for binding [^{3}H]α-factor. The other mutant receptors had a similar or slightly reduced binding affinity compared to that of the wild-type receptor. Photo-cross-linking of these Ala mutants to [Bpa^{13},K^{7}(biotinylamidocaproate), Nle^{12}] α-factor showed that cross-linking to the R58A mutant was highly diminished, but cross-linking to the F55A, G56A, and V57A mutants was not greatly affected. These cross-linking and site-directed mutagenesis results suggested that position 13 of α-factor interacted with R58 of Ste2p. The finding that [Bpa^{13}]α-factor and [Bio-DOPA^{13}]α-factor cross-link to Arg58 and Cys59, respectively, provides strong evidence that the carboxyl terminal residue of the pheromone binds to this region of Ste2p. The [Bio-DOPA^{1}]α-factor was observed to cross-link to Lys269 of Ste2p. It seems reasonable that the Tyr^{13} side chain is involved in a cation-π interaction with the Ste2p-Arg58 guanidinium moiety and a hydrogen bond with the Ste2p-Cys59 sulfhydryl group (Figure 13). In addition, the indole side chain of Trp^{1} of α-factor may be involve in a cation-π (or hydrogen bonding) interaction with the Ste2p-Lys269. Although the insertion of Ser or Ala greatly diminished cross-linking to Bio-DOPA-α-factor it did not eliminate it completely.

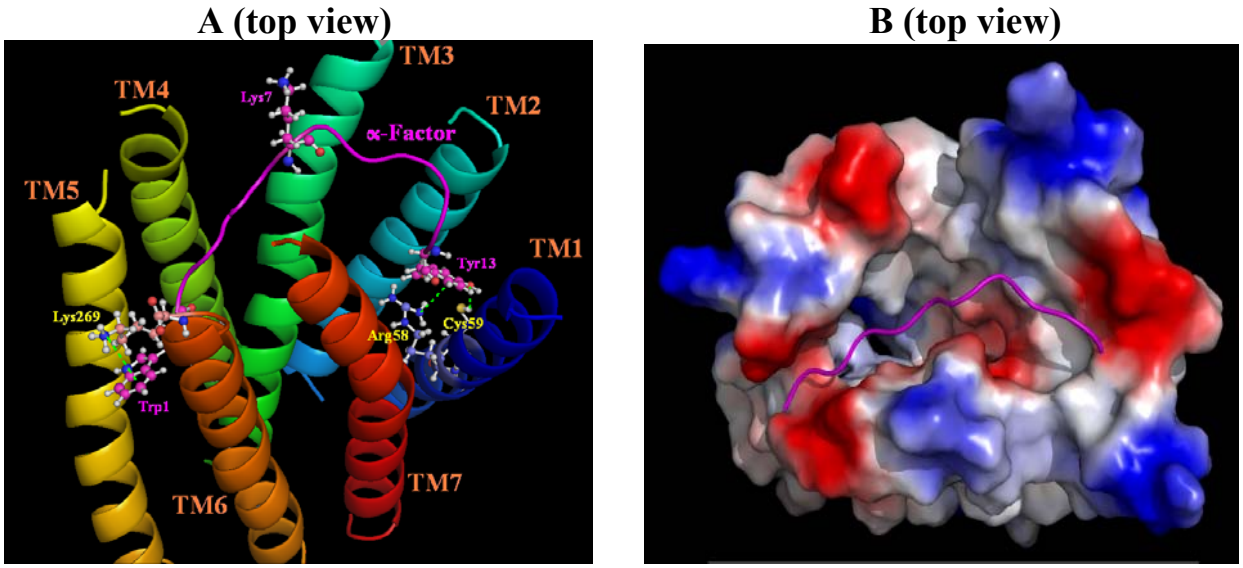

Figure 13: Proposed model of the interactions of Trp[1] and Tyr[13] of α-factor with Lys269, and Arg58/Cys59 residues of Ste2p, respectivcely. The transmembrane domains (TM) are labeled in different colors in A and α-factor is shown as a pink ribbon. **A:** Topview showing overall interactions of the N-terminus (close to TM5-TM6) and C-terminus (close to TM1) of α-factor with Ste2p. Trp[1] indole side chain of α-factor is propose to form a cation-π (or hydrogen bonding) interaction with Lys269 ε-amino group. The Tyr[13] side chain phenyl ring of α-factor is also proposed to be involved in a cation-π interaction with the Arg58 guanidinium moiety and the phenolic OH (Tyr[13]) forms a hydrogen bond with Cys59 sulfhydryl group. The interactions between the residues are indicated by broken green lines. **B:** Topview image of the electrostatic potential surface of Ste2p showing a potential binding pocket of α-factor.

In an elegant study using model PNAs to assure proximity between DOPA and potential nucleophiles, Kodadek and coworkers concluded that sulfhydryl (Cys), imidazole (His) and primary amines (Lys) could react with the orthoquinone oxidation product (19). Ser and Thr

hydroxyls were not found to interact under the experimental conditions reported by Kodadek and his group (19). Nevertheless, there are many examples of the nucleophilicity of Ser hydroxyl groups in proteins, and the hydroxyl oxygen has been shown to act as a nucleophile with a variety of electrophiles (*53*). Partially buried in the hydrocarbon core of the membrane, the solvation of the hydroxyl side chain of Ser59 in the Ste2p binding site might be quite different from that found in the aqueous buffers used with the PNA model compounds investigated by the Kodadek group. Thus, it seems plausible that Ser and Thr moieties of protein receptors may be potential sites for cross-linking to orthodiquinones produced on periodate activation of ligands.

At present the most detailed information pertaining to ligand binding sites of GPCRs comes from X-ray analysis of rhodopsin and β-adrenergic receptors (*11, 54-57*). These proteins bind retinal and inverse agonists, respectively, at sites located primarily in the TM core of these GPCRs. No high resolution information is available on GPCRs that bind medium sized peptide hormones; most of our knowledge on binding sites is inferred from biochemical data. The cross-linking information on α-factor-Ste2p interactions suggests that the carboxyl terminus of the tridecapeptide ligand contacts two polar residues (Arg58 and Cys59) that are near the extracellular end of TM1 of Ste2p (Fig. 9). Double mutant-cycle analyis (*44*) previously showed that Trp^1 and Trp^3 of α-factor interact strongly with N205 and Y266 residues that are located near the extracellular ends of TM5 and TM6, respectively (*17, 58*). Finally, the center of α-factor is thought to face toward the extracellular loop regions of Ste2p (*17, 33*). Thus, in contrast to covalently bound retinal and small biogenic amines, the α-factor tridecapeptide interacts primarily with the ends of TM domains and loops of Ste2p during activation of its GPCR. These interactions are consistent with the prevailing belief that the binding site for peptide ligands to their GPCRs involves ectodomains(*59, 60*).

Binding of α-factor is thought to elicit a significant conformational change in EL1 that is related to receptor activation. Intriguingly, the extracellular loop of rhodopsin is also believed to move during light activation of this GPCR, and the signaling role of extracellular loops in other Class A GPCRs is just starting to be revealed as well (*61*). Ste2p is a Class D GPCR and rhodopsin is a Class A GPCR. If extracellular loops are involved in activation of such evolutionary distinct receptors, it is not unreasonable to suggest that movements of extracellular loops may be an important, perhaps general, aspect of GPCR signal transduction. Evidently, different classes of GPCRs actuate these movements by distinct molecular interactions.

In conclusion, we have synthesized and characterized α-factor analogs (Bio-DOPA-α-factors) with DOPA replacing Trp^{1} or Tyr^{13} and biotin tagged on Lys^{7} and shown that these analogs linked covalently into Ste2p by periodate-mediated DOPA cross-linking. Mass spectrometric analyses of the cross-linked fragments demonstrated that Bio-$DOPA^{1}$ and Bio-$DOPA^{13}$ cross-linked into residues Leu264-Val280 (specifically Lys269) and Phe55-Met69 of Ste2p, respectively. Replacing cysteine at position 59 with serine or alanine drastically reduced the cross-linking with Bio-$DOPA^{13}$. Therefore, it is reasonable to conclude that Trp^{1} and Tyr^{13} of α-factor are in close proximity to Lys269 and Cys59 of Ste2p when α-factor is bound to Ste2p. Our results represent the first determination of a residue-to-residue contact point between α-factor and Ste2p and support the use of oxidative cross-linking to investigate peptide-GPCR interactions.

References for Part II

1. Lefkowitz, R. J. (2000) The superfamily of heptahelical receptors, *Nat Cell Biol 2*, E133-136.
2. Thompson, M. D., Percy, M. E., McIntyre Burnham, W., and Cole, D. E. (2008) G protein-coupled receptors disrupted in human genetic disease, *Methods Mol Biol 448*, 109-137.
3. Schoneberg, T., Schulz, A., Biebermann, H., Hermsdorf, T., Rompler, H., and Sangkuhl, K. (2004) Mutant G-protein-coupled receptors as a cause of human diseases, *Pharmacol Ther 104*, 173-206.
4. Rompler, H., Staubert, C., Thor, D., Schulz, A., Hofreiter, M., and Schoneberg, T. (2007) G protein-coupled time travel: evolutionary aspects of GPCR research, *Mol Interv 7*, 17-25.
5. Prossnitz, E. R., and Sklar, L. A. (2006) Modulation of GPCR conformations by ligands, G-proteins, and arrestins, *Ernst Schering Found Symp Proc*, 211-228.
6. Oldham, W. M., and Hamm, H. E. (2008) Heterotrimeric G protein activation by G-protein-coupled receptors, *Nat Rev Mol Cell Biol 9*, 60-71.
7. Dohlman, H. G., and Slessareva, J. E. (2006) Pheromone signaling pathways in yeast, *Sci STKE 2006*, cm6.
8. Dohlman, H. G., Thorner, J., Caron, M. G., and Lefkowitz, R. J. (1991) Model systems for the study of seven-transmembrane-segment receptors, *Annu Rev Biochem 60*, 653-688.
9. Fredriksson, R., and Schioth, H. B. (2005) The repertoire of G-protein-coupled receptors in fully sequenced genomes, *Mol Pharmacol 67*, 1414-1425.

10. Eilers, M., Hornak, V., Smith, S. O., and Konopka, J. B. (2005) Comparison of class A and D G protein-coupled receptors: common features in structure and activation, *Biochemistry 44*, 8959-8975.

11. Palczewski, K., Kumasaka, T., Hori, T., Behnke, C. A., Motoshima, H., Fox, B. A., Le Trong, I., Teller, D. C., Okada, T., Stenkamp, R. E., Yamamoto, M., and Miyano, M. (2000) Crystal structure of rhodopsin: A G protein-coupled receptor, *Science 289*, 739-745.

12. Dube, P., DeCostanzo, A., and Konopka, J. B. (2000) Interaction between transmembrane domains five and six of the alpha -factor receptor, *J Biol Chem 275*, 26492-26499.

13. Abel, M. G., Zhang, Y. L., Lu, H. F., Naider, F., and Becker, J. M. (1998) Structure-function analysis of the Saccharomyces cerevisiae tridecapeptide pheromone using alanine-scanned analogs, *J Pept Res 52*, 95-106.

14. Son, C. D., Sargsyan, H., Naider, F., and Becker, J. M. (2004) Identification of ligand binding regions of the Saccharomyces cerevisiae alpha-factor pheromone receptor by photoaffinity cross-linking, *Biochemistry 43*, 13193-13203.

15. Henry, L. K., Khare, S., Son, C., Babu, V. V., Naider, F., and Becker, J. M. (2002) Identification of a contact region between the tridecapeptide alpha-factor mating pheromone of Saccharomyces cerevisiae and its G protein-coupled receptor by photoaffinity labeling, *Biochemistry 41*, 6128-6139.

16. Son, C. D., Sargsyan, H., Hurst, G. B., Naider, F., and Becker, J. M. (2005) Analysis of ligand-receptor cross-linked fragments by mass spectrometry, *J Pept Res 65*, 418-426.

17. Lee, B. K., Khare, S., Naider, F., and Becker, J. M. (2001) Identification of residues of the Saccharomyces cerevisiae G protein-coupled receptor contributing to alpha-factor pheromone binding, *J Biol Chem 276*, 37950-37961.

18. Burdine, L., Gillette, T. G., Lin, H. J., and Kodadek, T. (2004) Periodate-triggered cross-linking of DOPA-containing peptide-protein complexes, *J Am Chem Soc 126*, 11442-11443.

19. Liu, B., Burdine, L., and Kodadek, T. (2006) Chemistry of periodate-mediated cross-linking of 3,4-dihydroxylphenylalanine-containing molecules to proteins, *J Am Chem Soc 128*, 15228-15235.

20. Li, W. W., Heinze, J., and Haehnel, W. (2005) Site-specific binding of quinones to proteins through thiol addition and addition-elimination reactions, *J Am Chem Soc 127*, 6140-6141.

21. Archer, C. T., Burdine, L., Liu, B., Ferdous, A., Johnston, S. A., and Kodadek, T. (2008) Physical and functional interactions of monoubiquitylated transactivators with the proteasome, *J Biol Chem 283*, 21789-21798.

22. Lim, H. S., Cai, D., Archer, C. T., and Kodadek, T. (2007) Periodate-triggered cross-linking reveals Sug2/Rpt4 as the molecular target of a peptoid inhibitor of the 19S proteasome regulatory particle, *J Am Chem Soc 129*, 12936-12937.

23. Hauser, M., Kauffman, S., Lee, B. K., Naider, F., and Becker, J. M. (2007) The first extracellular loop of the Saccharomyces cerevisiae G protein-coupled receptor Ste2p undergoes a conformational change upon ligand binding, *J Biol Chem 282*, 10387-10397.

24. Huang, L. Y., Umanah, G., Hauser, M., Son, C., Arshava, B., Naider, F., and Becker, J. M. (2008) Unnatural amino acid replacement in a yeast G protein-coupled receptor in its native environment, *Biochemistry 47*, 5638-5648.

25. Turcatti, G., Nemeth, K., Edgerton, M. D., Meseth, U., Talabot, F., Peitsch, M., Knowles, J., Vogel, H., and Chollet, A. (1996) Probing the structure and function of the tachykinin neurokinin-2 receptor through biosynthetic incorporation of fluorescent amino acids at specific sites, *J Biol Chem 271*, 19991-19998.

26. Sherman, F. (1991) Getting started with yeast, *Methods Enzymol 194*, 3-21.

27. Raths, S. K., Naider, F., and Becker, J. M. (1988) Peptide analogues compete with the binding of alpha-factor to its receptor in Saccharomyces cerevisiae, *J Biol Chem 263*, 17333-17341.

28. Eriotou-Bargiota, E., Xue, C. B., Naider, F., and Becker, J. M. (1992) Antagonistic and synergistic peptide analogues of the tridecapeptide mating pheromone of Saccharomyces cerevisiae, *Biochemistry 31*, 551-557.

29. David, N. E., Gee, M., Andersen, B., Naider, F., Thorner, J., and Stevens, R. C. (1997) Expression and purification of the Saccharomyces cerevisiae alpha-factor receptor (Ste2p), a 7-transmembrane-segment G protein-coupled receptor, *J Biol Chem 272*, 15553-15561.

30. Konopka, J. B., Jenness, D. D., and Hartwell, L. H. (1988) The C-terminus of the S. cerevisiae alpha-pheromone receptor mediates an adaptive response to pheromone, *Cell 54*, 609-620.

31. Kraft, P., Mills, J., and Dratz, E. (2001) Mass spectrometric analysis of cyanogen bromide fragments of integral membrane proteins at the picomole level: application to rhodopsin, *Anal Biochem 292*, 76-86.

32. Beavis, R., and Fenyo, D. (2004) Finding protein sequences using PROWL, *Curr Protoc Bioinformatics Chapter 13*, Unit 13 12.

33. Ding, F. X., Lee, B. K., Hauser, M., Patri, R., Arshava, B., Becker, J. M., and Naider, F. (2002) Study of the binding environment of alpha-factor in its G protein-coupled receptor using fluorescence spectroscopy, *J Pept Res 60*, 65-74.

34. Bauer, A., and Kuster, B. (2003) Affinity purification-mass spectrometry. Powerful tools for the characterization of protein complexes, *Eur J Biochem 270*, 570-578.

35. Lee, B. K., Lee, Y. H., Hauser, M., Son, C. D., Khare, S., Naider, F., and Becker, J. M. (2002) Tyr266 in the sixth transmembrane domain of the yeast alpha-factor receptor plays key roles in receptor activation and ligand specificity, *Biochemistry 41*, 13681-13689.

36. Lee, Y. H., Naider, F., and Becker, J. M. (2006) Interacting residues in an activated state of a G protein-coupled receptor, *J Biol Chem 281*, 2263-2272.

37. Robinette, D., Neamati, N., Tomer, K. B., and Borchers, C. H. (2006) Photoaffinity labeling combined with mass spectrometric approaches as a tool for structural proteomics, *Expert Rev Proteomics 3*, 399-408.

38. Proulx, C. D., Holleran, B. J., Lavigne, P., Escher, E., Guillemette, G., and Leduc, R. (2008) Biological properties and functional determinants of the urotensin II receptor, *Peptides 29*, 691-699.

39. Behar, V., Bisello, A., Rosenblatt, M., and Chorev, M. (1999) Direct identification of two contact sites for parathyroid hormone (PTH) in the novel PTH-2 receptor using photoaffinity cross-linking, *Endocrinology 140*, 4251-4261.

40. Behar, V., Bisello, A., Bitan, G., Rosenblatt, M., and Chorev, M. (2000) Photoaffinity cross-linking identifies differences in the interactions of an agonist and an antagonist with the parathyroid hormone/parathyroid hormone-related protein receptor, *J Biol Chem 275*, 9-17.

41. Boucard, A. A., Sauve, S. S., Guillemette, G., Escher, E., and Leduc, R. (2003) Photolabelling the rat urotensin II/GPR14 receptor identifies a ligand-binding site in the fourth transmembrane domain, *Biochem J 370*, 829-838.

42. Rihakova, L., Deraet, M., Auger-Messier, M., Perodin, J., Boucard, A. A., Guillemette, G., Leduc, R., Lavigne, P., and Escher, E. (2002) Methionine proximity assay, a novel method for exploring peptide ligand-receptor interaction, *J Recept Signal Transduct Res 22*, 297-313.

43. Naider, F., and Becker, J. M. (2004) The alpha-factor mating pheromone of Saccharomyces cerevisiae: a model for studying the interaction of peptide hormones and G protein-coupled receptors, *Peptides 25*, 1441-1463.

44. Naider, F., Becker, J. M., Lee, Y. H., and Horovitz, A. (2007) Double-mutant cycle scanning of the interaction of a peptide ligand and its G protein-coupled receptor, *Biochemistry 46*, 3476-3481.

45. Liu, S., Henry, L. K., Lee, B. K., Wang, S. H., Arshava, B., Becker, J. M., and Naider, F. (2000) Position 13 analogs of the tridecapeptide mating pheromone from Saccharomyces cerevisiae: design of an iodinatable ligand for receptor binding, *J Pept Res 56*, 24-34.

46. Shenbagamurthi, P., Kundu, B., Raths, S., Becker, J. M., and Naider, F. (1985) Biological activity and conformational isomerism in position 9 analogues of the des-1-tryptophan,3-beta-cyclohexylalanine-alpha-factor from Saccharomyces cerevisiae, *Biochemistry 24*, 7070-7076.

47. Dosil, M., Giot, L., Davis, C., and Konopka, J. B. (1998) Dominant-negative mutations in the G-protein-coupled alpha-factor receptor map to the extracellular ends of the transmembrane segments, *Mol Cell Biol 18*, 5981-5991.

48. Wilm, M. (2000) Mass spectrometric analysis of proteins, *Adv Protein Chem 54*, 1-30.

49. Blake, A. D., Bot, G., and Reisine, T. (1996) Structure-function analysis of the cloned opiate receptors: peptide and small molecule interactions, *Chem Biol 3*, 967-972.

50. Gurrath, M. (2001) Peptide-binding G protein-coupled receptors: new opportunities for drug design, *Curr Med Chem 8*, 1605-1648.

51. Kolb, P., Rosenbaum, D. M., Irwin, J. J., Fung, J. J., Kobilka, B. K., and Shoichet, B. K. (2009) Structure-based discovery of beta2-adrenergic receptor ligands, *Proc Natl Acad Sci U S A 106*, 6843-6848.

52. Eglen, R. M., and Reisine, T. (2009) New insights into GPCR function: implications for HTS, *Methods Mol Biol 552*, 1-13.

53. Kang, G. D., Lee, K. H., Ki, C. S., and Park, Y. H. (2004) Crosslinking reaction of phenolic side chains in silk fibroin by tyrosinase, *Fibers and Polymers 5*, 234-238.

54. Cherezov, V., Rosenbaum, D. M., Hanson, M. A., Rasmussen, S. G., Thian, F. S., Kobilka, T. S., Choi, H. J., Kuhn, P., Weis, W. I., Kobilka, B. K., and Stevens, R. C. (2007) High-resolution crystal structure of an engineered human beta2-adrenergic G protein-coupled receptor, *Science 318*, 1258-1265.

55. Rosenbaum, D. M., Cherezov, V., Hanson, M. A., Rasmussen, S. G., Thian, F. S., Kobilka, T. S., Choi, H. J., Yao, X. J., Weis, W. I., Stevens, R. C., and Kobilka, B. K. (2007) GPCR engineering yields high-resolution structural insights into beta2-adrenergic receptor function, *Science 318*, 1266-1273.

56. Warne, T., Serrano-Vega, M. J., Baker, J. G., Moukhametzianov, R., Edwards, P. C., Henderson, R., Leslie, A. G., Tate, C. G., and Schertler, G. F. (2008) Structure of a beta1-adrenergic G-protein-coupled receptor, *Nature 454*, 486-491.

57. Murakami, M., and Kouyama, T. (2008) Crystal structure of squid rhodopsin, *Nature 453*, 363-367.

58. Lin, J. C., Parrish, W., Eilers, M., Smith, S. O., and Konopka, J. B. (2003) Aromatic residues at the extracellular ends of transmembrane domains 5 and 6 promote ligand activation of the G protein-coupled alpha-factor receptor, *Biochemistry 42*, 293-301.

59. Marshall, G. R. (2001) Peptide interactions with G-protein coupled receptors, *Biopolymers 60*, 246-277.

60. Engel, S., and Gershengorn, M. C. (2007) Thyrotropin-releasing hormone and its receptors--a hypothesis for binding and receptor activation, *Pharmacol Ther 113*, 410-419.

61. Wheatley, M., Simms, J., Hawtin, S. R., Wesley, V. J., Wootten, D., Conner, M., Lawson, Z., Conner, A. C., Baker, A., Cashmore, Y., Kendrick, R., and Parslow, R. A. (2007) Extracellular loops and ligand binding to a subfamily of Family A G-protein-coupled receptors, *Biochem Soc Trans 35*, 717-720.

PART III

Unnatural Amino Acid Replacement in a Yeast G Protein-Coupled Receptor in its Native Environment

Part III was published (excluding MS/MS data on wild type Ste2p) in its entirety as: Huang LY, Umanah G, Hauser M, Son C, Arshava B, Naider F, Becker J. M. (2008). *Biochemistry*, **47**(20):5638-48. George K. Umanah was responsible for the mass spectrometric and cross-linking studies. LiYin Huang determined the expression conditions and biological activities of all mutants. Boris Arshava in Dr. Naider's laboratory was responsible for synthesis and purification of the pheromone peptides used in the study.

Chapter 1

Introduction

G protein-coupled receptors (GPCRs) are activated upon binding their cognate ligands. Ligand binding initiates a change in the conformation of these integral membrane proteins. This promotes signal transduction across the membrane, and the activation of the G protein-mediated signal transduction cascade (*1, 2*). The interactions between ligands and their receptors are defined for a number of GPCRs (*3*). However, the ligand-induced changes in protein structure, which initiate signal transduction, are difficult to study. Although site-directed mutagenesis has been used to address the issue of GPCR activation, more methods for studying ligand-dependent conformational changes upon receptor activation are needed. One promising approach which may be adapted to the study of the dynamics of GPCR structure is the use of orthogonal pairs of tRNA/ aminoacyl-tRNA synthetases evolved and expressed in the target cell to incorporate unnatural amino acids (*4-7*).

Non-naturally occurring amino acids can be synthesized to contain a variety of chemical moieties for use as photoaffinity labels or fluorescent and/or spectroscopic probes. To autonomously incorporate unnatural amino acids into proteins in living cells, the mutated tRNA is designed to recognize a specific codon, usually a nonsense codon, such as the amber TAG stop. The evolved cognate aminoacyl-tRNA synthetase specifically charges its orthogonal tRNA with an unnatural amino acid added to the growth medium. Provided that there is a sufficient quantity of the unnatural amino acid in the cytoplasm, the tRNA can be charged for delivery of the novel amino acid into the protein.

The genetic codes of *E. coli*, yeast and mammalian cells have been altered to allow the translational insertion of more than thirty unnatural amino acids with a variety of novel properties useful in the study of protein structure and function (*5, 8*). Thus far, these applications have focused primarily on soluble proteins. With respect to eukaryotic membrane proteins expressed in mammalian cells, unnatural amino acids have been introduced into the nicotinic acetycholine receptor in both CHO cells and cultured neuronal cells (*9*) and in the epidermal growth factor receptor in HEK293 cells (*10*). A heterologous *Xenopus* oocyte expression system has also been used extensively to insert non-natural amino acids into the nicotinic acetylcholine receptor (*11*) the neurokinin-2 receptor (*12*), the $GABA_A$ receptor (*13*), the NMDA receptor (*14*) and numerous channel proteins including the serotonin-gated ion channel (*15*), the inwardly rectifying potassium channel (*16*) and the voltage-sensitive sodium channel (*17*) . In both the mammalian and *Xenopus* expression systems, a tRNA chemically charged with the non-natural amino acid is introduced into the cell along with the target mRNA. While these systems are useful for the short-term studies of protein properties, they are not amenable to large-scale production of proteins into which unnatural amino acids have been incorporated. Recently, it was demonstrated in CHO cells that unnatural amino acids could be introduced into green fluorescent protein (GFP) using specific orthogonal tRNA/aminoacyl-tRNA synthetase pairs (*6*). Because the yeast *Saccharomyces cerevisiae* provides a tractable system in which to develop this methodology, we report here the genetic incorporation of an unnatural amino acid into a polytopic membrane protein in its native eukaryotic host cell .

To date in *S. cerevisiae* orthologous tRNA/aminoacyl-tRNA synthetase pairs have been used to incorporate a variety of unnatural amino acids, including the photoactivatable amino acid

analog *p*-benzoyl-*L*-phenylalanine (Bpa) (*4*), the fluorescent amino acid dansyl alanine (*18*) and acetylene and azide-containing amino acids (*7, 19*), into the soluble protein human superoxide dismutase. Here we report the site-specific incorporation of Bpa into Ste2p, a yeast GPCR, using an orthologous tRNA/aminoacyl tRNA synthetase pair. In this system, the amber TAG stop codon was engineered into specific sites within the *STE2* coding region. Bpa was supplied to the cells either as the free amino acid analog or as the dipeptide Met-Bpa. Upon translation of the message, Bpa was incorporated into the nascent Ste2p and ultimately expressed at the cell surface. Two of our Bpa-Ste2p receptors were used to selectively photocapture biotinylated α-factor. To our knowledge this is the first report of the expression in the native host cell of a GPCR containing a photoactivatable amino acid. The successful photocapture of α-factor by novel Ste2p mutants shows that GPCRs containing unnatural amino acids can be used to capture ligand and to study changes in domain-domain interactions during GPCR activation.

Chapter 2

Material and Methods

***Media, Reagents, Strains and Plasmids*:**

Saccharomyces cerevisiae strain DK102 (*MAT**a**, ura3-52 lys2-801^{am} ade201^{oc} trp1-Δ63 his3-Δ200 leu2-Δ1 ste2::HIS3 sst1-Δ5.*) was used for growth arrest and binding assays and the protease deficient strain BJS21 (*MAT**a**, prc1-407 prb1-1122 pep4-3 leu2 trp1 ura3-52 ste2::Kan^{R}.*) was used for protein isolation and immunoblot analysis. C-terminal FLAG and His tagged *STE2* was PCR amplified from plasmid pNED1 (*20*) and cloned into the plasmid p426-GPD (*21*) to yield plasmid pCL01. The plasmid pCL01was engineered by single-stranded mutagenesis to incorporate TAG stop codons at eight specific positions within the *STE2* coding region (Fig. 1). The sequence of all TAG mutants was verified by DNA sequence analysis completed by the Molecular Biology Resource Facility located on the campus of the University of Tennessee. Mutagenic and sequencing primers were purchased from Sigma/Genosys (The Woodlands, TX) or IDT (Coralville, IA). The pCL01 TAG mutant plasmids were co-transformed by the method of Geitz (*22*) into DK102 and BJS21 cells along with plasmid pECTyrRS/tRNACUA, encoding the orthogonal amber suppressor tRNA synthetase-tRNA pair genetically modified to allow for incorporation of *p*-benzoyl-*L*-phenylalanine (Bpa) (*4*). Transformants were selected by growth on minimal medium (*23*) lacking tryptophan and uracil (designated as MLWU) to maintain selection for the plasmids. Cells used in the assays described below were cultured in MLWU and grown to mid-log phase at room temperature with shaking (200 rpm) in the presence or absence of 2 mM Bpa, unless otherwise specified. Methionyl-Bpa was synthesized by standard solution phase techniques (*24*) and purified by reverse-phase HPLC

to greater than 99% homogeneity. All media components were obtained from BD (Franklin Lakes, NJ) and were of the highest quality available. Bpa was purchased from Bachem (Torrance, CA) and was dissolved in NaOH (1N) at a final concentration of 100 mM immediately before use.

Growth Arrest Assays:

DK102 cells expressing the wild-type (WT) or TAG constructs were grown at 30ºC in MLWU, harvested, washed three times with water and resuspended at a final concentration of 5 x 10^6 cells/ml. Cells (1 ml) were combined with 3.5 ml agar noble (1.1 %) with or without the addition of Bpa (2 mM final concentration) and poured as a top agar lawn onto MLWU medium. Filter disks (BD, Franklin Lakes, NJ) impregnated with the tridecapeptide pheromone α-factor (WHWLQLKPGQPNle^{12}Y) synthesized and characterized as previously described (*25*) were placed on the top agar and the plates were incubated at room temperature (23 ºC) for 48-72 hours.

***Immunoblots*:**

BJS21 cells expressing WT or TAG-*STE2* constructs grown in the presence or absence of Bpa were used to prepare total cell membranes isolated as previously described (*20*). Protein concentration was determined (BioRad, Hercules, CA) and membranes solubilized in SDS sample buffer. Proteins (2 µg/lane for wild type, 30 µg/lane for mutants) were fractioned by SDS-PAGE and immunoblotted. Blots were probed with FLAG antibody (Sigma/Aldrich Chemical, St. Louis, MO) or an antibody directed against the N-terminal 100 amino acids of

Ste2p generously provided by J. Konopka (*26*). The immunoblots were imaged and band density quantitated using Quantity One software (Version 4.5.1) on a Chemi-Doc XRS photodocumentation system (BioRad, Hercules, CA).

Binding Assays:

Tritiated α-factor (10.2 Ci/mmol, 12 μM) prepared as previously described (*25*) was used in saturation binding assays on whole cells. DK102 cells expressing WT or TAG constructs were harvested, washed three times with YM1 (*20*) and adjusted to a final concentration of 2 x 10^7 cells per ml. Cells (600 μl) were combined with 150 μl of ice cold 5X binding medium (YM1 plus protease inhibitors [YM1i (*20*)] supplemented with [^{3}H]α-factor) and incubated at room temperature for 30 minutes. The final concentration of [^{3}H]α-factor ranged from 0.5 x 10^{-10} to 1 x 10^{-6} M. Upon completion of the incubation interval, 200 μl aliquots of the cell-pheromone mixture were collected in triplicate and washed over glass fiber filter mats using the Standard Cell Harvester (Skatron Instruments, Sterling, VA). Retained radioactivity on the filter was counted by liquid scintillation spectroscopy. DK102 cells lacking Ste2p were used as a non-specific binding control for the assays. Specific binding for each mutant receptor was calculated by subtracting the non-specific values from those obtained for total binding. Specific binding data were analyzed by non-linear regression analysis for single-site binding using Prism software (GraphPad Software, San Diego, CA) to determine the K_m (nM) and B_{max} values (receptors/cell) for each mutant receptor.

MALDI-TOF:

BJS21 cells expressing either the WT or $G188^{TAG}$ Ste2p were grown in the presence or absence of Bpa and used to prepare total cell membranes as previously described (*20*). Approximately 3 mg cell membranes was resuspended in ice-cold solubilization buffer (50 mM Tris HCl, pH 7.4, 150 mM NaCl, 1 mM EDTA, 1% Triton X-100) with protease inhibitors (PMSF, pepstatin A and leupeptin) and incubated overnight at 4ºC with end-over-end mixing, then centrifuged at 15,000 x g for 30 minutes to remove non-soluble material. The solubilized proteins were then mixed with FLAG resin (Sigma/Aldrich Chemical Co., St. Louis, MO) and incubated at 4ºC with end-over-end mixing for 6 hours. The resin was collected by centrifugation at low speed (800 x g, 1 minute) and resuspended and collected four times in TBS buffer (25 mM Tris-HCl, 140 mM NaCl, 3 mM KCl, pH 7.4). Ste2p was eluted by resuspending the resin in 1 mL ice cold elution buffer (0.1 M glycine HCl, pH 3.5) and incubated at 4ºC with end-over-end mixing for 5 minutes. The resin was pelleted by centrifugation (2000 x g, 1 minute) and the supernatant, containing the eluted Ste2p, transferred to a fresh tube containing 20 µl of 0.5 M Tris HCl, pH 7.4, 1.5 M NaCl. Purity and concentration of samples was estimated by Coomassie blue and silver staining of SDS-PAGE gels. The samples were also analyzed by immunoblotting using an antibody to the FLAG epitope on the C-terminus of Ste2p.

Samples containing eluted Ste2p (~50 µg) were dried by vacuum centrifugation (Thermo Scientific, Waltham, MA) then dissolved in 100% trifluoroacetic acid (TFA) containing 10 mg/ml cyanogen bromide (CNBr). Deionized distilled water (ddH_2O) was then added to adjust the final TFA concentration to 70%, and the sample was incubated at 37°C in the dark for 18 hours. The samples were dried by vacuum centrifugation and washed three times with ddH_2O

and resuspended in 0.1% TFA. The resulting CNBr peptide fragments were further washed and concentrated using ZipTip pipette tips (Millipore Corporation, Billerica, MA) following the manufacturer's directions and resuspended in 70% acetonitrile 30% water (0.1% TFA). For MALDI-TOF analysis α-cyano-4-hydroxy-trans-cinnamic acid (ACHA, Sigma/Aldrich Chemical Company, St. Louis, MO) at a concentration of 20 mg/ml in 50% acetonitrile-50% water (0.1 % TFA) was used as the matrix. The digested samples (0.5 μL eluate from ZipTip), were either mixed with 0.5 μL of matrix before spotting on the target or 1.0 μL of matrix was spotted and allowed to dry before applying 1.0 μL of samples. MADLI-TOF spectra were acquired on a Bruker Daltonics (Boston, MA) Microflex using both reflector and linear methods.

Crosslinking:

A biotinylated form of α-factor [K^7(biotinylamidocaproate), Nle^{12}]α-factor was prepared as previously described (*27*). Membranes prepared from BJS21 cells expressing the $F55^{TAG}$, $G188^{TAG}$ and $Y193^{TAG}$ receptors, grown at room temperature in the presence or absence of Bpa (1 mM) were suspended in PPBi buffer (0.5 M potassium phosphate, pH 6.2, 10 mM TAME, 10 mM sodium azide, 10 mM potassium fluoride, and 0.1% BSA), incubated with biotinylated pheromone (1 μM) in the presence of absence of non-biotinylated pheromone (100 μM) for 30 minutes at room temperature, then chilled to 4ºC for the remainder of the procedure. Crosslinking was performed as previously described (*27*). Briefly, the membranes were exposed to UV light at 365 nm using a Stratalinker (Stratagene, La Jolla, CA) for three 15 minute intervals. The cross-linked membranes were washed three times with CAPS buffer [N-cyclohexyl-3-aminopropanesulfonic acid (Sigma, St. Louis, MO.), 10 mM, pH 10] by

centrifugation to remove non-crosslinked biotinylated α-factor, fractionated by SDS-PAGE and immunoblotted with antibody to Ste2p and with Neutravidin-HRP conjugate (Pierce, Rockford, IL) to detect the biotinylated pheromone covalently linked to the receptor. The signal generated by Neutravidin-HRP conjugate associated with the biotinylated ligand-receptor complex was quantitated by measurement of the band density using Quantity One software (Version 4.5.1) on a Chemi-Doc XRS photodocumentation system (BioRad, Hercules, CA). Before fractionation by SDS-PAGE the amount of protein in each sample was determined, and amounts specified in the text for each experiment were loaded into each lane.

Chapter 3

Results

Effect of Bpa Incorporation on Ste2p-Mediated Signal Transduction:

The amber stop codon TAG was inserted into the *STE2* coding sequence by site-directed mutagenesis at the eight sites indicated in Figure 1. The sites were located in the first transmembrane domain ($F55^{TAG}$), in the first ($S107^{TAG}$, $G115^{TAG}$, $V127^{TAG}$) and second ($Y193^{TAG}$ and $F204^{TAG}$) extracellular loops, at the border between the fourth transmembrane domain and the second loop ($G188^{TAG}$) and in the sixth transmembrane domain ($Y266^{TAG}$). These residues were selected based on several criteria: (i) location – either in an extracellular loop or near the interface between a TM and an extracellullar surface, (ii) prior site-directed mutagenesis studies indicating that the residues (S107, G115, V127, and G188) were tolerant to amino acid substitution (*28*), and (iii) conservation of the aromatic functional group (F55, F204, and Y266) (*29, 30*) . The plasmids bearing these mutations and the plasmid pECTyrRS/tRNACUA, which encoded the tRNA/tRNA synthetase pair, were transformed into DK102 and BJS21 cells.

To determine if the Ste2p-Bpa mutant proteins were able to bind ligand and ultimately transduce signal across the cell membrane, growth arrest or 'halo' assays were conducted on these transformed cells. Disks impregnated with α-factor were placed onto a top agar lawn of DK102 cells putatively expressing Ste2p-Bpa receptors, and the plates were incubated at room temperature for 48-72 hours. The rationale to conduct these studies was two-fold. In the absence of Bpa, the tRNA should not be charged, resulting in the production of truncated Ste2p. In this case, the cells should not respond to pheromone, and growth arrest should not occur.

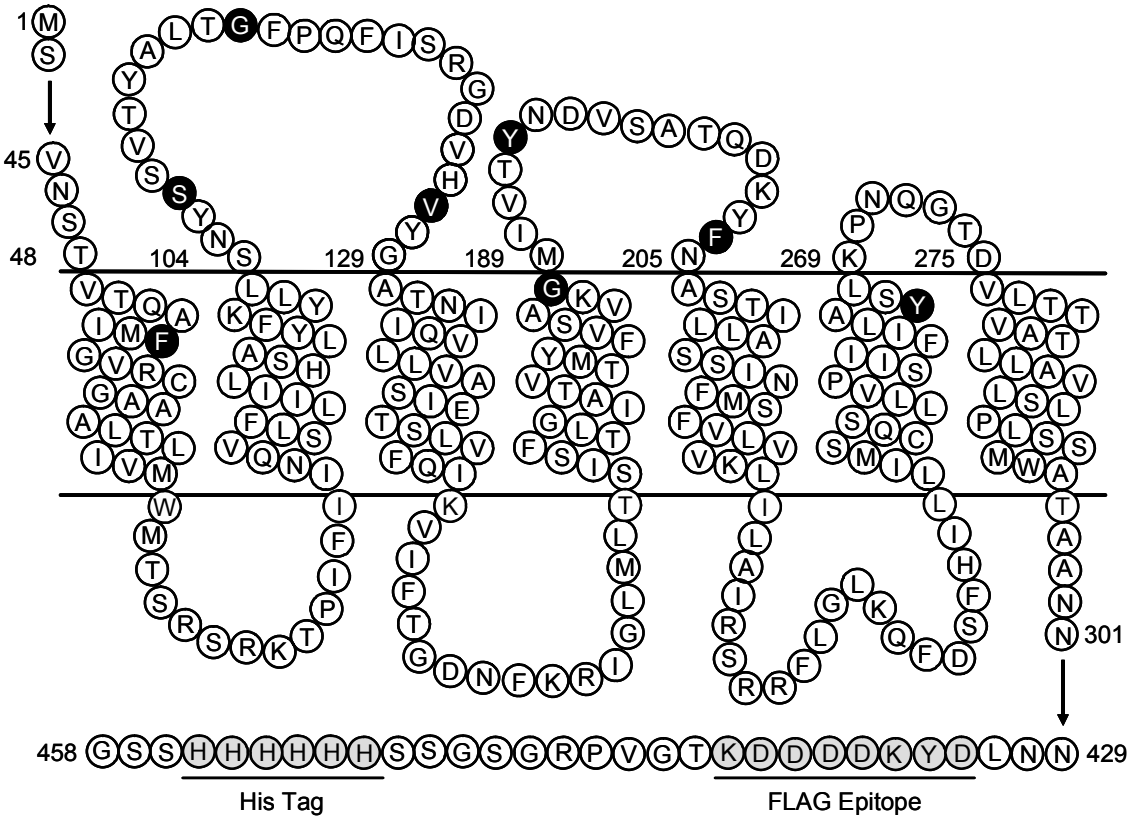

Figure 1: Sites targeted for Bpa insertion into Ste2p.The coding region of the *STE2* gene was modified to introduce the amber TAG codon, resulting in the insertion of Bpa into Ste2p at the sites indicated in black (F55, S107, G115, V127, G188, Y193, F204, and Y266). The FLAG and His tags are underlined and indicated by gray shading in the C-terminal tail.

In the presence of Bpa, the TAG codon should be suppressed by the charged tRNA and full-length protein should be synthesized. If the incorporation of Bpa is tolerated, the mutant Ste2p proteins might bind pheromone resulting in the initiation of signal transduction ultimately resulting in growth arrest, indicated by the formation of a clear halo around the disk.

For cells expressing wild-type Ste2p, dose-dependent halos were formed in both the presence and absence of Bpa indicating that Bpa addition to growth medium did not affect the

pheromone response (Figure 2A). For the mutant at position Y193, no halos were formed in the absence of Bpa, suggesting that no functional Ste2p was expressed. In contrast, in the presence of Bpa dose-dependent halos were formed indicating that Bpa was inserted in response to the TAG codon resulting in a functional protein. Although the halo diameters of the Y193 mutant were comparable to those of the wild type strain, the zone of inhibition was not as clear and the edges not as clearly defined as for the wild type strain. This is most likely due to decreased receptor number resulting from the Y193 mutation, as described below for the immunoblot results, or to more rapid desensitization of the Bpa mutant receptor, resulting in a recovery from the growth arrest response (*31, 32*).

To compare the pheromone-dependent growth arrest, the halo diameters were measured for the wild-type and for each of the eight mutant receptors (Figure 2B), plotted as a function of α-factor concentration, and the amount of pheromone per disk necessary to generate a 25 mm diameter halo was determined. In this bar graph the shorter the bar the more sensitive is the receptor to pheromone-induced growth arrest. For wild-type Ste2p, 0.84 ± 0.04 μg and 0.76 ± 0.01 μg per disk for cells grown in the absence and presence of Bpa, respectively, were required to reach 25 mm zone of growth inhibition. The $G188^{TAG}$ and $Y193^{TAG}$ receptors did not form halos in the absence of Bpa, but growth arrest did occur in the presence of Bpa. While neither receptor was as sensitive as the wild type to pheromone, the $Y193^{TAG}$ receptor was more sensitive (1.8 ± 0.02 μg per disk) than the $G188^{TAG}$ receptor (6.2 ± 1.0 μg per disk).

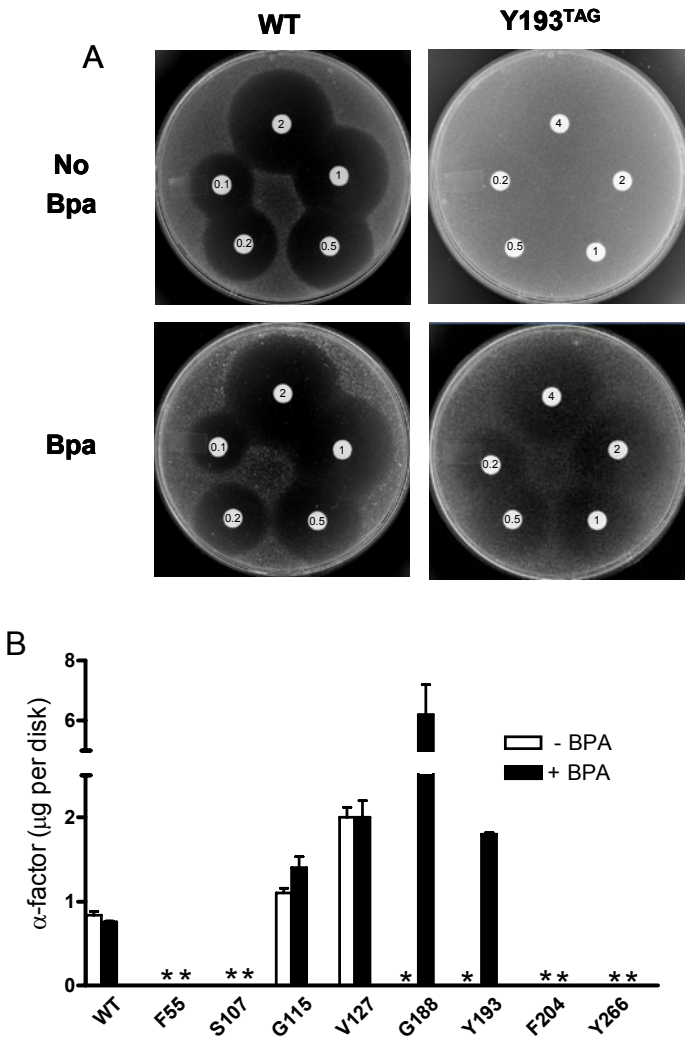

Figure 2: Halo assays of wild-type and Bpa mutant receptors. A. Wild-type or Y193^{TAG} mutant cells were plated onto medium in the presence and absence of Bpa. Disks containing α-factor as indicated (μg per disk) were placed onto the lawn of cells. **B.** Halo diameters were measured for each TAG mutant and plotted as a function of pheromone dose, and the amount of α-factor required to produce a 25 mm halo was determined. Open bars indicate cells grown in the absence of Bpa, filled bars indicate cells grown in the presence of Bpa, and an asterisk indicates no measurable halo. In this graph the shorter the bar the more sensitive is the receptor to pheromone-induced growth arrest.

For the G115^{TAG} and V127^{TAG} receptors halos formed in the absence of Bpa (1.1 ± 0.06 and 2.0 ± 0.2 μg per disk respectively), indicating that there was some "read-through" of the amber stop codon in the absence of Bpa. Several mutants (F55^{TAG}, S107^{TAG}, F204^{TAG}, Y266^{TAG}) did not support the production of halos in either the absence or presence of Bpa. For the F55^{TAG}, S107^{TAG}, F204^{TAG} receptors, immunoblot analysis (Figure 3) indicated that these receptors were expressed in the presence of Bpa, suggesting that Bpa was incorporated into Ste2p but was not tolerated at those positions, resulting in non-signaling receptors. In contrast, the Y266^{TAG} receptor was not functional in either the presence or absence of Bpa., and subsequent immunoblot analysis (Figure 3) indicated that this receptor was not expressed.

Expression of Ste2p-Bpa in Cell Membranes:

Cell membranes isolated from strain BJS21 expressing the TAG mutant constructs and the tRNA/tRNA synthetase pair were immunoblotted and probed with antibodies directed against the C-terminal FLAG epitope tag and the N-terminal 100 amino acids of Ste2p (*26*) to determine the effect of the amber stop codon on protein synthesis in the presence and absence of Bpa. Full-length wild-type Ste2p was synthesized in both the presence and absence of Bpa and could be detected by both N-terminal and C-terminal antibodies (Figure 3A and B). The F55^{TAG} and G188^{TAG} mutants were not detected in the absence of Bpa (Figure 3A). In the presence of Bpa a distinct band was observed for F55^{TAG} Ste2p and a weak but clearly discernible band was observed for the G188^{TAG} Ste2p receptor.

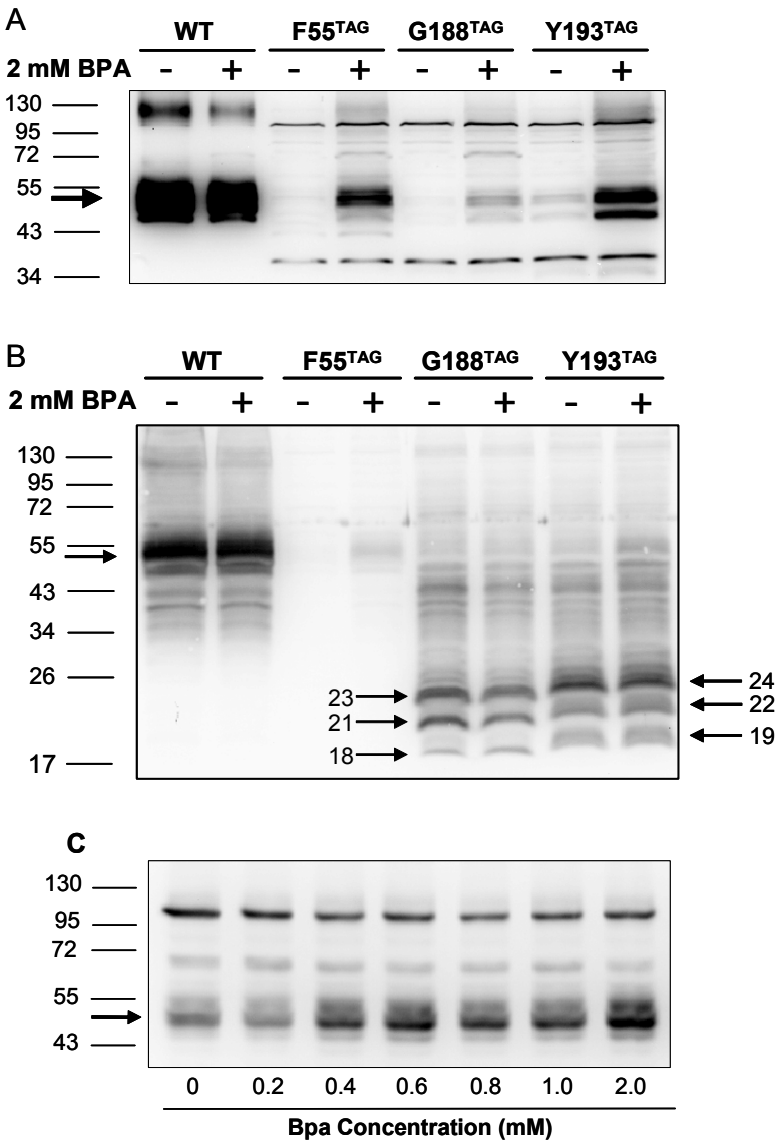

Figure 3: Immunoblots of membranes isolated from cells expressing Bpa-mutant Ste2p. In each panel the arrow at the left indicates the band corresponding to full length Ste2p. **A**. C-terminal FLAG and B. N-terminal anti-Ste2p immunoblots prepared from cells expressing the of F55, G188 and Y193 receptors grown in the presence and absence of 2 mM Bpa. In panel **B** the arrows in the lower portion of the figure indicate truncated forms of Ste2p. **C**. FLAG

immunoblot of membranes prepared from cells expressing the F55^{TAG} receptor in the presence of increasing concentrations of Bpa.

In both cases the expression was at relatively low levels; fifteen times more protein was loaded for the mutants to allow for detection by immunoblot compared to that of the wild type (30 μg vs. 2 μg). The G115^{TAG} and V127^{TAG} mutants were expressed in the presence of Bpa and their expression was not detected in the absence of Bpa (data not shown). In the absence of Bpa even though the amount of G115^{TAG} and V127^{TAG} receptors is below the limit of detection for the immunoblot, sufficient protein was made by read-through expression to give the biological response measured (Figure 2B). For the Y193^{TAG} mutant, a low level of expression was detected in the absence of Bpa, and this expression was enhanced in the presence of Bpa, but still not to the level of the wild type. Results similar to those for the Y193^{TAG} mutant were also observed for the S107^{TAG} and F204^{TAG} mutants (data not shown). The Y266^{TAG} mutant was not detected in the presence or absence of Bpa, indicating that this mutant is not expressed or is expressed at levels below the limit of detection for this system.

C-terminally truncated forms of the receptor can be seen for the G188^{TAG} and Y193^{TAG} receptors using antibody to the N-terminus (Figure 3B). Three major bands were detected at 23, 21, and 18 kDa for the G188^{TAG} and at 24, 22, and 19 kDa for the Y193^{TAG} receptor. These bands corresponded to the expected size of the non-glycosylated receptor and its two major glycosylated states truncated at the inserted stop codons (*33*). The origin of the bands of higher molecular weight (between 22 kD and 50 kD) in the G188^{TAG} and Y193^{TAG} lanes (Figure 3B)was not investigated, although these bands are not related to the absence or presence of Bpa. Truncated forms of the F55^{TAG} receptor were not detected with the N-terminus antibody (Figure

3B) since this antibody is directed against all 100 amino acids of the Ste2p N-terminus. Note that the full-length Ste2p band intensity (52 kD) for the wild type strain is less intense as detected by the N-terminal antibody than that of the same membranes probed with the FLAG antibody (Figure 3A). In our hands, the FLAG antibody always yields a stronger signal than the N-terminal antibody. This provides an explanation for the observation that although full length Bpa-containing proteins can be detected with the FLAG antibody, they are barely discernable by the N-terminal antibody. Expression of the full length $F55^{TAG}$ Bpa-containing receptor was enhanced in response to increased Bpa concentration in the growth medium (Figure 3C). At low concentration (0.2 mM Bpa) no increase over control (no Bpa) was observed, while at higher concentrations (2 mM) the signal corresponding to Ste2p on the immunoblot was enhanced, increasing by 2.6 fold over control as measured by band intensity. Similar results were obtained for the $G188^{TAG}$ and $Y193^{TAG}$ mutants (data not shown), suggesting that entry of Bpa into the cell is one factor determining the efficiency of Bpa insertion into the protein.

Effect of Bpa-containing Peptides on the Expression of Ste2p:

The data for the $F55^{TAG}$, $G188^{TAG}$ and $Y193^{TAG}$ receptors described above suggests that the expression of Bpa-containing Ste2p could be enhanced if Bpa were more efficiently delivered into the cell. It is known that small peptides enter yeast cells intact through the di-/tripeptide transporter Ptr2p (*34, 35*) and upon entry into the cell, these peptides are hydrolyzed to free amino acids. In an attempt to increase the delivery of Bpa into the cell, a Bpa-containing dipeptide (Met-Bpa) was synthesized. Methionyl dipeptides and tripeptides are excellent substrates for the yeast peptide transport system (*36*). Cells expressing the $F55^{TAG}$, $G188^{TAG}$ and

Y193^{TAG} receptor constructs were grown in the presence and absence of Met-Bpa, and membranes were isolated and probed with the C-terminal FLAG antibody to detect full-length protein. The expression of full length wild-type Ste2p was not affected by the presence of Met-Bpa confirming that this compound did not interfere with normal Ste2p expression at the concentrations indicated (Figure 4A). The Y193^{TAG} mutant expressed minimal FLAG-reactive Ste2p in the absence of Bpa, but in the presence of Met-Bpa (Figure 4B), full length protein was detected. Comparing the expression of Y193^{TAG} grown in the presence of 0.1 mM Met-Bpa to that grown in the presence of 0.1 mM Bpa (Figure 4B), expression was greater for the dipeptide (3.1 fold increase). At higher concentrations (0.5 mM and 2 mM) growth on Met-Bpa and Bpa yielded similar levels of expression (1.4 fold increase at each concentration). Similar results were obtained for the F55^{TAG} and Y193^{TAG} mutants. Growth on dipeptide at 0.1 mM resulted in 2.4 fold and 2.0 fold increases in expression for the F55^{TAG} and Y193^{TAG} mutants, respectively. At higher concentrations of peptide (0.5 mM and 2 mM), growth on Met-Bpa did not increase Ste2p expression when compared to the same concentration of Bpa.

***Cell Surface Expression of Bpa Mutants Determined by Saturation Binding Assay*:**

To characterize the cell surface expression and binding affinity of the Ste2p Bpa mutants DK102 cells expressing the F55^{TAG}, G188^{TAG}, and Y193^{TAG} receptors were used in whole-cell binding assays. Binding of radiolabeled α-factor was detected for cells expressing the wild-type receptor when cultured in either the presence or absence of Bpa.

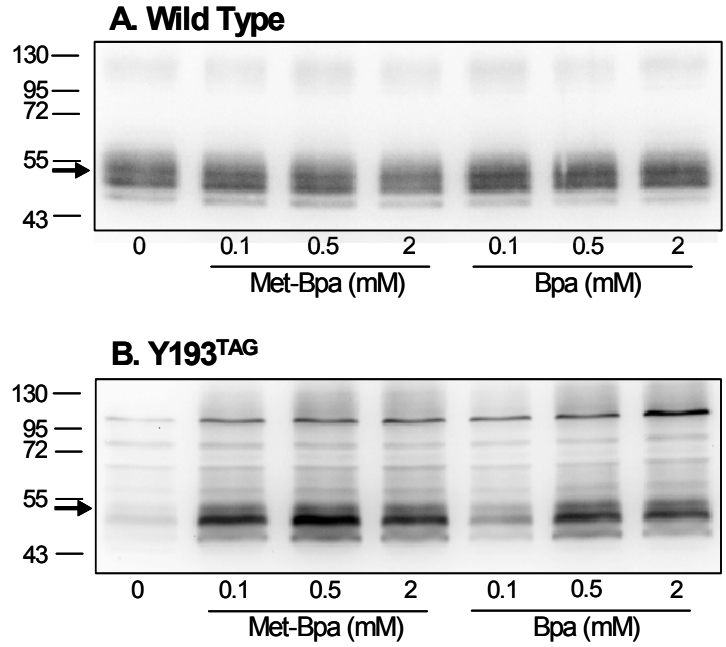

Figure 4: Utilization of a peptidyl form of Bpa. FLAG immunoblot analysis of membranes from cells expressing either wild type (A) or $Y193^{TAG}$ (B) Ste2p receptors grown in the presence of the dipeptide Met-Bpa or free Bpa at the concentrations indicated. Protein loads were 2 μg and 30 μg for the wild type and Y193 mutant, respectively.

In experiments using the wild type receptor, Bpa did not have any significant effect on the B_{max} and binding affinity (B_{max}= 152,470 ± 6,900 receptors per cell, K_D = 9.7 ± 1.4 nM) when compared to cells cultured in the absence of Bpa (B_{max}= 158,100 ± 6,500 receptors per cell, Kd = 11.0 ± 1.0 nM). For the mutant receptors, binding was not detected for cells grown in the absence of Bpa (data not shown). However, for cells grown in the presence of Bpa, saturable binding was observed. (Figure 5). The B_{max} values for the mutants were reduced by 10- to 20-fold compared to the wild-type receptor, which is consistent with the low level of expression observed in the immunoblots (Figure 3).

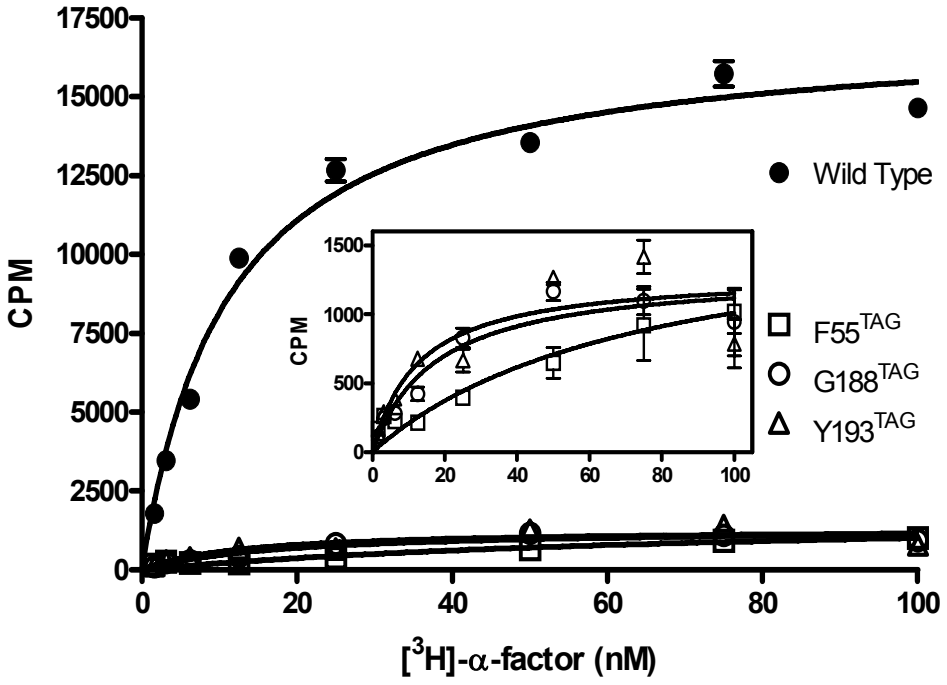

Figure 5: Whole cell saturation binding assay of [3H]α-factor to wild-type and TAG mutant receptors. Cells expressing the wild-type receptor and the indicated Bpa mutants were grown in the presence of 2 mM Bpa. Inset: Saturation binding assay for TAG mutant receptors plotted on an expanded scale. The data represents specific binding to cells as determined by subtracting the binding to an isogenic strain lacking the receptor from binding to cells containing the Bpa containing Ste2p mutant receptors.

The binding affinity (Kd) of the $Y193^{TAG}$ and $G188^{TAG}$ mutants (12.8 ± 4.9 nM and 17.5 ± 5.7 nM, respectively) were similar to that for the wild-type receptor, indicating that substitution of Bpa for the endogenous amino acid at these positions did not affect the interaction of the ligand with the receptor. In contrast, for the $F55^{TAG}$ mutant the binding affinity was reduced to 78.9 ±

46.1 nM, indicating that the substitution of Bpa for phenylalanine at this position affected ligand binding which correlates to the relative low signaling activity of this receptor.

MALDI-TOF indicates that Bpa is incorporated into Ste2p at position G188:

To confirm the incorporation of Bpa into Ste2p, MALDI-TOF mass spectrometric analysis of purified wild-type and $G188^{TAG}$ receptors was performed. We first carried out cyanogen bromide (CNBr) digest on purified wild type receptors and analyzed the fragments by MALDI-TOF as well as MS/MS to make sure that we can identify the Ste2p fragment containing Bpa using this method. Analysis of the purified wild type receptors using the silver staining technique on the samples resolved on 4-12% SDS-PAGE (Figure 6A) indicated that two prominent bands, corresponding in molecular weight to the glycosylated and non-glycosylated forms of Ste2p (51-53 kDa) were present. Immunoblot analysis confirmed that the two major bands were Ste2p (Figure 6B). The MALDI-TOF analysis of the CNBr fragmented wild type Ste2p revealed 5 out of 10 Ste2p predicted fragments (Figure 7). Whereas the MS/MS was able to identify and determined the amino acid sequences of 7 out the 10 predicted fragments covering about 65% of the entire Ste2p amino acid sequences. The MS/MS fragmentation spectra of residues 181-189 is shown on Figure 8.

The $G188^{TAG}$ receptor was chosen for to confirm the incorporation of Bpa into Ste2p based on nearby naturally-occurring methionine sites in Ste2p that would yield a small peptide (residues 181-189, easy to identify with MALDI-TOF, see Figure 7 and Figure 8) upon CNBr cleavage to facilitate mass spectroscopy.

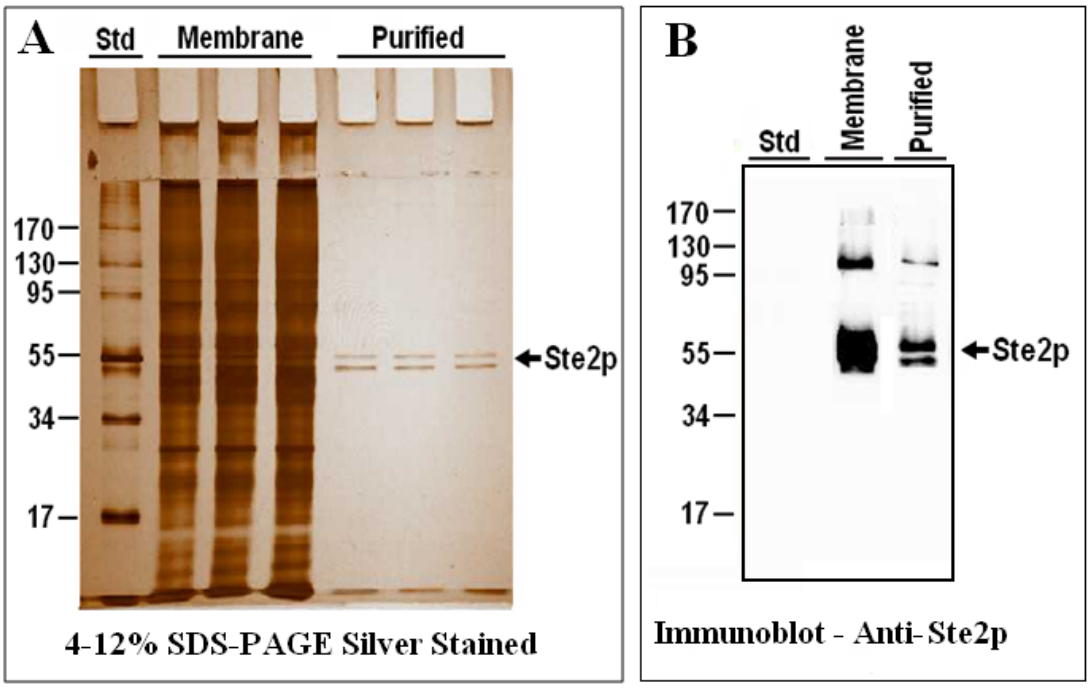

Figure 6: Analysis of purified wild type Ste2p samples. The solubilized membranes containing Ste2p (with His and FLAG epitope tags) were mixed anti-FLAG resin. The eluted samples from the FLAG resin were resolved on 4-12% SDS-PAGE and silver stained (**A**) and also immublotted using antibody directed against the N-terminus of Ste2p (**B**). Two prominent bands, corresponding in molecular weight to the glycosylated and non-glycosylated forms of Ste2p (51-53 kDa) were present in all purified samples (**A**). The bands were identified as Ste2p using the anti-Ste2p band. The dimer form of Ste2p was also observed on the immunoblot image (**B**).

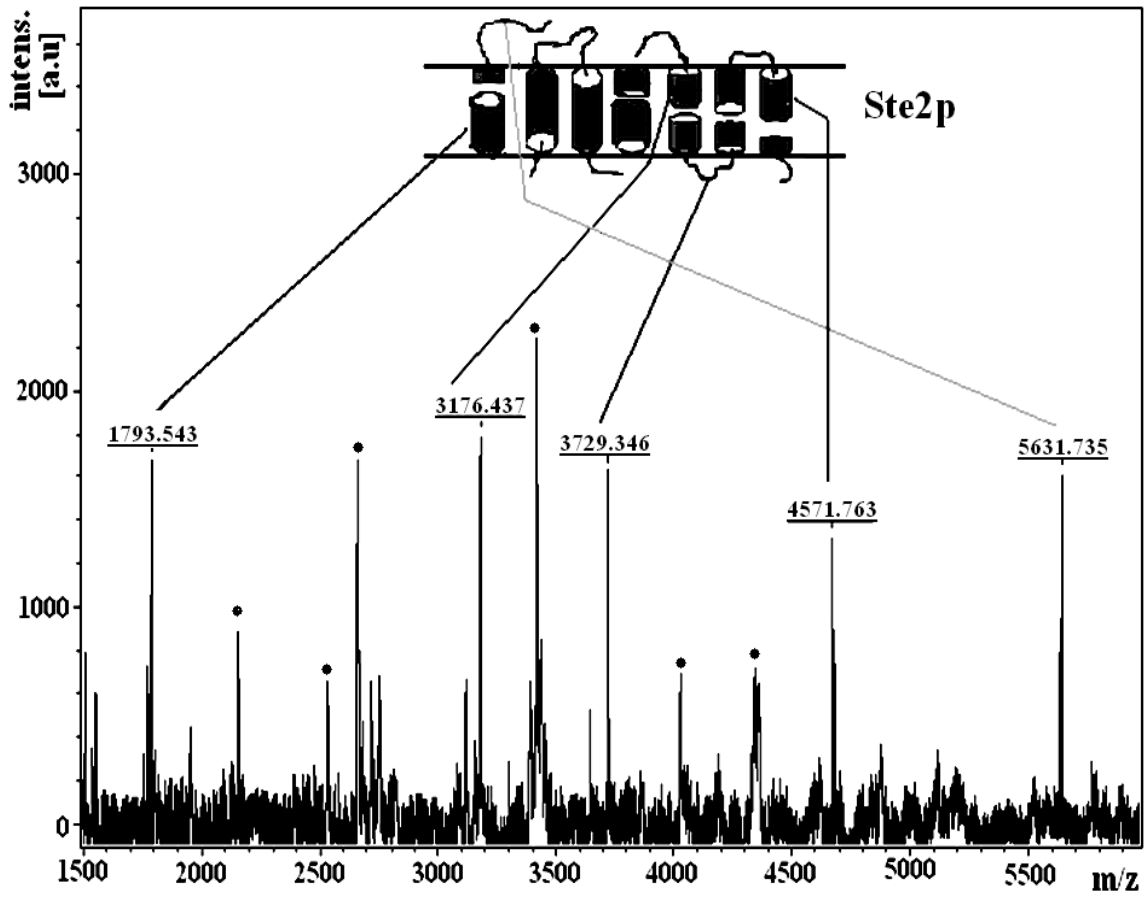

Figure 7: MALDI-TOF analysis of CNBr digests of wild-type Ste2p. Insert is a cartoon of Ste2p showing predicted CNBr fragments. Fragments that correspond to the transmembrane domains and loops of receptor are shown with lines to their corresponding fragments of Ste2p. Peaks labeled with a dot do not correspond to any of the theoretical masses for CNBr cleavage fragments of Ste2p. These are either fragments of proteins that were co-purified with Ste2p or degradation of Ste2p fragments whose masses do not correspond to the predicted CNBr fragment of Ste2p

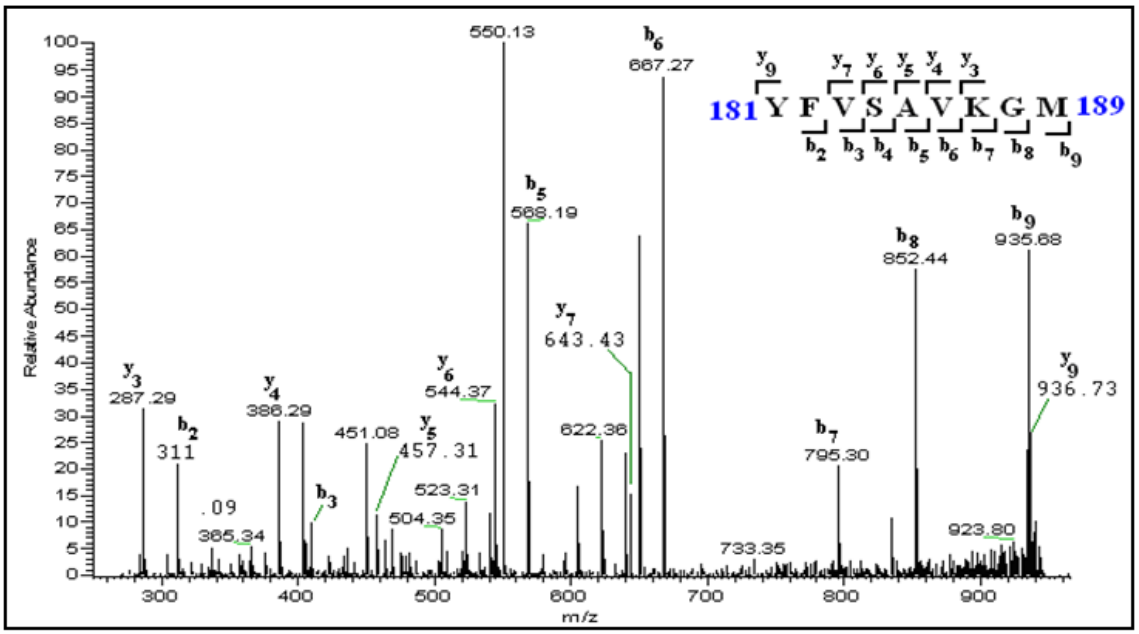

Amino acid sequence	Residues	Domains
•SDAA…TQAIM	(2-54)	N-terminus -TM1
•FGVR….LIVM	(55-69)	TM1
• LTSI…TVTM	(166 – 180)	TM4
• YFVSAVKGM	(181-189)	TM4
• IVTY…SINFM	(190 – 218)	EL3-TM5
• WATA…PVDM	(295-409)	TM7-C-terminus
• YTPDT…HSSG	(410- 458)	C-terminus

Figure 8: MS/MS analysis of CNBr fragments of wild type Ste2p. The samples were analyzed by reversed-phase liquid chromatography/tandem mass spectrometry. **Top panel:** MS/MS spectrum of fragment 181-189. Inserts are one-letter amino acid residue abbreviations of the fragment labeled with the identified ion types. The spectrum shows that 8 out 9 *b* ion fragments and 6 out of the 9 *y* ion fragments were identified. **Lower Panel:** A list of Ste2p CNBr fragments that were identified and sequenced. The overall sequence covers about 65% of the entire Sre2p amino acid sequence.

The substitution of glycine (75.07 Da) for Bpa (269.30 Da) at position 188 should result in a mass shift of 194 Da in the 188Bpa-containing peptide. To estimate purity and concentration of the samples prior to CNBr cleavage and MALDI-TOF analysis, Coomassie blue and silver staining of SDS-PAGE gels was performed on the purified $G188^{TAG}$ and wild-type receptors. In the Coomassie stained gel, only two bands, corresponding in molecular weight to the glycosylated and non-glycosylated forms of Ste2p (51-53 kDa) were observed. Using the more sensitive silver staining technique on the same sample, the same two bands were detected, along with some very faint bands not corresponding to Ste2p. Immunoblot analysis confirmed that the two major bands were Ste2p (data not shown). After CNBr cleavage of WT and $G188^{TAG}$ receptors, we carried out a MALDI-TOF analysis of the peptide fragments generated focusing on the molecular weight region corresponding to the peptide with the putative Gly to Bpa substitution.

Our analysis of the CNBr-cleaved wild-type and $G188^{TAG}$ receptors (Figure 9), revealed a mass shift from 954.154 Da in wild-type to 1146.46 Da in $G188^{TAG}$ corresponding to a 192 Da increase (Figure 9, table). Other peaks of identical mass corresponding to CNBr fragments of Ste2p were observed in both the wild-type (1473.81Da, 1505.39 Da) and G188Bpa (1474.45 Da, 1506.19 Da) receptors. Some peaks not corresponding to any of the theoretical masses of Ste2p CNBr fragments were also observed and are likely due to the degradation of Ste2p which occurred during the overnight incubation at 37C during CNBr cleavage or to the presence of other peptides in the preparation.

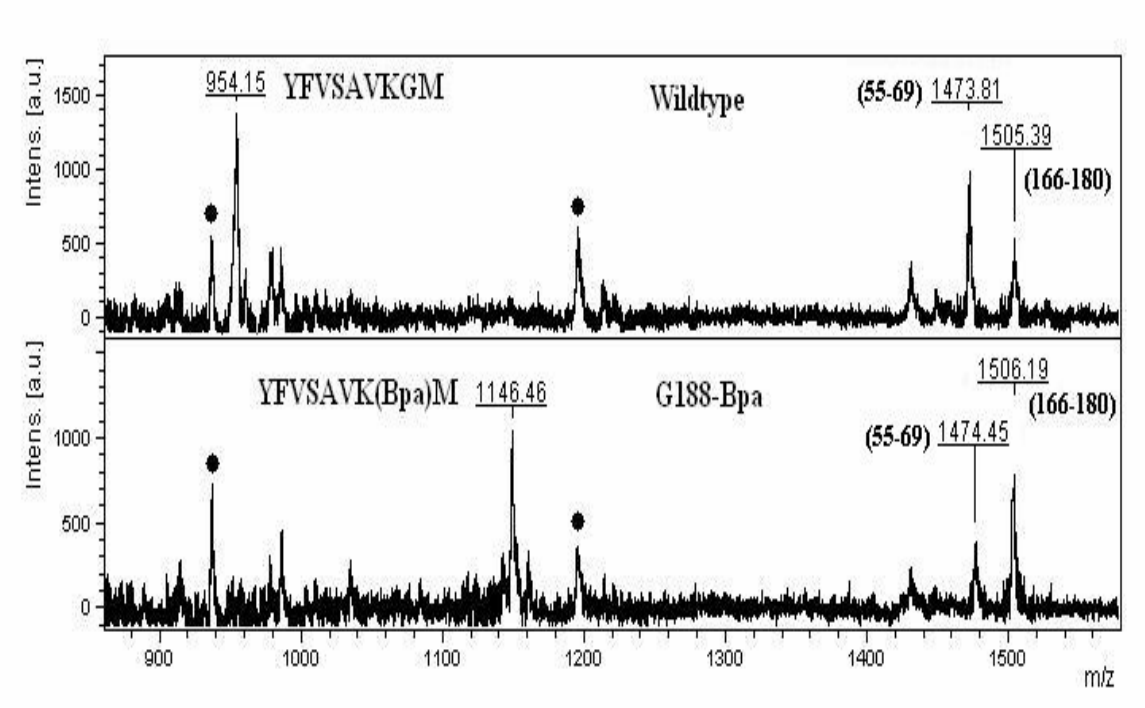

Wild-type		G188^{TAG} (+ Bpa)		Corresponding CNBr Fragment (residues of Ste2p)
Theoretical Mass	Observed Mass	Theoretical Mass	Observed Mass	
953.11	**954.15**	**1147.34**	**1146.46**	181 – 189
1474.82	1473.81	1474.82	1474.45	55 – 69
1506.77	1505.39	1506.77	1506.19	166 – 180

Figure 9: MALDI-TOF analysis of CNBr cleavage fragments of wild-type and G188TAG receptors. A peak (954.15 Da) corresponding to residues 181-189 (YFVSAVKGM) in the wild type receptor was not present in the G188^{TAG} receptor. A new peak (1146.46 Da) corresponding to 181-189 with Bpa at position 188 [YFVSAVK(Bpa)M] was detected. Other peaks corresponding to residues 55-69 and 166-180 were observed for both wild type and G188^{TAG} receptors. Peaks labeled with a black dot do not correspond to any to the theoretical masses for CNBr cleavage fragments of Ste2p. Summary of the MALDI-TOF results are shown on the table. The Masses of wild type fragment 181-189 and corresponding Bpa-mutant are in bold.

Bpa at positions F55 and Y193 can cross-link to the α-factor ligand:

To determine if Bpa incorporated in Ste2p could be used to cross-link to and thus capture the α-pheromone, cells expressing the wild type, $F55^{TAG}$, $G188^{TAG}$ and $Y193^{TAG}$ receptors as well as cells lacking Ste2p as a control were grown in the presence of Bpa. Membranes were prepared and incubated with or without [K^7(biotinylamidocaproate)]α-factor, an α-factor analog which contains biotin on the position seven lysine of the pheromone and binds to the receptor with high affinity (*27*). Crosslinking was also evaluated in the presence or absence of 100-fold excess non-biotinylated α-factor. Following incubation, the membranes were exposed to UV light to activate capture of pheromone to the Bpa-labeled receptor. The membranes were fractionated by SDS-PAGE, blotted and then probed with FLAG antibody to detect Ste2p (Figure 10A) or NeutrAvidin HRP to detect biotinylated ligand (Figure 10B). Wild-type receptor was expressed at levels higher than any of the mutant receptors as seen in previous experiments (Figure 3). When the immunoblots were probed with NeutraAvidin-HRP (Figure 10B) a distinct band was detected at the size expected for Ste2p in the $F55^{TAG}$ and $Y193^{TAG}$ receptors indicating that the biotinylated α-factor was cross-linked. Despite the fact that at least 20 times as much wild-type Ste2p was expressed when compared to the $F55^{TAG}$ or $Y193^{TAG}$ receptors (Figure 10A), labeling as detected with NeutraAvidin-HRP was significantly higher for the mutants (Fig. 7B). Moreover, labeling of the $F55^{TAG}$ and $Y193^{TAG}$ Bpa containing receptors was reduced in the presence of excess non- biotinylated α-factor (Figure 10B) by 83% and 64%, respectively, as determined by quantitation of band density. Similar results were observed in three independent replicates of this experiment.

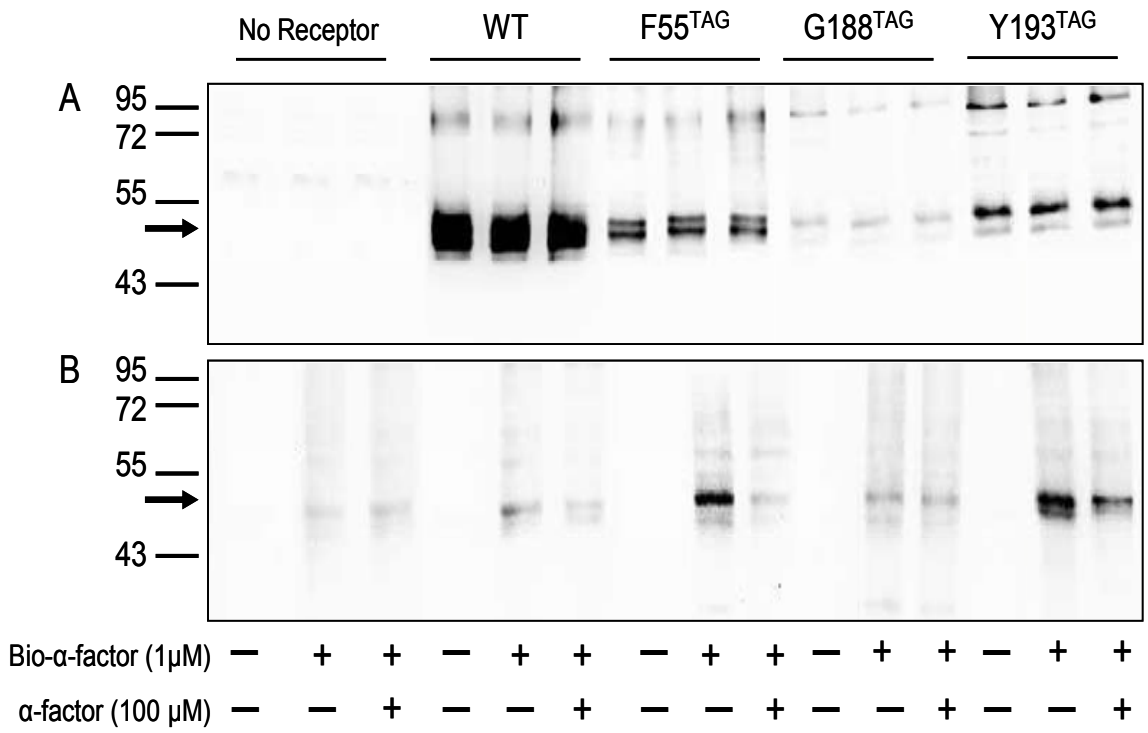

Figure 10: Cross-linking of biotinylated α-factor into Bpa-containing receptors.

Membranes prepared from cells expressing the wild-type, $F55^{TAG}$, $G188^{TAG}$, and $Y193^{TAG}$ receptors grown in the presence of Bpa were incubated with biotinylated-α-factor (1 μM) in the presence (+) or absence (-) of non-biotinylated-α-factor (100 μM) as indicated in the figure. Membranes were also prepared from cells lacking the receptor as a negative control. **A:** Following photoactivation, membranes (2 μg for wild-type and 25 μg for mutants and the negative control) were immublotted and probed with FLAG antibody to detect Ste2p. **B:** Membranes (25 μg for each lane) were immunoblotted and probed with avidin-HRP to detect biotinylated ligand. The arrow in both panels indicates the expected size for Ste2p.

For membranes prepared from cells lacking the receptor, as well as for the WT and the G188^{TAG} receptors a faint band at approximately 50 kD was observed (Figure 10B) that was dependent upon incubation of the membranes with biotinylated pheromone. The signal was not affected by the presence of non-biotinylated pheromone, and could be detected regardless of the Bpa-containing status of the receptor. Thus this signal is the result of non-specific association of the biotinylated pheromone with the membranes in a Ste2p-independent manner.

Chapter 4

Discussion

Many experiments have been performed with a variety of methodologies to provide a wealth of knowledge concerning GPCR structure and function. However, an understanding of the mechanism of activation is still in its infancy. The gold-standard would be to obtain crystal structures of the GPCR in both the resting and active state. Thus far, bovine rhodopsin and the human β-adrenergic receptor are the only GPCRs to have had their crystal structure solved (*37-39*). For rhodopsin, the receptor was crystallized in the inactive state, although recent reports of an active state crystal at moderate to low resolution (2.7–5.5 Å) have been published (*40*). Crystallization of the β-adrenergic receptor required expression as a fusion protein (*39*) or interaction with an inverse agonist (*38*) to stabilize receptor conformation. The use of unnatural amino acid replacement provides an alternate method for examining receptor structure as well as exploring the changes which occur in GPCRs upon receptor activation.

In an earlier study a fluorescent amino acid was incorporated into a GPCR, the neurokinin-2 receptor, using heterologous expression in *Xenopus* oocytes (*12*). In this communication we report the first evidence that an unnatural amino acid can be incorporated into the GPCR Ste2p expressed in its native environment in the yeast cell and still retain function. The incorporation was verified by mass spectrometry, and our studies indicate that once incorporated the photoactivatable Bpa in Ste2p can be used to covalently link the α-factor ligand to the receptor. Although there are many examples in the literature of photoactivated cross-linking of ligand to receptor, in all those cases the ligand contained the photoactivatable moiety. To our knowledge

our study represents the first example of cross-linking of ligand to a GPCR in which the receptor contained the photoactivatable group used to "capture" the ligand.

We demonstrated that incorporation of Bpa into both the F55 (located in TM1) and Y193 (located in EL2) receptors resulted in capture of biotinylated pheromone. Photochemical capture of the ligand could be largely inhibited by the presence of excess non-biotinylated pheromone. While F55 is positioned in the binding pocket of the receptor and was expected to interact with the pheromone (*27*), the ability of Y193 to capture the ligand suggests a possible role for EL2 in ligand binding. Previous studies using domain swapping indicated that EL2 was not a determinant of ligand specificity of the *S. cerevisiae* and *S. kluyveri* α-factor receptors (*41*). Thus our observation of a putative contact between the EL2 region of Ste2p and α-factor indicates the need for further study of EL2-α-factor interactions. In contrast the G188 receptor was not functional with respect to ligand capture, despite the fact that this receptor was determined to contain Bpa by mass spectrometry analysis (Fig. 6). The failure of the G188 receptor and the wild-type receptor to capture α-factor provides a critical control showing that the crosslinking with F55 and Y193 represent residue specific receptor-ligand interactions.

In addition to ligand capture experiments, we can envision other applications of this mutagenesis methodology such as studying changes in domain-domain interactions upon ligand binding which will shed light on the receptor activation mechanism. An advantage of using the orthologous tRNA/aminoacyl tRNA synthetase pair to incorporate Bpa into Ste2p in the yeast cell is that the GPCR remains in its native environment, and is thus able to interact with downstream effector molecules, such as the heterotrimeric G-proteins, thus making assessment of both ligand binding and signal transduction possible.

Although the use of unnatural amino acids has the potential to answer very important questions in GPCR biology, there are still obstacles to overcome. In the experiments presented in this paper, eight mutant *STE2* constructs ($F55^{TAG}$, $S107^{TAG}$, $G115^{TAG}$, $V127^{TAG}$, $G188^{TAG}$, $Y193^{TAG}$, $F204^{TAG}$ and $Y266^{TAG}$) were created with the amber TAG stop codon engineered at different sites within the open reading frame. Theoretically, when the cells expressing these mutant receptors were grown in the presence of Bpa, the unnatural amino acid would be incorporated into the protein by the cognate tRNA/aminoacyl-tRNA synthetase also expressed in the cell. In the absence of Bpa, it was expected that the TAG codon would result in termination of protein synthesis, resulting in a truncated protein. For the mutants $G188^{TAG}$ and $Y193^{TAG}$, this was the case –in the presence of Bpa, cells responded to pheromone (Fig. 2), full-length receptor was detected by immunoblot analysis (Fig. 3) and both bound ligand (Fig. 5) with near wild-type affinity. However, mutants with TAG amber stops at positions G115 and V127 exhibited significant amounts of inefficient stop codon recognition, or read-through, expression, as evidence by halo assay which in the context of the present experiments results in the production of full-length protein even in the absence of Bpa.

The efficiency with which nonsense codons – such as the UAG amber stop in mRNA – are suppressed can be affected by the context of the adjacent codons and poses a challenge (*42*). In *S. cerevisiae* nucleotides within 6 bases flanking the stop codon can influence the efficiency of termination (*43*) and it has been determined that "backup" or tandem stop codons can be found three codons downstream of the authentic stop for some genes (*44*). In the case of read-through, non-cognate tRNA species can misread the stop codon and insert an inappropriate amino acid. In the case of the UAG codon in yeast mRNA, the $tRNA^{Gln}_{GUC}$ can insert glutamine at the stop

codon when it is present in a context unfavorable for release factor recognition (*45*). In another tRNA/aminoacyl tRNA synthetase system evolved to incorporate the fluorescent amino acid dansyl-alanine in response to the amber stop codon, read-through in the absence of dansyl-alanine was eliminated by mutation of the aminoacyl-tRNA synthetase to increase selectivity of the enzyme for dansyl-alanine (*18*). Thus in order to optimize the system for insertion of Bpa into Ste2p, genetic manipulations in protein translation machinery (i.e. ribosomes, tRNAs, etc.) might be warranted. Interestingly, for the mutants $F55^{TAG}$, $S107^{TAG}$, and $F204^{TAG}$ protein function, but not expression, was eliminated when the cells were grown in the presence of Bpa (Fig. 2 and Fig. 3). This indicates the unnatural amino acid was incorporated into the protein, but did not result in a signal-transducing receptor at the cell surface. The presence of mutant Ste2p or other classes of GPCRs that bind ligand but do not signal has been extensively reported (*3*). Indeed binding without signaling is characteristic of antagonists and mutation of GPCRs to preferentially recognize antagonists has been documented (*29, 30*).

Incorporation of Bpa into the various TAG mutant receptors was not 100% efficient, as can be seen by the presence of truncated receptors on immunoblots (Fig. 3B), which could potentially interfere with the function of a full length receptor. However, previous studies showed that overexpression of 14 different truncated Ste2p receptors failed to produce any significant alteration in Ste2p function (*46*). Thus loss of signaling function ($F55^{TAG}$, $S107^{TAG}$, $F204^{TAG}$) in the halo assays that we observed likely results from intolerance of Bpa at the positions into which it was inserted, rather than to the interference by truncated receptors.

Using the orthologous tRNA/aminoacyl-tRNA synthetase pairs to incorporate Bpa at the engineered amber stop codon requires the presence of Bpa in the cytoplasm at sufficient

concentration to allow for effective charging of the tRNA. We have utilized a novel means to supply Bpa to yeast cells via the di/tripeptide transport system that is common to many eukaryotes (*47, 48*). In yeast, di/tripeptides as well as oligopeptides (tetra/pentapeptides) are not cleaved outside the cell, but are transported intact across the plasma membrane (*49, 50*). Expression of the $Y193^{TAG}$ receptor, as well as the $F55^{TAG}$ and $G188^{TAG}$ receptors was noticeably greater when the cells were grown in the presence of Met-Bpa at 0.1 mM when compared to Bpa (Fig. 4). Since peptide transporters are ubiquitous in living cells (*48*), this method might be used to enhance the delivery of unnatural amino acids and extend this approach to amino acids that cannot enter cells through amino acid permeases.

In summary, in this report we provide the first evidence that the unnatural photoactivatable amino acid *p*-benzoyl-*L*-phenylalanine can be incorporated into a G protein-coupled receptor in its native cell. Several of the mutant receptors responded to their natural ligand, the α-factor tridecapeptide, and bound this molecule with nM affinity. The mutant receptors were expressed at the membrane at levels from 5 to 10% of the wild-type receptor under identical conditions. Mass spectrometry proved that Bpa was incorporated at the expected position for the $G188^{TAG}$ receptor. Expression could be increased when the unnatural amino acid was delivered as a dipeptide via the peptide transport system of *S. cerevisiae*. Two Bpa-containing receptors were able to capture ligand after photoactivation providing evidence for the utility such labeled GPCRs to determine ligand-receptor interactions. These results set the stage for the use of unnatural amino acids technology in exploring the structure and function of integral membrane proteins in their native environment.

References for Part III

1. Eilers, M., Hornak, V., Smith, S. O., and Konopka, J. B. (2005) Comparison of class A and D G protein-coupled receptors: common features in structure and activation, *Biochemistry 44*, 8959-8975.
2. Karnik, S. S., Gogonea, C., Patil, S., Saad, Y., and Takezako, T. (2003) Activation of G-protein-coupled receptors: a common molecular mechanism, *Trends Endocrinol. Metab. 14*, 431-437.
3. Kristiansen, K. (2004) Molecular mechanisms of ligand binding, signaling, and regulation within the superfamily of G-protein-coupled receptors: molecular modeling and mutagenesis approaches to receptor structure and function, *Pharmacol. Ther. 103*, 21-80.
4. Chin, J. W., Cropp, T. A., Anderson, J. C., Mukherji, M., Zhang, Z., and Schultz, P. G. (2003) An expanded eukaryotic genetic code, *Science 301*, 964-967.
5. Wang, L., Xie, J., and Schultz, P. G. (2006) Expanding the genetic code, *Annu. Rev. Biophys. Biomol. Struct. 35*, 225-249.
6. Liu, W., Brock, A., Chen, S., and Schultz, P. G. (2007) Genetic incorporation of unnatural amino acids into proteins in mammalian cells, *Nat. Methods 4*, 239-244.
7. Chen, S., Schultz, P. G., and Brock, A. (2007) An improved system for the generation and analysis of mutant proteins containing unnatural amino acids in Saccharomyces cerevisiae, *J. Mol. Biol. 371*, 112-122.
8. Xie, J., and Schultz, P. G. (2005) Adding amino acids to the genetic repertoire, *Curr. Opin. Chem. Biol. 9*, 548-554.

9. Monahan, S. L., Lester, H. A., and Dougherty, D. A. (2003) Site-specific incorporation of unnatural amino acids into receptors expressed in Mammalian cells, *Chem. Biol. 10*, 573-580.

10. Sakamoto, K., Hayashi, A., Sakamoto, A., Kiga, D., Nakayama, H., Soma, A., Kobayashi, T., Kitabatake, M., Takio, K., Saito, K., Shirouzu, M., Hirao, I., and Yokoyama, S. (2002) Site-specific incorporation of an unnatural amino acid into proteins in mammalian cells, *Nucleic Acids Res. 30*, 4692-4699.

11. Rodriguez, E. A., Lester, H. A., and Dougherty, D. A. (2006) In vivo incorporation of multiple unnatural amino acids through nonsense and frameshift suppression, *Proc. Natl. Acad. Sci. U. S. A. 103*, 8650-8655.

12. Turcatti, G., Nemeth, K., Edgerton, M. D., Meseth, U., Talabot, F., Peitsch, M., Knowles, J., Vogel, H., and Chollet, A. (1996) Probing the structure and function of the tachykinin neurokinin-2 receptor through biosynthetic incorporation of fluorescent amino acids at specific sites, *J. Biol. Chem. 271*, 19991-19998.

13. Padgett, C. L., Hanek, A. P., Lester, H. A., Dougherty, D. A., and Lummis, S. C. (2007) Unnatural amino acid mutagenesis of the GABA(A) receptor binding site residues reveals a novel cation-pi interaction between GABA and beta 2Tyr97, *J. Neurosci. 27*, 886-892.

14. McMenimen, K. A., Dougherty, D. A., Lester, H. A., and Petersson, E. J. (2006) Probing the Mg2+ blockade site of an N-methyl-D-aspartate (NMDA) receptor with unnatural amino acid mutagenesis, *A.C.S. Chem. Biol. 1*, 227-234.

15. Beene, D. L., Brandt, G. S., Zhong, W., Zacharias, N. M., Lester, H. A., and Dougherty, D. A. (2002) Cation-pi interactions in ligand recognition by serotonergic (5-HT3A) and

nicotinic acetylcholine receptors: the anomalous binding properties of nicotine, *Biochemistry 41*, 10262-10269.

16. Tong, Y., Brandt, G. S., Li, M., Shapovalov, G., Slimko, E., Karschin, A., Dougherty, D. A., and Lester, H. A. (2001) Tyrosine decaging leads to substantial membrane trafficking during modulation of an inward rectifier potassium channel, *J. Gen. Physiol. 117*, 103-118.

17. Santarelli, V. P., Eastwood, A. L., Dougherty, D. A., Horn, R., and Ahern, C. A. (2007) A cation-pi interaction discriminates among sodium channels that are either sensitive or resistant to tetrodotoxin block, *J. Biol. Chem. 282*, 8044-8051.

18. Summerer, D., Chen, S., Wu, N., Deiters, A., Chin, J. W., and Schultz, P. G. (2006) A genetically encoded fluorescent amino acid, *Proc. Natl. Acad. Sci. U. S. A. 103*, 9785-9789.

19. Deiters, A., Cropp, T. A., Mukherji, M., Chin, J. W., Anderson, J. C., and Schultz, P. G. (2003) Adding amino acids with novel reactivity to the genetic code of Saccharomyces cerevisiae, *J. Am. Chem. Soc. 125*, 11782-11783.

20. David, N. E., Gee, M., Andersen, B., Naider, F., Thorner, J., and Stevens, R. C. (1997) Expression and purification of the Saccharomyces cerevisiae alpha-factor receptor (Ste2p), a 7-transmembrane-segment G protein-coupled receptor, *J. Biol. Chem. 272*, 15553-15561.

21. Mumberg, D., Muller, R., and Funk, M. (1995) Yeast vectors for the controlled expression of heterologous proteins in different genetic backgrounds, *Gene 156*, 119-122.

22. Gietz, D., St Jean, A., Woods, R. A., and Schiestl, R. H. (1992) Improved method for high efficiency transformation of intact yeast cells, *Nucleic Acids Res. 20*, 1425.

23. Sherman, F. (2002) Getting started with yeast, *Methods Enzymol. 350*, 3-41.

24. Naider, F., Becker, J. M., and Katzir-Katchalski, E. (1974) Utilization of methionine-containing peptides and their derivatives by a methionine-requiring auxotroph of Saccharomyces cerevisiae, *J. Biol. Chem. 249*, 9-20.

25. Raths, S. K., Naider, F., and Becker, J. M. (1988) Peptide analogues compete with the binding of alpha-factor to its receptor in Saccharomyces cerevisiae, *J. Biol. Chem. 263*, 17333-17341.

26. Konopka, J. B., Jenness, D. D., and Hartwell, L. H. (1988) The C-terminus of the S. cerevisiae alpha-pheromone receptor mediates an adaptive response to pheromone, *Cell 54*, 609-620.

27. Son, C. D., Sargsyan, H., Naider, F., and Becker, J. M. (2004) Identification of ligand binding regions of the Saccharomyces cerevisiae alpha-factor pheromone receptor by photoaffinity cross-linking, *Biochemistry 43*, 13193-13203.

28. Akal-Strader, A., Khare, S., Xu, D., Naider, F., and Becker, J. M. (2002) Residues in the first extracellular loop of a G protein-coupled receptor play a role in signal transduction, *J. Biol. Chem. 277*, 30581-30590.

29. Lee, Y. H., Naider, F., and Becker, J. M. (2006) Interacting residues in an activated state of a G protein-coupled receptor, *J. Biol. Chem. 281*, 2263-2272.

30. Lee, B. K., Lee, Y. H., Hauser, M., Son, C. D., Khare, S., Naider, F., and Becker, J. M. (2002) Tyr266 in the sixth transmembrane domain of the yeast alpha-factor receptor

plays key roles in receptor activation and ligand specificity, *Biochemistry 41*, 13681-13689.

31. Grishin, A. V., Weiner, J. L., and Blumer, K. J. (1994) Control of adaptation to mating pheromone by G protein beta subunits of Saccharomyces cerevisiae, *Genetics 138*, 1081-1092.

32. Weiner, J. L., Guttierez-Steil, C., and Blumer, K. J. (1993) Disruption of receptor-G protein coupling in yeast promotes the function of an SST2-dependent adaptation pathway, *J. Biol. Chem. 268*, 8070-8077.

33. Mentesana, P. E., and Konopka, J. B. (2001) Mutational analysis of the role of N-glycosylation in alpha-factor receptor function, *Biochemistry 40*, 9685-9694.

34. Island, M. D., Perry, J. R., Naider, F., and Becker, J. M. (1991) Isolation and characterization of S. cerevisiae mutants deficient in amino acid-inducible peptide transport, *Curr. Genet. 20*, 457-463.

35. Perry, J. R., Basrai, M. A., Steiner, H. Y., Naider, F., and Becker, J. M. (1994) Isolation and characterization of a Saccharomyces cerevisiae peptide transport gene, *Mol. Cell. Biol. 14*, 104-115.

36. Hauser, M., Kauffman, S., Naider, F., and Becker, J. M. (2005) Substrate preference is altered by mutations in the fifth transmembrane domain of Ptr2p, the di/tri-peptide transporter of Saccharomyces cerevisiae, *Mol. Membr. Biol. 22*, 215-227.

37. Palczewski, K., Kumasaka, T., Hori, T., Behnke, C. A., Motoshima, H., Fox, B. A., Le Trong, I., Teller, D. C., Okada, T., Stenkamp, R. E., Yamamoto, M., and Miyano, M.

(2000) Crystal structure of rhodopsin: A G protein-coupled receptor, *Science 289*, 739-745.

38. Rasmussen, S. G., Choi, H. J., Rosenbaum, D. M., Kobilka, T. S., Thian, F. S., Edwards, P. C., Burghammer, M., Ratnala, V. R., Sanishvili, R., Fischetti, R. F., Schertler, G. F., Weis, W. I., and Kobilka, B. K. (2007) Crystal structure of the human beta2 adrenergic G-protein-coupled receptor, *Nature 450*, 383-387.

39. Rosenbaum, D. M., Cherezov, V., Hanson, M. A., Rasmussen, S. G., Thian, F. S., Kobilka, T. S., Choi, H. J., Yao, X. J., Weis, W. I., Stevens, R. C., and Kobilka, B. K. (2007) GPCR engineering yields high-resolution structural insights into beta2-adrenergic receptor function, *Science 318*, 1266-1273.

40. Ridge, K. D., and Palczewski, K. (2007) Visual rhodopsin sees the light: structure and mechanism of G protein signaling, *J. Biol. Chem. 282*, 9297-9301.

41. Sen, M., and Marsh, L. (1994) Noncontiguous domains of the alpha-factor receptor of yeasts confer ligand specificity, *J. Biol. Chem*. *269*, 968-973.

42. Xie, J., and Schultz, P. G. (2006) A chemical toolkit for proteins--an expanded genetic code, *Nat. Rev. Mol. Cell. Biol. 7*, 775-782.

43. Williams, I., Richardson, J., Starkey, A., and Stansfield, I. (2004) Genome-wide prediction of stop codon readthrough during translation in the yeast Saccharomyces cerevisiae, *Nucleic Acids Res. 32*, 6605-6616.

44. Liang, H., Cavalcanti, A. R., and Landweber, L. F. (2005) Conservation of tandem stop codons in yeasts, *Genome Biol. 6*, R31.

45. Edelman, I., and Culbertson, M. R. (1991) Exceptional codon recognition by the glutamine tRNAs in Saccharomyces cerevisiae, *EMBO J. 10*, 1481-1491.

46. Martin, N. P., Leavitt, L. M., Sommers, C. M., and Dumont, M. E. (1999) Assembly of G protein-coupled receptors from fragments: identification of functional receptors with discontinuities in each of the loops connecting transmembrane segments, *Biochemistry 38*, 682-695.

47. Daniel, H., Spanier, B., Kottra, G., and Weitz, D. (2006) From bacteria to man: archaic proton-dependent peptide transporters at work, *Physiology (Bethesda) 21*, 93-102.

48. Saier, M. H., Jr. (2000) A functional-phylogenetic classification system for transmembrane solute transporters, *Microbiol. Mol. Biol. Rev. 64*, 354-411.

49. Becker, J. M., and Naider, F. (1995) in *Peptide-based drug design : controlling transport and metabolism* (Taylor, M. D., and Amidon, G. L., Eds.) pp xviii, 567 p., American Chemical Society, Washington, DC.

50. Hauser, M., Donhardt, A. M., Barnes, D., Naider, F., and Becker, J. M. (2000) Enkephalins are transported by a novel eukaryotic peptide uptake system, *J. Biol. Chem. 275*, 3037-3041.

PART IV

The Third Intracellular Loop of Ste2p, a Yeast G Protein-Coupled Receptor, is involved in a homo-dimer interface.

Part IV presents collaborative work with Dr. Fred Naider's laboratory at the City University of New York, Staten Island. George K. E. Umanah performed most the work, Liyin Huang assisted with the biochemical studies, Julie Maccarone determined the phenotypes of the Ste2p mutants and the peptides used were obtained from Dr. Naider's laboratory.

CHAPTER 1

Introduction

G-protein coupled receptors (GPCRs) are integral membrane proteins with seven transmembrane (TM) helical segments, which are known to play important roles in cell communication by activating intracellular events through both G protein-dependent and – independent processes (*1-3*). These receptors are encoded by the largest gene family in mammals, constitute the main target of prescribed drugs on the market, and still represent the most promising targets for new drug development (*1, 3-6*). Although these GPCRs are part of a very complex receptor-signaling system, this complexity is even higher when considering that these receptors can organize into homo-dimers and homo-oligomers (*7-11*). However, the existence of such high ordered GPCRs assemblies in native systems and their functional consequences remain unsolved (*12, 13*).

GPCRs have been observed to exist in membranes as monomers, dimers or oligomers in intact cells and in membranes prepared from cells, with the dimer often regarded as the minimal oligomeric arrangement required for G protein coupling. Animal model studies show that GPCR oligomers play an essential role in human pathologies (*4, 11, 13*). Although the monomer of GPCRs is capable of activating G proteins, the dimeric form couples the G protein more efficiently in some GPCRs (*7, 14, 15*). One of the earliest studies to show evidence of GPCR dimerization demonstrated that overexpressed, differentially tagged β_2-adrenergic receptors (β_2AR) form dimers and also showed that a peptide corresponding to the TM6 (transmembrane domain 6) region of the β_2AR could be used to disrupt the dimer and decrease receptor function implying that TM6 is important for dimer formation in β_2AR (*16*). Dimers between the two

different GABA receptors, $GABA_BR1$ and $GABA_BR2$, were shown to be required to form fully functional GABA receptors. The study also suggested that both GPCR subunits in a dimer seem to have distinct roles in the complex and that the $GABA_BR1$ seems to be responsible for ligand binding while the $GABA_BR2$ is required for G protein coupling (*12, 13*). Thus, whereas some GPCRs such as the metabotropic glutamate (mGlu) receptors are strict dimers, other GPCRs like the GABA receptors form oligomers that may couple with only one G protein (*13*).

Detailed examination of the crystallographic structure of rhodopsin suggested that TM1, TM2, TM4, TM5, the second intracellular loop (IL2), and the third intracellular loop (IL3) are all involved in the formation of rhodopsin oligomers. Thus, it seems that oligomerization of rhodopsin-like family of GPCRs involves more than one contact (*7, 14, 15*). Some GPCRs have been shown to use different oligomerization interfaces to achieve functional activities (*13*). The use of truncated receptors and other studies suggest that GPCR dimer formation may involve domain swapping or direct contacts of the receptor subunits. Mutation and computational analyses all provide evidence of the involvement of TM5, TM6 and IL3 in the dimerization interface in both the swapping and direct-contact models in some GPCRs tested (*9*). Even though many physiological activities have been assigned to the role of GPCRs oligomers, it is not clear whether GPCR oligomerization plays a role in the chaperoning and cell transport of receptors, or in the control of signaling specificity and efficacy. Nevertheless, evidence of dimerization in all GPCR families makes it an important phenomenon that needs investigation (*4, 11, 13*).

The yeast *Saccharomyces cerevisiae* GPCR, Ste2p, has been shown to form dimers in intact cells and membranes. Co-expression of Ste2p tagged with the cyan or yellow fluorescent

proteins (CFP or YFP) resulted in efficient fluorescence resonance energy transfer (FRET). The study also showed that dominant-interfering receptor mutants inhibited signaling by interacting with wild-type receptors rather than by sequestering G proteins (*17, 18*). Analysis of Ste2p truncated mutants showed that the N-terminal extracellular domain, TM1, and TM2 are all involved in receptor oligomerization (*19*). Recently, disulfide cross-linking studies have also shown TM1 and TM4 as dimer contacts in Ste2p similar to that of the rhodopsin family of GPCRs (*20*). Our lab has also shown that TM7 is a dimer contact in Ste2p (Kim, Heejung, personal communication). Subunits of Ste2p in a dimer complex have been found to be activated independently rather than cooperatively by agonist, but function together to promote G protein activation, possibly by contacting different subunits or regions of the G protein (*21*). Despite the intensive studies on Ste2p dimer formation, the role and organization of the dimers are not well defined.

This study identifies residues in IL3, the intracellular loop between TM5 and TM6, as a dimer contact in Ste2p. Residues in IL3 may be critical for dimer stability during receptor activation that involves rearrangement of the helices. Overall replacement of individual residues with cysteine did not significantly affect Ste2p activity, with the exception of R233C that displayed about 70% of wild type activity. Dimer formation via a Cys-Cys disulfide bond was reduced at the cytoplasmic ends of TM5 and TM6 in the presence of ligand implying that activation of Ste2p involves ligand-induced conformational changes in these portions of TM5 and TM6. This study is the first to identify IL3 as a dimer contact and also pinpoint specific residues that may be involved in stabilizing the oligomer form of Ste2p. We also propose an organization of an IL3-mediated dimer that fits with other dimer contacts identified in Ste2p.

CHAPTER 2

Materials and Methods

Media, Reagents, and Strains and Transformation:

Saccharomyces cerevisiae strain LM102 [*MAT**a**, bar1, leu2, trp1, ura3, FUS1-lacZ::URA3, ste2*Δ (*22*)] was used for Step2 growth arrest and *FUS1-LacZ* assays and the protease deficient strain BJS21 [*MAT**a***, *prc1-407 prb1-1122 pep4-3 leu2 trp1 ura3-52 ste2::Kan*^{R} (*23*)] was used for protein isolation and immunoblot analysis. The *STE2* mutant and *GPA1* plasmids were co-transformed by the method of Geitz (*24*) into LM102, and BJS21 cells along with *GPA1* mutant plasmids.

For all transformation cells were cultured in their selective media and grown to mid-log phase at 30^{o}C with shaking (200 rpm) overnight. The cells (5 ml culture) were then harvested and washed with sterile water and 100 mM LiAc (lithium acetate) by centrifugation at 4000g for 5 minutes. The pellet was resuspended in transformation mixture [240µl of 50% PEG (polyethylene glycol); 36µl of 1.0 M LiAc; 25µl of salmon sperm DNA; and 50µ water with plasmid DNA (5 µg)]. The mixture was incubated at 30^o C for 30 minutes and then heat shock at 42^o C for 25 minutes. The cells were separated from the mixture and resuspended in sterile water for plating on selective media. Transformants were selected by growth on minimal medium (*25*) lacking tryptophan and uracil (designated as MLTU) or tryptohan and histidine (designated as MLTH) to maintain selection for the plasmids. All media components were obtained from BD (Franklin Lakes, NJ) and were of the highest quality available.

Cysteine scanning mutagenesis:

C-terminal FLAG and His tagged *STE2* with the two cysteine residues (Cys59 and Cys252) substituted with serine and cloned into the plasmid p424-GPD to yield plasmid pBEC2 **(*22*)** was used for expressing Ste2p. The plasmid pBEC2 was engineered by site-directed mutagenesis to replace 22 residues, one at a time, in Ste2p (A228-I249) with cysteine. The open reading frame of *GPA1* was PCR amplified from the plasmid YepGαβγ **(*26*)** and cloned into the plasmid p426-GPD (*27*) to yield plasmid pBUG6. Primers used for the mutagenesis are listed in Table 1**.** The sequence of all cysteine mutants was verified by DNA sequence analysis completed by the molecular biology resource facility located on the campus of the University of Tennessee. Mutagenic and sequencing primers were purchased from Invitrogen (Carlsbad, CA)

Membrane extraction and Immunoblots:

BJS21 cells expressing S*TE2* and *GPA1* constructs grown in their selective media were used to prepare total cell membranes isolated as previously described (*28*). Cells were harvested and lysed by agitation with glass beads in 700 µL of HEPES buffer (50 mM HEPES, 150 mM NaCl, pH 7.5) and the following concentrations of protease inhibitors: 1.0 mM leupeptin, 10 µM pepstatin A, and 5.0 mM phenylmethanesulfonyl fluoride. The lysate was cleared by centrifugation at 3000g for 2 minutes. The membrane fraction was harvested by centrifugation at 15000g for 30 minutes and was then resuspended in the HEPES buffer with 20% glycerol. Protein concentration was determined by BioRad (BioRad, Hercules, CA) protein assay (*22*). For immunoblot analyses the membrane extract was solubilized in SDS sample buffer (BioRad, Hercules, CA) and 5 µg were fractioned by SDS-PAGE.

Table 1: Primers used for the mutagenesis.

Primer for Ste2p-IL3 Cys Mutants		Primer for Ste2p-IL3 Cys Mutants	
L228C Forward:	TTGATTTGCGCTATTAGATCAAGAAG	K239C Forward:	CCTTGGTCTCTGCCAGTTCGATAGTTTCC
L228C Reverse:	CTAATAGCGCAAATCAATTTAACTACC	K239C Reverse:	CTATCGAACTGGCAGAGACCAAGGAATC
A229C Forward:	GATTTTATGCATTAGATCAAGAAGATTCC	Q240C Forward:	GTCTCAAGTGCTTCGATAGTTTCCATATTTTAC
A229C Reverse:	GATCTAATGCATAAAATCAATTTAACTACC	Q240C Reverse:	CTATCGAAGCACTTGAGACCAAGGAATC
I230C Forward:	GATTTTAGCTTGCAGATCAAGAAGATTCCTTGG	F241C Forward:	CAAGCAGTGCGATAGTTTCCATATTTTAC
I230C Reverse:	CTTGATCTGCAAGCTAAAATCAATTTAACTACC	F241C Reverse:	GAAACTATCGCACTGCTTGAGACCAAGG
R231C Forward:	TTAGCTATTTGCTCAAGAAGATTCCTTGG	D242C Forward:	GCAGTTCTGCAGTTTCCATATTTTACTC
R231C Reverse:	CTTCTTGAGCAAATAGCTAAAATCAATTTAAC	D242C Reverse:	GGAAACTGCAGAACTGCTTGAGACCAAG
S232C Forward:	CTATTAGATGCAGAAGATTCCTTGG	S243C Forward:	CAGTTCGATTGCTTCCATATTTTACTC
S232C Reverse:	CTTCTGCATCTAATAGCTAAAATC	S243C Reverse:	TATGGAAGCAATCGAACTGCTTGAG
R233C Forward:	GATCATGCAGATTCCTTGGTCTCAAG	F244C Forward:	CGATAGTTGCCATATTTTACTCATAATG
R233C Reverse:	GGAATCTGCATGATCTAATAGCTAAAATC	F244C Reverse:	AATATGGCAACTATCGAACTGCTTGAGAC
R234C Forward:	CAAGATGCTTCCTTGGTCTCAAGC	H245C Forward:	TAGTTTCTGCATTTTACTCATAATGTC
R234C Reverse:	CAAGGAAGCATCTTGATCTAATAGC	H245C Reverse:	GTAAAATGCAGAAACTATCGAACTGCC
F235C Forward:	GAAGATGCCTTGGTCTCAAGCAGTTCGATAG	I246C Forward:	GTTTCCATTGCTTACTCATAATGTCATC
F235C Reverse:	CCAAGGCATCTTCTTGATCTAATAGC	I246C Reverse:	TGAGTAAGCAATGGAAACTATCGAAC
L236C Forward:	GATTCTGCGGTCTCAAGCAGTTCGATAG	L247C Forward:	TTCCATATTTGCCTCATAATGTCATCTC
L236C Reverse:	GACCGCAGAATCTTCTTGATC	L247C Reverse:	TATGAGGCAAATATGGAAACTATCG
G237C Forward:	GATTCCTTTGCCTCAAGCAGTTCGATAG	L248C Forward:	CATATTTTATGCATAATGTCATCTCAATC
G237C Reverse:	CTTGAGGCAAAGGAATCTTCTTG	L248C Reverse:	ACATTATGCATAAAATATGGAAACTATC
L238C Forward:	CTTGGTTGCAAGCAGTTCGATAG	I249C Forward:	ATTTTACTCTGCATGTCATCTCAATCTTTG
L238C Reverse:	CTGCTTGCAACCAAGGAATCTTC	I249C Reverse:	GATGACATGCAGAGTAAAATATGGAAAC

Blots were probed with FLAG antibody (Sigma/Aldrich Chemical, St. Louis, MO) to detect Ste2p. The signals generated were analyzed using Quantity One software (Version 4.5.1) on a Chemi-Doc XRS photodocumentation system (BioRad, Hercules, CA).

Growth Arrest Assays:

LM102 cells expressing C-terminal FLAG and His tagged Ste2p were grown at 30 ºC in MLT (minimal medium (*25*) lacking tryptophan), harvested, washed three times with water and resuspended at a final concentration of 5 x 10^6 cells/ml (*23*). Cells (1 ml) were combined with

3.5 ml agar noble (1.1 %) and poured as a top agar lawn onto MLT medium agar plates. Filter disks (BD, Franklin Lakes, NJ) impregnated with α-factor pheromone (0.125 – 2.0 μg) were placed on the top agar. The plates were incubated at 30 ºC for 18 hours and then observed for clear halos around the discs. The diameter of halos around the discs were measured and analyzed by linear regression analysis using Prism software (GraphPad Software, San Diego, CA). The experiment was repeated at least three times and reported values represent the mean of these tests.

Fus1-LacZ Assays:

LM102 cells expressing C-terminal FLAG and His tagged Ste2p Cys mutants were grown at 30 ºC in selective media, harvested, washed three times with fresh media and resuspended at a final concentration of 5 x 10^7 cells/ml. Cells (0.5 ml) were combined with α-factor pheromone (final concentration of 1 μM) and incubated at 30 ºC for 90 minutes. The cells were transferred to a 96-well flatbottom plate in triplicates, permeabilized with 0.5% Triton X-100 in 25 mM PIPE buffer and then β-galactosidase assays were carried out using fluorescein di-β-galactopyranoside (Molecular Probes, OR) as a substrate (*29*). The reaction mixtures were incubated at 37^{o}C for 60 min and 1.0 M Na_2CO_3 was added to stop the reaction. The fluorescence of the samples (excitation of 485nm and emission of 530 nM) was determined using a 96-well plate reader Synergy2 (BioTek Instruments, Inc., Winooski, VT). The data were analyzed using Prism software (GraphPad Software, San Diego, CA). The experiments were repeated at least three times and reported values represent the mean of these tests.

Disulfide cross-linking:

Membrane proteins (in HEPES buffer, 20% glycerol) extracted from BJS21 cells expressing Ste2p mutants or co-expressing with Gpa1p mutants were treated with Cu-P (1.0 μM Cu and 3.0 μM 1,10-phenanthroline) according to optimum concentrations for Cu-P determined in part 5 of the dissertation, Membrane samples were incubated with Cu-P at room temperature for 30 min. The reaction was quenched by addition of EDTA to final concentration of 10 mM. The cross-linked samples were resuspended in non-reducing SDS sample buffer (BioRad, Hercules, CA) and resolved on SDS-PAGE as described above. The disulfide reaction was reversed by reducing with 4% 2-mercaptoethanol (β-ME) in the SDS sample buffer before resolving it on SDS-PAGE. To investigate the effects of ligand or GTP on cross-linking, membrane fractions were incubated in HEPES buffer containing 5μM α-factor (WHWLQLKPGQPNle^{12}Y) or 20 μM α-factor antagonist (WLQLKPGQPNle^{12}Y) in the presence or absence of 0.1 mM GTP or GTP-γ-S (*1*) before Cu-P treatment.

For in vivo cross-linking, cells were grown to mid-log phase, harvested and washed with water by centrifugation (4000g for 5 min). The cells were resuspended in 100 mM LiAc and incubated at 30 ^{o}C for 30 min with mixing. After centrifugation, the cells were resuspended in 25% PEG with 250 mM LiAc for another 60 min incubation. Cells were washed with HEPES buffer three times after LiAc treatment. For whole cell ligand binding prior to cross-linking, cells were first incubated with KF (10 mM) and NaN_3(10mM) in HEPES buffer at room temperature for 15 min to inhibit receptor endocytosis (*30*) and then ligand added to final concentrations of 5μM for native α-factor or 20 μM for α-factor antagonist for another 30 min. Disulfide cross-linking was induced by adding Cu-P to final concentrations of 0.5 mM Cu and

1.5 mM 1,10-phenanthroline (*20*). Control cells without cross-linking were treated with equivalent volume of HEPES buffer. The mixture was incubated at room temperature for 60 min with end-over-end mixing. EDTA (ethylenediamine-tetraacetic acid) and NEM (N-Ethylmaleimide) to final concentrations of 10 mM were added to stop the reaction. The cells were washed three times with HEPES buffer containing EDTA (10 mM) and NEM (10 mM). Membrane extraction was carried as described above with HEPES buffer containing 10 mM EDTA/NEM. Reducing condition of disulfide bond were carried out by resuspending membrane samples in SDS-PAGE sample buffer containing 4% β-ME and incubating at room temperature for at least 15 min.

Prediction and modeling:

All models of 3-D structures were generated by the Phyre Structural Bioinformatics Group prediction tools (*31*). The structures were viewed and labeled with the PyMOL pdb viewer software (DeLano Scientific LLC, Palo Alto, CA).

CHAPTER 3

Results

Phenotypes of Ste2p IL3 Cys substitution mutants:

The signaling activities of the cysteine mutants were examined by α-factor induced growth arrest and *FUS1-LacZ* induction assays. The growth arrest assay is a sensitive test that measures the ability of cells expressing Ste2p to maintain pheromone-induced cell division arrest at the G_1 phase over a period of time. One of the early responses of the yeast cell to pheromone is the transcription of the gene *FUS1*. The *FUS1* gene product is involved in the fusion of cells during conjugation. The strains used in this study contain a reporter gene construct consisting of a fusion between *FUS1* promoter and the *lacZ* gene encoding the enzyme β-galactosidase (*32*). This allows for rapid, sensitive detection of mating pathway activation by assessing β-galactosidase activity in response to mating pheromone (*29*).

The Cys-less Ste2p engineered as the background for the specific cysteine mutations has been previously shown to have biological activities identical to the wild type receptor as determined by assays used in our lab. Both endogenous cysteine residues at positions 59 and 252 were substituted with serine to create a Cys-less receptor (*22*). We grouped the intracellular loop 3 (IL3) residues into three categories based on their phenotypes as follows: group 1 (TM5-IL3 boundary**)** residues, L228-S232; group 2 **(**middle IL3**)** residues, R233-Q240; and group 3 **(**IL3-TM6 boundary**)** residues, F241-I249. Ste2p with mutated group 1 residues (L228C-S232C) were expressed at levels similar to the Cys-less receptor as determined by FLAG immunoblot (Figure 1).

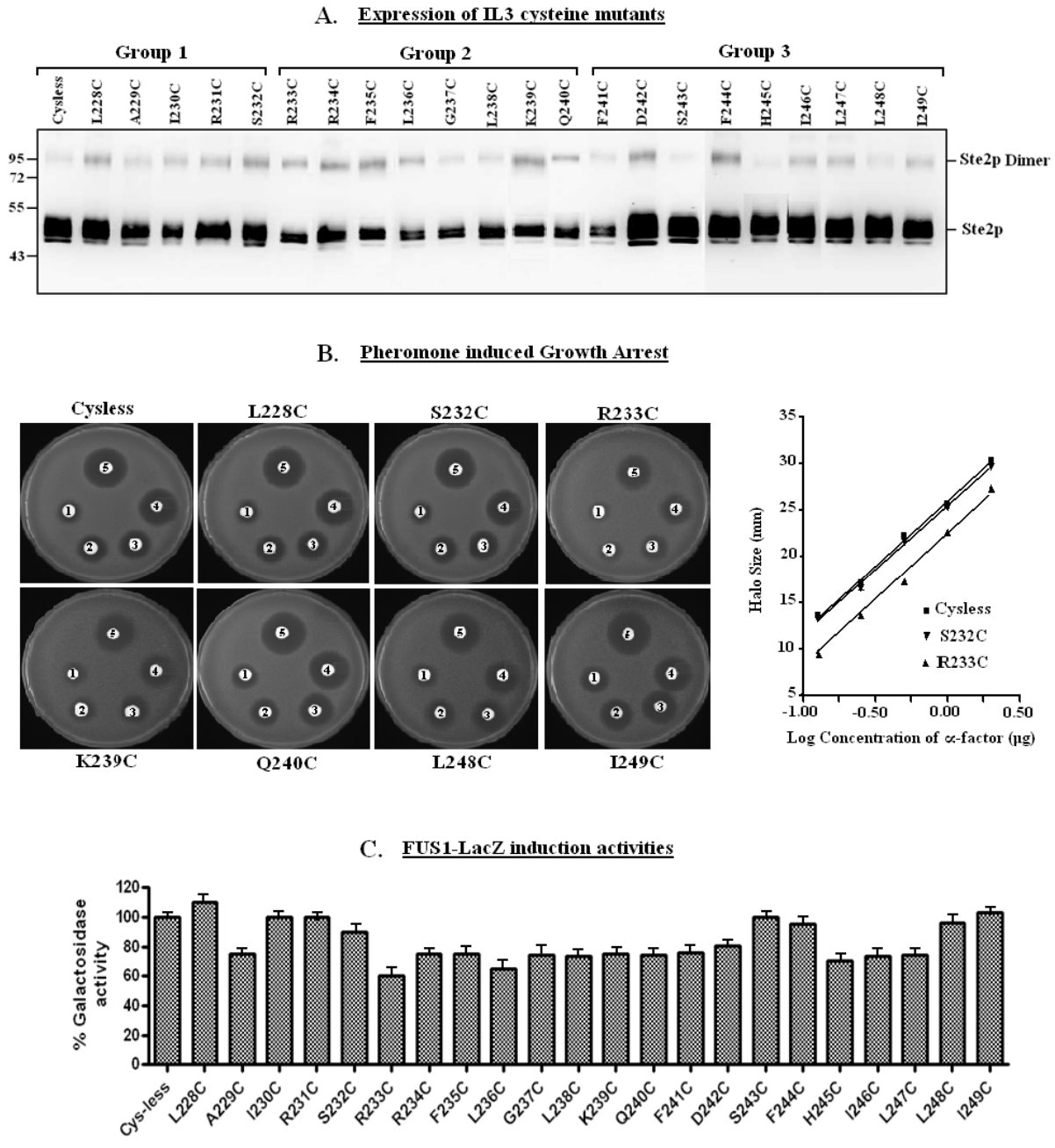

Figure 1: Phenotype of IL3 Cys mutants. **A**: Immunoblot analysis of IL3 Cys-mutants expression. The plots were probed with anti-FLAG to detect Ste2p. **B**: Representative images of growth arrest assay plates and graphs. **C**: Relative (%) β-galactosidase activity of the IL3 mutants.

They also exhibited biological activities similar to the Cys-less receptor. Group 2 (R233C-Q240C) mutants demonstrated 65-75% of Cys-less receptor expression level. These mutants have growth arrest activities similar to that of the Cys-less receptor, with the exception of R233C. The R233C mutant displayed about 65% activities relative to the Cys-less receptor. However, the *FUS1-LacZ* gene induction activities were less than the Cys-less receptor for the group 2 mutants. The differences in the growth arrest and *Fus1-LacZ* activities may be due to the fact that whereas growth arrest assay measures overall, long-term effects of the pheromone response pathways, the *Fus1-LacZ* measures the induction of a specific gene (*Fus1*) in the pathway. Hence, the group 2 mutations affected the induction of *Fus1* but overall did not have significant effects on cell cycle arrest required for mating. The group 3 mutants (F241C-I249C) have characteristics similar to those of the group 1 mutants. They are expressed at levels similar to the Cys-less receptor and have only slightly reduced (80-90%) growth arrest activities. However, the *FUS1*-lacZ activities vary among these mutants. Overall the substitution of cysteine into various positions in IL3 of Ste2p did not significantly affect receptor activity with the exception of the mutation of R233C, which displayed the strongest defects in all the assays tested. A summary of the mutant phenotypes is shown in the table below on Table 2.

Dimer formation in IL3 Cys-mutants:

The IL3 Cys mutants were generated to determine possible interactions with Gpa1p Cys mutants (see part V of dissertation), however preliminary Cu-P treatment of Ste2p R233C and R234C mutants showed that all the samples treated with Cu-P had increased dimer formation which could be reversed by reduction with 4% β-ME (Figure 2).

Table 2: Phenotypes of IL3 Cys substitution mutants.

	Mutation	Protein Expression (%)	Growth arrest activities (%)	Fus1-LacZ induction (%)
	Cys-less	100	100	100
Group 1	L228C	100	90	110
	A229C	100	90	75
	I230C	100	85	100
	R231C	100	90	100
	S232C	100	100	90
Group 2	R233C	65	70	60
	R234C	75	100	80
	F235C	75	100	80
	L236C	75	90	70
	G237C	75	100	75
	L238C	75	100	75
	K239C	75	100	80
	Q240C	75	100	80
Group 3	F241C	100	100	80
	D242C	85	85	85
	S243C	100	95	100
	F244C	100	90	95
	H245C	90	90	70
	I246C	100	90	70
	L247C	100	90	75
	L248C	100	85	95
	I249C	100	85	100

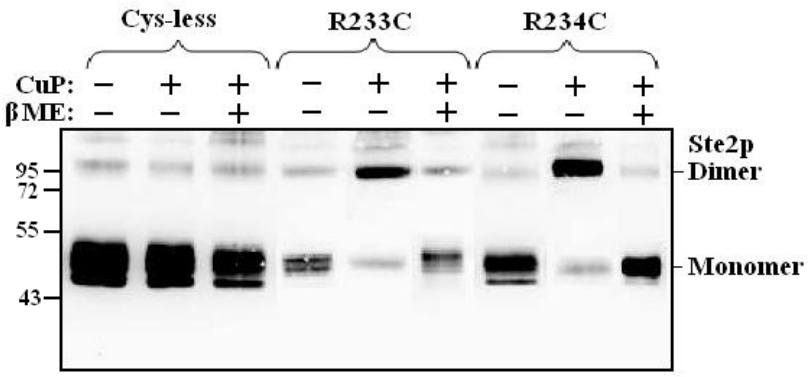

Figure 2: Copper treatment of Ste2p Cys mutants, R233C and R234C. The samples were untreated (lanes, -, -) or treated with 1.0 μM Cu-P (lanes, [-, +] and [+,+]). Dimer formation in R233C and R234C Ste2p mutants increased with copper oxidation. This was reversed by the reducing agent βME (4%) after the Cu-P treatment (compare lanes, [+, -] and [+, +]).

The IL3 of rhodopsin has been identified to be involved in oligomerization (*8*). We therefore hypothesized that IL3 of Ste2p may be involved in dimer (oligomer) formation. To investigate this we treated all IL3 Cys mutant receptors generated in this study with Cu-P to determine whether dimers were formed. The results showed that the IL3 Cys mutant receptors showed increased dimer formation when treated with Cu-P varying from 5% to 90% of monomer forms (Figure 3). The entire group 1 (L228C-S232C) and group 3 (F241C-I249C) residues, with the exception of A229C and H245C, had about 5-10% dimer formation. In contrast, Group 2 (R233C-Q240C) mutants showed elevated (45-95%) dimer formation. The higher degree of dimerization in these residues suggested that TM5-TM6 may be in a dimer interface for Ste2p. TM5 and TM6 have been predicted to be in a dimer interface in some GPCRs (*9*),

Group 1

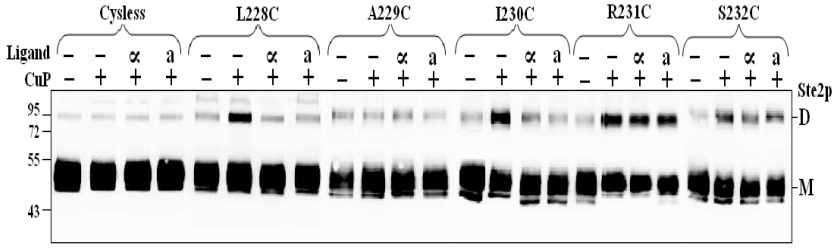

Group 2

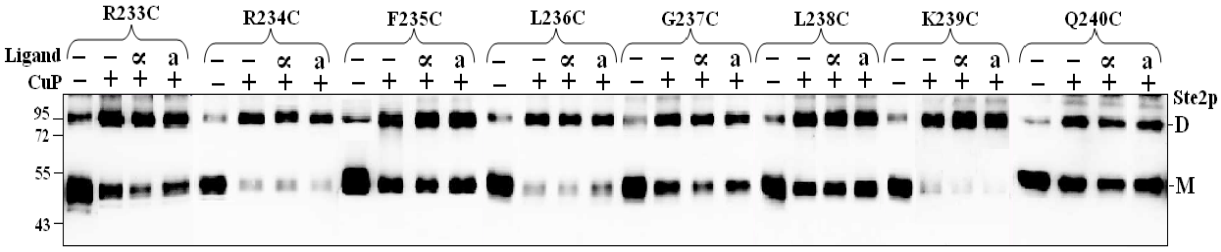

Group 3

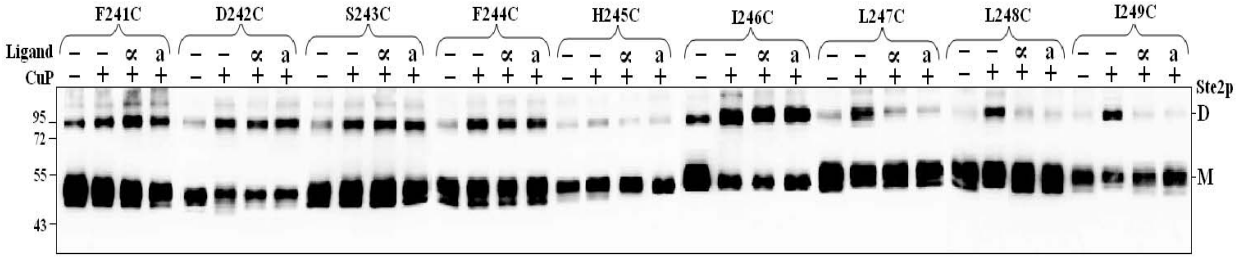

Figure 3: Analysis of IL3 Group 1 and 2 Cys-mutants for the ability to form dimer via a disulfide cross-links. The receptors were co-expressed with or without wild type Gpa1p. The blots were probed with anti-FLAG antibody to detect the presence of Ste2p at either the monomer (M, 53-55 kDa) or dimer (D, 106-110 kDa) positions, respectively. Each preparation was untreated (lanes -, -) or treated with Cu-P (lanes -, +) or with α-factor and Cu-P (lanes α, +) or with α-factor antagonist and Cu-P (lanes a, +).

However, we were concerned that protein-protein interactions may have occured using membranes which would not ordinarily occur in an intact cell. To determine whether dimer formation was the same or different in whole cells in comparison to membrane preparations, an in vivo Cu-P treatment assay was performed. Normally, Cu-P is not permeable to yeast cells; therefore, we adapted a method to permeabilize cells to Cu-P. Genetic transformation of the yeast *S. cerevisiae* by plasmid DNA is possible by pretreatment of the cells with LiAc and PEG. The treatment of cells with LiAc makes their membrane/cell wall more permeable without killing the treated cell; the treatment is temporary since the cells recover and can grow when cultured in growth media (*24, 33*). This approach was used to make the yeast strains expressing Ste2p Cys-mutants permeable to Cu-P for in vivo (whole cell) induced disulfide cross-linking.

Seven IL3 Cys-mutants were treated with Cu-P in vivo, using live permeabilized cells (Figure 4). Microscopic observation (Figure 4A) showed that the cells were not morphologically affected by Cu-P treatment and these cells were fully viable upon plating on growth media (data not shown). Comparison of dimer formation in vitro and in vivo (Figure 4B-C) shows that the dimer formation is not due to an artifact of the membrane preparation and does indeed occur in intact cells. On SDS-PAGE (4-12% gradient), the monomer, dimer, tetramer, hexamer were observed (Figure 4E). The monomer form predominates in SDS-PAGE because the non-covalent bonds between receptors in the oligomer are broken by the conditions of the SDS-PAGE and yet some of these interactions persist as seen in the cysless receptor samples. IL3, TM5 and TM6 all have been identified as dimer interface in separate studies using different receptors (*7, 8, 16*). We therefore propose that the cytoplasmic ends of TM5 and TM6 including IL3 in Ste2p are involve in dimer formation.

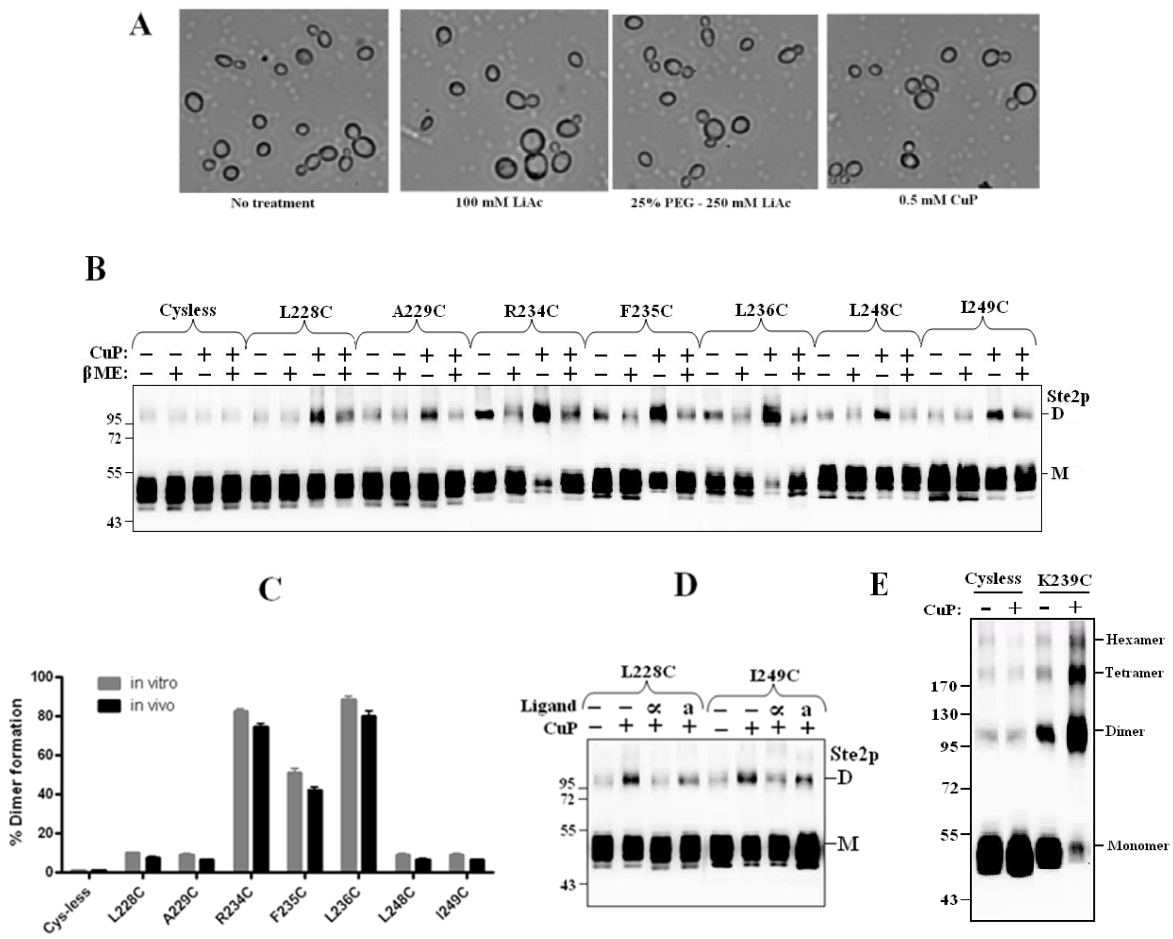

Figure 4: In vivo Cu-P treatment of IL3. The receptors were co-expressed with wild type Gpa1p. **A**: Images of cells at various stages of treatments during whole cell disulfide cross-linking Cu-P treatment. **B**: The blot images of seven mutants selected for whole cell cross-linking. The samples were probed with anti-FLAG antibody to detect the presence of Ste2p at either the monomer (M, 53-55 kDa) or dimer (D, 106-110 kDa) positions, respectively. Each preparation was untreated (lanes -, -) or treated with β-ME (lanes -, +) or Cu-P (lanes +, -) or with Cu-P and β-ME (lanes +, +). **C**: comparison of in vitro with in vivo cross-linking. **D**; Blot of whole cells expressing L228C and I249C treated with Cu-P in the presence of absence of ligand or antagonist. **E**: Blot image of Cys-less and K239C showing oligomer formation in Ste2p.

Conformational changes in TM5 and TM6 upon α-factor binding:

Since the cross-linking of Ste2p to Gpa1p was carried out in the absence and presence of ligand (α-factor), the Cu-P treatment of IL3 Cys-mutants was repeated on membranes incubated with α-factor prior to treating with Cu-P. While ligand binding did not affect dimer formation in receptors expressing receptors carrying mutations in residues R23I to I246 (See Figure 3 lanes labeled "α"), a reduction in dimerization was observed for mutation in the TM5 (L228C and I230C) and the TM6 boundaries (L247C to I249C). The results suggest that the TM5 and TM6 cytoplasmic boundaries undergo conformational changes upon α-factor binding to Ste2p such that these residues are shifted away from the "dimer interface", hence no dimers were formed when Cu-P was added. These α-factor-induced reductions in dimer formation in IL3 were also observed in vivo (Figure 4D) when whole cells were used for the disulfide cross-linking. The conformational changes at the cytoplasmic ends of TMs especially TM5 and TM6 are thought to play an important role in GPCR activation (*2, 34, 35*). We therefore suggest that conformational movements occur at the cytoplasmic end of TM5 and TM6 in Ste2p upon ligand binding.

Antagonist induced dimer reduction similar to agonist in the absence of Gpa1p:

Biochemical and cross-linking studies using both photoaffinity (*36*) and DOPA-mediated reactions (see part 2 of this dissertation) in our lab have shown that the N-terminus of α-factor is necessary for activation but not binding to Ste2p and that position 1 of α-factor most likely interacts with residues in the region of S251-M294 (TM6-EL3-TM7) of Ste2p. The question of whether the N-terminus of α-factor is important for the dimer reduction at the cytoplasmic ends of TM5 and TM6. The Cu-P treatment of receptors expressing the mutant IL3 residues were

repeated this time with both 5 μM α-factor (WHWLQLKPGQPNle^{12}Y) and 20 μM α-factor antagonist (WLQLKPGQPNle^{12}Y) binding before the Cu-P treatment. Because the α-factor antagonist was shown to bind to Ste2p at a slightly lower affinity than that of native α-factor (*37*), we therefore used 4-fold amount of α-factor for antagonist to make sure all Ste2p molecules were saturated. The results (Figure 3, compare lanes label "α" and "a") showed that both the native α-factor and antagonist almost completely blocked dimer formation at the TM5 (A228C and I230C) and TM6 (L247C to I249C) boundaries. Thus, the first two amino acids (WH) of α-factor may be essential for the reduction of dimer formation observed at the TM5 and TM6 cytoplasmic ends of Ste2p.

Gpa1p expression affected dimer formation in IL3:

The recent crystal structure of opsin with the 11 C-terminal residues of the Gα protein led the authors to conclude that the active conformation of this GPCR was stabilized by Gα (*38*). Another study also reported GTP may affect the interaction of receptor with Gα (*39*). We therefore determined whether co-expression (similar amount) of Ste2p and Gpa1p in the presence or the absence of GTP will affect IL3 dimer formation. To test these effects we co-expressed all the IL3 Cys-mutants with wild-type Gpa1p under the control of the same promoter and repeated the Cu-P treatment. Preliminary studies with A228C and I249C of IL3 indicated the presence of approximately equal levels of Ste2p and Gpa1p led to increased dimer formation in IL3 in comparison to when more Ste2p was expressed than was Gpa1p. In contrast, GTP addition had no affect on dimer formation with either equal level of Ste2p and Gpa1p expressed or with a high ratio of Ste2p to Gpa1p (Figure 5).

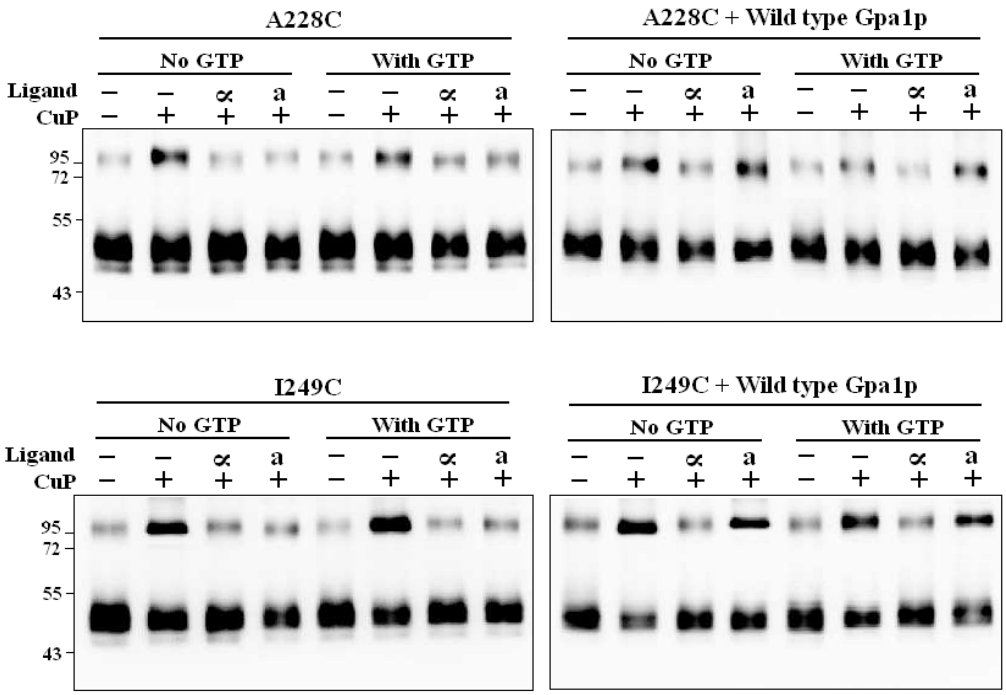

Figure 5: Effects of Gpa1p and GTP on IL3 conformation. The receptors, A228C and I249C were co-expressed with or without wild type Gpa1p and their membranes treated with or without ligand in the presence or absence of 0.1mM GTP prior to Cu-P treatments. The blots were probed with anti-FLAG antibody to detect the presence of Ste2p at either the monomer (M, 53-55 kDa) or dimer (D, 106-110 kDa) positions, respectively. Each preparation was untreated (lanes -, -) or treated with Cu-P (lanes -, +) or with α-factor and Cu-P (lanes α, +) or with α-factor antagonist and Cu-P (lanes a, +).

The results (Figure 6) of Cu-P treatment of all IL3 Cys mutants co-expressed with Gpa1p show that L228C and H245C that did not form dimer in the absence of Gpa1p expression (see Figure 3) but formed dimer when Ste2p and Gpa1p were co-expressed.

Group 1

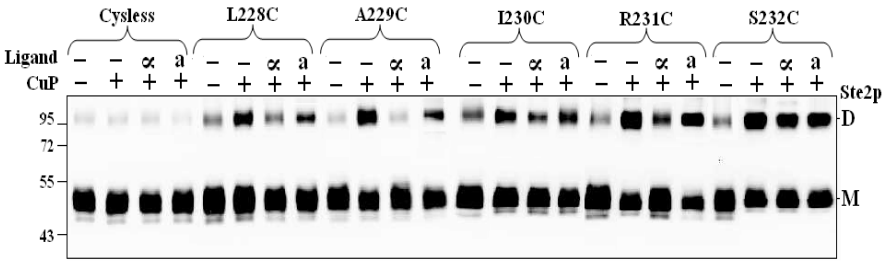

Group 2

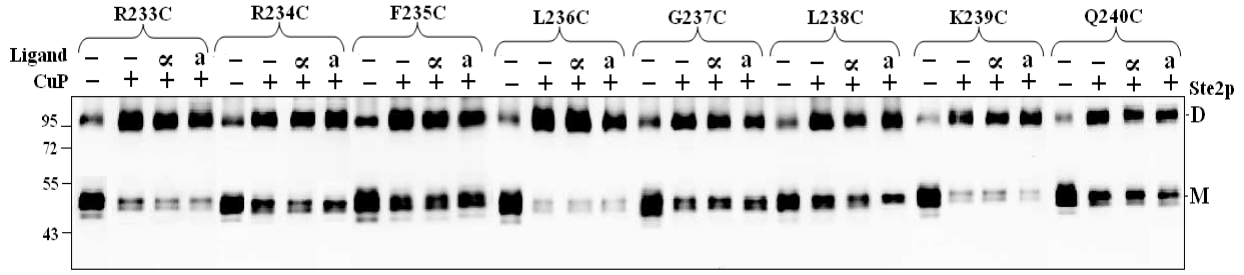

Group 3

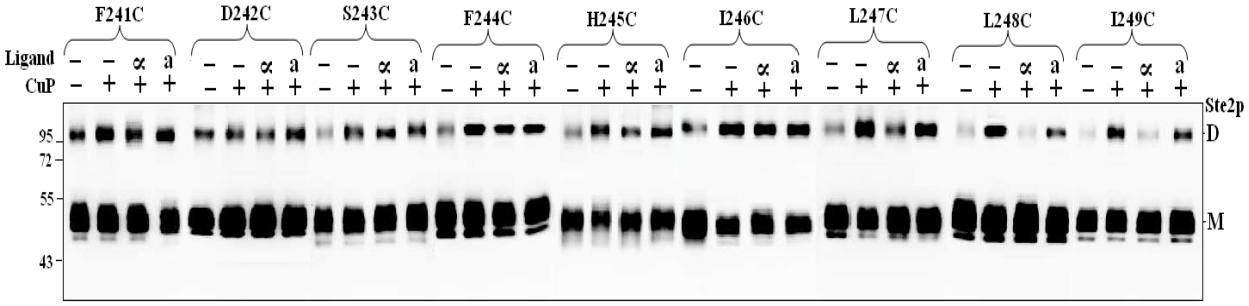

Figure 6: The Effects of Gpa1p expression on dimer formation. The receptors were co-expressed with wild type Gpa1p. The blots were probed with anti-FLAG antibody to detect the presence of Ste2p at either the monomer (M, 53-55 kDa) or dimer (D, 106-110 kDa) positions, respectively. Each preparation was untreated (lanes -, -) or treated with Cu-P (lanes -, +) or with α-factor and Cu-P (lanes α, +) or with α-factor antagonist and Cu-P (lanes a,+).

While dimer formation in receptors carrying mutations in residues S232-I246 was not affected, a reduction in dimerization was observed for mutation in the TM5 (L228C, A229C, I230C, and R231C) and the TM6 boundaries (L247, L248C, and I249C) in presence of α-factor (Figure 6, see lanes labeled "α").Although α-factor reduced dimer formation at the TM5 and TM6 cytoplasmic ends, the antagonist was only able to reduce dimerization by about 50% (Figure 6, compare lanes labeled "α" and "a"). Thus, antagonist may induce a different (or partial) conformation from α-factor-induced changes that are required for Ste2p activation in presence of an equal amount of Gpa1p. The first two amino acids of the ligand that are lacking in the antagonist may be essential for proper changes in the TM5 and TM6 of Ste2p. The co-expression of Ste2p and Gpa1p did not have any significant effects on the group 2 residues (R233C to Q240C) indicating that Gpa1p may not interact with these residues but rather the TM5 and TM6 boundaries where changes were observed.

CHAPTER 4

Discussion

Although the third intracellular loop (IL3) of Ste2p is suggested to directly interact with Gpa1p, there has been no report about its involvement in Ste2p homo-dimer formation. Most studies reported that individual residue mutations in IL3 did not significantly affect receptor activity. Most strong defects in receptor were observed in multiple or non-conservative mutations that altered the overall charges of specific regions that are suggested to interact with G proteins (*32, 40, 41*). Consistent with previous studies (*42*), IL3 was observed to tolerate Cys substitutions in our experiments except for the R233C receptor that displayed the most defects compared to the other mutants. Although the L236H and L236R mutations have been observed to cause partial defects in Ste2p activation (*42, 43*), the L236C mutant displayed only a slight decrease in activity relative to the Cys-less receptor as observed in previous studies. Overall the substitution of residues to cysteine in IL3 did not significantly affect the activities of the receptor. The tolerance for substitutions in IL3 suggests that activation of G protein by Ste2p involves multiple intramolecular interactions as observed for mammalian GPCRs (*44, 45*). Thus, the overall interactions of all IL3 residues are essential for proper Ste2p function and interaction with Gpa1p.

It is interesting to observe that strong dimer formation occurred in the IL3 Cys mutants; however this is not surprising since IL3 in rhodopsin has been identified to play a role in oligomerization (*7, 8, 14*). In addition, molecular dynamics simulations, correlated-mutation analysis and evolutionary-trace analysis all support the involvement of IL3 in the dimerization interface (*9*). The dimer formation observed in this study was also detected in intact cells,

indicating that the disulfide bond formation between the two units of Ste2p occurs in the native environment of the receptor. We therefore suggested that IL3 is a dimer contact in Ste2p oligomer formation. The presence of higher order of oligomers of Ste2p observed in this study (Figure 4E) indicates that Ste2p has multiple contacts in the oligomer form. Other studies have also shown that the N-terminal extracellular domain, TM1, TM2 (*19*), TM4 (*20*) , and TM7 (Heejung Kim, personal communication) are involved in oligomer formation in Ste2p similar to that of the rhodopsin family of GPCRs. In rhodopsin the strongest dimer contacts were found between TM5 and TM4, whereas TM1, TM2 and IL3 displayed fewer contacts. The weakest contact was the extracellular surface of TM1. The only interactions between the rhodopsin dimers observed were at the cytoplasmic ends, which involved K231, Q236, Q238 (all in IL3), K339 and T340 (all at the C-terminus). These IL3 and C-terminal residues in rhodopsin are thought to be involved in hydrogen bondings that stabilize the oligomers (*7, 8, 15*).

The role of IL3 in Ste2p oligomer formation is suggested to be similar to that of rhodopsin. The pattern of dimer formation in Ste2p IL3 (Figure 6) indicates that the side chains of R233, L236 and K239 all points towards the dimer interface. These residues form about 85-95% of dimer when treated with Cu-P. Interestingly, the residues in rhodopsin IL3 regions that are essential for dimer stabilization seem to be located at positions similar to those for Ste2p IL3 residues that are suggested to face the dimer interface. Although most individual mutations in IL3 do not display any significant defect in receptor activity, mutations of R233 (R233C) and L236 (L236H and L236R) have been observed to cause strong defects in Ste2p activation (*42, 43*). We therefore propose that these residues (R233, L236 and K239) in the IL3 region of Ste2p are involved in hydrogen bonding that stabilizes the Ste2p dimers. The similarity in dimer

interface sites between Ste2p and rhodopsin-like receptors provide further evidence that many aspects of structure and function are highly conserved across GPCRs, irrespective of primary amino acid sequence. A schematic arrangement of higher order organization of Ste2p compared with rhodopsin is shown in Figure 7. The model is based on the results of this study and other reports (*19, 20*).

Interactions of cognate ligands at the ligand-binding pocket of GPCRs, lead to conformational changes that are transferred from the extracellular surface of the receptor to the cytoplasmic domain involved in G-protein binding (*2*). One of the most commonly used strategies to investigate GPCRs agonist-induced conformational changes is disulfide cross-linking involving cysteine-substituted mutant GPCRs. This approach involves detection of dimer formation or intact receptor after enzymatic or chemical cleavage to assess disulfide bond formation between two Cys residues (*9, 15, 20*). Several recent disulfide cross-linking studies including those using β_2-adrenergic and M3 muscarinic acetylcholine receptors as models all showed that conformational changes in these receptors were associated with a clockwise rotation of the cytoplasmic end of TM6 of ~30^o (*35, 46-48*). The dimer disappearance of the Cys mutants at the cytoplasmic ends of TM5 and TM6 in Ste2p in the presence of bound ligand observed in this study indicates that these regions of the receptor undergo conformational changes similar to what has been observed in other GPCRs. Comparison of the crystal structure of opsin and rhodopsin also show that the cytoplasmic end of TM6 in opsin (active receptor) is shifted about 6 Å outwards from the center of the TM and undergoes a clockwise rotation of ~30^o at the cytoplasmic end.

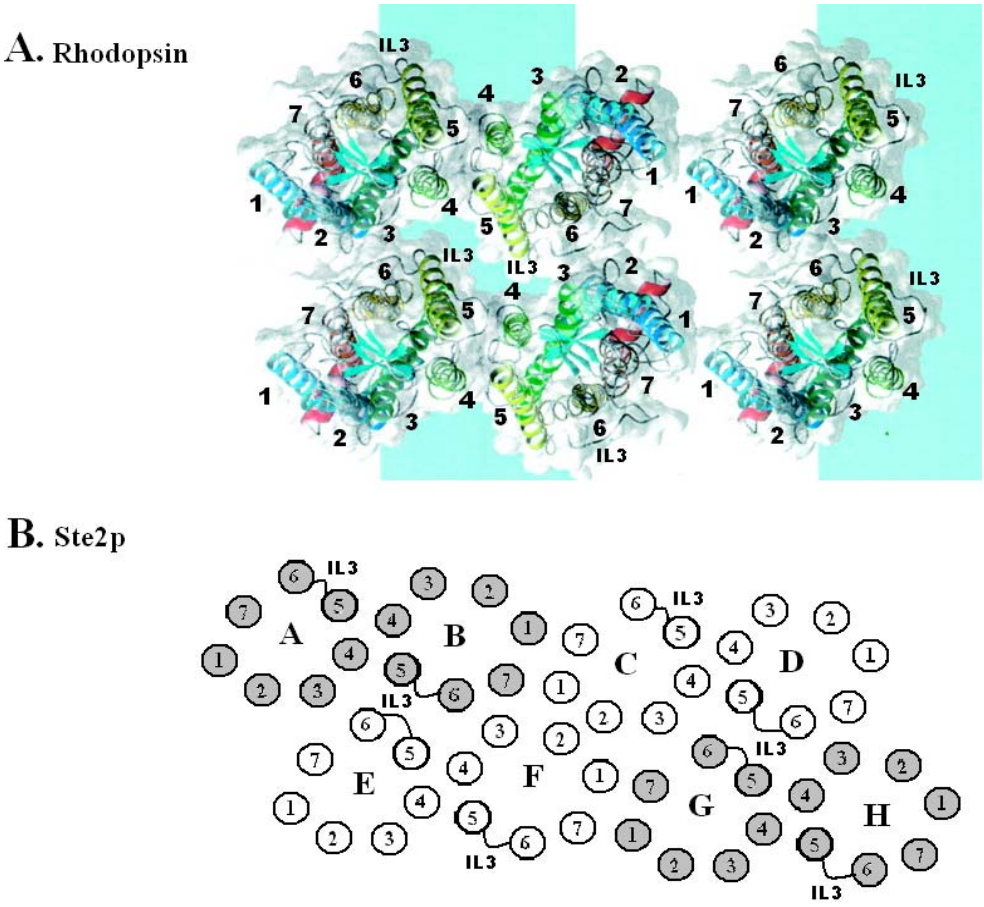

Figure 7: Model for the packing arrangement of rhodopsin and Ste2p in their oligomer forms. The transmembrane helices are labeled in numerical order 1-7. **A***:* rhodopsin assembles into dimers through a contact provided by TM4 and TM5. Dimers form rows as a result of contacts between IL3 and helices I and II from the adjacent dimer. Rows assemble through extracellular contacts formed by TM1. Figure taken from Liang et al (*8*). **B**: Ste2p assembles into dimers similar to rhodopsin. Dimers form rows through contacts of IL3. The IL3 regions are anti-parallel as predicted in some GPCRs (*9*) between dimers (e. g. AB - EF, or CD - GH). Dimers may also interact through contacts in TM1, TM2, TM4 and TM7 as observed in some studies (*19, 20*).

Both TM5 and TM6 were observed to move from their original positions in opsin. These changes, and other changes at TM3 and TM5, result in the creation of a binding domain which favors activation of the G protein transducin (*38*). We therefore propose that TM6 of Ste2p undergoes a clockwise rotation of about ~30^{o} at cytoplasmic surface, similar to other GPCRs (*35, 46-48*). The TM6 helix may also shift during Ste2p activation as observed in most GPCRs; however there is no evidence in the data presented in this study to support such movement. Based on the reduction of dimer formation observed in this study in residues at the ends TM5, we also propose that the TM5 cytoplasmic end undergoes a conformational change (probable an anti-clockwise rotation of about ~30^{o}). This needs further studies to confirm such movement. These proposed conformational changes at the cytoplasmic ends of TM5-TM6 in Ste2p did not alter IL3 involvement in dimer interactions as observed in the group 2 residues (Figure 6). This phenomena of ligand binding or receptor activation having no effects on dimerization in Ste2p has also been reported previously (*18*). Thus, the hydrophilic residues located in the middle of the loop (R233-Q240) that are proposed to be involved in hydrogen bonding in this study are required to stabilize dimers during rearrangements of the helices leading to receptor activation.

Dimer formation involving the cytoplasmic ends of TM5-TM6 and changes induced by ligand were affected by the expression of Gpa1p. Thus, the binding of Gpa1p may affect both IL3 and α-factor interactions. These phenomena have been observed when the crystal structure of opsin was compared with that of opsin-GαCT (opsin with the C-terminus of Gα transducin bound). The study suggested that GαCT binding plays a role in stabilizing the ligand binding pocket of the receptor as well as receptor conformation. The interactions of residues such as K296, S186, E181, Y268, C110 and C187 were found to be different in opsin when compared to

opsin-GαCT (*38*). Thus, the active conformation of the receptor is stabilized by both ligand and G protein binding. It is therefore not surprising that similar observations were made in this study when Ste2p was expressed with or without Gpa1p. When Gpa1p was co-expressed the side chain orientations of A229, I230, and R231 all at the cytoplasmic end of TM5 were altered so that their dimer formation was reduced in the presence of ligand binding, which was not observed in the absence of Gpa1p. At the cytoplasmic end of TM6, H245 also shows some reduction in the presence of ligand binding. The only change that occurred in the middle of the IL3 loop was a possible switch in orientation between R233 and R234. In the absence of Gpa1p, the side chain of R234 may point away from the receptor bundle facing towards the dimer interface, whereas the R233 side chain may point partially away from the dimer interface. In the presence of Gpa1p it seems that the opposite occurs, such that the R233 side chain may now points toward the dimer interface and the R234 may be oriented partially away from the interface. It is not clear whether these residues are involved in G protein interactions. However, some of these residues such as R231, R233, R234 and K239 may be involve in hydrogen bonding that are required for stabled Ste2p conformation. This study is the first to report that IL3 residues play essential role in mediating Ste2p-Ste2p interactions in the oligomer form.

The first amino acid of α-factor, Trp^{1} is suggested to interact with Ste2p residues, S251-M294 which comprises of TM6, the third extracellular loop (EL3), and part of TM7 [(*36*) and part 2 of this dissertation]. We investigated the role of the N-terminus of α-factor by examining the effects the α-factor antagonist (WLQLKPGQPNle^{12}Y), which lacks the first two amino acids, on dimer formation in the IL3 Cys mutants. In the absence of Gpa1p changes in dimer formation at the cytoplasmic ends of TM5-TM6 induced by the antagonist was similar to that of the native

α-factor ligand (WHWLQLKPGQPNle^{12}Y). However, co-expression of Ste2p Cys mutants with Gpa1p showed that the antagonist was able to reduce dimer formation by 50% compared to the native α-factor. Since co-expressing Ste2p and Gpa1p reflect the interactions in the natural environment, we suggest that antagonist binding to Ste2p does not induce the proper conformational changes at the TM5-TM6 cytoplasmic ends that are required for receptor activation. This implies that the first two amino acids of α-factor may be required for these changes and signaling in the presence of Gpa1p. The partial changes that were observed at TM5-TM6 ends induced by the antagonist may be due to the interactions of position 3 (Trp3) of α-factor that is still present in the antagonist. Previous studies have shown that Trp3 of α-factor may interact within the TM5-TM6-EL3 regions of Ste2p similar to Trp1 (*49*). Thus, conformational changes at the cytoplasmic ends of TM5 and TM6 in Ste2p require interactions of the N-terminal amino acids of α-factor, especially the first three (WHW) residues. It is therefore logical to propose that the first three amino acids of α-factor interact within a "signaling pocket" in Ste2p that may be comprised of residues in TM5 and TM6 as well as part of the EL2-TM5 and TM6-EL3 extracellular boundaries.

This study has revealed a unique characteristic of IL3 involvement in dimer formation in Ste2p that has not been observed for other GPCRs. Conformational changes at the cytoplasmic ends of TM5 and TM6 may be similar to other mammalian GPCRs. The N-terminus of α-factor is suggested to be important for changes in TM5 and TM6 in that the binding of an antagonist (lacking the first two residues) does not induce the same conformational changes in these regions as does binding of agonist. The information obtained in this study will serve as a platform for further understanding of GPCR oligomerization and their role in signal transduction.

References for Part IV

1. Ratnala, V. R., and Kobilka, B. (2009) Understanding the ligand-receptor-G protein ternary complex for GPCR drug discovery, *Methods Mol Biol 552*, 67-77.
2. Rosenbaum, D. M., Rasmussen, S. G., and Kobilka, B. K. (2009) The structure and function of G-protein-coupled receptors, *Nature 459*, 356-363.
3. Williams, C., and Hill, S. J. (2009) GPCR signaling: understanding the pathway to successful drug discovery, *Methods Mol Biol 552*, 39-50.
4. Panetta, R., and Greenwood, M. T. (2008) Physiological relevance of GPCR oligomerization and its impact on drug discovery, *Drug Discov Today 13*, 1059-1066.
5. De Amici, M., Dallanoce, C., Holzgrabe, U., Trankle, C., and Mohr, K. (2009) Allosteric ligands for G protein-coupled receptors: A novel strategy with attractive therapeutic opportunities, *Med Res Rev*.
6. Lundstrom, K. (2009) An overview on GPCRs and drug discovery: structure-based drug design and structural biology on GPCRs, *Methods Mol Biol 552*, 51-66.
7. Fotiadis, D., Liang, Y., Filipek, S., Saperstein, D. A., Engel, A., and Palczewski, K. (2003) Atomic-force microscopy: Rhodopsin dimers in native disc membranes, *Nature 421*, 127-128.
8. Liang, Y., Fotiadis, D., Filipek, S., Saperstein, D. A., Palczewski, K., and Engel, A. (2003) Organization of the G protein-coupled receptors rhodopsin and opsin in native membranes, *J Biol Chem 278*, 21655-21662.
9. Bouvier, M. (2001) Oligomerization of G-protein-coupled transmitter receptors, *Nat Rev Neurosci 2*, 274-286.

10. Milligan, G. (2006) G-protein-coupled receptor heterodimers: pharmacology, function and relevance to drug discovery, *Drug Discov Today 11*, 541-549.

11. Milligan, G., Canals, M., Pediani, J. D., Ellis, J., and Lopez-Gimenez, J. F. (2006) The role of GPCR dimerisation/oligomerisation in receptor signalling, *Ernst Schering Found Symp Proc*, 145-161.

12. Ferre, S., Baler, R., Bouvier, M., Caron, M. G., Devi, L. A., Durroux, T., Fuxe, K., George, S. R., Javitch, J. A., Lohse, M. J., Mackie, K., Milligan, G., Pfleger, K. D., Pin, J. P., Volkow, N. D., Waldhoer, M., Woods, A. S., and Franco, R. (2009) Building a new conceptual framework for receptor heteromers, *Nat Chem Biol 5*, 131-134.

13. Pin, J. P., Comps-Agrar, L., Maurel, D., Rives, M. L., Trinquet, E., Kniazeff, J., Rondard, P., and Prezeau, L. (2009) GPCR oligomers: two or more for what? Lessons from mGlu and GABAB receptors, *J Physiol*.

14. Filizola, M., Wang, S. X., and Weinstein, H. (2006) Dynamic models of G-protein coupled receptor dimers: indications of asymmetry in the rhodopsin dimer from molecular dynamics simulations in a POPC bilayer, *J Comput Aided Mol Des 20*, 405-416.

15. Park, P. S., Filipek, S., Wells, J. W., and Palczewski, K. (2004) Oligomerization of G protein-coupled receptors: past, present, and future, *Biochemistry 43*, 15643-15656.

16. Hebert, T. E., Moffett, S., Morello, J. P., Loisel, T. P., Bichet, D. G., Barret, C., and Bouvier, M. (1996) A peptide derived from a beta2-adrenergic receptor transmembrane domain inhibits both receptor dimerization and activation, *J Biol Chem 271*, 16384-16392.

17. Gehret, A. U., Bajaj, A., Naider, F., and Dumont, M. E. (2006) Oligomerization of the yeast alpha-factor receptor: implications for dominant negative effects of mutant receptors, *J Biol Chem 281*, 20698-20714.

18. Overton, M. C., and Blumer, K. J. (2000) G-protein-coupled receptors function as oligomers in vivo, *Curr Biol 10*, 341-344.

19. Overton, M. C., and Blumer, K. J. (2002) The extracellular N-terminal domain and transmembrane domains 1 and 2 mediate oligomerization of a yeast G protein-coupled receptor, *J Biol Chem 277*, 41463-41472.

20. Wang, H. X., and Konopka, J. B. (2009) Identification of amino acids at two dimer interface regions of the alpha-factor receptor (Ste2), *Biochemistry 48*, 7132-7139.

21. Chinault, S. L., Overton, M. C., and Blumer, K. J. (2004) Subunits of a yeast oligomeric G protein-coupled receptor are activated independently by agonist but function in concert to activate G protein heterotrimers, *J Biol Chem 279*, 16091-16100.

22. Hauser, M., Kauffman, S., Lee, B. K., Naider, F., and Becker, J. M. (2007) The first extracellular loop of the Saccharomyces cerevisiae G protein-coupled receptor Ste2p undergoes a conformational change upon ligand binding, *J Biol Chem 282*, 10387-10397.

23. Huang, L. Y., Umanah, G., Hauser, M., Son, C., Arshava, B., Naider, F., and Becker, J. M. (2008) Unnatural amino acid replacement in a yeast G protein-coupled receptor in its native environment, *Biochemistry 47*, 5638-5648.

24. Gietz, D., St Jean, A., Woods, R. A., and Schiestl, R. H. (1992) Improved method for high efficiency transformation of intact yeast cells, *Nucleic Acids Res 20*, 1425.

25. Sherman, F. (2002) Getting started with yeast, *Methods Enzymol 350*, 3-41.

26. Dosil, M., Giot, L., Davis, C., and Konopka, J. B. (1998) Dominant-negative mutations in the G-protein-coupled alpha-factor receptor map to the extracellular ends of the transmembrane segments, *Mol Cell Biol 18*, 5981-5991.

27. Mumberg, D., Muller, R., and Funk, M. (1995) Yeast vectors for the controlled expression of heterologous proteins in different genetic backgrounds, *Gene 156*, 119-122.

28. David, N. E., Gee, M., Andersen, B., Naider, F., Thorner, J., and Stevens, R. C. (1997) Expression and purification of the Saccharomyces cerevisiae alpha-factor receptor (Ste2p), a 7-transmembrane-segment G protein-coupled receptor, *J Biol Chem 272*, 15553-15561.

29. Slauch, J. M., Mahan, M. J., and Mekalanos, J. J. (1994) Measurement of transcriptional activity in pathogenic bacteria recovered directly from infected host tissue, *Biotechniques 16*, 641-644.

30. Jenness, D. D., and Spatrick, P. (1986) Down regulation of the alpha-factor pheromone receptor in S. cerevisiae, *Cell 46*, 345-353.

31. Kelley, L. A., and Sternberg, M. J. (2009) Protein structure prediction on the Web: a case study using the Phyre server, *Nat Protoc 4*, 363-371.

32. Clark, C. D., Palzkill, T., and Botstein, D. (1994) Systematic mutagenesis of the yeast mating pheromone receptor third intracellular loop, *J Biol Chem 269*, 8831-8841.

33. Zimkus, A., Chaustova, L., and V. Razumas. (2006) Effect of lithium and sodium cations on the permeability of yeast Saccharomyces cerevisiae cells to tetraphenylphosphonium ions, *BIOLOGIJA 2*, 47-49.

34. Lodowski, D. T., Angel, T. E., and Palczewski, K. (2009) Comparative analysis of GPCR crystal structures, *Photochem Photobiol 85*, 425-430.

35. Wess, J., Han, S. J., Kim, S. K., Jacobson, K. A., and Li, J. H. (2008) Conformational changes involved in G-protein-coupled-receptor activation, *Trends Pharmacol Sci 29*, 616-625.

36. Son, C. D., Sargsyan, H., Hurst, G. B., Naider, F., and Becker, J. M. (2005) Analysis of ligand-receptor cross-linked fragments by mass spectrometry, *J Pept Res 65*, 418-426.

37. Eriotou-Bargiota, E., Xue, C. B., Naider, F., and Becker, J. M. (1992) Antagonistic and synergistic peptide analogues of the tridecapeptide mating pheromone of Saccharomyces cerevisiae, *Biochemistry 31*, 551-557.

38. Scheerer, P., Park, J. H., Hildebrand, P. W., Kim, Y. J., Krauss, N., Choe, H. W., Hofmann, K. P., and Ernst, O. P. (2008) Crystal structure of opsin in its G-protein-interacting conformation, *Nature 455*, 497-502.

39. Smith, B., Hill, C., Godfrey, E. L., Rand, D., van den Berg, H., Thornton, S., Hodgkin, M., Davey, J., and Ladds, G. (2009) Dual positive and negative regulation of GPCR signaling by GTP hydrolysis, *Cell Signal 21*, 1151-1160.

40. Stefan, C. J., and Blumer, K. J. (1994) The third cytoplasmic loop of a yeast G-protein-coupled receptor controls pathway activation, ligand discrimination, and receptor internalization, *Mol Cell Biol 14*, 3339-3349.

41. Celic, A., Martin, N. P., Son, C. D., Becker, J. M., Naider, F., and Dumont, M. E. (2003) Sequences in the intracellular loops of the yeast pheromone receptor Ste2p required for G protein activation, *Biochemistry 42*, 3004-3017.

42. Choi, Y., and Konopka, J. B. (2006) Accessibility of cysteine residues substituted into the cytoplasmic regions of the alpha-factor receptor identifies the intracellular residues that are available for G protein interaction, *Biochemistry 45*, 15310-15317.

43. Schandel, K. A., and Jenness, D. D. (1994) Direct evidence for ligand-induced internalization of the yeast alpha-factor pheromone receptor, *Mol Cell Biol 14*, 7245-7255.

44. Slessareva, J. E., Ma, H., Depree, K. M., Flood, L. A., Bae, H., Cabrera-Vera, T. M., Hamm, H. E., and Graber, S. G. (2003) Closely related G-protein-coupled receptors use multiple and distinct domains on G-protein alpha-subunits for selective coupling, *J Biol Chem 278*, 50530-50536.

45. Kristiansen, K. (2004) Molecular mechanisms of ligand binding, signaling, and regulation within the superfamily of G-protein-coupled receptors: molecular modeling and mutagenesis approaches to receptor structure and function, *Pharmacol Ther 103*, 21-80.

46. Bhattacharya, S., Hall, S. E., and Vaidehi, N. (2008) Agonist-induced conformational changes in bovine rhodopsin: insight into activation of G-protein-coupled receptors, *J Mol Biol 382*, 539-555.

47. Jaakola, V. P., Griffith, M. T., Hanson, M. A., Cherezov, V., Chien, E. Y., Lane, J. R., Ijzerman, A. P., and Stevens, R. C. (2008) The 2.6 angstrom crystal structure of a human A2A adenosine receptor bound to an antagonist, *Science 322*, 1211-1217.

48. Ludeke, S., Mahalingam, M., and Vogel, R. (2009) Rhodopsin activation switches in a native membrane environment, *Photochem Photobiol 85*, 437-441.

49. Son, C. D., Sargsyan, H., Naider, F., and Becker, J. M. (2004) Identification of ligand binding regions of the Saccharomyces cerevisiae alpha-factor pheromone receptor by photoaffinity cross-linking, *Biochemistry 43*, 13193-13203.

PART V

Determination of specific residue-to-residue interaction between *Saccharomyces cerevisiae* α-factor Pheromone Receptor (Ste2p) and its G-alpha protein (Gpa1p) by disulfide cross-linking.

Part V presents collaborative work with Dr. Fred Naider's laboratory at the City University of New York, Staten Island. George K. E. Umanah performed most the work, Liyin Huang assisted with the biochemical studies, Julie Maccarone assisted with the phenotypes of the Gpa1p mutants and the peptides used were obtained from Dr. Naider's laboratory.

CHAPTER 1

Introduction

The *Saccharomyces cerevisiae* pheromone receptor encoded by the *STE2* gene belongs to the medically important family of G protein-coupled receptors (GPCRs) that transduce signals for a variety of stimuli (*1-3*). These receptors are comprised of seven transmembrane domains (TMs) and function by activating the Gα subunit of a heterotrimeric G protein. GPCRs are the most diverse group of membrane-bound receptors and are the targets of most of the current prescription drugs due to their association with a broad range of diseases, such as retinitis pigmentosa, inflammation, diabetes, cancer, and hypertension (*4, 5*). Despite the availability of crystal structures for G proteins (*6-8*) and GPCRs (*9-12*), the molecular mechanisms leading to activation of G proteins upon ligand binding to GPCRs remain unclear. GPCR–G protein interactions have recently found to have interesting implications with regards to drug discovery. If drugs can be identified that interfere or promote GPCR-G protein interaction, change the pattern of GPCR–G protein associations, or cause a GPCR to preferentially associate with one G protein and not others, then it would be possible to regulate the activities and functions of a specific receptor (*4, 13-15*)

Ligand binding to GPCRs induces receptors to undergo conformational changes, which enables them to activate Gα to exchange GDP for GTP. The GTP-bound Gα releases Gβγ and then either Gα or Gβγ can further activate downstream effectors, which result in increase or decrease of secondary (signal) molecules (*16-21*). Several biochemical and biophysical experiments suggest that the binding of ligand to GPCRs changes helix-helix interactions

between the TMs of the receptor which in turn affects the conformation of cytoplasmic domains that directly interact with G proteins (*14, 22-25*). Recently the crystal structure of opsin bound to the carboxyl-terminal peptide of transducin (Gα) revealed that the peptide occupies a cavity created between the cytoplasmic ends of TM3, TM5 and TM6 (*26*). Though this structure is the first to document that the C-terminus of the Gα interacts within a cavity in the receptor, the study did not define the mechanism that induces the activation of Gα upon interaction with the receptor. Several models have been proposed for signal transfer from the activated receptor to the G protein. The "gear shift", "lever arm" and "sequential fit" models have in common that the α5 helix (C-terminus) of Gα is the key transmission domain for the receptor-G protein signal transfer (*27-30*). Other regions of Gα such as the α4-helix, α2-helix, α2-β4 loop regions, and α4-β6 loop domain have also been implicated to directly interact with the receptor during signal transfer (*31, 32*).

Knowledge about the mechanism of GPCR-G protein signal transfer has been limited because of the problems working with membrane-bound receptor proteins and the difficulties in identifying conserved sequence motifs in the intracellular domains of GPCRs that might be involved in G protein activation. In addition, the complexity of mammalian GPCR cross-talk with different G proteins and other modulators within the same cell makes it difficult to assign specific signal transfer to a given GPCR and a specific Gα (*1, 3*). The mating pathway of *S. cerevisiae* has been a valuable tool for studying GPCR signal transduction mechanisms for many reasons such as the ease of mutagenizing components of the system and the ability to express active mammalian GPCRs in yeast. Furthermore, the yeast mating pheromone receptors activate only one Gα (Gpa1p) making it possible to identify specific interactions between the receptor

and its Gα (*3, 33, 34*). Ste2p, the α-factor pheromone receptor of *S. cerevisiae,* shows overall similar structural architecture to mammalian GPCRs and the yeast Gpa1p shows about 45% sequence similarity with mammalian Gα (*34, 35*). Comparison of Ste2p with the rhodopsin (class A) subfamily of GPCRs suggests that there are underlying similarities in the mechanism of signal transduction between Ste2p and the Class A GPCRs (*2*). These characteristics of Ste2p make it a good model for peptide-responsive GPCRs and other GPCRs that are difficult to study.

Studies on the interactions between Ste2p and Gpa1p indicate that Ste2p is similar to other GPCRs in that the third intracellular loop (IL3) is involved in Gpa1p activation (*2, 36-41*). Part of the Ste2p C-terminus was also shown to be involved in G protein interaction (*41*). However, specific residues that were important for G protein activation have not been identified to date because conservative mutations in any one residue did not result in significant defects (*2, 36-41*). Like the mammalian Gα, the region of Gpa1p that has been most commonly predicted to interact with Ste2p is the C-terminus (*42-44*). Truncation of the last five amino acids and lysine-to-proline substitution (K467P) of Gpa1p lead to pheromone signaling and mating defects suggesting that the C-terminal residues of Gpa1p, especially the last five amino acids, may be involved in Ste2p-Gpa1p interactions (*45*). Other studies have also proposed that the C-terminal domain of Gpa1p is critical for Ste2p-coupling, and that the C-terminus of Gpa1p forms a β-turn that correlates with the C-terminal region of mammalian Gpa1p (*46*). Mutagenesis studies suggest that residues in additional interface regions of Gpa1p contribute to activation of Ste2p and signaling (*32, 47*). Despite the intense studies carried out on the interactions of Ste2p with Gpa1p, the mechanisms of the interactions and specific residue-to-residue involved have not been determined.

This study identifies specific residue-to-residues interactions between Ste2p and Gpa1p. A proposed mechanism for receptor-Gα signal transfer involving conformational changes in both proteins is also discussed. To identify specific residue-to-residue contacts that are involved in the Ste2p-Gpa1p interaction, cysteine disulfide cross-linking was carried out on residues in IL3 of Ste2p and the C-terminus of Gpa1p. Disulfide cross-linking studies suggested that the extreme C-terminus of Gpa1p interacts with the cytoplasmic boundaries of TM5 and TM6 similar to the interaction of transducin with opsin (*26*). The pattern of Gpa1p interaction with the inactive and active forms of Ste2p suggest possible rotational and translational shift movements at the C-terminus of Ste2p that are required for proper Gpa1p coupling during activation of both proteins. This study is the first to identify specific residues in Ste2p that interact with specific residues in Gpa1p, and also provides experimental evidence of possible conformational changes at the C-terminus of a Gα during receptor-G protein activation. The information in this study will be crucial for future studies on Ste2p and Gpa1p interactions as well as most mammalian GPCRs that share similar structure-function relationships.

CHAPTER 2

Materials and Methods

Media, Reagents, and Strains and Transformation:

Saccharomyces cerevisiae strain TM5117 [*MAT**a**, bar1, leu2, his3, ura3, FUS1-lacZ::URA3, ste2*Δ*, gpa1*Δ (*48*)] was used for Gpa1p *Fus1-LacZ* activities and the protease deficient strain BJS21 [*MAT**a**, prc1-407 prb1-1122 pep4-3 leu2 trp1 ura3-52 ste2::Kan*^{R} (*49*)] was used for protein isolation and immunoblot analysis. The *STE2* and *GPA1* mutant plasmids were co-transformed by the method of Geitz (*50*) into TM5117 and BJS21 cells.

For all transformations, cells were cultured in their selective media and grown to mid-log phase at 30^{o}C with shaking (200 rpm) overnight. The cells (5 ml culture) were then harvested and washed with sterile water and 100 mM LiAc (lithium acetate) by centrifugation at 4000g for 5 minutes. The pellet was resuspended in transformation mixture [240µl of 50% PEG (polyethylene glycol); 36µl of 1.0 M LiAc; 25µl of salmon sperm DNA; and 50µ water with plasmid DNA (5 µg)]. The mixture was incubated at 30^o C for 30 minutes and then heat shocked at 42^o C for 25 minutes. The cells were separated from the mixture and resuspended in sterile water for plating on selective media. Transformants were selected by growth on minimal medium (*51*) lacking tryptophan and uracil (designated as MLTU) or tryptohan and histidine (designated as MLTH) to maintain selection for the plasmids. All media components were obtained from BD (Franklin Lakes, NJ) and were of the highest quality available.

Cysteine scanning mutagenesis:

The open reading frame of *GPA1* was PCR amplified from the plasmid YepGαβγ (*52*) and cloned into the plasmids p426 and p423-GPD (*53*) to yield plasmids pBUG6 and pBUG3, respectively. Primers used for the mutagenesis are listed in Table 1. The pBUG6 and pBUG3 were engineered by site-directed mutagenesis to replace 11 residues in Gpa1p (I461-I471) with cysteine. The sequence of all cysteine mutants was verified by DNA sequence analysis completed by the molecular biology resource facility located on the campus of the University of Tennessee. Mutagenic and sequencing primers were purchased from Invitrogen (Carlsbad, CA).

Membrane extraction and immunoblots:

BJS21 cells expressing S*TE2* and *GPA1* mutant constructs grown in their selective media were used to prepare total cell membranes isolated as previously described (*54*). Cells were harvested and lysed by agitation with glass beads in 700 µL of HEPES buffer (50 mM HEPES, 150 mM NaCl, pH 7.5) and the following concentrations of protease inhibitors: 1.0 mM leupeptin, 10 µM pepstatin A, and 5.0 mM phenylmethanesulfonyl fluoride. The lysate was cleared by centrifugation at 3000g for 2 minutes. The membrane fraction was harvested by centrifugation at 15000g for 30 minutes and was then resuspended in the HEPES buffer with 20% glycerol. Protein concentration was determined using the BioRad (BioRad, Hercules, CA) protein assay (*48*).

For immunoblot analyses the membrane extract was solubilized in SDS sample buffer (BioRad, Hercules, CA) and 5 µg were fractioned by SDS-PAGE.

Table 1: Primers used for the mutagenesis.

Primers for Gpa1p C-terminal Cys Mutants	
I461C Forward:	CCGATCTATGCATCCAGCAAAACCTT
I461C Reverse:	GCTGGATGCATAGATCGGTGACTGC
I462C Forward:	CGATCTAATCTGCCAGCAAAACCTTAAA
I462C Reverse:	GTTTTGCTGGCAGATTAGATCGGTGACTG
Q463C Forward:	CTAATCATCTGCCAAAACCTTAAAAAAAATTG
Q463C Reverse:	GGTTTTGGCAGATGATTAGATCGGTGAC
Q464C Forward:	ATCATCCAGTGCAACCTTAAAAAAATTGG
Q464C Reverse:	TTAAGGTTGCACTGGATGATTAGATCGGTG
N465C Forward:	CAGCAATGCCTTAAAAAAATTGG
N465C Reverse:	TTAAGGCATTGCTGGATGATTAGATC
L466C Forward:	CAAAACTGCAAAAAAATTGGTATTATATG
L466C REVERSE:	CAATTTTTTTGCAGTTTTGCTGGATGAT
K467C Forward:	ACCTTTGCAAAATTGGTATTATATG
K467C Reverse:	CAATTTTGCAAAGGTTTTGCTGGATG
K468C Forward:	CCTTAAATGCATTGGTATTATATGAGAATTCG
K468C Reverse:	AATACCAATGCATTTAAGGTTTTGCTGGATG
G470C Forward:	AAAAATTTGCATTATATGAGAATTCGATATCAAGC
G470C Reverse:	CGAATTCTCATATGCAACCAATTTTTTTAAGG
I471C Forward:	AAATTGGTTGCATATGAGAATTCGATATC
I471C Reverse:	CGAATTCTCATATGCAACCAATTTTTTTAAGG

Blots were probed with FLAG antibody (Sigma/Aldrich Chemical, St. Louis, MO) to detect Ste2p or an antibody directed against Gpa1p (Santa Cruz Biotechnology, Inc., CA). The signals generated were analyzed using Quantity One software (Version 4.5.1) on a Chemi-Doc XRS photodocumentation system (BioRad, Hercules, CA).

Fus1-LacZ Assays:

TM5117 cells co-expressing wild type Ste2p and the various Gpa1p mutants were grown at 30 ºC in selective media, harvested, washed three times with fresh media and resuspended at a final concentration of 5 x 10^7 cells/ml. Cells (0.5 ml) were combined with α-factor pheromone (final concentration of 1 μM) and incubated at 30ºC for 90 minutes. The cells were transferred to a 96-well flatbottom plate in triplicate, permeabilized with 0.5% Triton X-100 in 25 mM PIPES buffer and then β-galactosidase assays were carried out using fluorescein di-β-galactopyranoside (Molecular Probes, OR) as a substrate (*55*). The reaction mixtures were incubated at 37^{o}C for 60 min and 1.0 M Na_2CO_3 was added to stop the reaction. The fluorescence of the samples (excitation of 485nm and emission of 530 nM) was determined using a 96-well plate reader Synergy2 (BioTek Instruments, Inc., Winooski, VT). The data were analyzed using Prism software (GraphPad Software, San Diego, CA). The experiments were repeated at least three times and reported values represent the mean of these tests.

Disulfide cross-linking:

Membrane proteins (in HEPES buffer, 20% glycerol, pH 7.5) extracted from BJS21 cells expressing Ste2p Cys mutants co-expressed with Gpa1p Cys mutants were treated with Cu-P (1.0

μM Cu and 3.0 μM 1,10-phenanthroline) according to optimum concentrations for Cu-P determined in this part of the dissertation (see below), Membrane samples were incubated with Cu-P at room temperature for 30 min. The reaction was quenched by addition of EDTA to a final concentration of 10 mM. The cross-linked samples were resuspended in non-reducing SDS sample buffer (BioRad, Hercules, CA) and resolved on SDS-PAGE as described above. The disulfide reaction was reversed by reducing with 4% 2-mercaptoethanol (β-ME) in the SDS sample buffer before resolving it on SDS-PAGE. To investigate the effects of ligand or GTP on cross-linking, membrane fractions were incubated in HEPES buffer containing 5μM α-factor (WHWLQLKPGQPNle^{12}Y) or 20 μM α-factor antagonist (WLQLKPGQPNle^{12}Y) in the presence or absence of 0.1 mM GTP or GTP-γ-S (*15*) before Cu-P treatment.

For in vivo cross-linking, cells were grown to mid-log phase, harvested, and washed with water by centrifugation (4000g for 5 min). The cells were resuspended in 100 mM LiAc and incubated at 30^{o}C for 30 min with mixing.. After centrifugation, the cells were resuspended in 25% PEG with 250 mM LiAc for another 60 min incubation. Cells were washed with HEPES buffer three times after LiAc treatment. For whole cell ligand binding prior to cross-linking, cells were first incubated with KF (10 mM) and NaN_3 (10mM) in HEPES buffer at room temperature for 15 min to inhibit receptor endocytosis (*56*) and then ligand added to final concentrations of 5μM for native α-factor or 20 μM for α-factor antagonist for another 30 min. Disulfide cross-linking was induced by adding Cu-P to final concentrations of 0.5 mM Cu and 1.5 mM 1,10-phenanthroline (*57*). Control cells without cross-linking were treated with equivalent volume of HEPES buffer. The mixture was incubated at room temperature for 60 min with end-over-end mixing. EDTA (ethylenediamine-tetraacetic acid) and NEM (N-

ethylmaleimide) to final concentrations of 10 mM were added to stop the reaction. The cells were washed three times with HEPES buffer containing EDTA (10 mM) and NEM (10 mM). Membrane extraction was carried as described above with HEPES buffer containing 10 mM EDTA/NEM. Reducing condition of disulfide bond were carried out by resuspending membrane samples in SDS-PAGE sample buffer containing 4% β-ME and incubating at room temperature for at least 15 min.

Prediction and modeling:

All models of 3-D structures were generated by the Phyre Structural Bioinformatics Group prediction tools (*58*). The structures were viewed and labeled with the PyMOL pdb viewer software (DeLano Scientific LLC, Palo Alto, CA). Aligment of the last 11 amino acids of transducin (Gα of rhodopsin) with Gpa1p was carried out using European Bioinformatics Institute online sequence alignment tools (http://www.ebi.ac.uk/).

CHAPTER 3

Results

Expression and activities of Gpa1p Cys-mutants:

The expression and biological activities of the third intracellular loop (IL3) of Ste2p Cys mutants used for the disulfide cross-linking with Gpa1p have already been reported in a previous study (see part 4 of this dissertation). It was shown that all the IL3 Cys mutants displayed activities similar to the Cys-less receptor except for R233C which was about 30% reduced in biological activity compared to all of the other IL3 Cys mutant receptors. The Gpa1p Cys mutants generated in this study have expression levels similar to wild type Gpa1p (Figure 1B). The high molecular weight protein (denoted as NS in Figure 1B) that reacted with anti-Gpa1p was seen also in extracts from TM5117 cells deleted for Gpa1p (data not shown). The yeast strain TM5117 used to express the Gpa1p mutants has the endogenous *GPA1* deleted resulting in high basal *FUS1-LacZ* activities because the free Gβγ subunits constitutively activate the signal transduction pathway. When bound, the Gα subunit (GDP-state) renders the Gβγ subunits inactive. However in the presence an activated receptor, Gα-GDP exchanges GDP for GTP and the now active Gα-GTP subunit dissociates from Gβγ thus allowing these units to become active (*19*). The subsequent hydrolysis of GTP to GDP makes the Gα-GDP available for another cycle (*19*). Expression of the mutant Gα subunits showed that all could interact with the endogenous Gβγ subunits leading to reduced *FUS1-LacZ* activities in the TM5117 yeast strain (Figure 1C). In the presence of ligand bound Ste2p, the *FUS1-LacZ* activities increased, implying that all the various Gα mutants can couple with both the Ste2p receptor and the G protein βγ subunits.

A

```
Length:          11
Identity:        5/10 (50.0%)
Similarity:      7/10 (70.0%)

Transducin       340 ILENLKDCGLF 350
                     |.:|||..|:
Gpa1p            462 IQQNLKKIGII 472
```

B

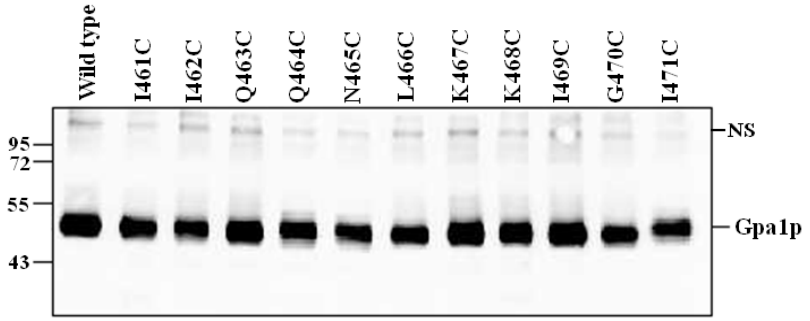

C

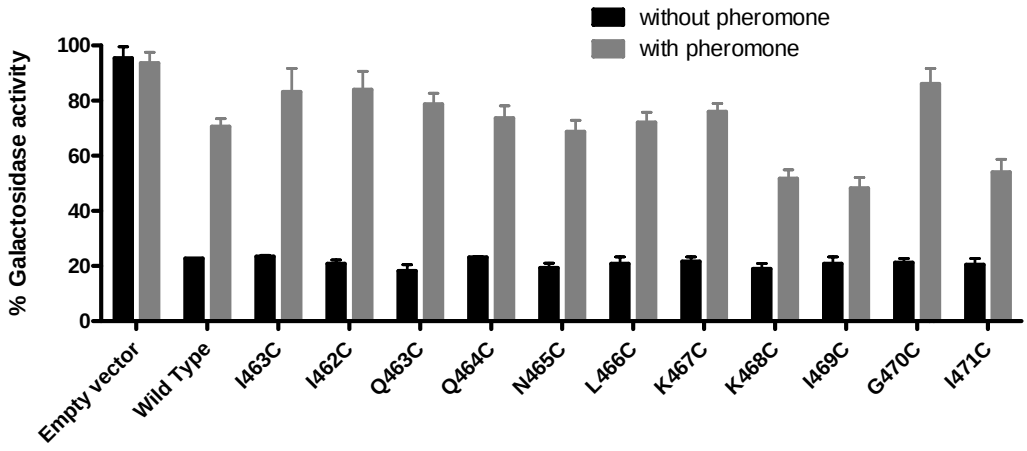

Figure 1: Expression and activities of Gpa1p Cys-mutants. A: alignment of Gpa1p and transducin Gα last 11 amino acids. B: immunoblot image of Gpa1p Cys mutants. All the mutants have similar expression level as wild type Gpa1p. A non-specific signal (NS) was observed on the blot in all samples. C: relative Fus1-LacZ activities of the mutants. All mutants could couple Gβγ subunits and responded to pheromone binding to Ste2p.

However, the mutants K468C, I469C and I471C all exhibited about 50% capacity to activate signal transduction as measured by *FUS1-LacZ* activity in comparison to the other Cys-mutants.

Copper treatment of IL3 Cys mutants and Gpa1p:

The initial studies involving copper treatment of membranes using 5-100 μM Cu showed that the Gpa1p could not be detected using anti-Gpa1p after the treatment. Copper interference with western blots observed in previous studies in another lab showed that aggregation of proteins occurred at high copper concentrations (*59*). Therefore, to determine the optimum concentration of Cu-P for cysteine disulfide cross-linking between IL3 Cys-mutants and Gpa1p C-terminal Cys-mutants, cells expressing R233C receptor (observed to form strong dimers) and wild type Gpa1p were treated with different amounts of copper. The amount that induced significant cross-linking with minimal effects on the detection of Gpa1p protein was 1.0 μM (Figure 2). Subsequently, for disulfide cross-linking, Cu-P [Cu(II) (1,10-phenanthroline)3] at a final concentration of 1.0 μM Cu and 3.0 μM 1,10-phenanthroline was added to membrane samples and incubated at room temperature for 30 min. The reaction was quenched by addition of EDTA to final a concentration of 10 mM. These treatment conditions were used for the disulfide studies unless otherwise stated.

***Disulfide cross-linking of Ste2p and Gpa1p*:**

To determine whether IL3 residues in Ste2p interacted with the C-terminal (I461-I471) residues in Gpa1p as measured by disulfide crosslinking, the IL3 Cys-mutants were each co-expressed with all the Gpa1p Cys-mutants including wild type Gpa1p.

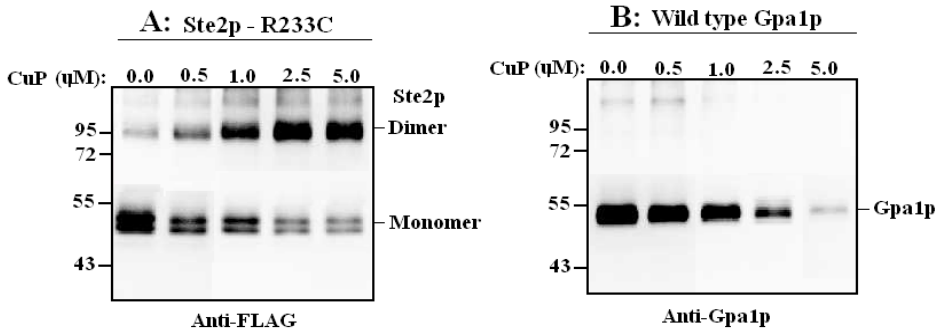

Figure 2: Copper treatment of Ste2p Cys mutants and wild type Gpa1p. The samples were incubated with different concentrations of copper at room temperature for 30 min. Significant disulfide bond was formed with 1.0 μM copper (A) with a minimal effect on Gpa1p detection (B).

Thus 23 different IL3 receptors each with only one Cys residue in IL3 were co-expressed with 12 different Gpa1p proteins each with only one Cys residue in the C-terminus to give 276 different combinations of Ste2p/Gpa1p Cys-mutants. Membranes extracted from all the different combinations were incubated with or without 5 μM α-factor and then treated with Cu-P as mentioned above (see materials and methods for detail).

The Cys-less Ste2p with His- and FLAG-epitope tags used to generate the IL3 Cys mutntants is about 51 kDa. This receptor is normally observed as a monomer (51-55 kDa, with three poorly dissociated bands due to N-glycosylation at two sites on the N-terminus) and a dimer (106-110 kDa) on blots [(*48*) also see part 4 of this dissertation]. The wild type Gpa1p used in this study is observed at a 52-54 kDa position (Figure 2). The Ste2p-Gpa1p disulfide cross-linked product (~103-108 kDa) is therefore expected to be at similar position as that of the Ste2p dimer (~102-110 kDa) on the immunoblots. Since the IL3 Cys mutants have been shown

to form homo-dimers (this dissertation, part 4) we were concerned that a 103-108 band would represent a Ste2p homo-dimer and and not a Ste2p-Gpa1p heterodimeric cross-linked product at similar position on immunoblots. To detect the Ste2p-Gpa1p cross-linked product we used an antibody directed against Gpa1p. This antibody should react with 52-54 kDa (Gpa1p) and 103-108 kDa Ste2p-Gpa1p heterodimer (if cross-linked) since Gpa1p does not form a homo-dimer; the only signal at the 103-108 position should correspond to the cross-linked product. The Ste2p-Gpa1p cross-linking results are shown in figures 3 showing those combinations that yielded cross-linked products. Those that were not included in the figures are combinations without any detectable cross-linked product, although for purposes of comparison, one example without detectable cross-linking is shown (Figure 3, I246C).

Out of the 22 Ste2p Cys-mutants tested, 5 mutants (L228C, S243C, L247C, L248C and I249C) showed a cross-linked band with 5 Gpa1p Cys-mutants (Q463C, N465C, K467C, I469C and G470C). In the inactive state (without α-factor) L248C in IL3 reacted with I469C in Gpa1p, whereas both L247C and I249C in IL3 reacted with N465C in Gpa1p. Although previous studies showed that I246C is highly accessible to a sulfhdryl reagent (*60*) this residue did not react with the Gpa1p residues tested in this study. No detectable disulfide product was observed in residues located in the middle of the IL3 loop or the TM5 boundary in the inactive conformation of Ste2p.

Thus, in the inactive state of Ste2p the C-terminus of Gpa1p may be in close proximity to, or tilted more towards, the cytoplasmic end of TM6 than TM5. In the ligand-bound, active conformation (α-factor "+" lanes) both A228C (TM5) and I249C (TM6) reacted with G470C of Gpa1p. S243C and L247C of the receptor reacted with Q463C of Gpa1, whereas receptor I249C reacted with I469C of Gpa1.

Ste2p-Cys-less

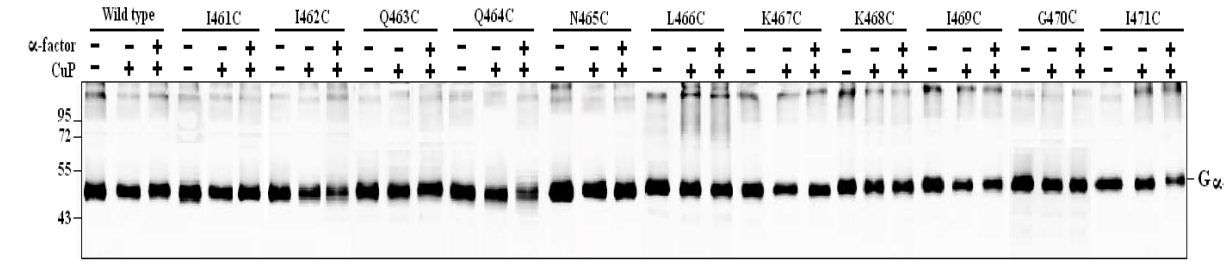

Ste2p-A228C

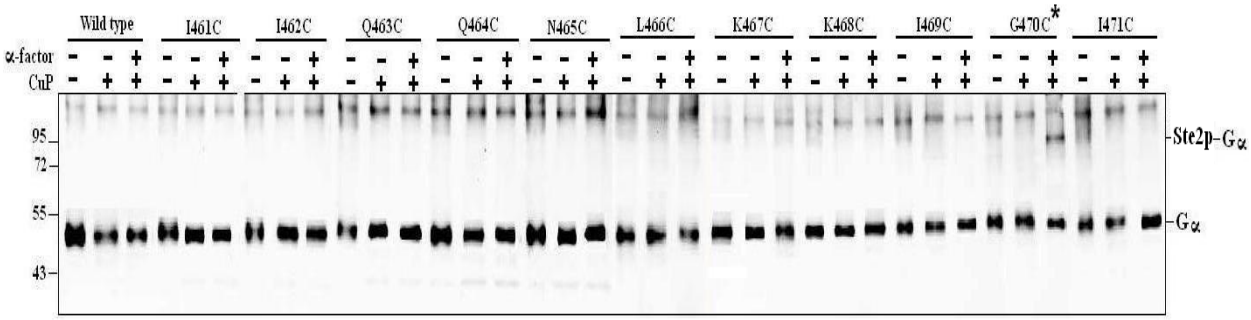

Ste2p-S243C

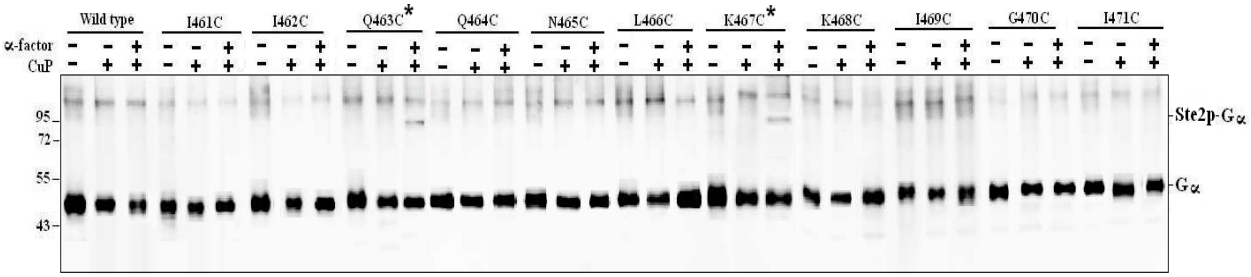

Ste2p-I246C

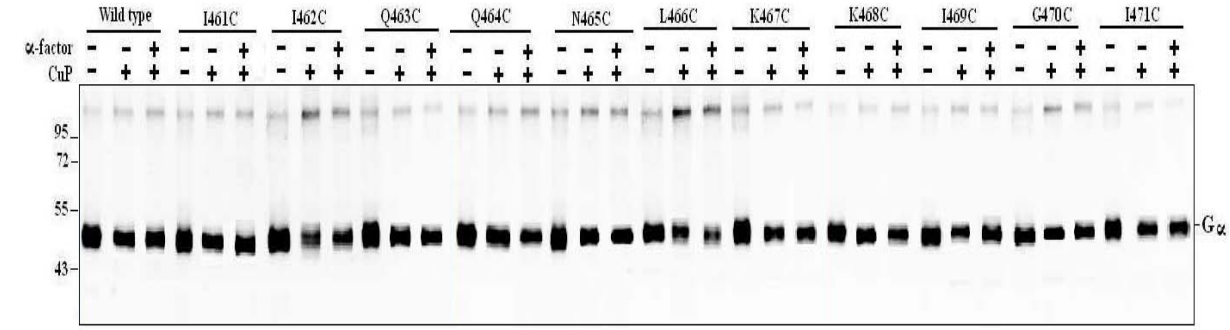

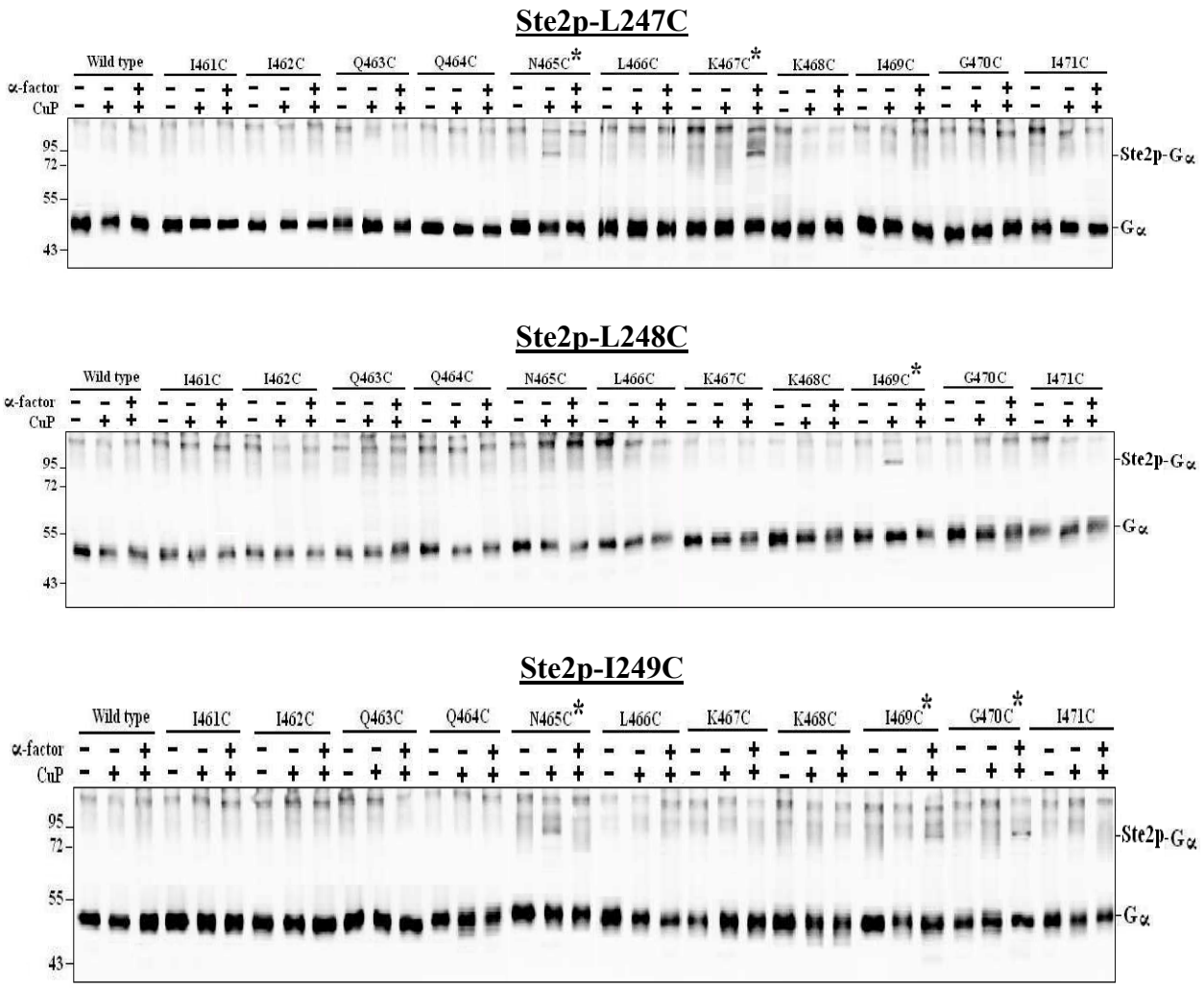

Figure 3: Disulfide cross-linking between of Ste2p and Gpa1p Cys-mutants. The blot images represent individual IL3 Cys-mutants co-expressed with Gpa1p Cys-mutants. Each preparation was untreated (lanes -, -) or treated with Cu-P (lanes -, +) or with α-factor and Cu-P (lanes +, +). The samples were probed with anti-Gpa1p antibody to detect the presence of Gpa1p (Gα) at either the 52-54 kDa or 103-108 kDa (Ste2p-Gα cross-linked) position. The blot images were spliced together from different gels to place the mutants in order according to residue number.

The Cu-P treatments of mutants with detectable cross-linked products were repeated (Figure 4). The samples were immunoblotted with both anti-Gpa1p and anti-FLAG to detect Ste2p-monomer (53-55 kDa), Ste2p-dimer (106-110 kDa) and Ste2p-Gpa1p cross-linked product (103-108 kDa). The Ste2p-Gpa1p cross-linked product was reversed by treatment with 4% β-ME (see Figure 4, last three lanes for I249C-G470C), indicating that there was a disulfide bond forming the heterodimeric Ste2p-Gpa1p.

To test whether the IL3-Gpa1p interactions observed in the membrane samples existed in the cell, in vivo CuP treatment was carried out on whole cells. For these experiments, cells co-expressing Ste2p-I249C and Gpa1p mutants, N465C, L466C, K467C, K468C, I469C, G470C and I471C in the presence or absence of α-factor were used. The results (Figure 5) show that the in vivo interaction of receptor mutant I249C with Gpa1p is similar to what was observed in membrane preparations.

The close proximity of A228, I247, L248, and L249 of Ste2p with the extreme C-terminus of Gpa1p indicate that these residues may be essential for Gpa1p coupling with Ste2p. The reaction of S243 (Ste2p) with Q463 and K467 (Gpa1p) suggest that these residues may be involved in a hydrogen bonding network.

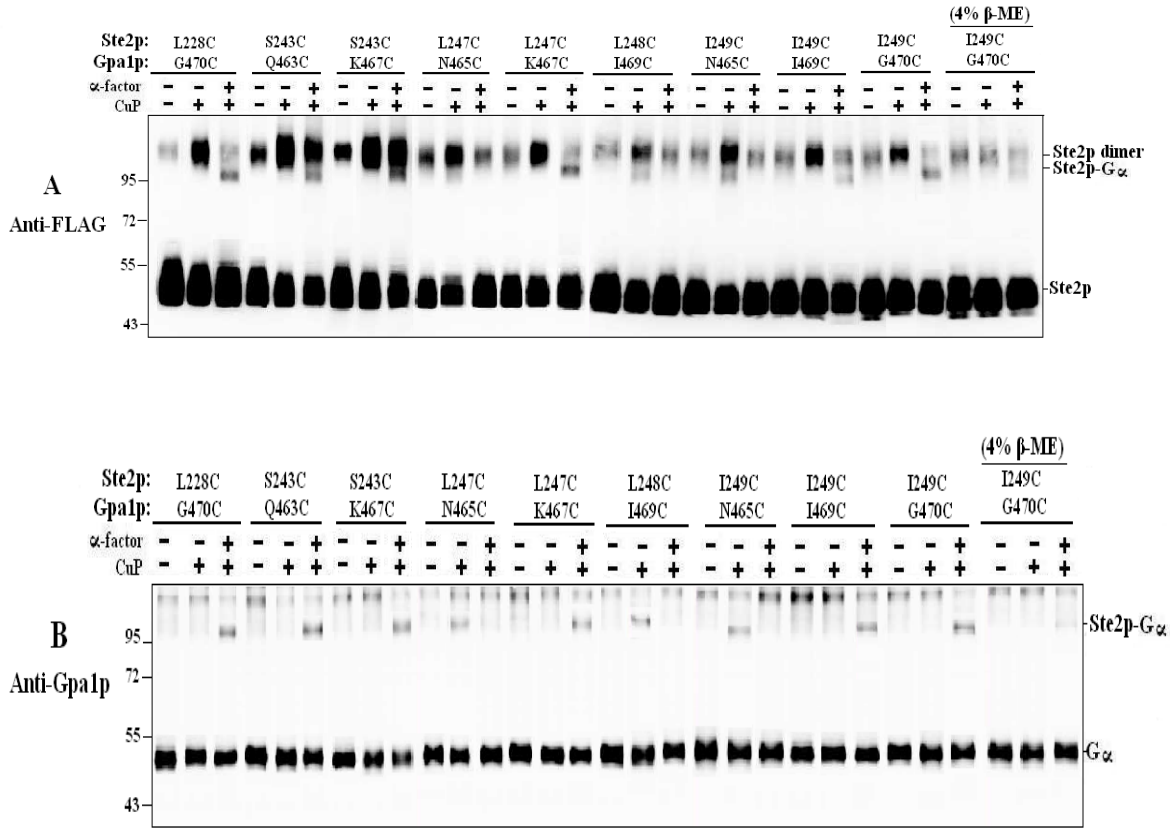

Figure 4: Disulfide cross-linking between of Ste2p IL3 and Gpa1p Cys-mutants. The samples were resolved on a 4-12 % gradient SDS-PAGE (non-reducing). **A**: The blots were probed anti-FLAG to detect the presence of Ste2p at either ~51-55 kDa (Ste2p monmer) or ~108-110 kDa (Ste2p-dimer) or ~103-108 kDa (Ste2p-Gα cross-linked) position. **B**: The blots were also probed with anti-Gpa1p antibody to detect the presence of Gpa1p (Gα) at either the ~53-54 kDa or ~103-108 kDa (Ste2p-Gα cross-linked) position. The blot images were spliced together from different gels. In the anti-FLAG blots a band below the Ste2p dimer position corresponding to Ste2p-Gpa1p cross-linked product was observed in lanes that show similar signal with the anti-Gpa1p. This product was reduced when samples were treated with (4% β-ME).

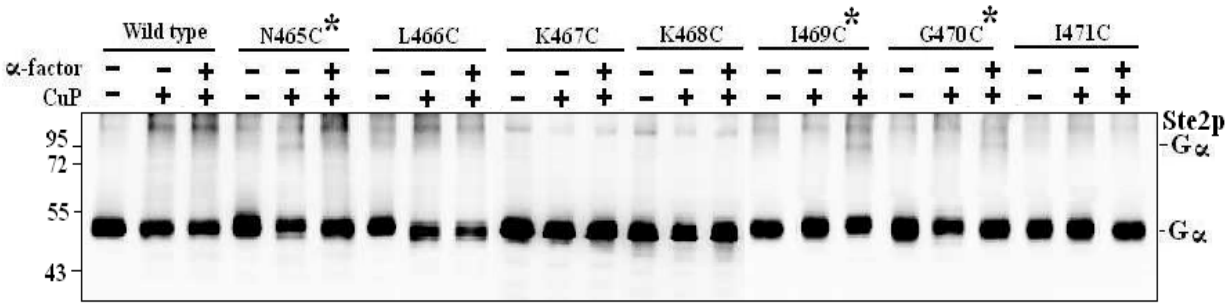

Figure 5: In vivo cross-linking of Ste2p and Gpa1p. Cells expressing Ste2p-I249C mutants the Gpa1p-Cys mutants (N465C-I471C) were treated with CuP for in vivo induced cross-linking. Membrane samples were probed with anti-Gpa1p. Ste2p-I249C show similar reactions with Gpa1p Cys mutants in vivo as observed in vitro. Each preparation was untreated (lanes -, -) or treated with Cu-P (lanes -, +) or with α-factor and Cu-P (lanes +, +).

CHAPTER 4

Discussion

Heterotrimeric G proteins transduce the signals for a wide range of medically important GPCRs (*4, 15, 61*). The Gα subunits are composed of two domains: the core and helical domains. The guanine nucleotide (GDP or GTP) is bound within a deep pocket between the core and helical domains. The C terminal regions of the Gα subunit, which is suggested to be involved in receptor interactions, consist of two α-helices and a β strand, where the α5-helix comprises the extreme C-terminus (*19, 46*). Activation of Gα subunit by GPCR alters interactions between GDP and residues of both the helical and core domains; these interactions are proposed to open the GDP-binding pocket, allowing GDP dissociation and the subsequent binding of GTP (*15, 25, 62*). Despite intensive studies on GPCR-G protein interactions the mechanisms by which Gα subunits are stimulated to bind GTP are not well defined. In this study specific residue-to-residue interactions between Ste2p, the *S. cerevisiae* pheromone receptor, and Gpa1p, its cognate Gα, have been identified by disulfide cross-liking. Conformational changes at the C-terminus of Gpa1p during Ste2p activation are also discussed.

The alignment of Gpa1p used in this study with the last 11 amino acids of transducin showed that these two proteins are 50% identical and 70% similar at the C-terminus (Figure 1A). This portion of transducin was suggested to directly interact with opsin and was used for co-crystallization with opsin to determine its binding to opsin (*26*). The C-terminus of Gpa1p has been identified to interact with Ste2p and truncation of the last five amino acid residues (K468-I472) of Gpa1p resulted in defects in the pheromone response pathway (*45*). Another report

showed that triple mutations to alanine at Q464, N465, and L466, at K467, K468, and I469 or at G470, I471, and I472 of the last nine amino acid residues resulted in defects in mating activities. Single alanine mutations within the QNL and KKI triplets did not affect mating, however the single mutants, K468P, G470A, I471A, I471T and I472T all resulted in mating defects (*46*). Activities of cysteine substitutions of the eleven residues (I461-I471) tested in this study indicated K468C, I469C and I471C all resulted in partial pheromone response activities consistent with previous studies (*32*), whereas the other eight mutants did not display any significant defects. Defects caused by mutations of the last five residues of Gpa1p have been consistent in most studies suggesting that these residues are indeed critical for proper receptor coupling and Gpa1p activation. None of these mutations affected the coupling of Gpa1p with the Gβγ protein subunits as observed in the *FUS1-LacZ* assay (Figure 1C), implying that the carboxyl tail of Gpa1p is essential for receptor coupling but not Gβγ proteins interaction as observed in mammalian cells (*36*).

The crystal structure of opsin in its G protein-interacting conformation shows that the cytoplasmic ends of TM5 and TM6 provides a surface for hydrophobic interactions with the C-terminus of transducin Gα. Residues at the cytoplasmic ends of TM3 also interact with the C-terminus of transducin Gα (*26*). The disulfide cross-linking studies presented in this dissertation indicated that the C-terminus of Gpa1p interacts with Ste2p at similar regions of TM5 and TM6. In opsin, TM5 and TM6 are involved in van der Waals interactions with the C-terminus of transducin and hydrogen bonding linking the transducin residues to opsin residues in the network (*26*). It has been shown in the fourth part of this dissertation that α-factor binding to Ste2p resulted in conformational changes in the hydrophobic residues at TM5 and TM6 cytoplasmic

ends. Out of the three residues (L228, A229 and I230) that were affected by conformational changes only L228 was observed to interact with G470C in the active conformation of the receptor. On the other hand, all residues (L247, L248 and L249) that were affected by changes at the intracellular end of TM5 were observed to interact with Gpa1p. The close proximity of A228, I247, L248, and L249 of Ste2p to the extreme C-terminus of Gpa1p indicates that these residues provide a hydrophobic environment that favors the Gpa1p C-terminus interactions. The reaction of S243 (Ste2p) with Q463 and K467 (Gpa1p) suggests that these residues are involved in a hydrogen bonding network, with hydrogen bridges between these three residues. These hydrogen bridges may be required for receptor activation, since this was only observed in the active form of the receptor. However, this is just a part of a network of interactions, so it may not be essential for full activation of the receptor and/or Gpa1p.

The last five residues (with the exception of I472 that was tested) of Gpa1p were all found to interact with IL3 residues. Most of these residues were found to interact at the cytoplasmic ends of TM6 in the active conformation of the receptor. In the opsin-GαCT complex it was observed that the binding of the Gα to the TM5-TM6 regions creates a network of interaction that stabilizes the ligand binding pocket of the receptor. We propose similar interactions between Gpa1p and TM5-TM6 in Ste2p. For instance, the deletion of the first two amino acids of α-factor prevents proper TM5-TM6 conformational changes as seen using the α-factor antagonist in part 4 of this dissertation. Thus, for receptor activation these two residues of α-factor may interact within a binding pocket that is stabilized by the interactions of the C-terminus of Gpa1p so that in the absence of these ligand residues (W^1H^2) the receptor does not undergo complete conformational changes. Thus, Gpa1p and α-factor binding to Ste2p are

coordinated for full activation of Ste2p. The fact that substitution of cysteine for residues in Gpa1p C-terminus did not significantly affect activities of either the receptor nor Gpa1p suggest that receptor-G protein coupling is mediated by more general structural features that involve network interactions between residues of both proteins. Since this study was done with a limited number of residues (L228-I249) it is likely that additional residues before L228 in TM5 and/or after I249 in TM6 and also some TM3 residues may interact with Gpa1p in Ste2p in the inactive/active state.

Activation of the G protein by the receptor has been observed to alter interactions of residues in the GDP binding domains that open the GDP-binding cleft, allowing GDP dissociation and the subsequent binding of GTP. Since the receptor binding domain of Gα is on the opposite face from the GDP-binding cleft, the interaction with the activated receptor must be transmitted by conformational changes to give rise to release of GDP. Mutagenesis studies of the C-terminus of Gpa1p suggest that the C-terminus adopts different conformations during interaction with Ste2p and Ste3p (*46*). However, this study could not predict the conformational changes that occur at the C-terminus of Gpa1p during receptor activation.

Several models have been proposed for the mechanism of G protein activation. In general, the models suggest that the α5-helix which comprises the C-terminus is the key transmission domain for signal transfer from the activated receptor to G protein (*31, 32*). Recently, conformational changes at the C-terminus of transducin Gα were proposed, based on structural and kinetic modeling by comparing the crystal structure of Gα and opsin-GαCT. This helix switch mechanism suggests that the α5 helix (C-terminus) undergoes a rotational and translational movement, which distorts the GDP binding site to cause GDP release. Thus, the

α5-helix rotates counter-clockwise around its axis by 90° and tilts relative to the membrane normal by 42°. This movement is accompanied by formation of hydrogen bonding networks between α5 and the active receptor (*30*).

In this study, two conformational changes are proposed based on the reactions of residues at the extreme end of the Gpa1p C-terminus with residues at the cytoplasmic ends of TM5-TM6 in Ste2p. The first conformational change observed was similar to the helix mechanism model of rotational movement of the C-terminus of Gpa1p (*30*). This movement is supported by the switch of the interactions from Gpa1p-N465C/Ste2p-L247C or Gpa1p-N465C/Ste2p-I249C in the inactive conformation to Gpa1p-K467C/Ste2p-L247C or Gpa1p-I469C/Ste2p-I249C in the active conformation respectively (see Figure 6). Since the C-terminus of the Gpa1p is predicted to have a helical structure (*32*) it will require about ~120^{o} rotation of the helix to move K467 from the inner core of the receptor to the IL3-Gpa1p interface, and vice-versa for N465. Also, since TM6 of Ste2p has been suggested in this study to undergo ~30^{o}C clockwise rotation upon ligand binding (see Part IV), similar to other GPCRs (*63*), it is proposed that Gpa1p may not have to undergo the full ~120^{o} rotation as noted, but rather ~90^{o} anti-clockwise rotation.

The second conformational change is what we call the "withdrawal" movement, similar to the "translational" movement predicted by the helix switch mechanism (*30*). This movement is observed in the switch of the interactions between Gpa1p-N465/Ste2p-I249 in the inactive conformation to Gpa1p-I469/Ste2p-I249 in the active conformation. These changes in interaction will require the C-terminus of Gpalp to move about the height of the pitch of a helix (~5.4 Å) and at the same time undergo a horizontal movement.

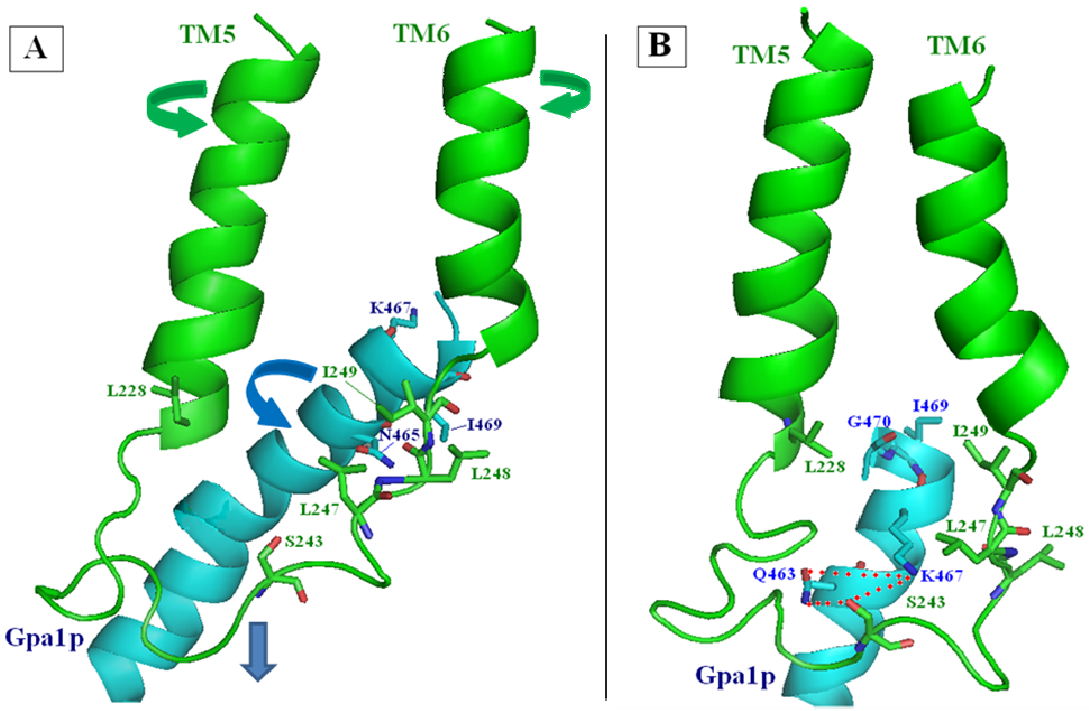

Figure 6: Proposed 3D model of conformational changes in Ste2p TM5-TM6 cytoplasmic ends and C-terminus of Gpa1p during activation. Ste2p and Gpa1p residues are labeled green and blue, respectively. A, (inactive state): The C-terminus of Gpa1p is suggested to be closer to TM6 than TM5 in the inactive state. Upon α-factor binding changes occur at the cytoplasmic ends of TM5 and TM6. TM5 and TM6 are proposed to undergo rotation of ~30^{o} in the anti-clockwise and clockwise directions, respectively (indicated by green arrows) similar to other GPCRs (*63, 64*). The C-terminus of Gpa1p undergoes two possible changes (indicated by blue arrows), an anti-clockwise rotation of ~90^{o} and a withdrawal of ~5.0 Å (horizontal and vertical shifts) from the inner core of the receptor to the cytoplasmic end. B (active state): TM5 and TM6 are closer due to a shift in TM6 towards TM5 as observed in other GPCRs (*63, 64*). The C-terminus of Gpa1p is now closer to TM5 and withdrawn into the cytoplasmic surface of TM5-TM6. There are possible H-bond links between S243 of Step and Q463/K467 of Gpa1p.

The vertical and horizontal movements result in a translational shift of the Gpa1p C-terminus from TM6 towards TM5 and probably TM3. Since the data presented in this study can not differentiate between vertical and tilt movements, we can not assign any angle of translational movement. However, the data show evidence for movement at the C-terminus of Gpa1p that results in about a 5.0 Å shift from the inner bundle of the receptor to the cytoplasmic surface. This "withdrawal" movement concurs with the α5-transmission rod concept that movement at the C-terminus of Gα opens the GDP-binding cleft, allowing GDP dissociation and the subsequent binding of GTP (*19*).

We therefore propose that the C-terminus of the Gpa1p, upon activation of Ste2p, undergoes a ~90^{o} anti-clockwise rotation and at the same time withdraws from the inner core of the receptor which involves a vertical shift of about 5.0 Å. These conformational changes bring TM5 and TM6 closer to each other positioning L228 (TM5) and I248 (boundary between IL3 and TM6) in close proximity to contact I469 and G470 of Gpa1p. It also generates new contacts between IL3 of Ste2p and C-terminal helix of Gpa1p; S243 interacts with Q463 and K467 with multiple hydrogen bonds, and L247 is located in close proximity with K467 probably mediated by hydrophobic interaction. . These conformational changes are consistent with a proposed model for transducin (*30*). These movements may be critical for GPCR-Gα coupling and activation. Further experimental work, such as identifying other residues in Ste2p and Gpa1p that are involved in these movements, will be needed to refine the mechanism of activation.

This study is the first to report specific residue-to-residue interactions between Ste2p IL3 and Gpa1p. The hydrophobic residues at the cytoplasmic ends of TM5 and TM6 are suggested to play essential roles in Ste2p coupling with Gpa1p. We also report for the first time

conformational changes that occur at the extreme C-terminus of Gpa1p that may be required for receptor coupling and activation. Overall the results presented indicate that Ste2p-Gpa1p interactions are similar to those observed for mammalian GPCRs especially the rhodopsin-like family receptors. The information obtained in this study will serve as a platform for further understanding of GPCR-G protein interactions in other systems.

References for Part V

1. Naider, F., and Becker, J. M. (2004) The alpha-factor mating pheromone of Saccharomyces cerevisiae: a model for studying the interaction of peptide hormones and G protein-coupled receptors, *Peptides 25*, 1441-1463.
2. Eilers, M., Hornak, V., Smith, S. O., and Konopka, J. B. (2005) Comparison of class A and D G protein-coupled receptors: common features in structure and activation, *Biochemistry 44*, 8959-8975.
3. Minic, J., Sautel, M., Salesse, R., and Pajot-Augy, E. (2005) Yeast system as a screening tool for pharmacological assessment of g protein coupled receptors, *Curr Med Chem 12*, 961-969.
4. Lundstrom, K. (2009) An overview on GPCRs and drug discovery: structure-based drug design and structural biology on GPCRs, *Methods Mol Biol 552*, 51-66.
5. Williams, C., and Hill, S. J. (2009) GPCR signaling: understanding the pathway to successful drug discovery, *Methods Mol Biol 552*, 39-50.
6. Wall, M. A., Coleman, D. E., Lee, E., Iniguez-Lluhi, J. A., Posner, B. A., Gilman, A. G., and Sprang, S. R. (1995) The structure of the G protein heterotrimer Gi alpha 1 beta 1 gamma 2, *Cell 83*, 1047-1058.
7. Lambright, D. G., Sondek, J., Bohm, A., Skiba, N. P., Hamm, H. E., and Sigler, P. B. (1996) The 2.0 A crystal structure of a heterotrimeric G protein, *Nature 379*, 311-319.
8. Sondek, J., Bohm, A., Lambright, D. G., Hamm, H. E., and Sigler, P. B. (1996) Crystal structure of a G-protein beta gamma dimer at 2.1A resolution, *Nature 379*, 369-374.

9. Palczewski, K., Kumasaka, T., Hori, T., Behnke, C. A., Motoshima, H., Fox, B. A., Le Trong, I., Teller, D. C., Okada, T., Stenkamp, R. E., Yamamoto, M., and Miyano, M. (2000) Crystal structure of rhodopsin: A G protein-coupled receptor, *Science 289*, 739-745.

10. Rasmussen, S. G., Choi, H. J., Rosenbaum, D. M., Kobilka, T. S., Thian, F. S., Edwards, P. C., Burghammer, M., Ratnala, V. R., Sanishvili, R., Fischetti, R. F., Schertler, G. F., Weis, W. I., and Kobilka, B. K. (2007) Crystal structure of the human beta2 adrenergic G-protein-coupled receptor, *Nature 450*, 383-387.

11. Jaakola, V. P., Griffith, M. T., Hanson, M. A., Cherezov, V., Chien, E. Y., Lane, J. R., Ijzerman, A. P., and Stevens, R. C. (2008) The 2.6 angstrom crystal structure of a human A2A adenosine receptor bound to an antagonist, *Science 322*, 1211-1217.

12. Warne, T., Serrano-Vega, M. J., Baker, J. G., Moukhametzianov, R., Edwards, P. C., Henderson, R., Leslie, A. G., Tate, C. G., and Schertler, G. F. (2008) Structure of a beta1-adrenergic G-protein-coupled receptor, *Nature 454*, 486-491.

13. De Amici, M., Dallanoce, C., Holzgrabe, U., Trankle, C., and Mohr, K. (2009) Allosteric ligands for G protein-coupled receptors: A novel strategy with attractive therapeutic opportunities, *Med Res Rev*.

14. Eglen, R. M., and Reisine, T. (2009) New insights into GPCR function: implications for HTS, *Methods Mol Biol 552*, 1-13.

15. Ratnala, V. R., and Kobilka, B. (2009) Understanding the ligand-receptor-G protein ternary complex for GPCR drug discovery, *Methods Mol Biol 552*, 67-77.

16. Simon, M. I., Strathmann, M. P., and Gautam, N. (1991) Diversity of G proteins in signal transduction, *Science 252*, 802-808.

17. Christopoulos, A. (2002) Allosteric binding sites on cell-surface receptors: novel targets for drug discovery, *Nat Rev Drug Discov 1*, 198-210.

18. Christopoulos, A., and Kenakin, T. (2002) G protein-coupled receptor allosterism and complexing, *Pharmacol Rev 54*, 323-374.

19. Cabrera-Vera, T. M., Vanhauwe, J., Thomas, T. O., Medkova, M., Preininger, A., Mazzoni, M. R., and Hamm, H. E. (2003) Insights into G protein structure, function, and regulation, *Endocr Rev 24*, 765-781.

20. Spiegel, A. M., and Weinstein, L. S. (2004) Inherited diseases involving g proteins and g protein-coupled receptors, *Annu Rev Med 55*, 27-39.

21. Leach, K., Sexton, P. M., and Christopoulos, A. (2007) Allosteric GPCR modulators: taking advantage of permissive receptor pharmacology, *Trends Pharmacol Sci 28*, 382-389.

22. Saidak, Z., Blake-Palmer, K., Hay, D. L., Northup, J. K., and Glass, M. (2006) Differential activation of G-proteins by mu-opioid receptor agonists, *Br J Pharmacol 147*, 671-680.

23. Nguyen-Ngoc, T., Afshar, K., and Gonczy, P. (2007) Coupling of cortical dynein and G alpha proteins mediates spindle positioning in Caenorhabditis elegans, *Nat Cell Biol 9*, 1294-1302.

24. Ahuja, S., and Smith, S. O. (2009) Multiple switches in G protein-coupled receptor activation, *Trends Pharmacol Sci 30*, 494-502.

25. Sato, M., and Ishikawa, Y. (2009) Accessory proteins for heterotrimeric G-protein: Implication in the cardiovascular system, *Pathophysiology*.

26. Scheerer, P., Park, J. H., Hildebrand, P. W., Kim, Y. J., Krauss, N., Choe, H. W., Hofmann, K. P., and Ernst, O. P. (2008) Crystal structure of opsin in its G-protein-interacting conformation, *Nature 455*, 497-502.

27. Rondard, P., Iiri, T., Srinivasan, S., Meng, E., Fujita, T., and Bourne, H. R. (2001) Mutant G protein alpha subunit activated by Gbeta gamma: a model for receptor activation?, *Proc Natl Acad Sci U S A 98*, 6150-6155.

28. Cherfils, J., and Chabre, M. (2003) Activation of G-protein Galpha subunits by receptors through Galpha-Gbeta and Galpha-Ggamma interactions, *Trends Biochem Sci 28*, 13-17.

29. Herrmann, R., Heck, M., Henklein, P., Kleuss, C., Hofmann, K. P., and Ernst, O. P. (2004) Sequence of interactions in receptor-G protein coupling, *J Biol Chem 279*, 24283-24290.

30. Scheerer, P., Heck, M., Goede, A., Park, J. H., Choe, H. W., Ernst, O. P., Hofmann, K. P., and Hildebrand, P. W. (2009) Structural and kinetic modeling of an activating helix switch in the rhodopsin-transducin interface, *Proc Natl Acad Sci U S A 106*, 10660-10665.

31. Blahos, J., 2nd, Mary, S., Perroy, J., de Colle, C., Brabet, I., Bockaert, J., and Pin, J. P. (1998) Extreme C terminus of G protein alpha-subunits contains a site that discriminates between Gi-coupled metabotropic glutamate receptors, *J Biol Chem 273*, 25765-25769.

32. Gladue, D. P., and Konopka, J. B. (2008) Scanning mutagenesis of regions in the Galpha protein Gpa1 that are predicted to interact with yeast mating pheromone receptors, *FEMS Yeast Res 8*, 71-80.

33. Burchett, S. A., Scott, A., Errede, B., and Dohlman, H. G. (2001) Identification of novel pheromone-response regulators through systematic overexpression of 120 protein kinases in yeast, *J Biol Chem 276*, 26472-26478.

34. Dohlman, H. G., and Thorner, J. W. (2001) Regulation of G protein-initiated signal transduction in yeast: paradigms and principles, *Annu Rev Biochem 70*, 703-754.

35. Dohlman, H. G. (2002) G proteins and pheromone signaling, *Annu Rev Physiol 64*, 129-152.

36. Slessareva, J. E., Ma, H., Depree, K. M., Flood, L. A., Bae, H., Cabrera-Vera, T. M., Hamm, H. E., and Graber, S. G. (2003) Closely related G-protein-coupled receptors use multiple and distinct domains on G-protein alpha-subunits for selective coupling, *J Biol Chem 278*, 50530-50536.

37. Kristiansen, K. (2004) Molecular mechanisms of ligand binding, signaling, and regulation within the superfamily of G-protein-coupled receptors: molecular modeling and mutagenesis approaches to receptor structure and function, *Pharmacol Ther 103*, 21-80.

38. Henry, L. K., Khare, S., Son, C., Babu, V. V., Naider, F., and Becker, J. M. (2002) Identification of a contact region between the tridecapeptide alpha-factor mating pheromone of Saccharomyces cerevisiae and its G protein-coupled receptor by photoaffinity labeling, *Biochemistry 41*, 6128-6139.

39. Son, C. D., Sargsyan, H., Naider, F., and Becker, J. M. (2004) Identification of ligand binding regions of the Saccharomyces cerevisiae alpha-factor pheromone receptor by photoaffinity cross-linking, *Biochemistry 43*, 13193-13203.

40. Lee, Y. H., Naider, F., and Becker, J. M. (2006) Interacting residues in an activated state of a G protein-coupled receptor, *J Biol Chem 281*, 2263-2272.

41. Duran-Avelar, M. J., Ongay-Larios, L., Zentella-Dehesa, A., and Coria, R. (2001) The carboxy-terminal tail of the Ste2 receptor is involved in activation of the G protein in the Saccharomyces cerevisiae alpha-pheromone response pathway, *FEMS Microbiol Lett 197*, 65-71.

42. Clark, C. D., Palzkill, T., and Botstein, D. (1994) Systematic mutagenesis of the yeast mating pheromone receptor third intracellular loop, *J Biol Chem 269*, 8831-8841.

43. Stefan, C. J., and Blumer, K. J. (1994) The third cytoplasmic loop of a yeast G-protein-coupled receptor controls pathway activation, ligand discrimination, and receptor internalization, *Mol Cell Biol 14*, 3339-3349.

44. Celic, A., Martin, N. P., Son, C. D., Becker, J. M., Naider, F., and Dumont, M. E. (2003) Sequences in the intracellular loops of the yeast pheromone receptor Ste2p required for G protein activation, *Biochemistry 42*, 3004-3017.

45. Hirsch, J. P., Dietzel, C., and Kurjan, J. (1991) The carboxyl terminus of Scg1, the G alpha subunit involved in yeast mating, is implicated in interactions with the pheromone receptors, *Genes Dev 5*, 467-474.

46. Kallal, L., and Kurjan, J. (1997) Analysis of the receptor binding domain of Gpa1p, the G(alpha) subunit involved in the yeast pheromone response pathway, *Mol Cell Biol 17*, 2897-2907.

47. Roginskaya, M., Connelly, S. M., Kim, K. S., Patel, D., and Dumont, M. E. (2004) Effects of mutations in the N terminal region of the yeast G protein alpha-subunit Gpa1p on signaling by pheromone receptors, *Mol Genet Genomics 271*, 237-248.

48. Hauser, M., Kauffman, S., Lee, B. K., Naider, F., and Becker, J. M. (2007) The first extracellular loop of the Saccharomyces cerevisiae G protein-coupled receptor Ste2p undergoes a conformational change upon ligand binding, *J Biol Chem 282*, 10387-10397.

49. Huang, L. Y., Umanah, G., Hauser, M., Son, C., Arshava, B., Naider, F., and Becker, J. M. (2008) Unnatural amino acid replacement in a yeast G protein-coupled receptor in its native environment, *Biochemistry 47*, 5638-5648.

50. Gietz, D., St Jean, A., Woods, R. A., and Schiestl, R. H. (1992) Improved method for high efficiency transformation of intact yeast cells, *Nucleic Acids Res 20*, 1425.

51. Sherman, F. (2002) Getting started with yeast, *Methods Enzymol 350*, 3-41.

52. Dosil, M., Giot, L., Davis, C., and Konopka, J. B. (1998) Dominant-negative mutations in the G-protein-coupled alpha-factor receptor map to the extracellular ends of the transmembrane segments, *Mol Cell Biol 18*, 5981-5991.

53. Mumberg, D., Muller, R., and Funk, M. (1995) Yeast vectors for the controlled expression of heterologous proteins in different genetic backgrounds, *Gene 156*, 119-122.

54. David, N. E., Gee, M., Andersen, B., Naider, F., Thorner, J., and Stevens, R. C. (1997) Expression and purification of the Saccharomyces cerevisiae alpha-factor receptor

(Ste2p), a 7-transmembrane-segment G protein-coupled receptor, *J Biol Chem 272*, 15553-15561.

55. Slauch, J. M., Mahan, M. J., and Mekalanos, J. J. (1994) Measurement of transcriptional activity in pathogenic bacteria recovered directly from infected host tissue, *Biotechniques 16*, 641-644.

56. Jenness, D. D., and Spatrick, P. (1986) Down regulation of the alpha-factor pheromone receptor in S. cerevisiae, *Cell 46*, 345-353.

57. Wang, H. X., and Konopka, J. B. (2009) Identification of amino acids at two dimer interface regions of the alpha-factor receptor (Ste2), *Biochemistry 48*, 7132-7139.

58. Kelley, L. A., and Sternberg, M. J. (2009) Protein structure prediction on the Web: a case study using the Phyre server, *Nat Protoc 4*, 363-371.

59. Dube, P., DeCostanzo, A., and Konopka, J. B. (2000) Interaction between transmembrane domains five and six of the alpha -factor receptor, *J Biol Chem 275*, 26492-26499.

60. Choi, Y., and Konopka, J. B. (2006) Accessibility of cysteine residues substituted into the cytoplasmic regions of the alpha-factor receptor identifies the intracellular residues that are available for G protein interaction, *Biochemistry 45*, 15310-15317.

61. Lodowski, D. T., and Palczewski, K. (2009) Chemokine receptors and other G protein-coupled receptors, *Curr Opin HIV AIDS 4*, 88-95.

62. Youn, H., Koh, J., and Roberts, G. P. (2008) Two-state allosteric modeling suggests protein equilibrium as an integral component for cyclic AMP (cAMP) specificity in the cAMP receptor protein of Escherichia coli, *J Bacteriol 190*, 4532-4540.

63. Wess, J., Han, S. J., Kim, S. K., Jacobson, K. A., and Li, J. H. (2008) Conformational changes involved in G-protein-coupled-receptor activation, *Trends Pharmacol Sci 29*, 616-625.

64. Rosenbaum, D. M., Rasmussen, S. G., and Kobilka, B. K. (2009) The structure and function of G-protein-coupled receptors, *Nature 459*, 356-363.

PART VI

Activities of *Saccharomyces cerevisiae* α-factor Pheromone Receptor (Ste2p) and its G alpha protein (Gpa1p) fusion protein.

Part VI presents collaborative work with Dr. Fred Naider's laboratory at the City University of New York, Staten Island. George K. E. Umanah performed all the work. The pheromone peptides used were obtained from Dr. Naider's laboratory.

CHAPTER 1

Introduction

Many external stimuli such as hormones, neurotransmitters and pheromones exert their effects in cells through G-protein-coupled receptors (GPCRs) that activate heterotrimeric G-proteins leading to changes in the activity of effectors. The heteromeric G proteins are comprised of three subunits, α (alpha), β (beta) and γ (gamma). Following ligand binding to GPCRs, a cascade of events occur (*1, 2*). The receptor interacts with a GDP-bound, inactive Gα subunit, which switches to a state where the guanine nucleotide binding site is empty. GTP binds and activates the Gα subunit, causing dissociation of the α subunit from the ligand-occupied receptor and dissociation of the βγ subunits. The activated Gα subunit now interacts with specific effector proteins, which results in changes in intracellular signaling. The GTPase activity of the Gα subunit hydrolyzes GTP to GDP, resulting in conformational changes such that the subunit dissociates from the effector(s). The inactive GDP-bound Gα subunit now reassociates with the βγ subunits, and the cycle can be repeated if an appropriate agonist-occupied receptor is available (*6-11*).

In humans, GPCRs are encoded by about 900 genes, whereas the various Gα subunit proteins are encoded by less than 20 genes. However, within a given cells type, GPCRs are usually co-expressed with at least 7 different Gα protein subunits, each expressed to varying degrees. This has been a major setback in understanding activation of G proteins by a GPCR in the mammalian system, and for pharmacologists who wish to understand aspects of GPCR–G protein interaction selectivity (*1, 2, 12*). These challenges have been approached in most studies by co-expressing a specific G protein with its GPCR, and yet it remains impossible to insure that

the expression levels and cellular distribution of the individual G proteins are such that GPCR to G protein stoichiometry is constant for different pairings (*5, 12*).

One of the most successful approaches used to maintain constant GPCR to G protein stoichiometry is the generation of a GPCR-Gα fusion protein. The 1:1 stoichiometry imposed in fusion proteins has been a very useful tool for understanding GPCR-G protein interaction. GPCR-Gα fusions have been used to obtained information about ligand efficacy, intrinsic activity, kinetics of the receptor G-protein interaction, and the importance of post-translational acylation (*12-15*). The fusion proteins, in most cases, are constructed by direct fusion of the GPCR C-terminus to the N-terminus of Gα (*5, 12*), however, some are constructed with a linker between the two proteins and/or truncation of the C-terminus of the receptor. Most of these fusions have been shown to display wild type or constitutive activities (*12*).

The use of GPCR-Gα fusions to obtain crystal structures of GPCRs has recently been given some attention. Recent tricks used to achieve the stability and conformational homogeneity required for GPCR crystallization included the use of antibody complexes, fusion proteins, binding ligands, stabilizing mutants, and special crystallization environments (*16-24*). Although the crystal structures were resolved using these tricks, there were concerned about the disruption or deletion of receptor regions, such as the third intracellular loop, that are essential for receptor activity; raising the questions about how the complete, intact receptor interacts with its G protein and cognate ligand (*25*). The use of a fusion protein to obtain crystal structures of GPCRs will provide new information regarding the structure of an intact receptor, which will be an advancement over the recent structures obtained.

The yeast *Saccharomyces cerevisiae* uses GPCRs for signal transduction in a manner similar to that observed in mammalian systems. The interactions between the *S. cerevisiae* α-factor pheromone receptor, Ste2p, and its cognate Gα subunit, Gpa1p, have been shown in several studies to serve as a good model system for most GPCRs, (*26-30*). It has also been shown that the Ste2p and Gpa1p fusion protein was functional with respect to signal transduction. In addition, even a fusion between Ste2p and a chimeric yeast–mammalian Gα subunit was able to transduce signal efficiently (*31*). However, detail activities of Ste2p-Gpa1p fusion was not reported . The success of this construct in yeast demonstrated that Ste2p-Gpa1p fusion can serve as a tool to understand the interactions between these two proteins and will provide critical information regarding interactions that regulate protein activation and ligand binding.

In this study, different variants of fusion proteins between Ste2p and the Gpa1p have been successfully constructed and shown to transduce signals efficiently. These fusion proteins have biological activities similar to wild type Ste2p or Gpa1p and are capable of complementing the deletion of Ste2p and/or Gpa1p. The fused proteins can be separated using factorXa protease to cleave a site that links the two proteins. Truncation of the C-terminus of Ste2p that is not essential for signaling but for endocytosis (*32*) in the fusion construct increased both expression and activities of the fusion protein. The use of the fluorescent guanine nucleotide analog BODIPY guanosine 5 ′-*O*-thiotriphosphate (BODIPY-GTPγS) has been adapted for use in an assay that allow for GTPase activities of the fusion protein to be measured. This assay is based on the fact that the binding of BODIPY-GTPγS to Gα subunits, or any protein with GTPase activity, will yield increasing fluorescence signal making it possible to determine the GTP

binding activities of these proteins (*33-35*). Results indicate that this assay will be very useful in determining the activities of purified and reconstituted GPCR-Gα complexes. The fusion construct will be used to investigate Ste2p-Gpa1p interactions using approaches such as the incorporation Bpa (described in part 3 of this dissertation) for photoaffinity cross-linking, cysteine disulfide cross-linking (described in part 5 of this dissertation) and ultimately to obtain a crystal structure of the Ste2p-Gpa1p complex.

CHAPTER 2

Materials and Methods

Media, Reagents, Strains and Plasmids:

Saccharomyces cerevisiae strain LM102 [*MAT**a**, bar1, leu2, trp1, ura3, FUS1-lacZ::URA3, ste2*Δ (*3*)] was used for Step2 growth arrest and binding assays; TM5117 [*MAT**a**, bar1, leu2, his3, ura3, FUS1-lacZ::URA3, ste2*Δ*, gpa1*Δ (*3*)] was used for *Fus1-LacZ* activities and the protease deficient strain BJS21 [*MAT**a***, *prc1-407 prb1-1122 pep4-3 leu2 trp1 ura3-52 ste2::Kan*^{R} (*36*)] was used for protein isolation and immunoblot analysis. GTPγS, GDP and BODIPY-GTPγS were obtained from Molecular Probes (Eugene, OR). The *STE2-GPA1* fusion plasmids were co-transformed by the method of Geitz (*37*) into LM102, TM5117 and BJS21. The plasmid pBKY1 containing STE2 with the cysteine residues and two known glycosylation sites replaced (Cys59Ser, Cys252Ser, Asn25Ser and Asn32Glu) and epitope tag comprising codons encoding a 9 amino acid sequence of rhodopsin (Rho-tag) introduced at the C-terminal end of the receptor sequence (*4*) was used in this study.

Construction of fusion Ste2p-Gpa1p proteins:

The following primers shown on table 1 were used for the constructions of the fusion proteins. For that first fusion construct the open reading frame of GPA1 was PCR amplified from the plasmid YepGαβγ (*38*) and cloned into the plasmid pBKY1 using the BKG1 set of primers to yield the plasmid pBKG1 (refered to as wild type). The pBKY1 was digested with *EcoRI* restriction enzyme and purified from an agarose gel for in vivo ligation with the GPA1 PCR product using the transformation procedure described below.

Table 1: Names of plasmids constructed and used in this study.

Plasmid	Protein type and tags	Primer Sequences
pBEC1:	Ste2p-Flag/His [Constructed by Hauser et al (*3*)]	
pBKY1:	Ste2p-Rho [Constructed by(*4*)]	
*pBKG1:	Fusion (Ste2p-Rho-Gpa1p)	Forward : CAGGTTGCTCCCGCTGATAATAATAATTTAATGGGGTGTACAGTCAGTACGC
	(Template: pBKY1)	Reverse: ATCGATAAGCTTGATATCGAATTCTCATATAATACCAATTTTTTTAAGGTTTTGCTGG
STE2 N-terminal rhodopsin (Rho) tagged and C-terminal truncated Fusion proteins		
pBKGR1 :	Fusion (Rho-Ste2p-Rho-Gpa1p)	Forward : ACCGAGACCTCGCAGGTCGCGCCTGCGCCTTCATTGAGCAAT
	(Template: pBKG1)	Reverse: CGCAGGCGCGACCTGCGAGGTCTCGGTAGCCGCATCAGACAT
pBKGR-300 :	Fusion (Rho-Ste2p?300-Gpa1p)	Forward : CATCAATGTGGGCCACGGCTGCTAATATGGGGTGTACAGTGAGTACG
	(Template: pBKGR1)	Reverse: GTTTGCGTACTCACTGTACACCCCATATTAGCAGCCGTGGCCCACATTG
pBKGR-310 :	Fusion (Rho-Ste2p?310-Gpa1p)	Forward : GCATCCAAAACAAACACAATTACTTCAATGGGGTGTACAGTGAGTACG
	(Template: pBKGR1)	Reverse: GCGTACTCACTGTACACCCCATTGAAGTAATTGTGTTTGTTTTGGATGC
pBKGR-320 :	Fusion (Rho-Ste2p?320 -Gpa1p)	Forward : GACTTTACAACATCCACAGATAGGTTTTATATGGGGTGTACAGTGAGTAC
	(Template: pBKGR1)	Reverse: CGTACTCACTGTACACCCCATATAAAACCTATCTGTGGATGTTGTAAAGTC
Fusion proteins with FactorXa cleavage sites (Xa) and GPA1 C-terminal Rho or FLAG tagged		
pBKGX1:	Fusion (Ste2p-Rho-Xa-Gpa1p)	Forward : ATTGAAGGTAGAATTGAAGGTAGAATGGGGTGTACAGTGAGTACGC
	(Template: pBKG1)	Reverse: TCTACCTTCAATTCTACCTTCAATTAAATTATTATTATCAGCGGGAGC
pBKGXf1:	Fusion (Ste2p-Rho-Xa-Gpa1p-Flag)	Forward : GACTATAAGGACGACGACGACACCGATCTAATCATC
	(Template: pBKGX1)	Reverse: GTCGTCGTCGTCCTTATAGTCGACTGCACTCAATAC
pBKGXr1:	Fusion (Ste2p-Rho-Xa-Gpa1p-Rho)	Forward : ACCGAGACCTCGCAGGTCGCGCCTGCGACCGATCTAATCATC
	(Template: pBKGX1)	Reverse: CGCAGGCGCGACCTGCGAGGTCTCGGTGACTGCACTCAATAC
C-terminal GPA1 Rho or FLAG tagged		
*pBUG1:	Gpa1p	Forward: GTTTCGACGGATCTAGAACTAGTGGATCCATGGGGTGTACAGTGAGTACGCAAAC
	(Template: p424GPD)	Reverse: CGAGGTCGACGGTATCGATAAGCTTTCATATAATACCAATTTTTTTAAGGTTTTGC
pBUGf1:	Gpa1p-Flag	Forward : GACTATAAGGACGACGACGACACCGATCTAATCATC
	(Template: pBUG1)	Reverse: GTCGTCGTCGTCCTTATAGTCGACTGCACTCAATAC
pBUGr1:	Gpa1p-Rho	Forward : ACCGAGACCTCGCAGGTCGCGCCTGCGACCGATCTAATCATC
	(Template: pBUG1)	Reverse: CGCAGGCGCGACCTGCGAGGTCTCGGTGACTGCACTCAATAC

*The primers were used to amplify GPA1 from the plasmid YepGαβγ (*38*) and cloned into their templates by in vivo ligation.

The rhodopsin (TETSQVAPA) tag (Rho) was inserted between Ala5 and Pro6 of at the N-terminal of STE2 in the fusion construct to produce the plasmid, pBKGR1. This plasmid was used as the template for C-terminus truncated STE2 fusion plasmids, pBKG300, pBKG310, pBK320. FactorXa restriction sites were incorporated between the STE2 and GPA1 using the pBKG1 as template to yield the plasmid pBKGX1. Both FLAG (DYKDDDDK) and rhodopsin tags were inserted between residues Val457 and Thr458 of GPA1 in the pBUG1 and pBKGX1 plasmids to generate the plasmids pBUGf1 /pBUGr1 and pBKXf1/pBKXr1 respectively. All constructs except pBKG1 and pBUG1 were made by Dpn1 mediated site directed mutagenesis using the primers and templates listed on table 1. The mutated plasmids were amplify in *E. coli* and isolated for DNA sequencing to verify the mutations. The sequence of all constructs was verified by DNA sequence analysis completed by the molecular biology resource facility located on the campus of the University of Tennessee. Three primers (F1424: [GTATATAAAGACG-GTAGGTATTG] (*3*), STE2B: [GGGATTGCTACAGTTACCATG] and GPA1B: [CTAGTGG-ATCCATGGGGTGTACAGTGAG]) were used to sequence the fusion plasmids. The GPA1 plasmids were sequenced using two primers (F1424 and GPA1B). DNA sequencing results were analyzed using the Megalign Lasergene V8.0.2 by DNASTAR Inc. (Madison, WI). Mutagenic and sequencing primers were purchased from Invitrogen (Carlsbad, CA).

Transformation and cell growth:

For all transformation cells were cultured in selective media and grown to mid-log phase at 30^{o}C with shaking (200 rpm) overnight. The cells were treated with LiAc (lithium acetate) as previously described. Transformants were selected by growth on minimal medium (*39*) lacking

tryptophan (designated as MLT) to maintain selection for the plasmids. All media components were obtained from BD (Franklin Lakes, NJ) and were of the highest quality available.

Membrane extraction and Immunoblots:

BJS21 cells expressing S*TE2 and GPA1 mutant* constructs grown in their selective media were used to prepare total cell membranes isolated as previously described (*40*). Cells were harvested and lysed by agitation with glass beads in 700 µL of HEPES buffer (50 mM HEPES (pH 7.5), 150 mM NaCl) and the following concentrations of protease inhibitors: 1.0 mM leupeptin, 10 µM pepstatin A, and 5.0 mM phenylmethanesulfonyl fluoride. The lysate was cleared by centrifugation at 3000g for 2 minutes. The membrane fraction was harvested by centrifugation at 15000g for 30 minutes, and was then resuspended in the HEPES buffer with 20% glycerol. Protein concentration was determined by BioRad (BioRad, Hercules, CA) protein assay (*3*). For immunoblot analyses the membrane extract was solubilized in SDS sample buffer (BioRad, Hercules, CA) and 5 µg were fractioned by SDS-PAGE. Blots were probed with antibody directed against the N-terminal 60 amino acids of Ste2p [generously provided by J. Konopka (*32*)], FLAG and rhodopsin antibodies (Sigma/Aldrich Chemical, St. Louis, MO) to detect Ste2p/Gpa1p or an antibody directed against Gpa1p (Santa Cruz Biotechnology, Inc., CA). The signals generated were analyzed using Quantity One software (BioRad, Hercules, CA).

Growth Arrest Assays.

LM102 cells expressing the various fusion proteins or receptor alone were grown at 30 ºC in MLT, harvested, washed three times with water and resuspended at a final concentration of 5 x 10^6 cells/ml (*36*). Cells (1 ml) were combined with 3.5 ml agar noble (1.1 %) and poured as

a top agar lawn onto MLT medium agar plate. Filter disks (BD, Franklin Lakes, NJ) impregnated with α-factor pheromone (0.125 – 2.0 μg) were placed on the top agar. The plates were incubated at 30 ºC for 18 hours and then observed for clear halos around the discs. The diameter of halos around the discs were measured and analyzed by linear regression analysis using Prism software (GraphPad Software, San Diego, CA). The experiment was repeated at least three times and reported values represent the mean of these tests.

FUS1-LacZ Assays:

LM102 and TM5117 cells expressing the various fusion proteins or Ste2p alone were grown at 30 ºC in selective media, harvested, washed three times with fresh media and resuspended at a final concentration of 5 x 10^7 cells/ml. Cells (0.5 ml) were combined with α-factor pheromone (final concentration of 1 μM) and incubated at 30 ºC for 90 minutes. The cells were transferred to a 96-well flatbottom plate in triplicates, permeabilized with 0.5% Triton X-100 in 25 mM PIPE buffer and then β-galactosidase assays were carried out using fluorescein di-β-galactopyranoside (Molecular Probes, OR) as a substrate (*41*). The reaction mixtures were incubated at 37^{o}C for 60 minutes and 1.0 M Na_2CO_3 was added to stop the reaction. The absorbance of the samples at excitation of485nm and an emission of 530 nMwas determined using a 96-well plate reader Synergy2 (BioTek Instruments, Inc., Winooski, VT). The data were analyzed using Prism software (GraphPad Software, San Diego, CA). The experiment was repeated at least three times and reported values represent the mean of these tests.

Whole cell saturation Binding Assay:

This assay was performed using LM102 cells expressing expressing the fusion protein, BKG1 or receptor alone (BKY1). The cells were grown at 30 ºC in MLT, harvested, washed three times with YM1 [0.5 M potassium phosphate (pH 6.24) containing 10 mM TAME, 10 mM sodium azide, 10 mM potassium fluoride,and 1% BSA] and resuspended at a final concentration of 4×10^7 cells/ml in YM1i (YM1 plus potassium fluoride (1 mg/ml), *p*-toluene-sulfonyl-l-arginine methyl ester (3.8 mg/ml), NaN_3 (0.6 mg/ml), bovine serum albumin (5 mg/ml) and tosyl-lysine chloromethyl ketone (1 mg/ml). (*40*)]. Cells (600 µl) were combined with 150 µl of ice-cold 5× binding medium (YM1i supplemented with ^{3}H-labeled α-factor) and incubated on ice for 30 min. The final 1× concentrations of pheromone ranged from 0.8 to 100 nm. Upon completion of the incubation interval, 200-µl aliquots of the cell/pheromone mixture were collected in triplicate and washed over glass fiber filter mats using the Standard Cell Harvester (Skatron Instruments, Sterling, VA). Retained radioactivity on the filter was counted by liquid scintillation spectroscopy. LM102 cells lacking Ste2p, expressing only the empty vector (p424-GPD), were used as a nonspecific binding control for the assays. Specific binding for each mutant receptor was calculated by subtracting the nonspecific values from those obtained for total binding. Specific binding data were analyzed by nonlinear regression analysis for single-site binding using Prism software (GraphPad Software, San Diego, CA) to determine the B_{max} (receptors/cell) and Kd (binding affinity) values. (*42*).

FactorXa cleavage of fusion proteins:

The optimal conditions for factorXa activities were tested. The initial conditions were to test factorXa activities at 4 ^{o}C and room temperature at different incubation time. For the digestion, about 250 µg of membrane from BJS21 cells expressing fusion protein with factorXa cleavage sites (BKGXa) was resuspended in 250 µl 1X factorXa digesting buffer containing 5units of factorXa enzyme in two separate tubes. One of the tubes was incubated at 4 ^{o}C and the other at room temperature. About 40 µl of the mixtures were aliquoted into fresh eppendorf tubes containing 20 µl of 3X SDS-PAGE sample buffer at 0 mins, 30 mins, 1 hour, 2 hours, 4 hours and overnight (16 hours). The extent of digestion of the fusion protein by factorXa was analyzed by Western blot using antibodies against Ste2p and Gpa1p. To determine the optimum factorXa enzyme concentration, about 50 µg of membrane samples were resuspended in 40 µl 1X factorXa digesting buffer containing different concentrations (0, 0.015, 0.03, 0.06, 0.12, 0.25 and 0.50 Units) of factorXa enzyme. The reaction mixtures were incubated at 4^{o}C for 4 hours. About 20 µl of 3X SDS-PAGE sample buffer was added to each reaction mixture to stop the reaction and samples analyzed by immunoblot using antibodies against Ste2p and Gpa1p.

BODIPY assay for GTPase activities of fusion proteins:

BJS21 cells expressing Ste2p membranes were resuspended in MES buffer (20mM MES, 10mM $MgCl_2$, 2mM EDTA). To determine the time course for fluorescence signal membranes samples (with or without 2.5 µM GTP) were mixed with 25 µM BODIPY-GTPγS in the presence or absence of 0.1 µM α-factor. The fluorescence measurements was read every 5 minutes with shaking before reading using a CytoFluor 4000 fluorescence plate reader

(Biosystems, Inc., Framingham, MA) at excitation of 485 nm and emission of 530 nm (*33*). All experiments were done in opaque plastic 96-well plates at 25^{o} C. Fluorescence signal in different BODIPY-GTPγS (0.25-2.0 μM) and α-factor (1.0 -1000 nM) concentrations were tested. The effects of pH (6.0, 6.5, 7.0), NaCl (5.0-300mM), and GDP (0.5-400 μg/ml) were also investigated. The data were analyzed using Prism software (GraphPad Software, San Diego, CA). The experiments were done in triplicate and repeated at least three times and reported values represent the mean of these tests.

The effects of GTP and GDP on Ste2p binding in fusion proteins:

Membranes from BJS21 cells expressing the fusion proteins or Ste2p alone were extracted as described above. Membranes (700 ml) were resuspended at a final concentration of 0.25 mg/ml in YM1i containing 5.0 nM ^{3}H-labelled α-factors and incubated for 60 minutes at 4^{o} C in the presence of GTP-γ-S or GDP at different concentrations ($1x10^{-4}$ – $1x10^{-10}$ M). Upon completion of the incubation interval, 200-μl aliquots of the membrane mixture were collected in triplicate and washed over glass fiber filter mats using the Standard Cell Harvester (Skatron Instruments, Sterling, VA). Retained radioactivity on the filter was counted by liquid scintillation spectroscopy. Membrane from BJS21 cells lacking Ste2p, expressing only the empty vector (p424-GPD) was used as a nonspecific binding control for the assays. Specific binding for each mutant receptor was calculated by subtracting the nonspecific values from those obtained for total binding. Specific binding data were analyzed by nonlinear regression analysis for single-site binding using Prism software (GraphPad Software, San Diego, CA).

CHAPTER 3

Results

Plasmid Constructs:

The plasmids encoding the *STE2-GPA1* fusion and *GPA1* constructed in this study are shown below. These plasmids served as parental templates for site-directed mutagenesis which was used to generate the different constructs used in this study. Site directed mutagenesis was undertaken using a primer mediated PCR based protocol. This approach involves using primers synthesized to contain specific site-directed mutations (see Table 1) to replicate the parental plasmids, thus incorporating the mutation into the newly synthesized plasmid. For selection of mutagenized plasmids, the PCR reaction mixture (containing a mixture of parental and mutagenized plasmids) was digested with the restriction endonuclease, *Dpn*I (recognition target sequence: 5-Gm6ATC-3, where adenine residue is methylated) which selectively cuts the non-methylated parental plasmid. The mutant plasmid generated in vitro is not methylated. Thus, only the parental plasmid used as template in the mutagenesis reaction will be digested by *Dpn*I, leaving the PCR mutagenized plasmid intact (*43*). The *BamHI* and *EcoRI* digest of the plasmids showed the vector (~6.5 kb) in all plasmids (Figure 1). The fusion *STE2-GPA1* fragment (~2.9 kb) comprising of *STE2* (~1.35 kb) and *GPA1* (~1.45 kb) and differences in sizes of truncated fusion plasmids were also observed.

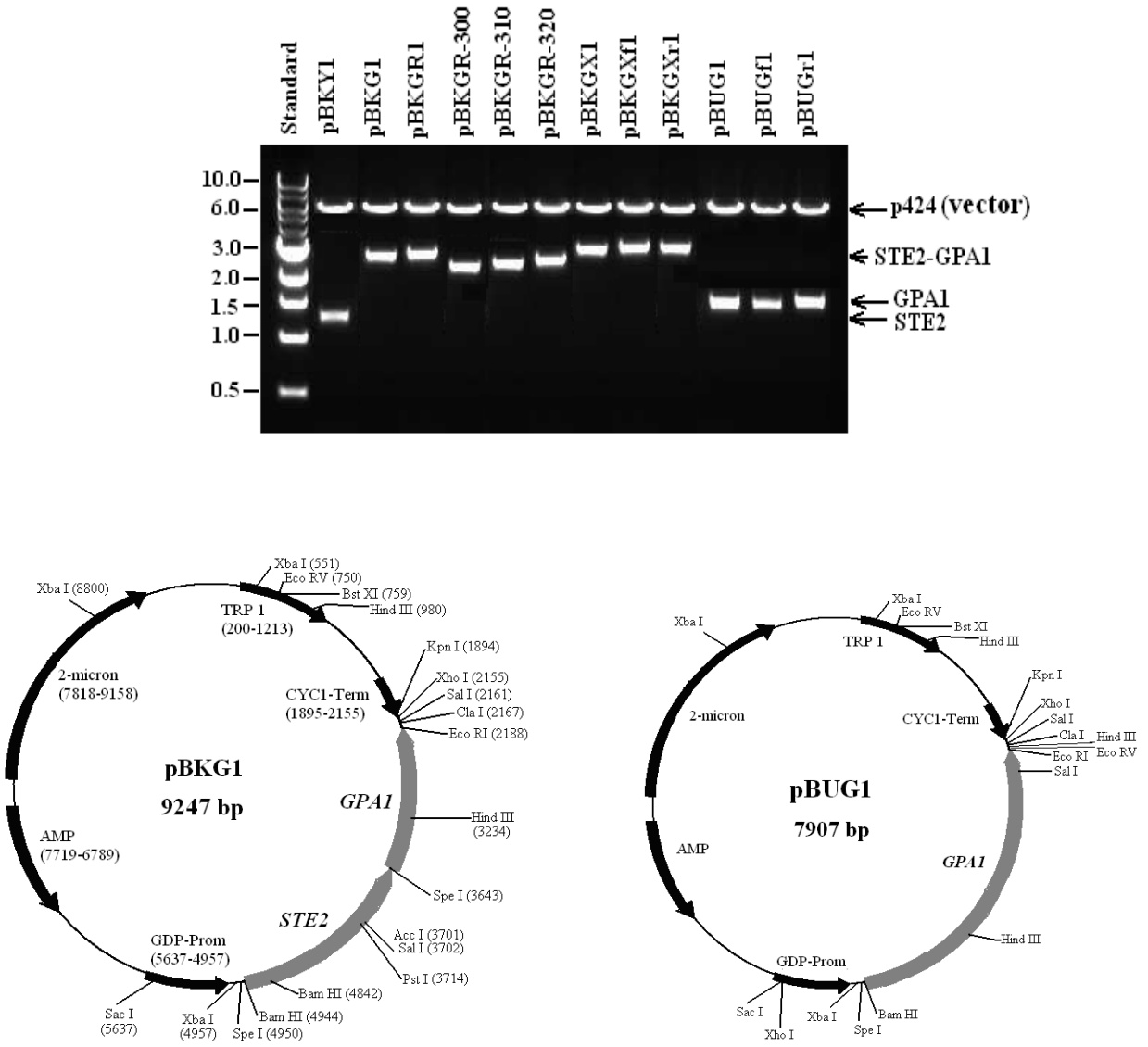

Figure 1: Agarose gel electrophoresis of the plasmids constructed in this study and maps of pBKG1 and pBUG1. All plasmids were digested with *BamH1* and *EcoRI* restriction enzymes from Biolabs Inc. (New England, Ipswich, MA). The vector fragment (~6.5 kb) was observed in all plasmids. The fusion STE2-GPA1 fragment (~2.9 kb) comprising of STE2 (~1.35 kb) and GPA1 (~1.45 kb). Differences in sizes of truncated fusion plasmids were also observed.

Expression of fusion protein:

To create a Ste2p-Gpa1p fusion protein the C-terminus of Ste2p was linked directly to the N-terminus of Gpa1p. To verify that the fusion protein was expressed, total membranes were isolated from BJS2, a proteases deficient yeast strain, expressing either the fusion protein (BKG1) or Ste2p (BKY1). Membranes from both strains were run on SDS-PAGE, immunoblotted, and probed with antibodies directed against Ste2p or Gpa1p. The Ste2p (BKY1) used in this study to create the Ste2p-Gpa1p fusion protein is Cys-less (C59S and C252S), lacks glycosylation sites (N25G and N32G), and contains a 9 amino acid rhodopsin epitope tag (rho-tag) introduced at the C-terminal end of the receptor. This version of Ste2p was observed on blots at the 48 kDa position (*4*). When membrane fractions containing Ste2p was resolved by SDS-PAGE a band corresponding to 48 kDa was observed on the anti-Ste2p blot, whereas a band of approximately 100 kDa was detected in samples containing the fusion protein (Figure 2A). The yeast Gpa1p was observed at the 52-54 kDa position (*44*). On the anti-Gpa1p blot a band at 52-54 kDa, corresponding to endogenous Gpa1p expressed in the BJS21 strain, was observed in all the lanes. A band of approximately 100 kDa was observed on an anti-Gpa1 immunoblot of membrane fraction containing the fusion Ste2p-Gpa1p protein, indicating that the high molecular weight band observed in the anti-Ste2p blot is indeed a signal from the fusion protein. The fusion protein was expressed at significantly reduced levels, ~50% compared to the non-glycosylated, Cys-less receptor as determined by quantitation of band density.

A: Expression of fusion (BKG1) & Ste2p (BKY1)

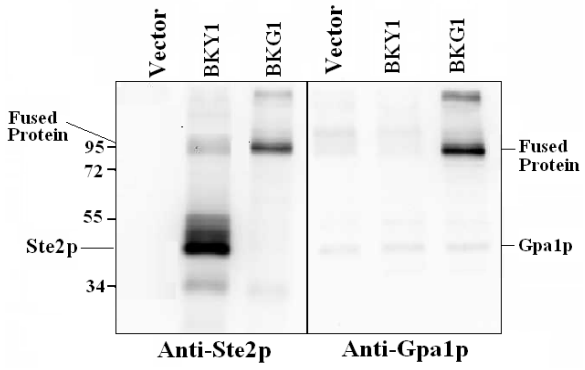

B: Growth arrest activities

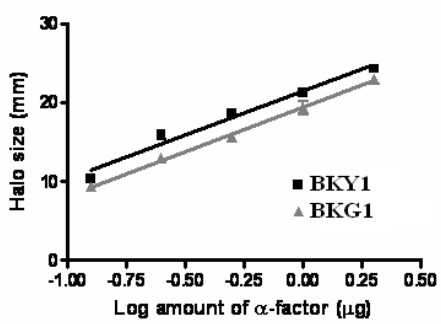

C: Pheromone induced *FUS1-LacZ* transcription

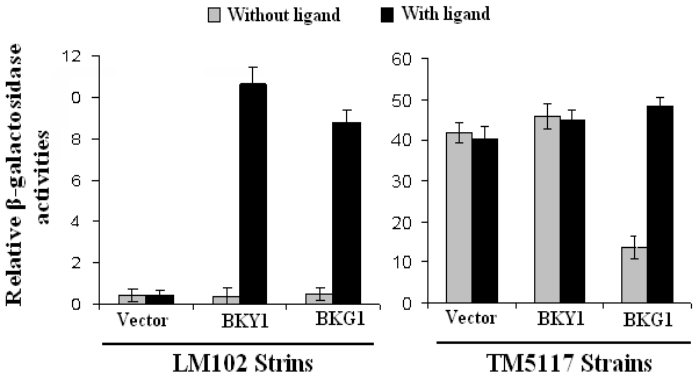

D: Pheromone binding activities

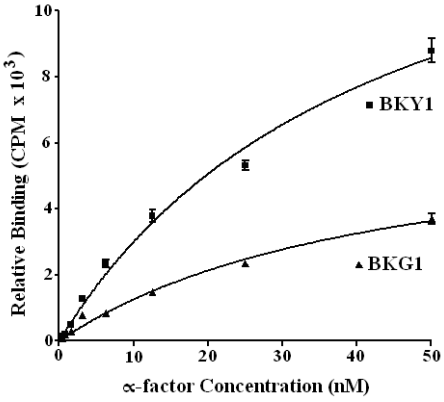

Figure 2: Biological activities of Ste2p-Gpa1p fusion protein. **A**: Images of blots showing the expression of the fusion protein (BKG1) and Ste2p (BKY1). A band at the ~100 kDa position corresponding to the fusion protein is observed on both the anti-Ste2p and anti-Gpa1p blots. About a 48 kDa band corresponding to Step was observed only in the anti-Ste2p blot, whereas a weak band corresponding to the endogenous Gpa1p expressed in the BJS21 cells was observed in all lanes on the anti-Gpa1p blot. **B:** A plot of halo sizes (pheromone induced growth arrest) around discs on lawn of cells. **C:** Pheromone induced β-galactosidase activities. **D:** The binding curves for fusion protein and Ste2p used to determine their binding affinity for α-factor.

Fusion protein complements Ste2p and Gpa1p deletion:

The functional activities of the fusion protein were examined by pheromone binding assay, α-factor induced cell cycle arrest (halo assay) and *FUS1*-LacZ reporter gene activity. Comparison of halo (zone of growth arrest) size demonstrated that the fusing of Gpa1p to the C-terminus of Ste2p did not compromise the fusion protein's ability to mediate growth arrest in response to α-factor (Figure 2B). The fusion protein showed about 90% of the control Ste2p growth arrest activities. One of the earliest responses of the yeast cell to pheromone is the transcription of the gene *FUS1*. The *FUS1* gene product is involved in the fusion of cells during conjugation. The strains (LM102 and TM5117) used in this study contain a reporter gene construct consisting of a fusion between *FUS1* promoter and the *lacZ* gene encoding the enzyme β-galactosidase (*45*). This allows for rapid, sensitive detection of mating pathway activation by assessing β-galactosidase activity in response to mating pheromone (*41*). The LM102 strain is Ste2p deficient but expresses endogenous Gpa1p, whereas the TM5117 strain is deficient in both Ste2p and Gpa1p. The absence of Gpa1p in the TM5117 strain results in high basal *FUS1-LacZ* activities since the free Gβγ subunits are constitutively active. Ordinarily, the Gα subunit (GDP-bound, inactive state) binds Gβγ and renders the subunits inactive. However in the presence an activated receptor, Gα exchanges bound GDP for GTP and the now active Gα-GTP subunit dissociates from Gβγ thus allowing these units to become active (*9*). Assessment of β-galactosidase (LacZ) activity in response to α-factor in LM102 cells indicated that the fusion protein induce the transcription of the *FUS1* gene at levels similar to Ste2p (Figure 2C). In the TM5177 strains the expression of the fusion protein was capable of reducing the Gβγ mediated β-galactosidase activity, and also responded to pheromone by increasing the activity. The

reduction of basal β-galactosidase activity in TM5117 implies that the fusion protein also interacts with the Gβγ protein subunits in the cell. Thus, the fusion protein was able to complement the deletion of both Ste2p and Gpa1p in the strains that were tested in this study.

Fusion protein has similar affinity for α-factor to that of Ste2p:

Although the immunoblot analysis (Figure 2A) showed that the fusion protein was expressed in the total membrane fraction, information about the cell surface expression could not be determined from this analysis. Cell surface expression was examined using LM102 in a whole cell saturation binding assay to measure the *Bmax* (receptors/cell) and *Kd* (ligand binding affinity) values (Figure 2D). Previous studies indicated that the control Ste2p used in this study has a binding affinity (~ 13 nM) similar to that of wild type Ste2p (*4*). The *Kd* value measured for the fusion protein was 14.5 nM compared to 13.8 nM for the control Ste2p used in this study. The *Bmax* values that indicate the number of receptor molecules per cell was 37,600 for control Ste2p compared to 16,000 fusion protein receptors per cell. Though the surface expression level of the fusion protein is about 50% that of Ste2p both proteins have similar affinity for the ligand, α-factor as determined by the *Kd* values.

Expression and activities of Fusion protein containing factorXa:

Some of the approaches that will be used in the fusion protein to determine the interactions between Ste2p and Gpa1p include cross-linking via disulfide bond formation or photoaffinity covalent linkage using Bpa. In order to identify if a cross-link formed between Ste2p and Gpa1p in the fusion protein, two factorXa protease sites (IEGRIEGR) were inserted

between the two proteins to generate the BKGX1 construct. This fusion protein is expressed and has functional activities similar (see Figure 3A-C) to the wild type fusion protein (BKG1). Both proteins have a *Kd* value of about 15 nM. Experiments were conducted to determine the optimum conditions for factorXa digestion of the Ste2p-Gpa1p fusion protein. The effects of temperature and incubation time were examined by treating membrane samples containing the fusion protein with 0.1 units of factorXa protease at 4 ^{o}C and at room temperature. Aliquots of the reaction mixtures were transferred into fresh eppendorf tubes containing 3X SDS-PAGE sample buffer at 30 min, 1 hour, 2 hours, 4 hours and overnight (16 hours). The extent of cleavage of the fusion protein by factorXa digestion was analyzed by immunoblotting using antibodies against Ste2p and Gpa1p (Figure 3D). The appearance of a Ste2p band on the anti-Step blot and a Gpa1p band on the anti-Gpa1p blot in fusion protein samples treated with factorXa indicate that the protease was capable of cutting the fusion protein into two separate proteins. The results showed that treatment at 4 ^{o}C was better than at room temperature and that 4 hours of incubation was sufficient enough to cleave most of the proteins. Shorter periods of incubation (30 mins and 1 hour) were not sufficient for adequate cleavage, whereas longer periods (overnight, 16 hours) resulted in degradation of the proteins as a result of non-specific digestion.

The enzyme concentration required for optimum cleavage was also examined. The results showed that 0.5 unit of the factorXa enzyme was sufficient to digest most of the fusion protein present in 50 μg of membrane (Figure 3E).

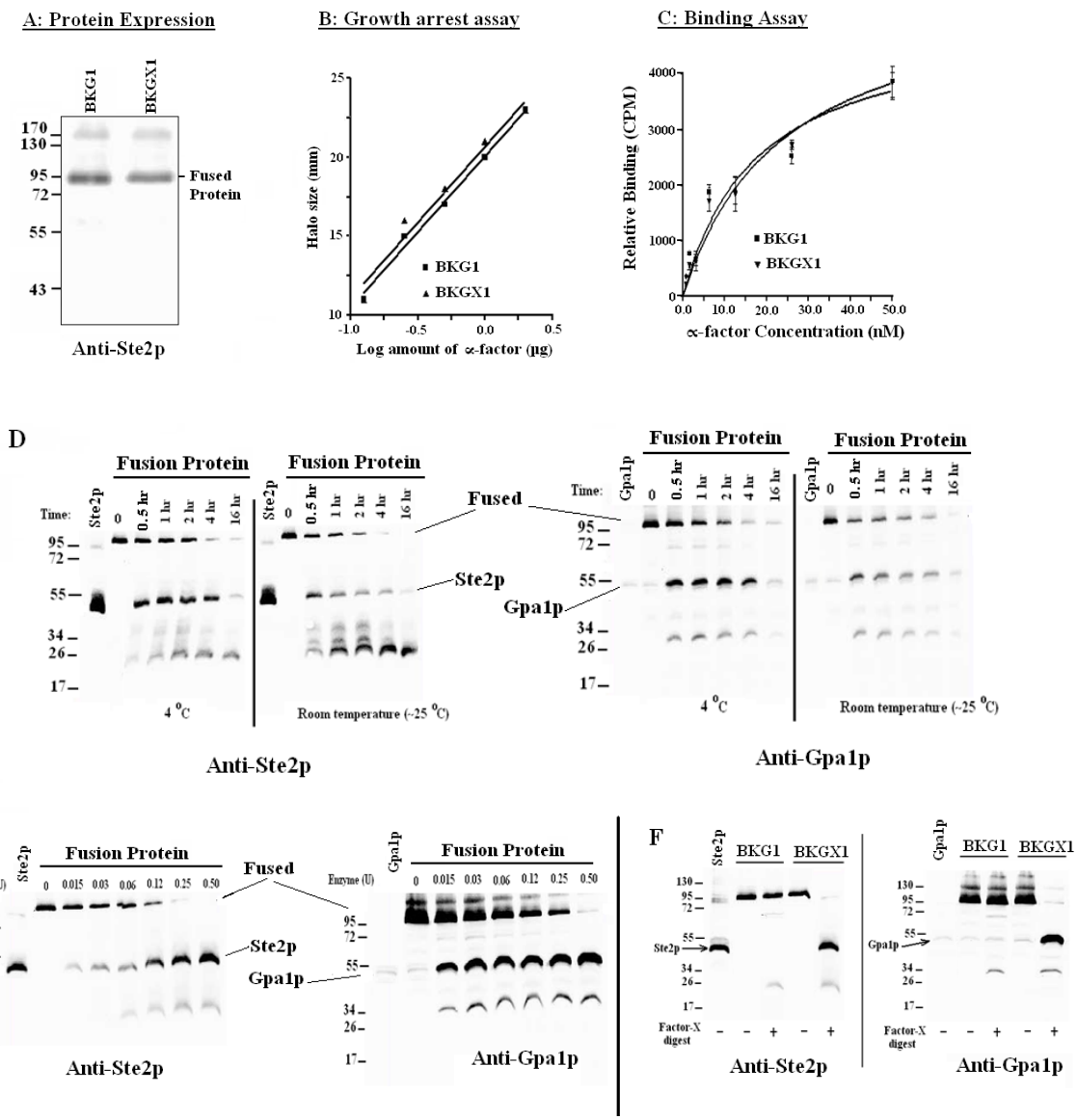

Figure 3: Activities of fusion protein with factorXa site.. **A**: Images of blots showing the expression of the fusion protein with factorXa site (BKGX1). **B:** A plot for growth arrest. **C:** The binding curves for BKG1 (wild type) and BKGX1. **D-E:** Blot images showing results for optimizing temperature, incubation time and enzyme concentrations for factorXa digest of fusion protein. **F:** Blot images showing example of results of digested fusion protein using the optimum conditions determined in this study for the factorXa.

Based on these results the protocol for factorXa digestion of the fusion protein in typical cross-linking studies was standardized to include 50 µg of membrane proteins suspended in 40 µl 1X factorXa buffer containing 0.5 units of factorXa enzyme and then incubated at 4 ^{o}C for 4 hours. Approximately 20 µl of 3 X SDS-PAGE sample buffer is added to stop the reaction, and the resulting product is analyzed by immunoblotting using antibodies against both Ste2p and Gpa1p. An example of the results of this protocol is shown in Figure 3F using a fusion protein without factorXa as a control. Thus Ste2p and Gpa1p in the fusion protein can be separated by factorXa enzymatic cleavage.

Phenotypes of N-terminal tagged and C-terminal truncated Ste2p fusion protein:

One of the reasons for constructing the fusion protein is to obtain a Ste2p-G protein complex that will stable for X-ray crystallographic studies. These studies require the use of a large quantity of purified protein. The low level of Ste2p-Gpa1p fusion protein expression is a major concern if this protein will be used for such studies. To improve on the expression levels we truncated part of the C-terminal region of Ste2p that has been identified to be essential for endocytosis of the receptor (*46, 47*). The rhodopsin epitope tag (TETSQVAPA) was inserted between residues Ala5 and Pro6 of Ste2p for detection and affinity purification resulting in the creation of the BKGR1 protein. This BKGR1 was used as the template for C-terminal truncation of Ste2p. Three different truncations were constructed, BKGR-300 (last 131 residues of Ste2p deleted at position Asn300), BKGR-310 (last 121 residues deleted at position Ser310) and BKGR-320 (last 111 residues deleted at position Tyr320). The N-terminal tagged fusion protein (BKGR1) was expressed at levels similar to the wild type protein (BKG1) as shown in figure 4A.

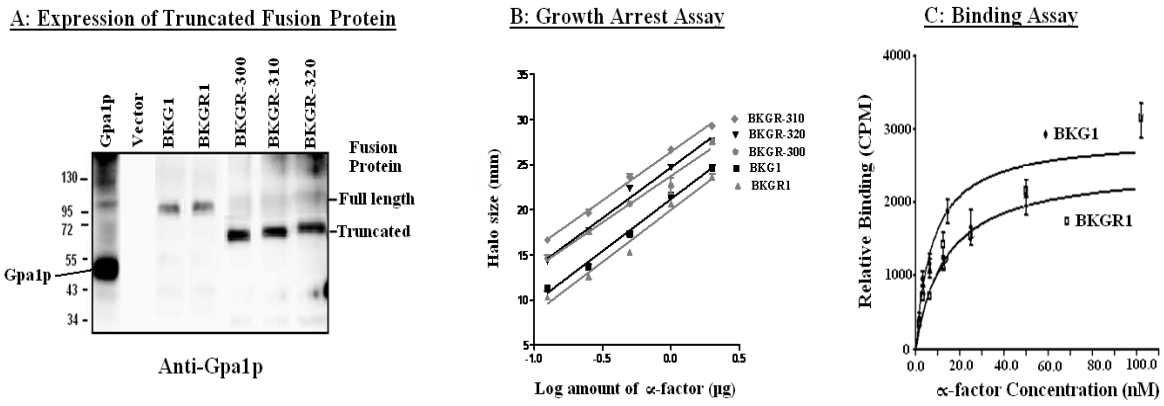

Figure 4: Activities of truncated fusion proteins. **A**: Blots images of wild type (full length) and truncated fusion and Gpa1p as control. The samples were probed with anti-Gpa1p antibody. **B**: A plot of the sizes of halos formed as a result of cell cycle arrest in cells responds to pheromone, α-factor. **C**: The binding curves to measure the binding affinity of the Step N-terminal tagged fusion protein (BKGR1).

However, both growth arrest and ligand binding results indicated that the N-terminal tagged fusion protein was slightly less active than the wild type fusion protein. The binding affinity of BKGR1 was determined to be 18 nM (Figure 4C). These results imply that N-terminal tagging of Ste2p did not significantly affect the activities of the fusion protein. The immunoblot analysis revealed three bands at about the 87, 88 and 89 kDa positions in lanes of membrane samples containing Ste2p-C-terminal truncated fusion proteins, BKGR-300, BKGR-310 and BKGR-320 respectively (Figure 4A) verifying that the proteins were indeed truncated. All of the truncated mutants had increased expression levels and growth arrest activities compared to the full-length fusion proteins. The BKGR-310 protein was approximately 2-fold more active in the growth arrest assay than the non-truncated fusion proteins.

Activities of C-terminal tagged Gpa1p fusion proteins:

The wild type fusion protein (BKG1) constructed in this study had only one epitope tag (rhodopsin tag) located at the extreme C-terminus of Ste2p. Gpa1p fusion to Ste2p reduced accessibility of antibody to the epitope tag, making it difficult to detect the fusion protein on blots. The Ste2p N-terminal Rho-tagged fusion protein (BKGR1 described above) is one of the alternative solutions to this problem. Another alternative is to insert an epitope tag at the C-terminal portion of Gpa1p for both detection and purification purposes. Both Rho (TETSQVAPA) and FLAG (DYKDDDDK) epitope tags were inserted between residues Val457 and Thr458 of Gpa1p using the wild type plasmids pBKG1 (fusion protein) and pBUG1 (Gpa1p) to generate the plasmids pBKGr1 (fusion-Rho)/pBKGf1 (fusion-Flag) and pBUGr1 (Gpa1p-Rho)/pBUGf1 (Gpa1p-Flag) respectively (Figure 5). The proteins were expressed in BJS21 cells and membranes were extracted for immunoblot analyses. The immunoblot analyses (Figure 5A) show that all proteins were expressed except for those with the Rho tag (BKGr1 and BUGr1). The DNA sequences of these plasmids were checked again. The sequence results showed there was no other mutation apart from the Rho tag inserted. To check if these proteins were expressed at very low levels, the amount of membrane protein loaded on the gel was increased by 10-fold, but a signal was not observed (data not shown). In addition TM5117 cells expressing these proteins did not display any activity (Figure 5C) indicating that the inclusion of the Rho tag was not tolerated by these mutants. In contrast the insertion of the FLAG epitope tag at the same position did not affect the activities of either the fusion protein (BKGf1) or Gpa1p alone (BUGf1). The biological activities showed that BKGf1 had similar binding (Kd value of 16 nM) and cell cycle arrest activities to that of the wild type fusion protein (BKG1).

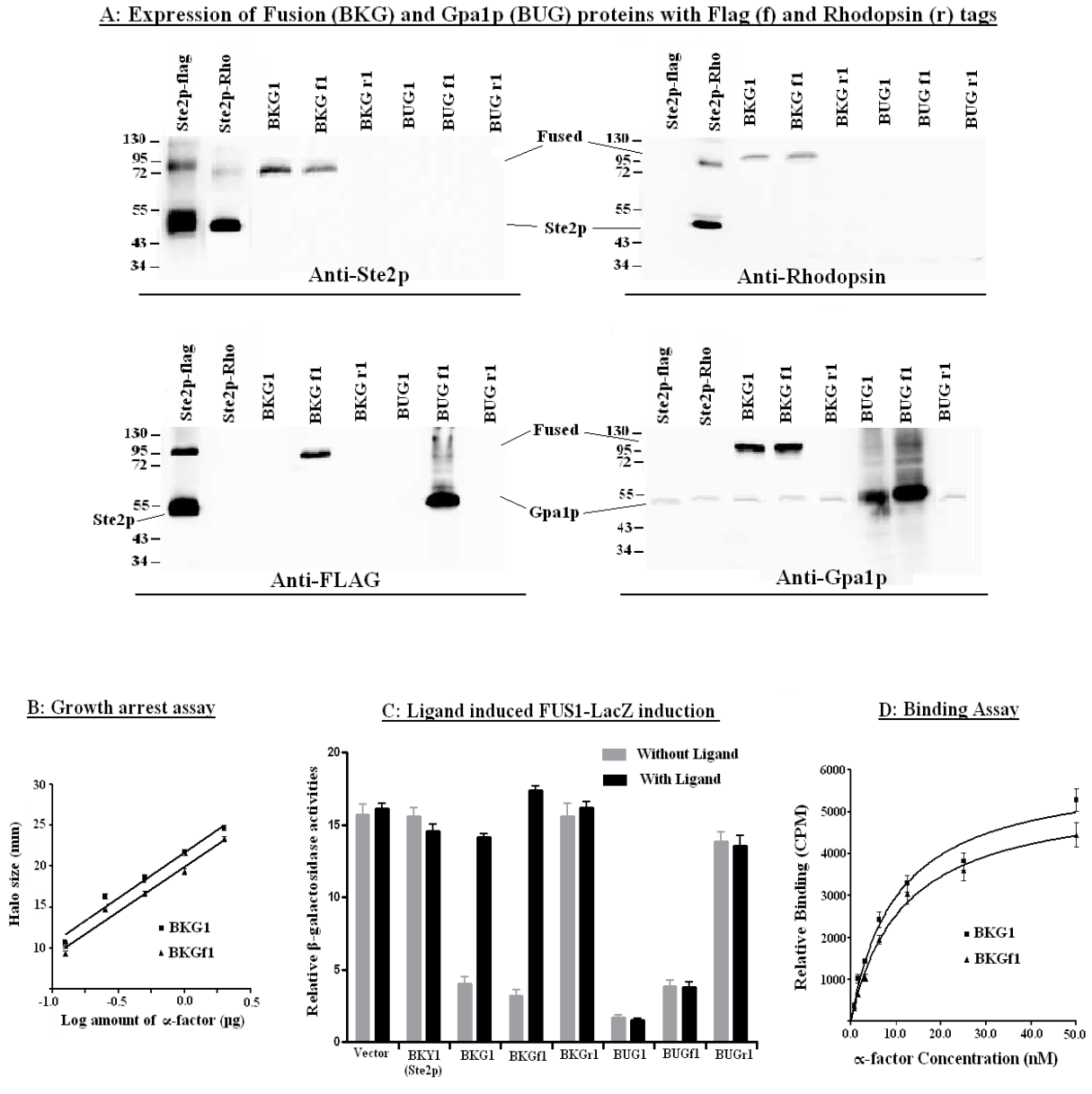

Figure 5: Activities of C-terminal tagged Gpa1p in fusion protein. **A**: Images of blots showing the expression of the fusion protein (BKG) and Gpa1p (BUG) with FLAG (f) or Rho (r) tags. **B:** A plot of pheromone induced halo (growth arrest). **C:** Pheromone induced β-galactosidase activities. **D:** The binding curves for wild type fusion protein (BKG1) and fusion protein with FLAG tagged at the C-terminal of Gpa1p (BKGf1).

BODIPY assay for GTPase activities of Ste2p-Gpa1p Fusion protein:

To determine whether the fusing of Gpa1p to Ste2p affects its ability to bind GTP, a GTPase fluorescence assay that depends on GTP binding (*33-35*) was adapted and modified for this study. This method uses BODIPY guanosine 5′-*O*-thiotriphosphate (BODIPY-GTPγS, referred to as BODIPY in this study) as a probe for GTPase activity. It has been shown that the interaction of GTPase with BODIPY results in increased fluorescence signal corresponding to GTP binding (*35*). This property of BODIPY was exploited to design an assay for determining the GTPase activities of the fusion protein. For preliminary studies membrane extracted from BJS21 expressing Ste2p and endogenous Gpa1p was used. It was proposed that when Ste2p and Gpa1p are in the membrane, binding of α-factor to Ste2p will induce activation of Gpa1p leading to an increased affinity for GTP. Thus in the presence of α-factor the binding of BODIPY to Gpa1p is expected to increase fluorescence signal. However, initial studies showed that although GTP (1 μM) was able to reduce BODIPY (5 μM) signal, the presence of the α-factor pheromone (1 μM) caused reduction rather than enhancement of fluorescence signal (Figure 6A). We tested whether α-factor had any quenching effects on fluorescence signal by mixing different concentrations of α-factor and BODIPY without membrane (Figure 6B). The results indicated that fluorescence signal is reduced in the presence of α-factor (as low as 1 nM) even in the absence of membrane. The most drastic reduction was seen in the presence of pheromone concentrations of more than 10 nM. For subsequent studies 10 nM α-factor and 0.5 μM BODIPY was used. The effect of pH was also determined by testing pH 6.0, 6.5 and 7.0 using BJS21 membranes containing Ste2p and Gpa1p. The results suggest that ligand induced increase in fluorescence at pH 7.0 was better than pH 6.0 or 6.5.

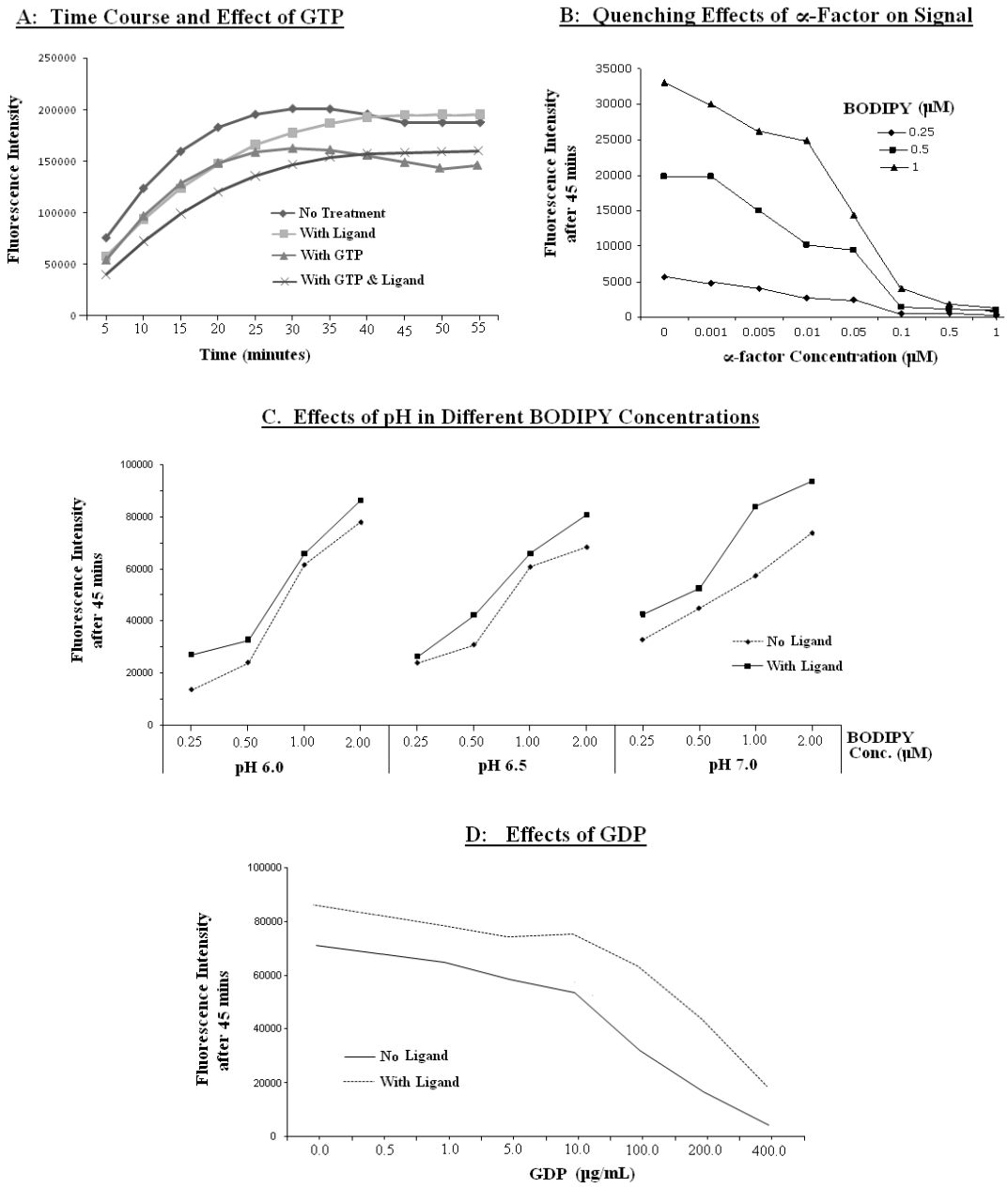

Figure 6: Optimizing condition for BODIPY-GTP assay. A: Time course curves showing the effects of GTP. **B:** a plot of different concentrations of α-factor showing the signal quenching effects of the pheromone. **C:** a graph of different pH conditions and BODIPY concentrations in the presence and absence of ligand. **D:** Curves showing the effects of different concentrations of GDP on fluorescence signal.

The concern of the BODIPY binding to any protein with GTPase activity other than Gpa1p was addressed by adding GDP to the mixture to occupy all guanine nucleotide binding sites in GTPase-like proteins. The effects of GDP on fluorescence signal in the presence and absence of pheromone were examined (Figure 6D) by mixing membranes with GDP and incubating for 15 minutes at 4^{o}C before adding α-factor and BODIPY. GDP at concentrations between 10 – 100 μg/mL reduced non-specificity of the BODIPY binding and also displayed increased fluorescence signal upon α-factor binding to Ste2p. Based on these results it was determined that a typical BODIPY assay should involve 20 mg membrane proteins resuspended in 90 μl of HEPES or MES buffer at pH 7.0 containing, 10 mM $MgCl_2$, and 10 μg/mL of GDP. The mixture is incubated for 15 minutes at 4^{o}C before adding α-factor (10 nM) and BODIPY (1.0 μM). To eliminate background (non-specific) signals, a parallel set of reactions is carried out in membranes in the absence of Ste2p, Gpa1p, or fusion proteins. The fluorescence signals of the background are subtracted from that of the test samples and the differences are plotted.

GTP and GDP binding to Gpa1p in the fusion protein affect Ste2p affinity for α-factor:

The GTPase activity of the wild type fusion protein (BKG1) expressed in BJS21 cells were examined using the BODIPY assay designed in this study. The results shown in figure 7 indicate that BJS21 (expressing endogenous Gpa1p) membranes containing the Ste2p-Gpa1p fusion protein displayed a higher increased in fluorescence signal compared to membranes containing control Ste2p. The membrane sample containing the fusion protein also had high basal fluorescence due to the high level of Gpa1p (fusion) present compared to the low level of endogenous Gpa1p present in all the membrane samples.

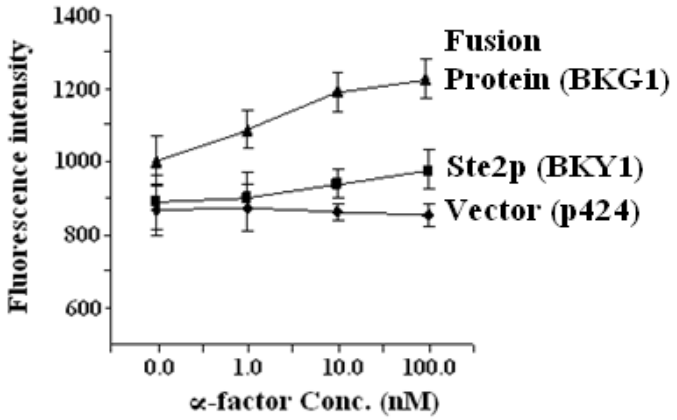

Figure 7: GTPase activities of fusion protein. The fluorescence signal of membranes extracted from BJS21 cells expressing wild type fusion protein (BKG1), Ste2p (BKY1) or empty vector (p424) using the BODIPY assay optimum conditions determined in this study. The fusion protein showed better response to α-factor than Ste2p.

These results indicate that the BODIPY assay can be used to determine GTPase activity of the fusion protein, and it will be very useful for studies of GTPase activity in purified samples. Ligand binding to a GPCR results in reduction in the affinity of GDP bound to the Gα protein, and an increase in its affinity for binding to GTP. It has been shown that increasing concentrations of GDP reduce the binding affinity of ligand for the GPCR (*14*). The binding affinity of the wild type fusion protein in the presence of increasing concentrations of GDP was examined using BJS21 membranes containing Ste2p or the fusion proteins. The membrane samples (also contain endogenous Gpa1p expressed by the BJS21 cells) were incubated with different concentrations of GDP for 20 minutes before adding 10 nM ^{3}Hα-factor to each reaction mixture for another 30 minutes of incubation at 4^{o}C. The membranes were washed (see materials and methods for details) to get rid of unbound ^{3}Hα-factor and then the amount of ^{3}Hα-

factor associated with the membrane were counted by counting ^{3}H. For background membranes transformed with empty plasmids were treated in similar manner. The ^{3}H count of the background was substrated from the counts of the control Ste2p and fusion protein samples to obtain specific binding counts. The specific counts were plotted as percentage (using samples with no GDP as 100%) against the different concentrations of GDP. The % $^{3}H\alpha$-factor binding results (Figure 8 A) suggest that increasing concentrations of GDP leads to a reduction in the affinity of Ste2p for α-factor in both the control Ste2p and the fusion protein. However, the fusion was more sensitive to the GDP effects than the control Ste2p. Thus, whereas $1x10^{-4}$ M of GDP reduced the binding affinity in the control Ste2p by 50% only $1x10^{-8}$M of GDP was required to cause similar effect in the fusion proteins. When GDP was added to membranes after $^{3}H\alpha$-factor binding no significant reduction in receptor affinity for α-factor was observed (Figure 8A).

The effect on the Ste2p-α-factor interaction caused by GTP binding to Gpa1p was also examined by conducting the fusion binding to 10 nM $^{3}H\alpha$-factor in the presence of increasing concentrations of GTPγS. The results (Figure 8B) suggest that increasing the concentration of GTP led to decreased affinity of Ste2p for α-factor, and similar results were obtained whether the GTP was added before or after $^{3}H\alpha$-factor binding. GTP treatement reduced α-factor binding was by about 65% in fusion protein. While only about a 40% reduction was observed in Ste2p membrane samples. Again the fusion was observed to be more sensitive to GTP than the Ste2p as observed for the effects of GDP. Thus, whereas $1x10^{-5}$ M of GTP reduced the binding affinity in the control Ste2p by 40% only $1x10^{-8}$M of GTP was required for similar effect..

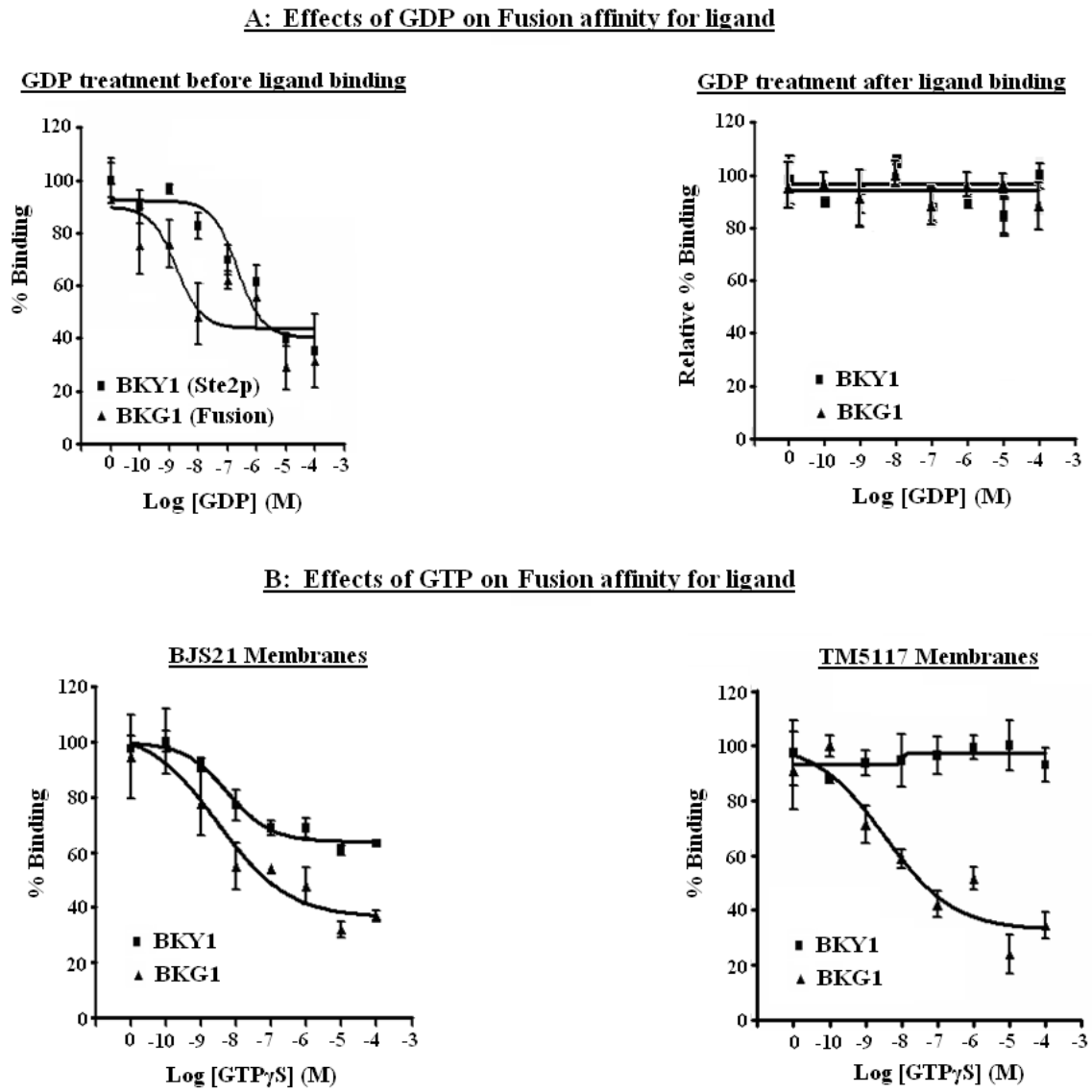

Figure 8: GDP/GTP effects on α-factor binding to fusion. A: Binding curves of membranes extracted from BJS21 (expresses Gpa1p) cells expressing fusion (BKG1) or Ste2p (BKY1) proteins. The binding affinities of the proteins were measured before or after GDP treatment at different concentrations. B: Binding curves of membranes from BJS21 and TM5117 expressing the fusion and Ste2p proteins. The binding was conducted in the presence of varying amount of GTPγS.

Since the BJS21 strained used for these assays also expresses Gpa1p, it was possible that the effect of GDP/GTP binding might be mediated by this endogenous Gpa1p, rather than the Gpa1p physically fused to Ste2p in the fusion protein. To investigate this, the effect of GTP on receptor-ligand affinity was tested using membranes from the strain TM5117 (both Step and Gpa1p deleted) expressing either fusion or control Ste2p proteins. While the fusion protein affinity for α-factor was reduced by the presence of increasing GTP concentration there was no significant changes in the Ste2p affinity (Figure 8B). These results imply that the Gpa1p in the fusion protein binds to GDP or GTP and this affects the interactions of Ste2p with α-factor in a manner similar to when the two proteins are expressed separately.

CHAPTER 4

Discussion

Although crystal structures for four GPCRs have been obtained, there are no structures for physiologically active GPCR-Gα complexes and details of the signal transduction mechanisms employed by GPCRs remains unclear (*25*). Signaling in the GPCR transduction cycle involve complexes of the receptors with other proteins including other GPCRs (dimer formation) and its cognate G proteins. The use of GPCR fusions to understand the complex interactions between the receptor and its Gα subunit has become very popular since such fusion proteins provide a defined 1:1 stoichiometry of GPCR to Gα. In this manner, bias in the analysis of ligand potencies and efficacies caused by varying ratios of receptor to G proteins can be eliminated. This approach has been very useful in providing information about ligands and G protein interactions with GPCRs (*5, 12, 14, 25*). Recently the crystal structure of opsin in its transducin C-terminus bound form and the various tricks used to obtained crystal structures of GPCRs indicate that GPCR complexes purified as conformationally homogeneous species may be more stable than monomeric receptors, hence more suitable for crystallization (*23, 25, 48*). Thus, the use of fusions proteins, such as GPCR-Gα, should enhance stability and prove very useful for crystallographic and other biophysical studies. This part of the dissertation describes the expression and activities of different variants of the yeast GPCR Ste2p fused to its cognate Gα, Gpa1p. Although, the Ste2p-Gpa1p fusion protein has been reported earlier (*31*), the authors did not carry out detailed characterization of this fusion protein. The study only reported mating, growth arrest and *FUS1-LacZ* activities of the Ste2p-Gpa1p fusion protein that lacks the last 60

amino acids of Ste2p. In this report detailed activities of full length and truncated Ste2p-Gpa1p fusion proteins are discussed.

Analysis of the expression of the full length Ste2p-Gpa1p fusion indicates that the protein is expressed at 50% of the level of Ste2p. This reduced expression may be due to a low rate of folding or trafficking of the large fusion protein to the membrane, compared to the trafficking of the smaller, separate proteins. The ability of the Ste2p-Gpa1p fusion protein to function as a Gα subunit, and also as a receptor was addressed by expressing the protein in yeast cells devoid of Ste2p and/or Gpa1p. The functionality of the fusion as a receptor was first examined by expressing the fusion protein in cells devoid of Ste2p. Pheromone induced cell cycle arrest and *FUS1-LacZ* activities all indicated the fusion can complement the deletion of Ste2p. Though the Bmax value indictaed that the fusion is expressed at the cell surface at only 50% of the Ste2p level, it has a binding affinity (~14 nM) similar to that of the WT receptor. This implies that the direct attachment of Gpa1p to Ste2p did not alter its ability to function as a receptor and that it still maintains wild type activities as indicated by the biological assay.. The functionality of the fusion as a Gα protein was also examined by determining the activities in Ste2p and Gpa1p deleted strain (TM5117). The deletion of Gpa1p results high basal *FUS1-LacZ* activities in TM5117 because the free Gβγ subunits are constitutively active. When bound, the Gα subunit (GDP-state) renders the Gβγ subunits inactive. However in the presence of an activated receptor, Gα-GDP exchanges GDP for GTP and the active Gα-GTP subunit dissociates from Gβγ thus allowing these units to become active. The subsequent hydrolysis of GTP to GDP makes the Gα-GDP subunit available for another cycle (*9*). Expression of the fusion protein in TM5117 showed that this protein could interact with the endogenous Gβγ subunits leading to reduced

basal *FUS1-LacZ* activities (Figure 2C). However, in the presence of ligand, the *FUS1-LacZ* activities increased, implying that Gpa1p in the fusion was able to couple with the Ste2p (directly attached) and the Gβγ subunits.

Further analysis of Gpa1p in the fusion indicate that it still binds effectively to GTP and GDP, and that these interactions with GTP and GDP affect Ste2p binding with α-factor, as observed in other GPCRs (*14, 49*). The high GTPase activities (BODIPY assay) of the fusion observed in response to α-factor also show that the coupling between Ste2p and Gpa1p proteins is not affected. Although the BODIPY assay was able to measure the GTPase activities of the fusion protein, the assay still needs to be further refined. For instance, the quenching effects of the pheromone may be a setback for fusion or Gpa1p mutants that require high pheromone concentration to trigger a detectable biological response. Nevertheless, the results obtained from this assay indicate that it is very promising for determining the GTPase activities of purified proteins. In the presence of GTP, a 65% reduction of binding was observed in the fusion protein compared to 40% when the two proteins were expressed independently. The high sensitivity of the fusion protein to the effects of GDP or GTP can be attributed to the fact that the fusion provide 1:1 stoichiometry of Ste2p to Gpa1p; hence all ligand-bound-Ste2p in the fusion will be associated with a Gpa1p that will alter the binding affinity if the Gpa1p is bound to a GDP or GTP whereas not all ligand-bound-Ste2p is associated with Gpa1p in the control sample. Thus, results from biochemical studies of GPCRs interactions with G proteins are most likely to be more precise using fusion proteins than the separate proteins.

One of the reasons for constructing the Ste2p-Gpa1p fusion was to use the protein for cross-linking studies between the two proteins. To do this, two factorXa protease sites

(IEGRIEGR) were inserted between the two proteins. The fusion protein containing the factorXa site displayed functional activities identical to the wild type fusion. A factorXa digestion protocol, developed for this study, was used to analyze both the wild type and the factorXa-mutant fusions. The results indicated that the factorXa fusion mutant can be separated by enzymatic cleavage using the factorXa enzyme. The disappearance of the fusion band and the appearance of bands of equivalent intensity at the Ste2p and Gpa1p positions on the immunoblots indicate that almost all the fusion were completely separated into Ste2p and Gpa1p. This enzymatic cleavage of the fusion protein proved to be very successful and reliable. Thus, covalent interactions or cross-linking between Ste2p and Gpa1p in the fusion can be assessed using this methodology. In this approach, when a covalent bond is formed by chemical cross-linking between residues of Step and Gpa1p, the two proteins will still be attached via the covalent bond even after digestion of the complex with factorXa. However, in the absence of a covalent bond the two proteins will run as separate entities on SDS-PAGE following factorXa digestion. This technique will be very useful in identifying residue to residue interactions between the two proteins.

The Ste2p-Gpa1p fusion was also constructed for crystallographic and other biophysical studies that will provide structure-function information. These studies require the use of a large quantity of purified protein. The fusion protein in this study is expressed at levels about 50% of that observed for Ste2p. To improve the expression level of the fusion protein, parts of the C-terminal region of Ste2p that have been suggested to be essential for down-regulation by endocytosis were truncated. Although, the N-terminus of Ste2p has been implicated to be essential for activity of the receptor (*50, 51*), a Rho (TETSQVAPA) epitope tag inserted between

Ala5 and Pro6 of Ste2p in the fusion protein (also in all truncated mutants) did not significantly affect its activity. Three different truncations created by deleting the last 131 (Gpa1p attached to Asn300), 121 (Gpa1p attached to Ser310) or 111 (Gpa1p attached to Tyr320) residues of Ste2p displayed better expression and function (about 2-fold activities) than the wild type fusion. The high functional activities of these truncated fusion mutants could be due to the increase in receptor number (as observed on the immunoblot, Figure 4A) and/or as a result of the reduced ability to down-regulate by endocytosis as observed for C-terminally truncated Ste2p mutants (*32*). However, the expression level of these truncation mutants was about 70% of that for WT Ste2p. Although truncation of the C-terminus increased the expression level of the fusion protein, this increase is still not enough for the production of large quantities of purified protein required for X-ray crystallographic studies. It is therefore suggested that some further modifications be made to the protein, or alternately an expression system other than *S. cerevisiae* should be employed to improve expression levels.

The insertion of the FLAG epitope tag (DYKDDDDK) between residues Val457 and Thr458 in Gpa1p of the fusion did not alter its activity to function as a Gpa1p protein. This fusion protein displayed activities identical to wild type Gpa1p or similarly tagged Gpa1p mutant. It also retained receptor functions similar to those of Ste2p. Interestingly when the Rho tag was inserted at the same position, no detectable expression of either the fusion protein or free Gpa1p was observed on immunoblots using antibodies against Ste2p, Gpa1p and/or the Rho epitope. Cells transformed with plasmids bearing these constructs did not display any observable activities. The α5 helix (C-terminus) of the Gpa1p is known to play a critical role in mediating Ste2p coupling. However, several studies have shown that the last five amino acids of Gpa1p are

critical for such activities (*44, 52*), therefore residue Val457 (16 residues away from the C-terminus) was chosen as the site to insert the epitope tag. It is not clear why the Rho tag affected protein expression of both the fusion and Gpa1p proteins, while the FLAG tag did not. One possible explanation is that the FLAG epitope tag is more hydrophilic than the Rho tag. Thus, that region of Gpa1p can tolerate the very hydrophilic FLAG tag but not the moderately hydrophilic Rho epitope tag. Since N-terminal Rho tagging of Ste2p in the fusion protein displayed expression and activities similar to those of the the wild type fusion, it will not be necessary to put the Rho tag on Gpa1p.

This study is the first to report detailed activities of a full length Ste2p-Gpa1p fusion protein that retains the function (both in vivo and in vitro) of each individual protein, and can complement the deletion of both proteins. The fusion protein functions as a receptor (Ste2p) with near wild type affinity for α-factor and as a tethered Gα protein (Gpa1p) with affinity for GTP/GDP similar to that for the native Gα. The fusion protein could be separated by cleaving a protease site that was engineered between the two proteins. Truncation of the C-terminus of Ste2p in the fusion increased both expression and activities of the construct. This fusion protein will be a very useful tool to study the structure-function relationship between the receptor and Gα proteins, and should help to develop an understanding of the critical interactions required for GPCRs coupling with G proteins.

References for Part VI

1. Eglen, R. M., and Reisine, T. (2009) New insights into GPCR function: implications for HTS, *Methods Mol Biol 552*, 1-13.
2. Williams, C., and Hill, S. J. (2009) GPCR signaling: understanding the pathway to successful drug discovery, *Methods Mol Biol 552*, 39-50.
3. Hauser, M., Kauffman, S., Lee, B. K., Naider, F., and Becker, J. M. (2007) The first extracellular loop of the Saccharomyces cerevisiae G protein-coupled receptor Ste2p undergoes a conformational change upon ligand binding, *J Biol Chem 282*, 10387-10397.
4. Lee, B. K., Jung, K. S., Son, C., Kim, H., VerBerkmoes, N. C., Arshava, B., Naider, F., and Becker, J. M. (2007) Affinity purification and characterization of a G-protein coupled receptor, Saccharomyces cerevisiae Ste2p, *Protein Expr Purif 56*, 62-71.
5. Suga, H., and Haga, T. (2007) Ligand screening system using fusion proteins of G protein-coupled receptors with G protein alpha subunits, *Neurochem Int 51*, 140-164.
6. Simon, M. I., Strathmann, M. P., and Gautam, N. (1991) Diversity of G proteins in signal transduction, *Science 252*, 802-808.
7. Christopoulos, A. (2002) Allosteric binding sites on cell-surface receptors: novel targets for drug discovery, *Nat Rev Drug Discov 1*, 198-210.
8. Christopoulos, A., and Kenakin, T. (2002) G protein-coupled receptor allosterism and complexing, *Pharmacol Rev 54*, 323-374.
9. Cabrera-Vera, T. M., Vanhauwe, J., Thomas, T. O., Medkova, M., Preininger, A., Mazzoni, M. R., and Hamm, H. E. (2003) Insights into G protein structure, function, and regulation, *Endocr Rev 24*, 765-781.

10. Spiegel, A. M., and Weinstein, L. S. (2004) Inherited diseases involving g proteins and g protein-coupled receptors, *Annu Rev Med 55*, 27-39.

11. Leach, K., Sexton, P. M., and Christopoulos, A. (2007) Allosteric GPCR modulators: taking advantage of permissive receptor pharmacology, *Trends Pharmacol Sci 28*, 382-389.

12. Milligan, G., Parenty, G., Stoddart, L. A., and Lane, J. R. (2007) Novel pharmacological applications of G-protein-coupled receptor-G protein fusions, *Curr Opin Pharmacol 7*, 521-526.

13. Holst, B., Hastrup, H., Raffetseder, U., Martini, L., and Schwartz, T. W. (2001) Two active molecular phenotypes of the tachykinin NK1 receptor revealed by G-protein fusions and mutagenesis, *J Biol Chem 276*, 19793-19799.

14. Seifert, R., Wenzel-Seifert, K., Gether, U., and Kobilka, B. K. (2001) Functional differences between full and partial agonists: evidence for ligand-specific receptor conformations, *J Pharmacol Exp Ther 297*, 1218-1226.

15. Welsby, P. J., Carr, I. C., Wilkinson, G., and Milligan, G. (2002) Regulation of the avidity of ternary complexes containing the human 5-HT(1A) receptor by mutation of a receptor contact site on the interacting G protein alpha subunit, *Br J Pharmacol 137*, 345-352.

16. Cherezov, V., and Caffrey, M. (2007) Membrane protein crystallization in lipidic mesophases. A mechanism study using X-ray microdiffraction, *Faraday Discuss 136*, 195-212; discussion 213-129.

17. Cherezov, V., Rosenbaum, D. M., Hanson, M. A., Rasmussen, S. G., Thian, F. S., Kobilka, T. S., Choi, H. J., Kuhn, P., Weis, W. I., Kobilka, B. K., and Stevens, R. C. (2007) High-resolution crystal structure of an engineered human beta2-adrenergic G protein-coupled receptor, *Science 318*, 1258-1265.

18. Day, P. W., Rasmussen, S. G., Parnot, C., Fung, J. J., Masood, A., Kobilka, T. S., Yao, X. J., Choi, H. J., Weis, W. I., Rohrer, D. K., and Kobilka, B. K. (2007) A monoclonal antibody for G protein-coupled receptor crystallography, *Nat Methods 4*, 927-929.

19. Rasmussen, S. G., Choi, H. J., Rosenbaum, D. M., Kobilka, T. S., Thian, F. S., Edwards, P. C., Burghammer, M., Ratnala, V. R., Sanishvili, R., Fischetti, R. F., Schertler, G. F., Weis, W. I., and Kobilka, B. K. (2007) Crystal structure of the human beta2 adrenergic G-protein-coupled receptor, *Nature 450*, 383-387.

20. Rosenbaum, D. M., Cherezov, V., Hanson, M. A., Rasmussen, S. G., Thian, F. S., Kobilka, T. S., Choi, H. J., Yao, X. J., Weis, W. I., Stevens, R. C., and Kobilka, B. K. (2007) GPCR engineering yields high-resolution structural insights into beta2-adrenergic receptor function, *Science 318*, 1266-1273.

21. Jaakola, V. P., Griffith, M. T., Hanson, M. A., Cherezov, V., Chien, E. Y., Lane, J. R., Ijzerman, A. P., and Stevens, R. C. (2008) The 2.6 angstrom crystal structure of a human A2A adenosine receptor bound to an antagonist, *Science 322*, 1211-1217.

22. Park, J. H., Scheerer, P., Hofmann, K. P., Choe, H. W., and Ernst, O. P. (2008) Crystal structure of the ligand-free G-protein-coupled receptor opsin, *Nature 454*, 183-187.

23. Scheerer, P., Park, J. H., Hildebrand, P. W., Kim, Y. J., Krauss, N., Choe, H. W., Hofmann, K. P., and Ernst, O. P. (2008) Crystal structure of opsin in its G-protein-interacting conformation, *Nature 455*, 497-502.

24. Warne, T., Serrano-Vega, M. J., Baker, J. G., Moukhametzianov, R., Edwards, P. C., Henderson, R., Leslie, A. G., Tate, C. G., and Schertler, G. F. (2008) Structure of a beta1-adrenergic G-protein-coupled receptor, *Nature 454*, 486-491.

25. Marino, S. F. (2009) High-level production and characterization of a G-protein coupled receptor signaling complex, *FEBS J 276*, 4515-4528.

26. Dohlman, H. G., and Thorner, J. W. (2001) Regulation of G protein-initiated signal transduction in yeast: paradigms and principles, *Annu Rev Biochem 70*, 703-754.

27. Dohlman, H. G. (2002) G proteins and pheromone signaling, *Annu Rev Physiol 64*, 129-152.

28. Eilers, M., Hornak, V., Smith, S. O., and Konopka, J. B. (2005) Comparison of class A and D G protein-coupled receptors: common features in structure and activation, *Biochemistry 44*, 8959-8975.

29. Naider, F., and Becker, J. M. (2004) The alpha-factor mating pheromone of Saccharomyces cerevisiae: a model for studying the interaction of peptide hormones and G protein-coupled receptors, *Peptides 25*, 1441-1463.

30. Minic, J., Sautel, M., Salesse, R., and Pajot-Augy, E. (2005) Yeast system as a screening tool for pharmacological assessment of g protein coupled receptors, *Curr Med Chem 12*, 961-969.

31. Medici, R., Bianchi, E., Di Segni, G., and Tocchini-Valentini, G. P. (1997) Efficient signal transduction by a chimeric yeast-mammalian G protein alpha subunit Gpa1-Gsalpha covalently fused to the yeast receptor Ste2, *EMBO J 16*, 7241-7249.

32. Konopka, J. B., Jenness, D. D., and Hartwell, L. H. (1988) The C-terminus of the S. cerevisiae alpha-pheromone receptor mediates an adaptive response to pheromone, *Cell 54*, 609-620.

33. McEwen, D. P., Gee, K. R., Kang, H. C., and Neubig, R. R. (2001) Fluorescent BODIPY-GTP analogs: real-time measurement of nucleotide binding to G proteins, *Anal Biochem 291*, 109-117.

34. Jameson, E. E., Roof, R. A., Whorton, M. R., Mosberg, H. I., Sunahara, R. K., Neubig, R. R., and Kennedy, R. T. (2005) Real-time detection of basal and stimulated G protein GTPase activity using fluorescent GTP analogues, *J Biol Chem 280*, 7712-7719.

35. Willard, F. S., Kimple, A. J., Johnston, C. A., and Siderovski, D. P. (2005) A direct fluorescence-based assay for RGS domain GTPase accelerating activity, *Anal Biochem 340*, 341-351.

36. Huang, L. Y., Umanah, G., Hauser, M., Son, C., Arshava, B., Naider, F., and Becker, J. M. (2008) Unnatural amino acid replacement in a yeast G protein-coupled receptor in its native environment, *Biochemistry 47*, 5638-5648.

37. Gietz, D., St Jean, A., Woods, R. A., and Schiestl, R. H. (1992) Improved method for high efficiency transformation of intact yeast cells, *Nucleic Acids Res 20*, 1425.

38. Dosil, M., Giot, L., Davis, C., and Konopka, J. B. (1998) Dominant-negative mutations in the G-protein-coupled alpha-factor receptor map to the extracellular ends of the transmembrane segments, *Mol Cell Biol 18*, 5981-5991.

39. Sherman, F. (2002) Getting started with yeast, *Methods Enzymol 350*, 3-41.

40. David, N. E., Gee, M., Andersen, B., Naider, F., Thorner, J., and Stevens, R. C. (1997) Expression and purification of the Saccharomyces cerevisiae alpha-factor receptor (Ste2p), a 7-transmembrane-segment G protein-coupled receptor, *J Biol Chem 272*, 15553-15561.

41. Slauch, J. M., Mahan, M. J., and Mekalanos, J. J. (1994) Measurement of transcriptional activity in pathogenic bacteria recovered directly from infected host tissue, *Biotechniques 16*, 641-644.

42. Lee, B. K., Khare, S., Naider, F., and Becker, J. M. (2001) Identification of residues of the Saccharomyces cerevisiae G protein-coupled receptor contributing to alpha-factor pheromone binding, *J Biol Chem 276*, 37950-37961.

43. Fisher, C. L., and Pei, G. K. (1997) Modification of a PCR-based site-directed mutagenesis method, *Biotechniques 23*, 570-571, 574.

44. Kallal, L., and Kurjan, J. (1997) Analysis of the receptor binding domain of Gpa1p, the G(alpha) subunit involved in the yeast pheromone response pathway, *Mol Cell Biol 17*, 2897-2907.

45. Clark, C. D., Palzkill, T., and Botstein, D. (1994) Systematic mutagenesis of the yeast mating pheromone receptor third intracellular loop, *J Biol Chem 269*, 8831-8841.

46. Jenness, D. D., and Spatrick, P. (1986) Down regulation of the alpha-factor pheromone receptor in S. cerevisiae, *Cell 46*, 345-353.

47. Dosil, M., Schandel, K. A., Gupta, E., Jenness, D. D., and Konopka, J. B. (2000) The C terminus of the Saccharomyces cerevisiae alpha-factor receptor contributes to the formation of preactivation complexes with its cognate G protein, *Mol Cell Biol 20*, 5321-5329.

48. Blois, T. M., and Bowie, J. U. (2009) G-protein-coupled receptor structures were not built in a day, *Protein Sci 18*, 1335-1342.

49. Smith, B., Hill, C., Godfrey, E. L., Rand, D., van den Berg, H., Thornton, S., Hodgkin, M., Davey, J., and Ladds, G. (2009) Dual positive and negative regulation of GPCR signaling by GTP hydrolysis, *Cell Signal 21*, 1151-1160.

50. Shi, C., Kendall, S. C., Grote, E., Kaminskyj, S., and Loewen, M. C. (2009) N-terminal residues of the yeast pheromone receptor, Ste2p, mediate mating events independently of G1-arrest signaling, *J Cell Biochem 107*, 630-638.

51. Shi, C., Kaminskyj, S., Caldwell, S., and Loewen, M. C. (2007) A role for a complex between activated G protein-coupled receptors in yeast cellular mating, *Proc Natl Acad Sci U S A 104*, 5395-5400.

52. Gladue, D. P., and Konopka, J. B. (2008) Scanning mutagenesis of regions in the Galpha protein Gpa1 that are predicted to interact with yeast mating pheromone receptors, *FEMS Yeast Res 8*, 71-80.

PART VII

General Conclusions and Future Studies

CHAPTER 1

General Conclusions and Discussion

This dissertation details how three different cross-linking approaches have been used to understand the interactions between the *Saccharomyces cerevisiae* pheromone receptor, Ste2p, its ligand, α-factor, and its cognate Gα protein, Gpa1p. Chemical cross-linking using DOPA-α-factor analogs have provided insights into the interactions of the C-terminus of α-factor with specific residues in Ste2p. The incorporation of benzoyl-*L*-phenylalanine (Bpa) into Ste2p for photoaffinity cross-linking to identify specific residues that contact or are in close proximity with α-factor is also reported. The use of cysteine disulfide cross-linking to determine specific residue-to-residue interactions in the Ste2p-Ste2p homo-dimer and the Ste2p-Gpa1p hetero-dimer revealed conformational changes in Ste2p and Gpa1p that occur during signal transduction. Finally different variants of Ste2p-Gpa1p fusion proteins that displayed biological activities similar to Ste2p and Gpa1p proteins are also discussed. In this final part of the dissertation, the major findings of these studies are summarized, including how these results contribute to current knowledge of GPCRs interactions with their ligands and G proteins, and an outline for future experiments that will provide further details on the mechanism(s) of signal transduction through GPCRs upon ligand binding.

Interactions of α-factor with Ste2p:

Though there have been several reports on the interactions of α-factor with Ste2p (*1-3*), specific residue-to-residue interactions have not been reported. Previously it was reported that

α-factor analogs containing Bpa at positions 1 and 13 cross-linked into portions of Ste2p comprising residues Ser251-M294 and Phe55 – Arg58, respectively (*1, 2, 4*). The studies with Bpa analogs did not identify the exact residue of Ste2p that interacted with position 1 or 13 of α-factor. Although Bpa-α-factor analogs have been useful for photoaffinity labeling of Ste2p the diphenylketone side chain in Bpa is considerably larger than the side chain of any natural amino acid. Because of the structural similarity of DOPA to Tyr and Trp, DOPA should be a better replacement than Bpa. In this study the periodate-mediated chemical cross-linking of [$DOPA^{1}$ Lys^{7}(BioACA),Nle^{12}]α-factor (Bio-$DOPA^{1}$) and [Lys^{7}(BioACA),Nle^{12}, $DOPA^{13}$]α-factor (Bio-$DOPA^{13}$) into Ste2p were investigated. These α-factor analogs were potent agonists, and comparison to the α-factor control indicated that the replacement of Trp at postion 1 or Tyr at 13 with DOPA did not significantly affect the ability of the peptide ability to bind and activate Ste2p. Thus, the reduction in the activities of Bio-$DOPA^{1}$ and Bio-$DOPA^{13}$ were mainly due to tagging with biotin (for detection) and not the DOPA replacement. Matrix-assisted laser-desorption ionization-time-of-flight (MALDI-TOF) analysis revealed that Bio-$DOPA^{1}$ and Bio-$DOPA^{13}$ α-factor analogs cross-linked to fragments of Ste2p comprising residues Leu264-Thr284 and Phe55 – Met69, respectively, similar to previous report using the Bpa analogs (*1, 2, 4*). Cross-linking of the Bio-$DOPA^{13}$ α-factor analog into a Ste2p mutant (Cys59Ser) devoid of cysteine was greatly diminished suggesting that $DOPA^{13}$ of the α-factor analog interacted directly with Cys59 of Ste2p. These results indicate that the N-terminus of α-factor interacts with residues near the extracellular surface of TM5-TM6-TM7 whereas the C-terminus interacts

with residues near the TM1 region. The precise mechanism of α-factor binding to Ste2p is not well defined.

Despite variations in ligand specificity of the GPCRs, there are some similarities in the ligand interactions among the GPCR families. GPCRs ligands are classified as full agonist, partial agonists, inverse agonists, antagonist, synergist and allosteric regulators. These ligands induce different conformational changes in GPCRs, which can result in the production of different intracellular signals (*6-10*). The development of drugs targeting GPCRs are mostly based on the mechanisms of full, partial and inverse agonists, antagonist, and allosteric modulators. Thus, understanding the activities of these ligands will facilitate the design of drugs that target GPCRs (*9, 11, 12*). Although several studies have reported on the activities of partial and inverse agonists, antagonists and allosteric modulators, not much has been reported on synergist activities. The proposed mechanism by which the α-factor synergist enhances the activities of α-factor is critical for designing drugs that are required to selectively increase the activities of GPCRs only in their ligand-bound state. In this approach if the signaling pocket of the ligand in the GPCR is known, a specific molecule or peptide can be generated that will only interact within the signaling pocket without inhibiting the activities of the agonist. Such drugs will be very selective since they will target only agonist bound receptors so that a mutant agonist that can not fully activate its receptor can, through interaction with the synergist, induce full activation.

The cross-linking of the Bio-DOPA α-factor analogs to Ste2p was prevented in the presence of a 100-fold molar excess native α-factor (WHWLQLKPGQPNleY) and an α-factor

antagonist (WLQLKPGQPNleY) but it was not influenced by the presence of BSA. However, an α-factor synergist (WHWLQLKPGQP) reduced cross-linking of Bio-DOPA^{1} by 70% but had no significant effect on Bio-DOPA^{13} cross-linking. This α-factor synergist lacking the last two residues of α-factor has been shown to have significantly reduced binding affinity for Ste2p, however it enhances the activity of the wild-type α-factor (*5*). The interaction sites of the synergist is unknown. The data collected in this dissertation suggest that the synergist is most likely to interact within the signaling pocket. The differential inhibition of cross-linking by the α-factor synergist suggests that the synergist interacts within a similar site as the N-terminus of α-factor in Ste2p. Though the synergist does not bind to Ste2p, the results of this dissertation suggest that the binding of α-factor to Ste2p induce conformational changes at the extracellular surface of the receptor that opens the signaling pocket, allowing the synergist to interact with the receptor. Thus, in the absence of a potent agonist that binds Ste2p the synergist does not interact within this pocket since this pocket is only exposed upon binding of a potent agonist. This scenario explains why the synergist can not activate receptor by itself, but in the presence of α-factor it increases the activities of the receptor to greater than wild type level.

Non-naturally occurring amino acids can be synthesized to contain a variety of chemical moieties for use as photoaffinity labels. To incorporate unnatural amino acids into proteins in living cells, a novel method has been developed that uses orthogonal pairs of tRNA/ aminoacyl-tRNA synthetases evolved and expressed in the target cell (*13*). In *S. cerevisiae* orthologous tRNA/aminoacyl-tRNA synthetase pairs have been used to incorporate a variety of unnatural amino acids, including the photoactivatable amino acid analog *p*-benzoyl-*L*-phenylalanine [Bpa]

(*14*). This dissertation reports the site-specific incorporation of Bpa into Ste2p using an orthologous tRNA/aminoacyl tRNA synthetase pair.

In this system, the amber TAG stop codon was engineered into specific sites within the *STE2* coding region. The results showed that the mutant receptors were expressed at the membrane at levels from 5 to 10% of the wild-type receptor. Whereas some mutants displayed defects in activities others have activities similar to wild type receptor as determined by growth arrest and binding assays. Mass spectrometry proved that Bpa was incorporated at the expected position for the $G188^{TAG}$ receptor. Ste2p-Bpa mutant expression increased when the unnatural amino acid was delivered as a dipeptide via the peptide transport system of *S. cerevisiae*.

Bpa-Ste2p receptors were used to selectively photocapture biotinylated α-factor. These cross-linking results indicate that Ste2p residues Phe55 and Tyr193, but not Gly188, are in close proximity to α-factor in the ligand bound conformation of Ste2p. The close proximity of Ste2p residue Tyr193 to α-factor suggests that this aromatic residue may interact with the highly aromatic and hydrophobic N-terminus ($W^1H^2W^3L^4$) of α-factor. This idea is very speculative and therefore Tyr193 remains a target for future studies. The cross-linking of Phe55Bpa Ste2p mutant with α-factor was not surprising since this the TM1 region of Ste2p has been suggested to be the site of interaction for the C-terminus of the ligand. The exact residues in α-factor that interact with Phe55 and Tyr193 were not identified, so this issue still needs to be addressed.

Binding mechanism of α-factor to Ste2p:

The multi-step processes in which peptides bind to their receptors are thought to provide the basis for understanding ligand interactions with GPCRs (*9, 15*). Understanding the mechanism of α-factor binding to Ste2p will be critical for elucidating other GPCRs-peptide ligand interactions. A two-step model for the binding of α-factor to Ste2p, described in part II of this dissertation, should provide more information on how pheromone and other peptides bind to their cognate GPCRs. In this model it is suggested that the C-terminus of α-factor first interacts with Ste2p within a binding pocket that includes residues (Phe55-Met69) in TM1. These interactions induce conformational changes at the extracellular surface of the receptor allowing the N-terminus to bind and penetrate, thus activating the receptor. The interactions with the N-terminus also induce additional conformational changes that are propagated to the cytoplasmic ends of the receptor leading to G protein activation. This model is consistent with a report that suggested that α-factor associates with Ste2p via a two-step process involving an initial interaction that places the ligand in a hydrophobic environment, followed by a conversion to a state in which the ligand moves to a more polar environment (*16*).

N-terminus of α-factor required for conformational changes at TM5-TM6 in Ste2p:

Cysteine disulfide bonds formed by the third intracellular loop (IL3) Cys mutants suggest that IL3 is a dimer contact surface in Ste2p homo-dimer. The observed presence of higher order oligomers of Ste2p indicates that multiple contacts interact in the oligomer. The reduction of dimer formation through residues at the cytoplasmic ends of TM5 and TM6 in presence of α-

factor, but not the α-factor antagonist, also suggests that the interactions of the pheromone N-terminus with Ste2p induce conformational changes in these regions of TM5 and TM6, similar to what has been reported for other GPCRs (*17-19*). These conformational changes at the cytoplasmic ends of TM5 and TM6 were shown to be affected by Gpa1p expression. Thus the binding of α-factor and Gpa1p to Ste2p coordinated to stabilize the active conformation of the receptor. The Bio-DOPA cross-linking studies revealed that the N-terminus of α-factor interacts with residues Ser251-Met294 (TM6-TM7) consistent with the results that the α-factor antagonist (lacking the first 2 N-terminal residues) does not induce proper conformational changes in residues at the cytoplasmic ends of TM5-TM6. Conformational changes in TM5, TM6 and TM7 have been observed to be critical for GPCRs activation (*17-19*). It is therefore suggested that the N-terminus of α-factor is responsible for inducing activation of Ste2p required for conformational changes in TM5 and TM6. However, agonist binding did not effect the high level of dimer formation mediated by residues located in the middle of IL3, suggesting that these residues may play a role in stabilizing Ste2p homo-dimers during receptor activation.

TM5 and TM6 in Ste2p interact with Gpa1p:

Ste2p residues L228 (at TM5 boundary), L247, L248 and L249 (all at TM6 boundary) were observed to interact with Gpa1p. The close proximity of these residues with the C-terminus of Gpa1p indicates that they provide a hydrophobic environment that favors the Gpa1p C-terminus interactions, similar to the reported interactions of opsin with transducin (*20*). The reaction of S243 (Ste2p) with Q463 and K467 (Gpa1p) suggests that these residues are involved

in a hydrogen bonding network, with hydrogen bridges between these three residues. These hydrogen bridges may be required for receptor activation, since this was only observed in the ligand-bound form of the receptor. The interactions of Gpa1p residues with different Ste2p residues in the active and inactive states suggest that the C-terminus of Gpa1p undergoes conformational changes during activation. These changes involve two movements; the first is an anti-clockwise 90^{o} rotational movement similar to the helix mechanism model of transducin (*21*), and the second, termed "withdrawal" movement, involves both vertical and horizontal displacement that result in about a 5.0 Å shift from the inner bundle of the receptor to the cytoplasmic surface (see part 5, Figure 6). These conformational changes bring TM5 and TM6 closer to each other, positioning L228 (TM5) and I248 (junction between IL3 and TM6) in close proximity to contact I469 and G470 of Gpa1p. It also generates new contacts between IL3 of Ste2p and C-terminal helix of Gpa1p; S243 interacts with Q463 and K467 with multiple hydrogen bonds, and L247 is located in close proximity with K467, probably mediated by hydrophobic interaction. The information obtained from this study will be critical for understanding the mechanism by which Gα proteins are activated by GPCRs to transduce signal to effector molecules.

Ste2p and Gpa1p fusion:

The Ste2p-Gpa1p fusion proteins displayed biological activities similar to wild type Ste2p or Gpa1p, and are capable of complementing the deletion of Ste2p and/or Gpa1p. The analyses of the functionality of the fusion as a receptor (Ste2p) and/or Gα protein (Gpa1p) indicate that the protein has affinity for α-factor and GTP/GDP similar to the wild type of the

separate proteins. The fusion construct could be separated by cleaving a protease site that was placed between the two proteins. Truncation of the C-terminus of Ste2p in the fusion increased both expression and activities. This fusion protein will be a very useful tool to study the structure-function relationship of both proteins and also the critical interactions that are required for GPCRs coupling with G proteins.

Working model for α-factor and Gpa1p binding to Ste2p and receptor activation:

The results presented in this dissertation, combined with the work of others including receptor mutagenesis analyses and structure-activity relationships of α-factor analogs, allowed the proposal of a binding model for the peptide ligand. The model (Figure 1) suggests a bend in the α-factor around the Pro8-Gly9 (*22*), with the Lys^7 side chain facing away from the TMs domains and interacting with a binding pocket formed by the extracellular loops (*23*). Studies of the N-terminus of α-factor indicated a strong preference for a large hydrophobic residue at the amino-terminal position of the pheromone (*4, 24, 25*). Analyses of α-factor Trp^3 activities indicated that the side chain of this residue is in a hydrophobic pocket (*1, 2, 16*). Based on data obtained from part II in this dissertation and other cross-linking studies (*1, 2, 4*) it is likely that the N-terminus of α-factor interacts with a pocket consisting of aromatic residues from the extracellular ends of TM5, TM6, and TM7 and the loops EL2 and EL3 attached to these TMs. In addition, the C-terminus of the pheromone interacts with TM1, where Gln^{10} of α-factor is in close proximity to residues 47 and 48 of Ste2p (*3*) and Tyr^{13} is in close proximity to Arg58 and Cys59 of Ste2p.

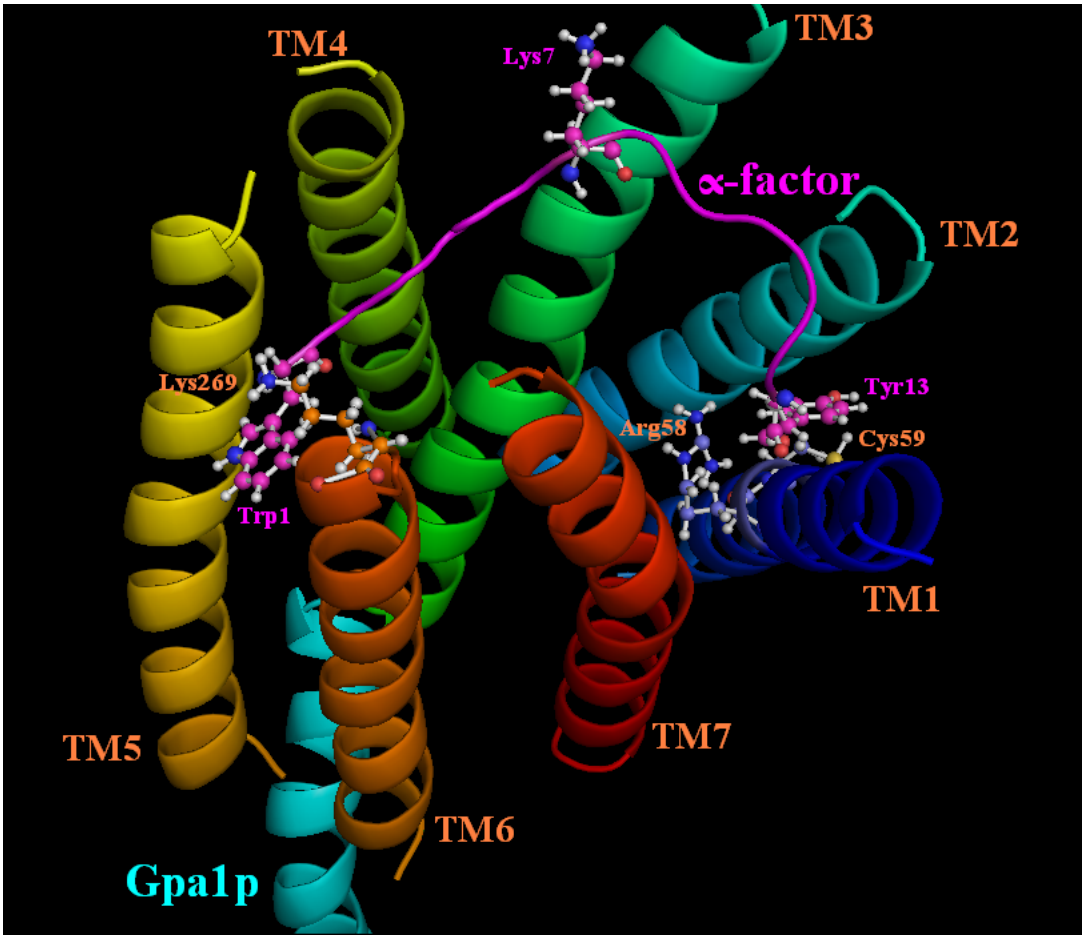

Figure 1: Working model for α-factor and Gpa1p binding to Ste2p. The transmembrane domains (TM) of Ste2p are labeled in different colors, α-factor is shown as a pink ribbon and Gpa1p C-terminus is colored in pale blue (positioned between TM5-TM6). The α-factor is suggested to bind with the Lys^{7} side chain facing away from the transmembrane domains and interacting with a binding pocket formed by the extracellular loops. The C-terminus (Tyr^{13}) of α-factor interacts with TM1 residues Arg58 and Cys59. The N-terminus (Trp^{1}) interacts with a pocket consisting of aromatic residues from the extracellular ends of TM5, TM6, and TM7 where it is in close proximity to Lys269 of Ste2p. The C-terminus of Gpa1p (pale blue) is shown to be in close proximity to TM5 and TM6.

The data obtained from part IV and V suggest that the binding and interactions of the N-terminus of α-factor to the TM5-TM6 regions of Ste2p induce conformational changes at the cytoplasmic ends of these TMs. This in turn leads to activation of the receptor and ultimately interactions with Gpa1p.

In the inactive form of Ste2p, the C-terminus of Gpa1p is suggested to be close to TM6 where residues L247 and L248 in TM6 are in close proximity to N465 and I469 in Gpa1p, respectively. Upon α-factor binding to Ste2p conformational changes (most likely rotational movements) at the ends of TM5 and TM6 occur that also induce conformational changes at the C-terminus of the Gpa1p. The changes at the C-terminus of Gpa1p are suggested in this study to involve a ~90^{o} anti-clockwise rotation, and at the same time a withdrawal from the inner core of the receptor which involves a vertical shift of about 5.0 Å. These changes cause the C-terminus of Gpa1p to move closer to TM5 and be withdrawn into the cytoplasmic surface of TM5-TM6. The conformational changes at the TM5 and TM6 regions did not affect the strong dimer formation of the IL3 region (connects the two TMs), suggesting that Ste2p dimers are not affected by receptor activation. The data in part 4 also suggest that residues in IL3 may be involved in stabilizing the Ste2p homo-dimers during the receptor activation. Overall, the results indicate that the binding of α-factor and Gpa1p are coordinated to stabilize the active conformation of Ste2p. This coordination was also reported in part 6 of the dissertation where the binding of GTP or GDP to Gpa1p in a Ste2p-Gpa1p fusion protein affected the binding of α-factor to Ste2p.

CHAPTER 2

Future Studies

Although great progress has been made in understanding the structure-function relationships of GPCRs and their G proteins, the mechanism underlying the interactions between these proteins still remains unclear, and only partial information is available concerning the binding sites for most molecules, including peptides, within the GPCR. The data obtained during the course of research for this dissertation will be important in understanding the complexity of GPCR signal transduction. However, in order to fully understand the activation mechanism of GPCRs upon agonist binding and their interactions with G proteins further studies are necessary to reveal additional details. This final part of the dissertation outlines a few suggestions to elucidate the interactions between the Ste2p with α-factor and Gpa1p.

Cross-linking studies:

The results obtained in part 2 indicate that DOPA α-factor analogs are indeed very useful to study Ste2p regions that interact with specific residues in α-factor. Although cross-linked fragments were identified by MALDI-TOF analysis based on the fragment size observed compared to predicted sizes of Ste2p fragments, the sequencing of this fragment to obtain the amino acid sequence will be more substantial. However, the data analyses from this dissertation were limited due to relatively low sensitivity of the instruments used, lack of proper algorithms to analyze complex fragmentation patterns, and difficult-to-interpret fragmentation of branched peptides. It is therefore recommended that analysis of $DOPA^{1}$ and $DOPA^{13}$ cross-linked

fragments should be carried out using instruments that will provide more information, such as the amino acid sequencing of the fragments to determine specific residues that interact with DOPA. The incorporation of DOPA at different positions of α-factor will be very helpful to determine the exact binding site and receptor residues involve in the binding.

This dissertation work revealed that L228 (at TM5 boundary) S243, L247, L248 and I249 (all at TM6 boundary) are in close proximity to C-terminus of Gpa1p. The crystal structure of opsin in its G protein-interacting conformation shows that TM5, TM6, TM3 and IL2 all interaction with the C-terminus of transducin Gα (*20*). Since this dissertation only tested a limited number of Ste2p residues (L228-I249) it is most likely that some residues N-terminal to L228 in TM5 and/or C-terminal to I249 in TM6 and also some TM3 residues may interact with Gpa1p in Ste2p in the inactive state. The cross-linking studies should be expanded to include residues in IL2. The incorporation of Bpa in these target regions of Ste2p (as described in part III of the dissertation) is also recommended.

The Ste2p and Gpa1p fusion constructs generated in this study displayed activity similar to that of non-fused Ste2p and Gpa1p. The separation of fused Ste2p and Gpa1p using factorXa indicated that this fusion is a useful tool for studying the interactions between Ste2p with Gap1p. The 1:1 stoichiometry of Ste2p to Gpa1p provides an ideal condition to capture any interactions between the two proteins. An outline of how this fusion protein can be used for cross-linking studies using either cysteine disulfide bond formation or Bpa photoaffinity labeling is shown in Figure 2. This approach will be very useful in defining specific interactions between the two proteins.

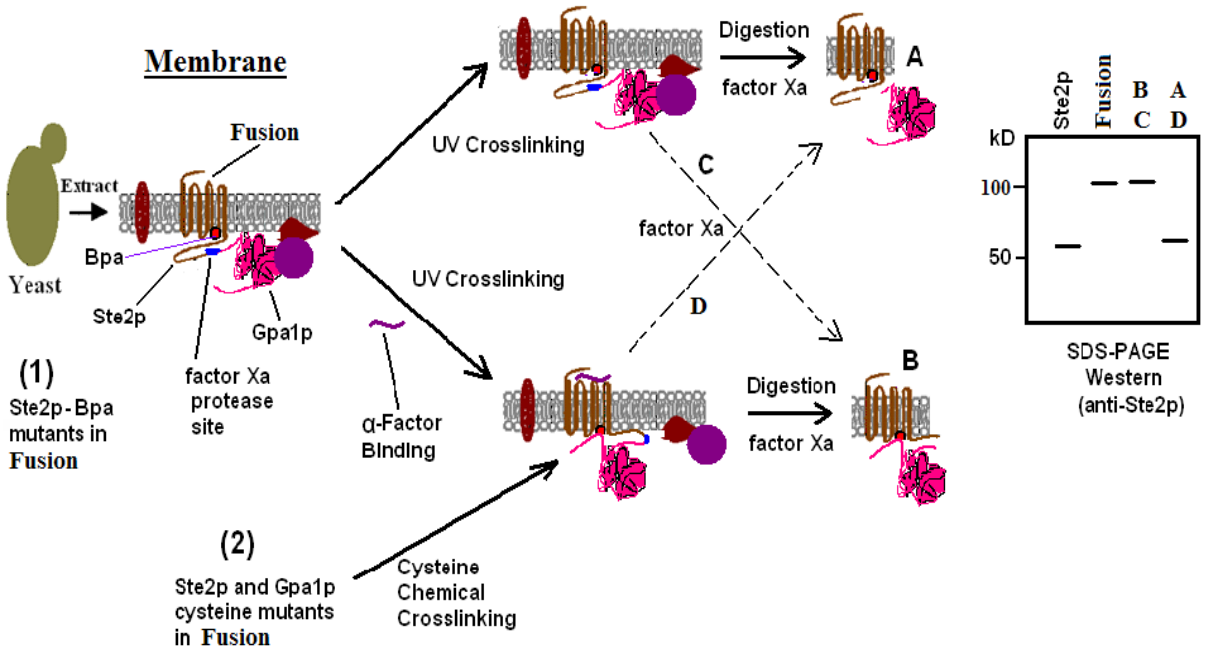

Figure 2: Ste2p and Gpa1p fusion cross-linking studies. The membrane extract containing the fusion protein is subjected to either UV-cross-linking (**1**. using Bpa-Fusion mutants) or chemical oxidation (**2**. using cysteine-Fusion mutants) in the presence or absence of α-factor binding. The fusion protein is then digested with factorXa to separate the two proteins. The samples are then resolved on SDS-PAGE to determine their sizes on the immunoblots using antibodies against Ste2p and Gapa1p (Figure 3 only shows the blots for anti-Ste2p). If Ste2p and Gpa1p are cross-linked then whether with ligand binding (product **B**) or without ligand binding (product **C**) a band similar to the size of the fusion should be observed even after the factorXa treatment. On the other hand if Ste2p and Gpa1p are not cross-linked then whether with ligand binding (product **D**) or without ligand binding (product **A**) a band similar to the size of the Ste2p should be observed after the factorXa digest.

References for Part VII

1. Son, C. D., Sargsyan, H., Hurst, G. B., Naider, F., and Becker, J. M. (2005) Analysis of ligand-receptor cross-linked fragments by mass spectrometry, *J Pept Res 65*, 418-426.
2. Son, C. D., Sargsyan, H., Naider, F., and Becker, J. M. (2004) Identification of ligand binding regions of the Saccharomyces cerevisiae alpha-factor pheromone receptor by photoaffinity cross-linking, *Biochemistry 43*, 13193-13203.
3. Lee, B. K., Khare, S., Naider, F., and Becker, J. M. (2001) Identification of residues of the Saccharomyces cerevisiae G protein-coupled receptor contributing to alpha-factor pheromone binding, *J Biol Chem 276*, 37950-37961.
4. Henry, L. K., Khare, S., Son, C., Babu, V. V., Naider, F., and Becker, J. M. (2002) Identification of a contact region between the tridecapeptide alpha-factor mating pheromone of Saccharomyces cerevisiae and its G protein-coupled receptor by photoaffinity labeling, *Biochemistry 41*, 6128-6139.
5. Eriotou-Bargiota, E., Xue, C. B., Naider, F., and Becker, J. M. (1992) Antagonistic and synergistic peptide analogues of the tridecapeptide mating pheromone of Saccharomyces cerevisiae, *Biochemistry 31*, 551-557.
6. Gregory, K. J., Sexton, P. M., and Christopoulos, A. (2007) Allosteric modulation of muscarinic acetylcholine receptors, *Curr Neuropharmacol 5*, 157-167.
7. Leach, K., Sexton, P. M., and Christopoulos, A. (2007) Allosteric GPCR modulators: taking advantage of permissive receptor pharmacology, *Trends Pharmacol Sci 28*, 382-389.

8. De Amici, M., Dallanoce, C., Holzgrabe, U., Trankle, C., and Mohr, K. (2009) Allosteric ligands for G protein-coupled receptors: A novel strategy with attractive therapeutic opportunities, *Med Res Rev*.

9. Eglen, R. M., and Reisine, T. (2009) New insights into GPCR function: implications for HTS, *Methods Mol Biol 552*, 1-13.

10. Williams, C., and Hill, S. J. (2009) GPCR signaling: understanding the pathway to successful drug discovery, *Methods Mol Biol 552*, 39-50.

11. Lundstrom, K. (2009) An overview on GPCRs and drug discovery: structure-based drug design and structural biology on GPCRs, *Methods Mol Biol 552*, 51-66.

12. Ratnala, V. R., and Kobilka, B. (2009) Understanding the ligand-receptor-G protein ternary complex for GPCR drug discovery, *Methods Mol Biol 552*, 67-77.

13. Wang, L., Xie, J., and Schultz, P. G. (2006) Expanding the genetic code, *Annu Rev Biophys Biomol Struct 35*, 225-249.

14. Chin, J. W., Cropp, T. A., Anderson, J. C., Mukherji, M., Zhang, Z., and Schultz, P. G. (2003) An expanded eukaryotic genetic code, *Science 301*, 964-967.

15. Chapter, M. C., White, C. M., De Ridder, A., Chadwick, W., Martin, B., and Maudsley, S. (2009) Chemical modification of Class II G-protein-coupled receptor ligands: Frontiers in the development of peptide analogs as neuroendocrine pharmacological therapies, *Pharmacol Ther*.

16. Bajaj, A., Celic, A., Ding, F. X., Naider, F., Becker, J. M., and Dumont, M. E. (2004) A fluorescent alpha-factor analogue exhibits multiple steps on binding to its G protein coupled receptor in yeast, *Biochemistry 43*, 13564-13578.

17. Wess, J., Han, S. J., Kim, S. K., Jacobson, K. A., and Li, J. H. (2008) Conformational changes involved in G-protein-coupled-receptor activation, *Trends Pharmacol Sci 29*, 616-625.

18. Reynolds, K. A., Katritch, V., and Abagyan, R. (2009) Identifying conformational changes of the beta(2) adrenoceptor that enable accurate prediction of ligand/receptor interactions and screening for GPCR modulators, *J Comput Aided Mol Des 23*, 273-288.

19. Rosenbaum, D. M., Rasmussen, S. G., and Kobilka, B. K. (2009) The structure and function of G-protein-coupled receptors, *Nature 459*, 356-363.

20. Scheerer, P., Park, J. H., Hildebrand, P. W., Kim, Y. J., Krauss, N., Choe, H. W., Hofmann, K. P., and Ernst, O. P. (2008) Crystal structure of opsin in its G-protein-interacting conformation, *Nature 455*, 497-502.

21. Scheerer, P., Heck, M., Goede, A., Park, J. H., Choe, H. W., Ernst, O. P., Hofmann, K. P., and Hildebrand, P. W. (2009) Structural and kinetic modeling of an activating helix switch in the rhodopsin-transducin interface, *Proc Natl Acad Sci U S A 106*, 10660-10665.

22. Zhang, Y. L., Marepalli, H. R., Lu, H. F., Becker, J. M., and Naider, F. (1998) Synthesis, biological activity, and conformational analysis of peptidomimetic analogues of the Saccharomyces cerevisiae alpha-factor tridecapeptide, *Biochemistry 37*, 12465-12476.

23. Ding, F. X., Lee, B. K., Hauser, M., Davenport, L., Becker, J. M., and Naider, F. (2001) Probing the binding domain of the Saccharomyces cerevisiae alpha-mating factor receptor with rluorescent ligands, *Biochemistry 40*, 1102-1108.

24. Zhang, Y. L., Lu, H. F., Becker, J. M., and Naider, F. (1997) Position one analogs of the Saccharomyces cerevisiae tridecapeptide pheromone, *J Pept Res 50*, 319-328.

25. Lee, B. K., Lee, Y. H., Hauser, M., Son, C. D., Khare, S., Naider, F., and Becker, J. M. (2002) Tyr266 in the sixth transmembrane domain of the yeast alpha-factor receptor plays key roles in receptor activation and ligand specificity, *Biochemistry 41*, 13681-13689.

VITA

George K. Essien Umanah was born in Cape coast, Ghana. He graduated from Odorgonno High School and then trained as a medical technician at the Korle-Bu Teaching Hospital, Accra, Ghana. He attended The University of Ghana and received his B.Sc in Biochemistry. During his studies at the university he worked for MEDLAB medical center a Switzerland company in Ghana as a medical lab technician. After graduation he was employed by the Biochemistry Department at The University of Ghana as a research and teaching assistant helping with undergraduate s programs. He also worked as research technician in Ghana for DIVERSA Corporation in San Diego, USA, isolating and characterizing microbial DNA from reserved forest. He then moved to the England and received his Master of Research in Medical Biotechnology from The University of Essex. He was accepted to the Ph.D. program in Microbiology department at the University of Tennessee, Knoxville. He did his graduate work in Dr. Jeffrey M. Becker's laboratory. Throughout the course of his time in this program, he served as a Graduate Teaching and Research Assistant and received several awards. He received a Doctor of Philosophy degree in Microbiology.